GENOMIC ENZYMOLOGY STUDY OF THE AMINOGLYCOSIDE ANTIBIOTIC ACETYLTRANSFERASES

GENOMIC ENZYMOLOGY STUDY OF THE AMINOGLYCOSIDE ANTIBIOTIC ACETYLTRANSFERASES

By EMILY BORDELEAU, M.Sc.

A thesis submitted to the School of Graduate Studies in partial fulfillment of the requirements for the degree of Doctor of Philosophy

DESCRIPTIVE NOTE

McMaster University DOCTOR OF PHILOSOPHY (2022) Hamilton, Ontario
(Biochemistry and Biomedical Sciences)

TITLE: Genomic enzymology study of the aminoglycoside antibiotic acetyltransferases

AUTHOR: Emily A. Bordeleau, M.Sc.

SUPERVISOR: Gerard D. Wright, Ph.D.

NUMBER OF PAGES: xiii, 182

Foreword

Lay abstract

Pathogens continue to learn new ways to protect themselves from antibiotics. With the discovery of new antibiotics becoming more challenging, global antibiotic resistance has the potential to become the next global pandemic. One solution is to redesign traditional antibiotics to escape resistance. A reliable, effective class of antibiotics currently under development are aminoglycosides. There is considerable knowledge into the sequence-structure-function relationships of proteins traditionally regarded as the sole contributors to a form of aminoglycoside resistance. My work describes the use of computational and biochemical techniques to investigate resistant elements beyond what we know is prevalent in clinical pathogens. Through these efforts I uncover structurally, and mechanistically distinct proteins capable of broad-spectrum, high-level aminoglycoside resistance produced by bacteria in various environments. These results are invaluable for the informed design of less-resistance prone aminoglycosides and antibiotic stewardship programs to limit these forms of resistance from becoming clinically prevalent.

Abstract

Since their discovery over 40 years ago, considerable knowledge has been obtained on the diversity, and structure-function relationships of aminoglycoside acetyltransferases (AACs), responsible for antibiotic resistance among priority clinical pathogens. In recent years, investigations have expanded to biochemical characterizations of AACs found in environmental reservoirs. The successful design of next-generation aminoglycosides (AGs) depends on an up-to-date understanding of the broader AG resistome.

Towards this goal, I present the first structural analysis for the unique apramycin modifying enzyme, ApmA. Apramycin is a veterinary antibiotic that is in development for clinical use. The atypical chemical scaffold provides inherent protection from many clinically relevant resistance mechanisms. Prior to the work presented herein, *apmA* was an uncharacterized apramycin resistance element among environmental species. I heterologously expressed and subsequently purified ApmA to characterize the nature of resistance towards this unique aminoglycoside. The results report the first acetyltransferase of the left-handed β-helix (LβH) superfamily involved in AG detoxification.

Secondly, I completed a comprehensive characterization of ApmA utilizing a structurally diverse panel of AGs for susceptibility testing, protein engineering, steady-state kinetics, and x-ray crystallography. Through these approaches, I establish the structural and functional features that define ApmA's place within the LβH superfamily and set it apart from other known AACs. The biochemical data presented describes a chemical mechanism dependent on the substrate specificity. Furthermore, I describe the molecular determinants behind AG-modification of clinically relevant AGs.

Lastly, I describe the first comprehensive structural and functional study of clinical and environmental Antibiotic_NAT (A_NAT) inactivating enzymes. A pan-family antibiogram was obtained and mapped to the reconstructed phylogeny for the A_NAT family. Crystallographic analysis of representatives from each clade was completed with our collaborators from the University of Toronto. Through the analysis of several ligand-bound A_NAT complexes, I contributed to the elucidation of structural features responsible for substrate specificity.

The collective findings from these chapters have extended the protein landscape involved in AG-acetylation from one commonly used fold to three distinct architectures, each unique in underlying chemical mechanism and dissemination.

Acknowledgements

Gerry – I don't think either of us could have anticipated the ups and downs of my Doctoral studies. Thank you for being an incredible mentor, your passion for science is inspiring. Thank you for always pushing me to become the researcher I am now, while helping me create a safe, positive, work-life balance as I encountered the most difficult situations I'll ever have to face in life.

To my committee members, Marie and Eric – thank you for all your guidance with my research. I am so grateful for your time, support and understanding as I navigated challenges inside and outside the lab.

To all the past and present members of the Wright lab – there are so many people I want to thank but don't have enough pages. Each of you have impacted my life in so many ways and I am so grateful to all of you. I cannot imagine this experience without you.

To my friends outside the lab and family – it's been an adventure that's for sure! Lisa and Luke, I love you both so much and I am so grateful we could stay in touch all these years. Thank you for endlessly pushing me to fight for what I deserve. Stephen – best little brother a girl could ask for and I am so thankful to have your support, thank you for being available at all hours to proofread the smallest of paragraphs or listen to me vent. Dad – there are too many things to thank you for, I know you will always be rooting for me in everything I do moving forward.

Lastly, Andrew – husband to be, my best friend. I have reached the happiest and healthiest version of myself because of you. There are no words for how thankful I am that we found each other when we did.

Table of contents

List of figures

Chapter 1

Chapter 2

Chapter 3

List of tables

Chapter 2

Chapter 3

Chapter 4

List of abbreviations

A_NAT	antibiotic *N*-acetyltransferase
AAC	aminoglycoside acetyltransferase
AG	aminoglycoside
AME	aminoglycoside modifying enzyme
ANT	aminoglycoside nucleotidyltransferase
APH	aminoglycoside phosphotransferase
CAT	chloramphenicol acetyltransferase
CARD	comprehensive antibiotic resistance database
CoA	coenzyme A
COOT	crystallographic object-oriented toolkit
DOS	deoxystreptamine ring
FMG	functional metagenomics
GNAT	GC*N*5-related *N*-acetyltransferase
HMBC	heteronuclear multiple bond correlation
HMM	hidden Markov model
HR-ESI-MS	high-resolution electrospray ionization mass spectrometry
LC	liquid chromatography
LβH	left-handed β helix
NMR	nuclear magnetic resonance spectroscopy
PDB	protein data bank
Pfam	protein families (database)
RMTase	16S rRNA methyltransferase
SAD	single anomalous diffraction
XAT	xenobiotic acetyltransferase

Declaration of academic achievement

I have performed all the research in this body of work except where indicated in the preface of each chapter.

Chapter One: Aminoglycoside *N*-acetyltransferases

Introduction

Bacterial pathogens have acquired and evolved through natural selection, a diverse collection of resistance strategies to protect against all antibiotic classes. One of the major resistance mechanisms employed is to reduce a drug's affinity for its bacterial target through enzyme-mediated antibiotic modification[1]. Aminoglycosides (AGs) are a class of natural and semi-synthetic antibiotics that are impacted by highly diverse modification mechanisms. The commonly used AGs incorporate a 2-deoxystreptamine ring varying in substitution by amino-sugars. Their decorated structures provide ample centers for functionalization by AG-modifying enzymes (AMEs) that phosphorylate, acetylate, or adenylate key AG sites **(Fig. 1)**. These structural alterations lead to a loss in affinity for one of the most reliable targets in drug development, the bacterial ribosome. AGs primarily bind to the 16S rRNA and disrupt the codon-anticodon pairing mechanism. This result compromises the fidelity of protein synthesis by creating mistranslated or truncated proteins. Modifications of hydroxyl or primary amine groups on the AG molecule block essential interactions within the ribosome A-site resulting in high levels of resistance for the host[2]. Among the classes of AMEs, the most prominent in the clinic are the *N*-acetyltransferases (AACs). AACs catalyze the acetyl-coenzyme A-dependent acetylation of primary amine functional groups to reduce the affinity of AGs for their molecular target. Semi-synthesis of natural product AGs leverages the stereochemistry and positioning of functional groups to evade AAC-mediated inactivation. Substantial structure-activity studies have informed the design of analogs less prone to resistance with improved activity. These attributes, in combination with their well-established clinical history as effective bactericidal drugs for the treatment of infections caused by Gram negative pathogens, have revitalized investigations for next-generation AGs to combat serious multi-drug resistant infections[3-6].

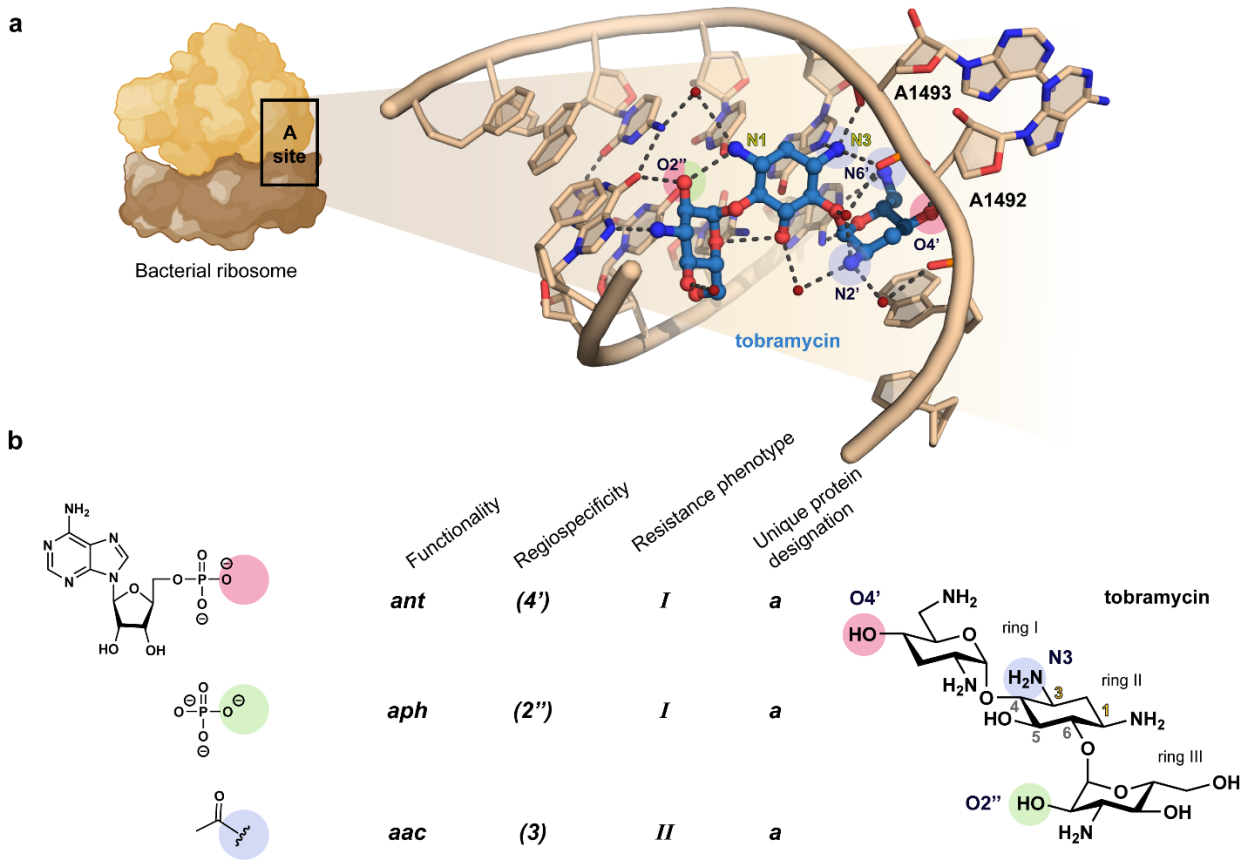

Figure 1. Nomenclature for aminoglycoside modifying enzymes reflects the diversity of functionalization to reduce affinity for 16S rRNA. (a) Primary mechanism of action for AG antibiotics. (b) There are three subclasses of AG-modifying enzymes that differ based on form of chemical modification: ANTs (adenylation), APHs (phosphorylation) and AACs (acetylation). The nomenclature for genes encoding three tobramycin modifying enzymes are broken down into the four components first described in ref. 12 (functionality, regiospecificity, resistance phenotype and protein designation). A three-letter italicized abbreviation indicates the functional group to be added to tobramycin. The regiospecificity, or site of modification, is indicated in parentheses. A roman numeral indicates the resistance phenotype when the protein is expressed in the host. The last component of the nomenclature is a lower-case letter to differentiate between modifying enzymes of the same function, regiospecificity and resistance phenotype. Functional groups that are susceptible to modification on tobramycin by ANT(4')-Ia, APH(2'')-Ia and AAC(3)-Ia are highlighted pink, green and lavender respectively. Figure in part created with BioRender.com

Canonical members of the AG resistome: GC*N*5-related *N*-acetyltransferases

The GC*N*5-related *N*-acyltransferases (GNATs) are a protein superfamily in which a common fold has evolved to facilitate the acylation of a wide variety of important biological molecules. The functional diversity observed for this superfamily is reflected in the low primary sequence similarities and architecture of the acyl-accepting substrate region[7]. GNATs are found across all domains of life and are involved in processes such as detoxification, post-translation regulation, and biosynthesis of the bacterial cell wall. Their ability to partake in various critical acetylating activities is a consequence of the conserved fold involved in binding the pyrophosphate group of acetyl-CoA. The pyrophosphate binding loop is the only structural feature with a sequence motif shared between GNATs (R/Q-X-X-G-X-A/G). Several hydrogen bonds are formed between the peptide backbone and the pyrophosphate group within this region. Other distinguishing secondary structural attributes are parallel beta sheets with interspersed alpha helices[8].

With regards to the AACs of the AG resistome, GNATs were the first members to be identified[9]. Until relatively recently, the GNATs have been recognized as the sole contributors to AG resistance through acetylation for over 50 years. Consequently, a wealth of knowledge has been obtained regarding the diversity of their sequences, structures, and functions **(Fig. 2)**. The nomenclature initially adapted for AMEs and is still in use today, was a system built to describe gene and enzyme function with a useful short-hand[10-12]**(Fig. 1b)**. Genes encoding acetyltransferases are named with the three-letter abbreviation *aac* followed by a numerical value that indicates the site of modification on the AG molecule. A Roman numeral represents the resistance phenotype of the host when the gene is expressed. Lastly, a lower-case letter is assigned to distinguish between unique genes that confer identical resistance profiles. Around the same

time, an alternate nomenclature was also introduced by Novick et al. as a part of a proposal for plasmid and strain designations[13]. This less frequently used naming system shortens the abbreviation by removing a label that differentiates between isoforms. A capital letter followed by a single numerical value is used to describe the regiospecificity and its position in the discovery sequence. The review of these two systems by Shaw et al. in 1993 serves as the key starting reference for resistance phenotypes and in-depth analysis of sequence-function relationships across all AMEs known at the time of its publication[10].

The GNATs involved in AG acetylation are the most diverse in terms of regiospecificity for their activity **(Fig. 2)**. Each enzyme primarily targets sites N3, N6', and N2' of AGs and are therefore referred to as AAC(3), AAC(6'), and AAC(2'), respectively **(Fig 1b)**. The coexisting naming systems have, over time, created discrepancies in the literature for assigning a designation for a newly identified acetyltransferase. Vanhoof et al. were the first to address concerns regarding coexisting nomenclature systems after unintentionally assigning a new protein to a designation already in use[14]. There have since been mischaracterized resistance elements and incorrect functional assignments to sequences encoding acetyltransferases. For example, AAC(1) is an *N*-acetyltransferase responsible for N1 acetylation of AGs[15-17]. There are two reported enzymes belonging to this group, with the point of differentiation in substrate specificity being apramycin[16]. The activity was last reported in 1999 and, despite a lack of supporting protein sequence or structure, continues to be cited as a member of the GNAT superfamily[18-20]. There was also a shift in the literature where the nomenclature was assumed to imply protein familial relationships. To date, enzymes harboring AAC(3) activity can be categorized into ten subgroups based on their AG resistance profile. AAC(3)-I[21] and AAC(3)-XI[22] are the only known AACs that belong to the GNAT superfamily. Before structures of the remaining eight subgroups became available, only a

few publications recognized through protein sequence that two different protein families harbored AAC(3) activity[10,21,23]. However, these reports were outnumbered by a surge in structural data for GNATs AAC(3)-I and AAC(6')-I isoforms, accompanied by detailed functional and mechanistic studies. The result was the classification of all AG-modifying enzymes with AAC(3) activity belonging to the GNAT superfamily. The low percent identity among sequences of true GNATs further supported defining all AAC(3)s as such, even when structures of a distinct fold were published years later.

We highlight these discrepancies in the literature to create a solid foundation for developing next-generation AGs. The appropriate designations of these proteins are crucial to understanding how resistance functions evolve within their respective superfamily. There are many examples of acetyltransferases chromosomally encoded where their actual physiological function has yet to be determined, and it is proposed that antibiotic resistance may play a secondary role[24-26]. Insight into these connections will help us to better predict which genes have the evolutionary potential to inactivate AGs. Working towards this goal, the following sections will review the sequence, structure and function of GNATs studied to date with AG-modifying activities.

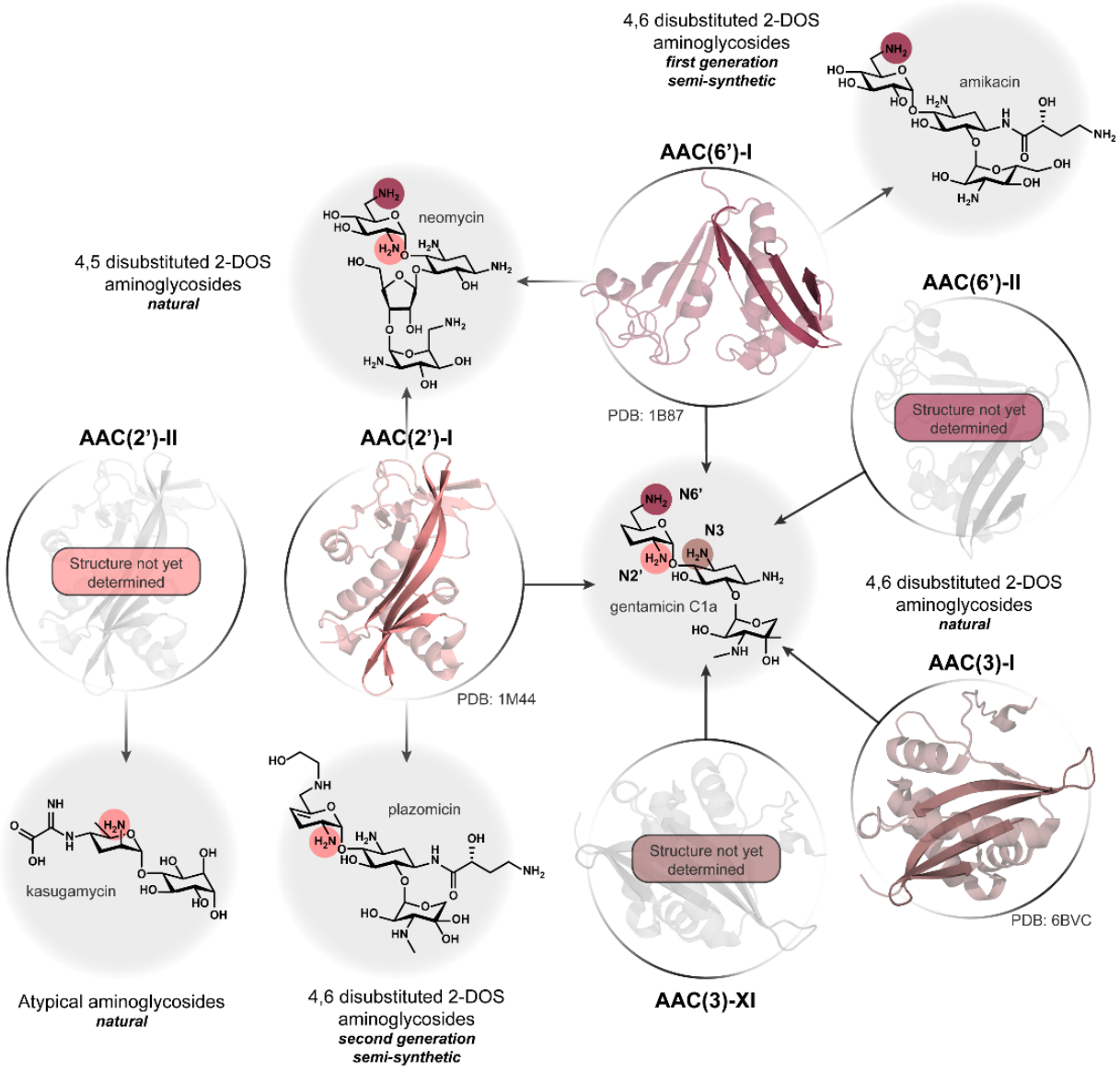

Figure 2. Overview of GNATs involved in AG-modification. Monomers from solved GNAT crystal structures of each subgroup are shown. The network of GNAT structures highlights the diversity in substrate specificity and regiospecificity. Structural and mechanistic studies have primarily focused on resistance elements already mobilized in the clinic or chromosomally encoded among pathogenic bacteria. Critical gaps remain in structures for newly identified AACs and those found in AG-producing organisms.

AAC(3)

The first protein sequence identified in the GNAT superfamily belongs to a 3-*N*-acetyltransferase commonly found in clinical isolates that conferred resistance towards gentamicin, fortimicin, and sisomicin[9,10]. Later designated AAC(3)-Ia, a 3-*N*-acetyltransferase from *Serratia marcescens,* also provided the first 3D-crystal structure of an AG-modifying acetyltransferase[27]. A truncated form of the protein (residues 1-168) was co-crystalized with CoA to a resolution of 2.3 Å. The initial structure provided invaluable insight into the binding mechanism of the acetyl-donor and conserved catalytic region of GNATs. However, the truncated AAC(3)-Ia isoform was later found to lack an α-helix observed in other AACs[28]. We recently determined the crystal structure of the full-length protein (residues 1-177) in complex with CoA to a resolution of 1.8 Å[29] **(Fig. 2)**. Our structure includes the C-terminal region, identifying changes in positioning of a β-strand and the addition of the aforementioned α-helix that impacts the positioning of CoA[29].

The emergence of AAC(3)-Ia in the 1970s compromised the usefulness of the popular clinical AG gentamicin[30-32]. To combat multi-drug resistance and improve the pharmacological properties of the class, first-generation semi-synthetic AGs were designed to evade modification and reduce toxicity. Amikacin is the most successful of those developed during this period and is still widely used today[33]. Described in 1972, amikacin is a semi-synthetic derivative of kanamycin A modified at C1 with an L-(γ)-amino-α-hydroxybutyryl chain, inspired by the natural product AG butirosin, an L-(γ)-amino-α-hydroxybutyryl derivative of ribostamycin that has improved activity against AAC-expressing bacteria[34]. The substitution at this position was found to provide protection against AAC(3)s.

There are currently four known isoforms of AAC(3)-I (a-d) that are found mobilized in various Gram-negative pathogens[35,36]. The distribution of these isoforms among clinical isolates

is mainly mediated by mobile gene cassettes inserted into integrons[21,35,37,38]. A fifth isoform, AAC(3)-Ie, was reported in 2004 in a multi-drug resistant *Salmonella enterica* sample[38]. However, the protein sequence shares 100 % amino acid identity with AAC(3)-Id and should be referenced as such.

More recent investigations have explored the diversity of GNATs with AAC(3) activity in the environment. We followed up on previously identified environmental metagenomic sequences[39], and found AG-acetylating activities comparable to those found in clinical isolates[28]. To establish approximate relationships between subgroups, we pooled clinical representatives and metagenomic sequences for phylogenetic analysis. While clinical isoforms of AAC(3)-I clustered together, selected sequences from metagenomics sampling exhibited great diversity, belonging to several subgroups within the GNAT superfamily. For this review, we re-constructed the phylogenetic tree to include AACs of varying regiospecificity **(Fig. 3)**. Our results demonstrate the depth of functional diversity that remains to be characterized within environmental reservoirs.

Crystal structures of meta-AACs and AAC(3)-Ib verified the shared GNAT fold for acetyl-CoA binding. Our *in vitro* kinetic experiments revealed greater rates of AG-acetylation for meta-AACs than the AAC(3)-I isoforms already circulating in clinic[28]. We selected meta-AACs near in phylogeny to clinical AAC(3)-I isoforms for susceptibility testing and found they exhibited an expanded AG resistance profile. A handful of meta-AACs exhibited activity towards tobramycin, a resistance profile noted to be reminiscent of AAC(3)-II. However, to designate these meta-AACs an AAC(3)-II GNAT, susceptibility testing with additional AGs would be required to distinguish from other AG-modifying GNATs[10].

AAC(3)-XI is a GNAT originating from clinical samples of the opportunistic pathogen, *Corynebacterium striatum*. The strains were found to exhibit a similar AG resistance profile as our

meta-AACs with the addition of activity observed towards kanamycin B and dibekacin[22]. Purification of the 3'-*N*-acetylated dibekacin product *in vitro* supported the classification of the enzyme to the AAC(3) subgroup with its unique activity profile justifying the assignment of subgroup XI. The authors did not purify the acetylated-kanamycin B product, which may be modified at a different site. A lack of resistance was observed towards kanamycin A, which only differs from kanamycin B at the N2' position. It is possible that the binding mode of kanamycin B results in *N*-acetylation instead on the prime ring. The positioning of AAC(3)-XI in our GNAT phylogenetic tree **(Fig. 3)** shows a distant relationship with the AAC(3) subgroup and instead falls within a clade of verified AAC(6') enzymes. Without supporting spectroscopic data of the acetylated kanamycin B product, the activity of AAC(3)-XI remains to be fully characterized.

AAC(6')

GNATs responsible for modifying the N6' position can be categorized into two subclasses based on their resistance profiles **(Fig. 2)**. AAC(6')-I confers resistance towards amikacin, neomycin, and naturally occurring 4,6-disubstituted subclass of AGs, with minimal activity observed towards gentamicin C1. In contrast, AAC(6')-II is active towards all gentamicins and cannot confer resistance towards amikacin[40]. AAC(6')-I isoforms have become widely disseminated among priority pathogens. They exhibit the greatest sequence diversity among AMEs and are distributed among three known GNAT clades harboring N6' acetylating activity **(Fig. 3)**. The most prevalent isoform is AAC(6')-Ib. It was first discovered in *Klebsiella pneumoniae* in 1986 and remains the most frequently reported in clinical isolates today[33,41,42]. Several variants of AAC(6')-Ib have been identified, with the most notable being the bifunctional variant AAC(6')-Ib-cr[43]. Due to two single amino acid substitutions, Trp102Arg and Asp179Tyr, the substrate specificity of this enzyme expanded to include fluoroquinolones that incorporate a pendant

184 piperazine ring such as ciprofloxacin. Despite being a synthetic antibiotic, this minor change in
185 protein sequence permits the modification of the available secondary nitrogen of the piperazine
186 heterocycle[43]. Fusion proteins with AAC(6')-I activity have also been found with either terminal
187 region found to have an additional AAC(6')-I, an AAC with different regiospecificity[44], a
188 nucleotidyltransferase[45], or a phosphotransferase[46]. The most clinically relevant bifunctional
189 enzyme is AAC(6')-APH(2'')[46,47]. The domain involved in AG acetylation is designated AAC(6')-
190 Ie. This isoform uniquely *N*-acetylates fortimicin and is the only AAC verified to *O*-acetylate
191 lividomycin and paromomycin to confer resistance[47,48].

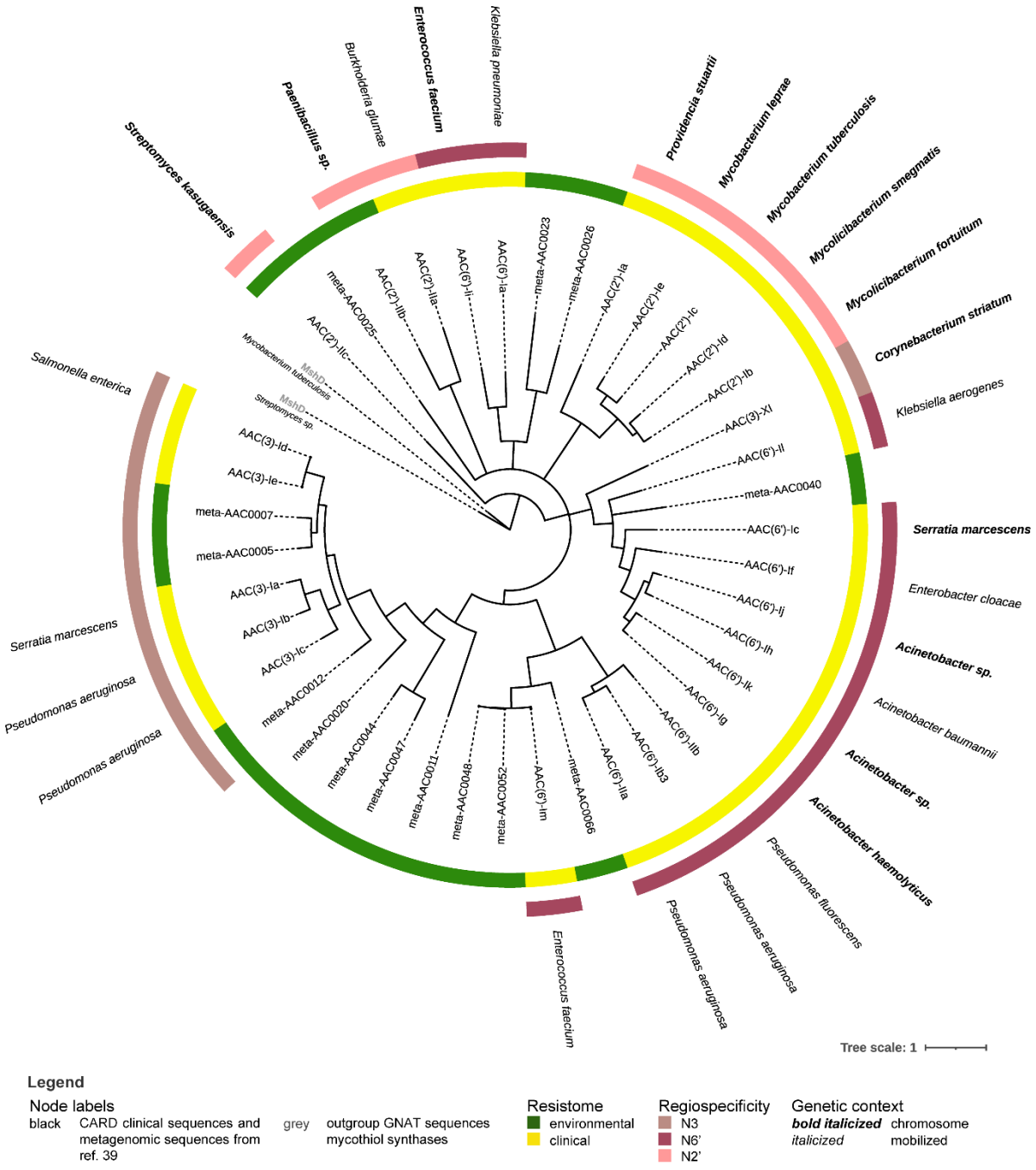

Figure 3. Radial phylogram of clinical and metagenomic sequences identified as members of the GNAT superfamily. AG-modifying GNATs exhibit great sequence diversity with variable regiospecificity. GNATs involved in AG-detoxification are not constrained to any one form of genetic element and have been identified across Gram-negative and -positive bacteria of different environments. Outgroup sequences are for mycothiol synthases, MshD, with GenBank protein accession identifiers WP_003404307.1 and WP_012380250.1. Inner radial colour strip indicates if the sequence originates from an environmental or clinical sample. Outer radial colour strip indicates the confirmed regiospecificity of acetylation. Representative bacterial species are listed in bold or italics to indicate if the sequence is known to be chromosomally encoded or associated with mobile genetic elements.

The chromosomal genes *aac(6')-Ii*[49] and *aac(6')-Iy*[50] encode for isoforms of AAC(6')-I in *Enterococcus faecium* and *Salmonella enterica,* respectively. Biochemical investigations of these isozymes have laid the groundwork for understanding the molecular mechanisms of GNAT-mediated AG acetylation. AAC(6')-I isozymes have been the subject of rigorous steady-state kinetic analyses across broad AG and acyl-CoA panels to describe details of substrate specificity, catalytic activity, and chemical mechanism[26,47,50,51]. Elucidation of kinetic parameters found AAC(6')-Ii to be relatively inefficient as a detoxifying enzyme, with a correlation between k_{cat} (the rate at saturating levels of the antibiotic substrate) and minimal inhibitory concentration[26]. The *N*-acetylating activity of AAC(6')-Ii and -Iy was found to include histones in a discriminate manner[52,53]. There are several crystal structures available for clinically derived AAC(6')-I isozymes that have contributed to understanding substrate specificity[52] and in connection to the sequence diversity within this subgroup of GNATs[54]. At a molecular level, AAC(6')-I isoforms have undergone rigorous mechanistic investigations to learn which residues are critical for binding AGs or catalysis[50,55,56]. GNATs involved in AG-modification have been found to utilize different chemistries to facilitate acetylation[47,51]. Overall, these GNATs have been described to lack conserved residues involved in critical chemistries.

The combined efforts from these investigations informed the second generation semi-synthetic AG, plazomicin[6,57,58]. The naturally occurring AG sisomicin was used as a parent scaffold as the inherent unsaturation present in ring I provides protection from 4'-*O*-nucleotidyltransferases. The addition of an L-(γ)-amino-α-hydroxybutyryl chain to C1 renders the AG to the activity of AAC(3) enzymes. Protection from inactivation by AAC(6') enzymes is provided through the addition of a hydroxyethyl substituent at the 6' position[58].

AAC(2')

The subgroup of AAC(2') has been commonly recognized as chromosomally encoded *N*-2'-acetyltransferases universally found in *Providencia stuartii*[59-61] with more recent identifications made in *Mycobacteria*[24,25,62,63] and *Mycolicibacteria*[25,64]. GNATs classified as AAC(2')-I confer resistance towards disubstituted 2-deoxystreptamine subclasses of AGs containing an N2' group, including the second-generation semi-synthetic AG, plazomicin[58] **(Fig. 2)**. The *O*-acetylation of AGs, such as amikacin and kanamycin A, has been suggested by AAC(2')-Ic but the literature currently lacks supporting cell-based susceptibility assays to confirm the acetylating activities observed *in vitro* correlate to protection *in vivo*[24]. However, alternative substrates for AAC(2')-I isoforms have been identified. Peptidoglycan is readily *O*-acetylated by AAC(2')-Ia, with host AG-resistance under conditions where *aac(2')-Ia* is highly expressed[60,65]. Both acetyl-CoA and *N*-acetylglucosamine have been demonstrated to be accepted by AAC(2')-Ia as acetyl-donors in AG-modification[65]. These studies were the first conversations about the physiological roles these enzymes may serve for the host. Early kinetic analyses of AAC(2')-I isoforms, and later of AAC(6')-I isoforms, also included AG-susceptibility testing to investigate the relationships of *in vitro* activity and AG-resistance phenotypes. It's suggested that the primary roles these enzymes hold in secondary metabolism have been co-opted fortuitously to provide protection from antibiotics[61].

Mechanistic studies of AAC(2')-I isoforms subsided in the early 2000s[24,61,62]. The last of these studies generated several crystal structures of apo-AAC(2')-Ic as well as ternary complexes with co-enzyme A and either tobramycin, kanamycin A or ribostamycin. The structural and biochemical data obtained were compared with glucosamine-6-phosphate acetyltransferase to investigate the alternative physiological role of AAC(2')-Ic. The structures were the first detailed reports highlighting water-mediated interactions involved in AG-binding and possible role in the

chemical mechanism[62]. Crystallographic analysis of other AAC(2')-I ligand-bound complexes resumed upon report of plazomicin susceptibility[58]. The molecular determinants for plazomicin binding and other AG substrates have been explored in detail[64,66,67]. Structural analyses of other AAC(2')-I isoforms have also been completed with varying disubstituted AGs. These structures have increased our knowledge of the complex networks within the AG-binding pocket for these chromosomally encoded acetyltransferases. However, mutagenesis studies are still lacking to compare elements necessary for binding and underlying chemistries.

Albeit a less recognized AAC, AAC(2')-II is a subclass of N2' GNATs responsible for the acetylation of kasugamycin **(Fig. 2)**. Kasugamycin is an atypical AG, composed of a D-*chiro*-inositol moiety and a kasugamine moiety (2,4-diamino-2,3,4,6-tetradeoxy-D-arabino-hexose), containing a carboxy-imino-methyl group[68]. The lack of a 2-deoxystreptamine ring, directs kasugamycin to the mRNA-binding tunnel between the E- and P-sites of the 30S ribosomal subunit. Consequently, kasugamycin blocks the initiation of translation at different stages[69,70]. Kasugamycin is an agricultural control agent for fungal and bacterial pathogens in different crops. AAC(2')-IIa is responsible for kasugamycin resistance in isolates of the seed-borne rice pathogens, *Burkholderia glumae* and *Acidovorax avenae* subsp. *avenae*. The encoding gene, *aac(2')-IIa*, is mobilized on the IncP genomic island that can be inserted into the host chromosome[71] and IncP-1β plasmid pAAA83[72]. The isoform AAC(2')-IIb provides intrinsic kasugamycin resistance for *Paenibacillus sp. LC231*, a multi-drug resistant strain isolated from the pristine environment of Lechuguilla Cave[73]. Chromosomally encoded isoforms have also been identified from the kasugamycin producer, *Streptomyces kasugaensis*. Of the 23 putative proteins encoded within the biosynthetic gene cluster[74], *kasF* and *kasH*, have been recently verified to encode kasugamycin N2' acetyltransferases[75]. KasH, herein referred to as AAC(2')-IIc, is the primary determinant for

self-resistance against kasugamycin. The weak acetylating KasF *in vitro* does not correlate to resistance *in vivo*, leaving its purpose to be determined[75].

Although GNATs have been the subject of rigorous biochemical studies for several decades, the knowledge obtained primarily looks to what is currently circulating among priority pathogens[48,55,56,76]. Critical gaps in structural knowledge remains in each AAC subgroup[22], particularly for GNATs involved in AG biosynthesis[75]. Phylogenetic analysis has also been limited to AACs falling within the same regiospecificity subgroup[66,77]. The GNAT phylogeny presented in this chapter is based on all AAC subgroups, providing greater insight into the functional diversity of varying genetic backgrounds. The metagenomic AAC sequences identified in previous works[28] I show are putative AACs of varying regiospecificity and substrate specificity. Such sequences within the GNAT superfamily can be investigated further for the evolution or adaptation of physiological functions to confer AG resistance. The chapters presented in this thesis are how we can begin establishing these connections within different protein superfamilies of the AG resistome. The knowledge obtained through a genomic enzymology strategy can be leveraged in the identification of novel resistance mechanisms and subsequent surveillance.

Purpose and goals of thesis

The purpose of this thesis started as an investigation of resistance elements towards the atypical AG apramycin to aid in its development as a next-generation therapeutic. As I uncovered incredible structural and mechanistic diversity for modifying enzymes, this project widened to a genomic enzymology study of AACs within the AG resistome.

Genomic enzymology is an interdisciplinary strategy that incorporates genetic context and evolution into the paradigm of protein sequence-structure-function. The partnership of these concepts provides insight into the evolution of function within a protein superfamily. Such information is critical to inform next-generation antibiotic development, surveillance, and stewardship strategies in all settings.

In chapter 2, I present ligand-bound and apo-crystal structures of ApmA, publishing the first report of an LβH AAC involved in aminoglycoside detoxification. Through spectroscopic techniques, I show ApmA acetylates apramycin with a previously unreported regiospecificity to confer high-level resistance. Chapter 3 presents a comprehensive characterization of ApmA utilizing protein engineering, x-ray crystallography, steady-state kinetics, and antimicrobial susceptibility assays. I demonstrate that ApmA deviates from the chemical mechanism LβH's are well known for. These results highlight the liability of this resistance element to other AGs if it becomes clinically prevalent. I show ApmA confers broad-spectrum resistance and provide a detailed structural analysis to inform the development of next-generation scaffolds.

Chapter 4 incorporates bioinformatics with the approaches mentioned above to explore the diversity within the underestimated protein family of A_NATs. For this study, my contributions included the curation of clinical and environmentally derived A_NATs and completion of all antimicrobial susceptibility testing to map the function of encoded A_NATs to the phylogeny.

Chapter 5 will bring together the major findings presented and outline future directions for understanding the evolution of these functions in each protein family.

Chapter Two: ApmA is a unique aminoglycoside modifying enzyme

Preface

The work presented in the following chapter has been published in:

Bordeleau, E., Stogios, P. J., Evdokimova, E., Koteva, K., Savchenko, A., & Wright, G. D. (2021). ApmA is a unique aminoglycoside antibiotic acetyltransferase that inactivates apramycin. *Mbio*, 12(1), e02705-20.

E.B. and G.D.W. conceived the study and designed the experiments. E.B. completed all antimicrobial susceptibility testing and wrote the published manuscript. Purification of ApmA and acetylated apramycin was completed by E.B., K.K. completed spectroscopic characterization of acetylated apramycin. P.J.S. solved all crystal structures, wrote the manuscript and E.B. completed protein sequence and structural analysis. E.E. performed protein purification and crystallization. A.S. and G.D.W. oversaw the work and wrote the manuscript.

Abstract

Apramycin is an aminoglycoside antibiotic with the potential to be developed to combat multi-drug resistant pathogens. Its unique structure evades the clinically widespread mechanisms of aminoglycoside resistance that currently compromise the efficacy of other members in this drug class. Of the aminoglycoside-modifying enzymes that chemically alter these antibiotics, only AAC(3)-IVa has been demonstrated to confer resistance to apramycin through *N*-acetylation. Knowledge of other modification mechanisms is important to successfully develop apramycin for clinical use. Here, we show that ApmA is structurally unique among the previously described aminoglycoside-modifying enzymes and capable of conferring a high level of resistance to apramycin. *In vitro* experiments indicated ApmA to be an *N*-acetyltransferase, but in contrast to AAC(3)-IVa, ApmA has a unique regiospecificity of the acetyl transfer to the N2' position of apramycin. Crystallographic analysis of ApmA conclusively showed that this enzyme is an acetyltransferase from left-handed β helix protein superfamily (LβH) with a conserved active site architecture. The success of apramycin will be dependent on consideration of the impact of this potential form of clinical resistance.

Introduction

Waksman's tandem discoveries of streptomycin and neomycin over 65 years ago ushered in the clinical use of the aminoglycoside antibiotics (AGs) for the treatment of bacterial infections (1, 2). Since then, a variety of AGs have found clinical success. All AGs have a six-membered aminocyclitol core that serves to distinguish sub-families of the class. For example, the 4,6-deoxstreptamine antibiotics tobramycin, gentamicin, and amikacin are particularly effective against Gram negative pathogens. These antibiotics offer improved oto- and nephrotoxicity profiles over the 4,5-deoxstreptamine containing scaffolds such as neomycin (3, 4). Most AGs act through noncovalent binding to the small ribosomal subunit in a fashion that disrupts the proofreading property of translation (5). The result is subversion of the genetic code followed by the production of aberrant proteins and peptides, resulting in cell death.

Soon after the introduction of AGs in clinical practice, acquired resistance mediated by mobile genetic elements was reported (6). Over the past decades, a plethora of AG resistance genes have been identified, many of them moving through bacterial populations by lateral gene transfer (7). In addition to the upregulation of efflux systems and mutations in outer membrane porins occurring in some bacteria such as *Pseudomonas aeruginosa* (8), two general mechanisms of resistance dominate in pathogens, drug inactivation and target modification. Both mechanisms result in a decreased affinity of the AG for its ribosomal target (9, 10). Inactivation of AGs occurs via chemical modification by one of the following three classes of aminoglycoside-modifying enzymes (AMEs); *O*-phosphorylation (APHs), *O*-adenylylation (ANTs), or *N*-acetylation by aminoglycoside acetyltransferases (AACs) (11–13). Modification of the drug target is the most recent form of aminoglycoside resistance to emerge in the clinic (14). The 16S rRNA methyltransferases (RMTases) are responsible for the N7 methylation of G1405 (e.g., *Escherichia*

coli numbering; ArmA, Rmt family) or N1 methylation of A1408 (14, 15) (e.g., NpmA, KamB) within the 16S rRNA, respectively, conferring resistance to only 4,6-disubstituted or all 4,5- and 4,6-disubstituted AGs. RMTases are increasingly found in carbapenem-resistant isolates, greatly limiting therapeutic options for infections caused by these bacteria (16).

The broad mechanistic and genetic diversity of AG resistance impacts the use of existing drugs and dampens enthusiasm in the discovery of new members of this family of antibiotics, despite their highly desirable bactericidal activity toward Gram-positive and Gram-negative pathogens. In response to this challenge, the group at Achaogen embarked on an effort to deliver a next generation semi-synthetic AG that was not susceptible to common AMEs. The result of this effort is plazomicin (Zemdri) approved by the FDA in 2018, which retains antibiotic activity in the presence of most AMEs (17, 18). However, plazomicin remains ineffective against isolates coexpressing many RMTases, resistance genes that were not in significant circulation when the development program was launched (19). This fact emphasizes the potential for rapid dissemination of new resistance elements in the clinic that may move more rapidly through bacterial populations than the drug development process.

Apramycin is an unusual AG where the deoxystreptamine (DOS) aminocyclitol ring is monosubstituted and is linked to an octadiose element **(Figure 1)** (20). Apramycin has been used in veterinary medicine for decades but more recently has been found to exhibit broad activity against WHO prioritized multi-drug resistant (MDR) pathogens such as carbapenemase-producing Enterobacteriaceae and *Acinetobacter baumannii* (3, 21–24). The unique monosubstitution of apramycin's DOS ring prevents both inactivation by a majority of common AMEs and resistance due to target alteration by N7 RMTases (24). This characteristic makes apramycin particularly attractive as a candidate next-generation AG for clinical use in humans (25).

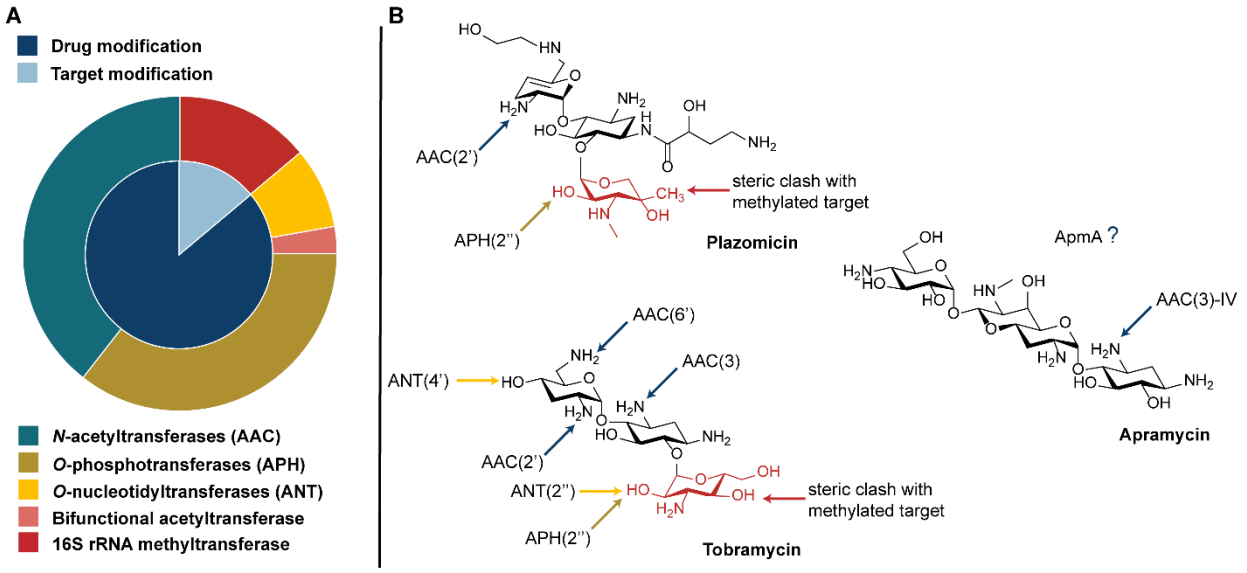

Figure 1. Apramycin's advantage to overcome aminoglycoside resistance in the clinic. (A) Aminoglycoside resistance elements explored in this study (Table S1, Figure S1). Inner circle represents the two main modes of aminoglycoside resistance: drug inactivation and target modification. Outer circle highlights the individual enzymes (Figure S1), coloured based on chemical modification made to the target or antibiotic. (B) Apramycin's unique monosubstitution of the DOS ring with the octadiose element limits the number of inactivating mechanisms. Lack of substitution at C6 allows avoidance of clinically relevant 16S rRNA methyltransferases.

Prior to the introduction of this antibiotic into the clinic, knowledge of the apramycin resistome is important. The *N*-acetyltransferase AAC(3)-IVa, a common selectable antibiotic resistance marker for molecular biology studies in actinomycetes, confers high level apramycin resistance and is occasionally found in clinical isolates of Enterobacteriaceae (26–28). AAC(1) has been reported to be associated with apramycin resistance; however, the sequence of this gene is unavailable and the original isolates lost (A. Lovering, personal communication) (29, 30). ApmA is another acetyltransferase linked to apramycin resistance. ApmA was first reported in 2011 from bovine and porcine methicillin-resistant *Staphylococcus aureus* (MRSA) isolates (31, 32). The gene was found as the sole resistance element on a smaller plasmid as well as a larger antimicrobial multiresistance plasmid that also contained heavy metal resistance genes and potential virulence elements (32, 33). AAC(3)-IVa adopts the structural fold for the more recently studied AAC(3)

enzymes belonging the Antibiotic_NAT family (PDB 6MN4). Primary sequence alignment suggests that ApmA does not share this three-dimensional structure. Given the growing interest in apramycin as a drug candidate we have investigated ApmA's activity towards apramycin and determined its three-dimensional structure. We identify ApmA as a member of the left-handed β-helix (LβH) superfamily, similar to chloramphenicol and streptogramin *O*-acetyltransferase resistance enzymes. This is the first report of an AG resistance element with this protein fold and reflects the diversity and enzymatic opportunism of antibiotic resistance.

Results

The apramycin resistome is limited to four known genes

The resistome of apramycin was evaluated through susceptibility testing against our in-house antibiotic resistance platform consisting of a panel of isogenic strains of *Escherichia coli* BW25113 Δ*tolC*Δ*bamB*, each expressing unique aminoglycoside resistance elements (34). Apramycin susceptibility was surveyed against 27 aminoglycoside resistance elements, consisting of 11 AACs, 11 APHs, 2 ANTs, and 4 RMTases. Gene expression levels were under the control of the constitutive promoter P_{bla}. A control strain not expressing an aminoglycoside resistance element was used as a reference for apramycin potency. We found only the four previously reported apramycin resistance elements to confer resistance **(Figure S1)**. The two N1-A1408-directed RMTases, NpmA and KamB, and the two acetyltransferases, AAC(3)-IVa and ApmA, each confer a high level of resistance to apramycin (≥ 64 μg/mL; **Table 1**). ApmA remains the only member of these apramycin resistance elements uncharacterized with respect to its structure and function.

Table 1. Apramycin resistance elements identified through susceptibility testing of *E. coli* BW25113 Δ*tolC*Δ*bamB* expressing aminoglycoside resistance enzymes.

Aminoglycoside resistance mechanism	Resistance gene	MIC (μg/mL) *E. coli* BW25113 Δ*tolC* Δ*bamB*
None	None	4
Drug modification	*aac(3)-IVa*	≥ 512
	apmA	64
Target modification	*kamB*	≥ 512
	npmA	≥ 512

ApmA acetylates apramycin at 2'-NH_2

Purified recombinant ApmA was used to produce acetylated apramycin *in vitro* to determine the regiospecificity of acetyl group transfer. Characterization of the acetylated product was carried out using high resolution electrospray ionization mass spectrometry (HR-ESI-MS), which revealed a single acetylation of the apramycin core (mass increase of 42.0 Da) (**Table 2**).

Table 2. HR-ESI-MS analysis of ApmA-catalyzed acetylated aminoglycosides in positive ion mode.

Modified Aminoglycoside	Molecular formula	Exact mass [M + H]	
		Calculated	Observed
apramycin	$C_{21}H_{42}N_5O_{11}$	540.2875	540.2891
N-acetyl apramycin	$C_{23}H_{45}N_5O_{12}$	582.2986	582.2989

Further characterization of the regiospecificity of acetyl transfer was accomplished using a combination of one- and two- dimensional nuclear magnetic resonance spectroscopy (1D and 2D NMR) of purified, ApmA-inactivated apramycin. **(Table S1, Figure S4-S8)** Acetyl apramycin NMR spectra were compared with those reported in the literature for the apramycin-free base (35). We noted significant deshielding of the 2' proton from 3.02 ppm in apramycin to 4.06 ppm in the acetylated product in the ^{1}H NMR. This change is a result of the effect of a carbonyl group attached to a neighboring atom (N2'). In the ^{13}C NMR, two new carbon shifts were observed at 21.8 ppm and at 172.89 ppm, corresponding to a methyl group carbon and carbonyl carbon chemical shifts. Lastly, heteronuclear multiple bond correlation spectra (HMBC) revealed correlations between the carbonyl carbon and methyl protons, as well as their correlation with the 2' proton. **(Figure 2)** These data are consistent with acetylation of apramycin by ApmA at the 2'-NH_2 of ring I.

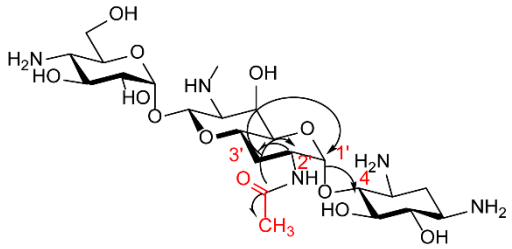

Figure 2. HMBC correlations. Correlations between carbonyl carbon of the acetyl group, methyl protons and 2' proton are indicated with the arrows.

ApmA is an *N*-acetyltransferase from the left-handed β helix protein superfamily

Primary sequence analysis of ApmA identified a seven-hexapeptide repeat motif, suggesting it is a member of the LβH superfamily of acetyltransferases that includes the xenobiotic acetyltransferases (XAT) subclass of LβHs, responsible for the inactivation of streptogramin group A antibiotics (36, 37) (Vat) and chloramphenicol (38, 39) (CATB). Crystals of the apoenzyme and ApmA in complex with apramycin or acetyl-CoA were obtained, and their structures solved to resolutions of 2.08 Å, 1.85 Å and 2.30 Å respectively **(Table S2)**. Analysis of these complexes showed ApmA to be a trimeric protein and confirmed it to be a member the LβH superfamily.

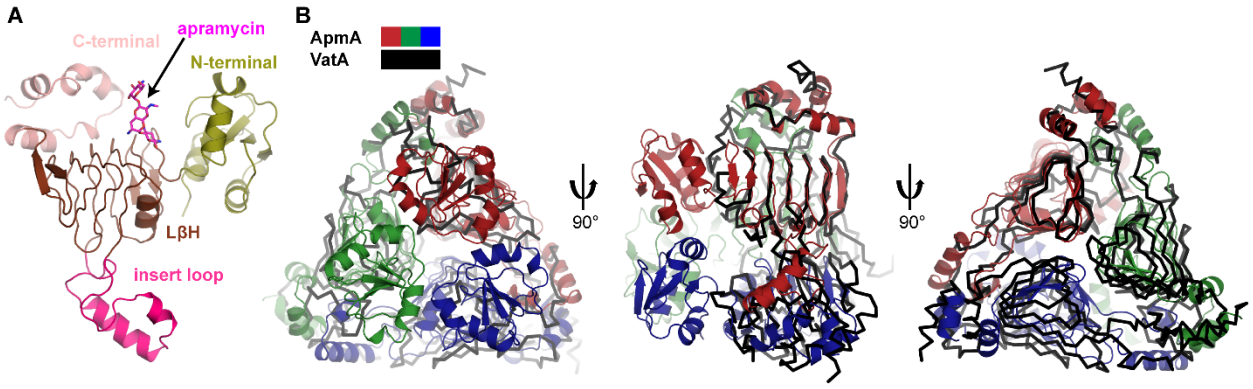

Figure 3. Structural comparison of ApmA to XAT subclass of LβH superfamily. (A) Domain architecture represented in ApmA monomer. (B) Structural superimposition of ApmA and VatA (PDB 4HUS) in complex with apramycin and virginiamycin respectively (substrates not shown). ApmA chains are coloured in red, blue and green, and VatA chains are all coloured in black.

The overall structure of ApmA is consistent with the canonical XAT architecture (36): it consists of a C-terminal region comprised of three α-helices (residues 232 to 274), a central LβH

domain where the hexapeptide motif is repeated seven times (residues 83 to 231) and an insert located in the center of the LβH fold, characterized by two α-helices (residues 132 to 176). Unlike other XATs, ApmA contains an additional N-terminal region, comprised of four β-sheets and two α-helices (residues 1 to 82). **(Figure 3A and 3B)** The LβH domains of three neighbouring chains together form a tunnel to shuttle the pantothenate arm of acetyl-CoA into the apramycin binding pocket. **(Figure 4A)** The N-terminal region appears to play a role in distorting the first two β-strands from the 7-stranded β-sheet of the LβH domain relative to their position in VatA and XAT (PDB 2XAT) **(Figure S2)**. These β-strands are twisted nearly 90° from their position in VatA and XAT and significantly alter the shape and volume of the substrate binding pocket **(Figure S2).**

Three acetyl-acceptor binding pockets were identified with the positioning of the central DOS ring consistent with other AMEs, which typically are lined with aspartate and glutamate residues (40). In the ApmA-apramycin complex, the N3 atom of the AG's aminocyclitol ring is coordinated by two aspartic acids (Asp144 and Asp145) in a helix within the C-terminal domain, and one glutamic acid (Glu85) positions the N1 atom. Ring III of apramycin interacts with several residues from one of the helices of the insert loop region of the LβH domain (Gln147, Gln159, and Tyr172). The 6'-OH of ring I interacts with N113 from within the LβH domain. **(Figure 4A & 4B) Consistent** with the NMR structure of 2'-acetyl-apramycin, we observed the 2'-NH_2 of the antibiotic positioned for acetylation.

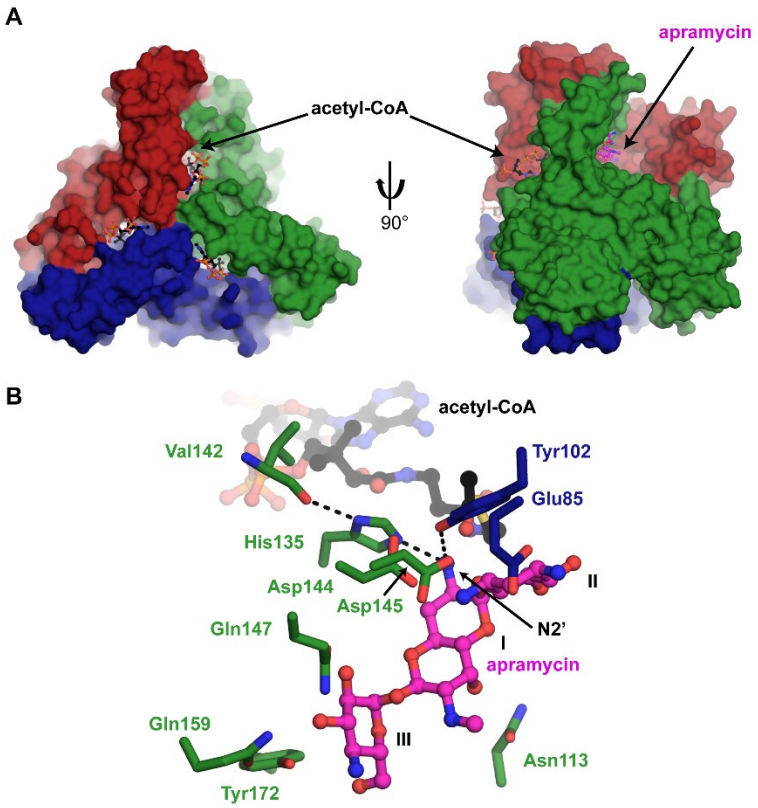

Figure 4. LβH domain creates a tunnel for acetyl-CoA binding. (A) Surface view of ApmA•acetyl-CoA complex superimposed on ApmA•apramycin complex. Chains are coloured red, green and blue. Apramycin and acetyl-CoA are shown in sticks. (B) Active site of superimposed ApmA substrate complexes highlighting residues suspected to be involved in apramycin binding and acetylation.

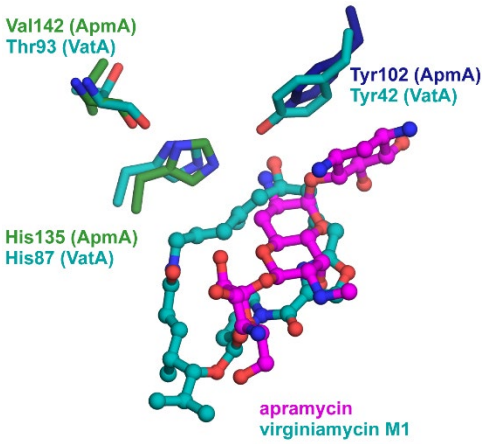

Figure 5. Superimposition of active site for VatA (PDB 4HUS) onto ApmA. Important catalytic residues for VatA and the equivalent residues found in ApmA are identified.

Upon superimposition of the two binary complexes (root mean square deviation [R.M.S.D], 0.29 Å), the 2'-NH_2 lies between 3.1 to 3.7 Å from the carbonyl carbon of the acetyl moiety. **(Figure 4B)** Tyr102 participates in a network of hydrogen bonds between the 2'NH_2 and Asp144 that may be important for antibiotic binding. The imidazole side chain from His135 is within 2.8 to 3.1 Å of apramycin's 2'-NH_2. Consistent with other XAT enzymes, the N1 of this imidazole is hydrogen bonded to a carbonyl of the peptide backbone (Val142). **(Figure 4B)** It is suspected that interaction increases the basicity of imidazole's N2 to help in a role as a general base (37, 38). Superimposition of ApmA with VatA, in complex with their antibiotic substrates, demonstrates that the His135 of ApmA is geometrically equivalent to the catalytic histidine for VatA (His87) (36). **(Figure 5)** Tyr102 of ApmA was also found in the same position of Tyr42 of VatA, a residue responsible for stabilizing the oxyanion intermediate for *O*-acetylation (36). To further assess the significance of His135 at the sequence level, we gathered reference sequences for Vats and CATBs from the Comprehensive Antibiotic Resistance Database (CARD) (41) to construct a multiple sequence alignment. Our analysis revealed that His135 of ApmA aligns with the conserved catalytic histidine found across all Vat and CATB sequences, essential for the *O*-acetylation of their respective substrates (36). **(Figure S3)** We next generated the alanine mutant of His135 to evaluate the impact of this substitution on ApmA's detoxification of apramycin through cell-based assays. Upon expression of the His135Ala mutant in *E. coli*, resistance to apramycin remained within 2-fold of when the wild-type enzyme was expressed (32 to 64 μg/mL). These results suggest the role of this histidine in the acetylation of apramycin does not hold the same significance as for the function of other XATs and requires further investigation.

Discussion

Apramycin's atypical structure in comparison with other AGs has garnered considerable attention for its potential as a next-generation AG antibiotic. The development of derivatives termed apralogs, has focused on retaining apramycin's low ototoxic potential while increasing potency coupled with evading resistance to apramycin through AAC(3)-IV-mediated modification (42, 43). Molecular modeling of 3-acetyl-apramycin bound to the ribosome indicates that reduced binding to the target results from a steric clash between the 16S rRNA phosphate backbone and the amide positioned at C3 of apramycin (24). We show that ApmA is an acetyltransferase that instead modifies apramycin at the N2' position of the octadiose element to confer high level drug resistance. However, N2' does not make direct contacts with the 16S rRNA and could spatially accommodate the acetyl group. We suggest that acetylation at this position reduces the affinity of the overall molecule for its target. The N2' participates in an intramolecular interaction with O5 of the 2-DOS ring. Intramolecular interactions between AG sugar rings have been suggested to play an important role in the recognition and binding of AGs to the 16S rRNA (44). The octadiose element of apramycin participates in important hydrogen bonds with A1408 of the 16S rRNA, creating a glycoside-adenine pseudo-base pair (43, 45, 46). Acetylation of N2' would disrupt the orientation of the 2-DOS and octadiose ring. The carbonyl would also have the potential to create new intramolecular interactions that alter the configuration of the molecule. Unfavourable intermolecular interactions would also be introduced if the carbonyl group approaches the negatively charged phosphate backbone, creating an electronic clash. Lastly, the overall charge of apramycin will be impacted by the replacement of the primary amine with an amide. The removal of the positively charged amine would further hinder its ability to interact with the negatively charged RNA. **(Figure 6)**

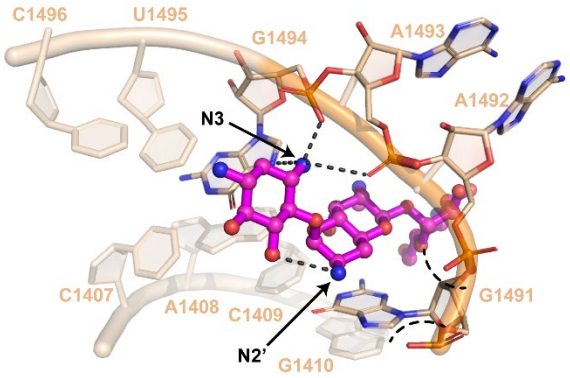

Figure 6. Impact of 2'-acetylation on ribosomal binding of apramycin. Crystal structure of apramycin bound to the ribosome (PDB 4AQY). Important interactions between N3 and the ribosome for recognition of the 2-DOS ring are indicated. Intramolecular interaction between N2' and O5 is highlighted. Acetylation at position N3 creates steric clash with the phosphate backbone. Acetylation of the N2' position is predicted to create an electronic clash with the negatively charged backbone of A1492 and G1491.

The regiospecificity of the acetyl transfer phenotypically assigns ApmA to the AAC(2') family of AMEs. However, unlike ApmA, AAC(2') enzymes are members of the GNAT superfamily (19) and found chromosomally encoded in *Providencia stuartii* and *Mycobacterium tuberculosis* (47, 48). Our analysis of AG resistance shows that AAC(2')-Ia from *P. stuartii* does not confer resistance toward apramycin, making ApmA the first AAC(2') enzyme documented to do so. Furthermore, initial reports of *apmA* found the sequence mobilized on plasmids from *Staphylococci* isolates from bovine and swine (31–33). The most recent report of the gene has also identified *apmA* in *Campylobacter* isolated from pork, demonstrating an expansion of host and crossover to Gram-negative pathogens (49).

The findings of this study highlight the adaptation of a common protein fold to generate new functions in antibiotic resistance. Concerns that other XAT enzymes capable of conferring resistance to other classes of antibiotics were discussed over 20 years ago (50). Antibiotic acetyltransferases are products of convergence of function, with CoA-dependent acetylation

spanning several protein scaffolds (39, 51–55). Our crystallographic data demonstrate ApmA belongs to the LβH superfamily of acetyltransferases, which had not previously been linked to the detoxification of AG antibiotics. The substrate specificity of the LβH scaffold has expanded to accommodate AGs, reminiscent of other sugar-containing substrates of LβH *N*-acetyltransferases involved in *O*-antigen biosynthesis (56, 57). Previously, XATs were observed to only *O*-acetylate their respective antibiotic substrates with the help of a conserved catalytic histidine. There are also LβH *N*-acetyltransferases that contain a histidine in the active site and have been shown to be important in the acetylation of their respective nucleotide-linked sugar substrates (56, 58). We show that the His135Ala ApmA mutant is still capable of *N*-acetylating apramycin to confer an equivalent level of resistance to when the wild-type protein is expressed. This suggests that the molecular mechanism of acetyl transfer is similar to that of the GCN5 family AAC(6') enzymes where no catalytic base is necessary. Here, acyl transfer occurs due to the alignment and proximity of acetyl-CoA and the nucleophilic receptor amine of the antibiotic (59). Overall, this work has the potential to aid in the identification of apralogs with reduced susceptibility to ApmA. Furthermore, the distribution of *apmA* should be monitored for the further transfer into clinical isolates. This unique AME threatens not only the success of apramycin's introduction into the clinic but may impact other AGs susceptible to its modification as well.

Methods

Bacterial strains and *apmA* cloning

apmA (Genbank ID: FN806789.3) was synthesized as a gBlock by Integrated DNA Technologies (IDT) for cloning into pGDP3(34) and pET19b-TEV using *Nde*I and *Xho*I restriction sites. The pET19b-TEV plasmid consists of an N-terminal His_{10}-tag cleavable by a tobacco etch virus protease (TEV). The pGDP3 construct of *apmA* was transformed into hyperpermeable, efflux-deficient mutant *E. coli* BW25113 Δ*tolC*Δ*bamB* (for antimicrobial susceptibility testing). Construct of pET19b-TEV:*apmA* was transformed into BL21(DE3)-Gold competent cells (for crystallography). All constructs were verified through Sanger sequencing at the Mobix sequencing facility, McMaster University.

Site-directed mutagenesis

Nucleotide substitutions (indicated by bold text in primers) were introduced in *apmA* with PCR site-directed mutagenesis by primer extension (60) using pGDP3:*apmA* as a template and the following mutagenic oligonucleotide primers to produce *apmA*:H135A.

Forward 5'-AGAGATCCATGCGAAC**GCT**CAGTTAAACATGACCTTTG-3'

Reverse 5'-AAGGTCATGTTTAACTG**AGC**GTTCGCATGGATCTCTG-3'.

The final construct was verified through Sanger sequencing at the Mobix sequencing facility, McMaster University.

Antimicrobial susceptibility testing

Screening against our in-house antibiotic resistance platform was carried out as previously described (34). Apramycin susceptibility testing of *E. coli* BW25113 Δ*tolC*Δ*bamB* expressing

apmA and *apmA*(H135A) was completed in triplicate following the Clinical and Laboratory Standards Institute (CLSI) protocols for the microbroth dilution method (61). Strains were cultured in cation-adjusted Mueller-Hinton broth (CAMHB) in a 96-well format. Plates were incubated in a shaking incubator at 37 °C for 18 hrs.

Protein expression and purification

For acetylated product characterization, *E. coli* BL21(DE3) Rosetta-gami pLysS transformed with pET19b-TEV constructs of *apmA* were grown in autoinduction medium supplemented with selection antibiotics for 3 days at 25 °C and 180 rpm. Cells were collected by centrifugation at 6400 x g, 4 °C and resuspended in binding buffer (25 mM HEPES [pH 7.5], 300 mM NaCl, 10 mM imidazole]. Resuspended cells were lysed using a continuous cell disrupter at 20,000 psi, 4 °C followed by centrifugation at 30,000 x g to remove cell debris. ApmA was purified from the lysate by nickel-nitrilotriacetic acid (Ni-NTA) affinity chromatography (Qiagen) at 4 °C. A 2 mL volume of Ni-NTA resin was pre-equilibrated with binding buffer and incubated with the lysate for 1 hr on ice prior to purification. The resin was washed with wash buffer (25 mM HEPES [pH 7.5], 300 mM NaCl, 25 mM imidazole) and proteins were eluted with a 4-step wise gradient (25 %, 50 %, 75 %, 100 %) of elution buffer (25 mM HEPES [pH 7.5], 300 mM NaCl, 250 mM imidazole). Elutions were dialyzed overnight against dialysis buffer (25 mM HEPES [pH 7.5], 300 mM NaCl). SDS-PAGE gel electrophoresis was performed to assess sample purity. To prepare stock solutions, concentrated ApmA was diluted to a final concentration ranging from 30 µM to 150 µM in dialysis buffer. Protein dilutions were flash frozen in liquid nitrogen and stored at – 80 °C.

For crystallography studies, native ApmA was expressed in gold competent *E. coli* BL21(DE3). A 3 mL overnight culture was diluted into 1 L of LB media containing selection antibiotics and grown at 37 °C, shaking. Expression of selenomethionine-derivatized ApmA was carried out in M9 minimal media following the manufacturer's instructions (Shanghai Medicilon). Expression was induced with isopropyl β-D-1-thiogalactopyranoside (IPTG) at 17 °C when OD_{600} reached 0.6−0.8. The overnight cell culture was then collected by centrifugation at 7000 x g. Cells were resuspended in binding buffer (100 mM HEPES [pH 7.5], 500 mM NaCl, 5 mM imidazole, and 5% glycerol [v/v]), lysed with a sonicator, and cell debris was removed by centrifugation at 30 000 x g. The cell lysate was loaded on a 4 mL Ni-NTA column (Qiagen) pre-equilibrated with 250 mL of binding buffer. The resin was washed with wash buffer (100 mM HEPES [pH 7.5], 500 mM NaCl, 30 mM imidazole, and 5% glycerol [v/v]), and the proteins were eluted with elution buffer (100 mM HEPES [pH 7.5], 500 mM NaCl, 250 mM imidazole, and 5% glycerol [v/v]). The His_{10}-tagged proteins were then subjected to overnight TEV cleavage using 50 μg of TEV protease per mg of His_{10}-tagged protein in binding buffer and dialyzed overnight against the binding buffer. The His_{10}-tag and TEV were removed by running the protein again over the Ni-NTA column. The tag-free proteins were dialyzed against dialysis buffer [50 mM HEPES (pH 7.5), 500 mM NaCl) overnight, and the purity of the protein was analyzed by SDS-polyacrylamide gel electrophoresis.

Spectroscopic characterization of ApmA catalyzed acetylated apramycin

ApmA catalyzed acetylated apramycin was produced from 50 mL *in vitro* reactions (50 mM HEPES, pH 7.5) consisting of 500 μM aminoglycoside, 500 μM acetyl-CoA and 1 μM ApmA. Reactions were incubated at room temperature until acetylated products (mass increase of 42.0 Da) were detected by LC/ESI-MS. Enzymes were removed by centrifugation using an Amicon

Ultra-15 Centrifugal Filter and the flow-through subsequently concentrated. Acetyl-apramycin was purified from the concentrate using AG50W-X8 strong cation resin. The resin was pre-equilibrated with 1 % NH_4OH and washed with H_2O until a neutral pH was obtained. Fractions containing acetylated products were identified by LC/ESI-MS, followed by detailed analysis with NMR and HR-ESI-MS. LC/ESI-MS data was acquired using a QTRAP 2000 (Applied Biosystems) system equipped with an Agilent 1100 LC interface. HR-ESI-MS data was acquired using an Agilent 1290 UPLC separation module and qTOF G6550A mass detector in positive ion mode. NMR analysis was completed using a Bruker AVIII 700 MHz instrument in deuterated water as the solvent. The chemical shifts are reported in parts per million (ppm).

Crystallization and structure determination

All crystals were grown at room temperature using the vapor diffusion sitting drop method with 0.5 µL of protein solution mixed with 0.5 µL of reservoir solution. Crystals were grown using the following reservoir solutions: ApmA•apramycin complex (0.2 M CaCl, 20% PEG 3350, 5 mM apramycin) and ApmA•acetyl-CoA complex (0.1 M citric acid pH 3.6, 30% PEG 200, 5 mM apramycin, 2mM acetyl-CoA). All crystals were cryoprotected with Paratone-N or ethylene glycol and then flash-frozen in liquid nitrogen prior to diffraction data collection. Diffraction data were collected at the Advanced Photon Source, Argonne National Laboratory, beamlines 19-ID or 21-ID. All data were processed by HKL-3000. The ApmA•apramycin structure was solved using the single anomalous diffraction (SAD) method, and this was used to solve all additional complexes by MR. Structure refinement was performed using Phenix.refine plus manual building with Coot. The presence of substrate molecules was identified by building into the Fo − Fc difference density after the initial rounds of refinement.

689 **Sequence and structural analysis**

690 PyMOL (62) was used to identify potential interacting residues (≤ 4.0 Å in distance) of
691 ApmA with substrates apramycin and acetyl-CoA. Structural superimpositions with VatA (4HUS)
692 were constructed using the cealign function in PyMol. XAT representative sequences were
693 obtained from the CARD (41). ApmA and Vat sequences were aligned with the Expresso (63–65)
694 function of T-COFFEE (66, 67) to build a profile hidden Markov model (HMMER 3.3.1) (68). All
695 sequences were aligned with the resulting HMM profile and visualized using Jalview (69).

696

697 **Data availability statement**

698 PDB validation reports for crystal structures obtained in this study have been submitted
699 with the manuscript. Accession numbers are as follows: 7JM0 (ApmA apoenzyme), 7JM1 (ApmA
700 complex with acetyl-CoA), 7JM2 (ApmA complex with apramycin).

701

Acknowledgements

We thank Zdzislaw Wawrzak, Life Sciences Collaborative Access Team, Advanced Photon Source, Argonne National Laboratory for diffraction data collection. Crystal structures solved in this work were funded in whole or in part with U.S. Federal funds from the National Institute of Allergy and Infectious Diseases, National Institutes of Health, Department of Health and Human Services, under Contract No. HHSN272201700060C (Center for Structural Genomics of Infectious Diseases (CSGID, http://csgid.org). This research was funded by a Canadian Institutes of Health Research grant (FRN-148463), the Ontario Research Fund, and by a Canada Research Chair to G.D.W.

References

1. Schatz A, Bugle E, Waksman SA. 1944. Streptomycin, a substance exhibiting antibiotic activity against gram-positive and gram-negative bacteria.*. Exp Biol Med 55:66–69.

2. Waksman SA, Lechevalier HA. 1949. Neomycin, a new antibiotic active against streptomycin-resistant bacteria, including tuberculosis organisms. Science. 109:305–307.

3. Hu Y, Liu L, Zhang X, Feng Y, Zong Z. 2017. *In vitro* activity of neomycin, streptomycin, paromomycin and apramycin against carbapenem-resistant *Enterobacteriaceae* clinical strains. Front Microbiol 8:1–7.

4. Hobbie SN, Akshay S, Kalapala SK, Bruell CM, Shcherbakov D, Bottger EC. 2008. Genetic analysis of interactions with eukaryotic rRNA identify the mitoribosome as target in aminoglycoside ototoxicity. Proc Natl Acad Sci 105:20888–20893.

5. Davies J, Gorini L, Davis BD. 1965. Misreading of RNA codewords induced by aminoglycoside antibiotics. Mol Pharmacol 1:93–106.

6. Davies J. 1995. Vicious circles: looking back on resistance plasmids. Genetics 139:1465–8.

7. Courvalin P. 1994. Transfer of antibiotic resistance genes between gram-positive and gram-negative bacteria. Antimicrob Agents Chemother 38:1447–1451.

8. Pang Z, Raudonis R, Glick BR, Lin T-J, Cheng Z. 2019. Antibiotic resistance in *Pseudomonas aeruginosa*: mechanisms and alternative therapeutic strategies. Biotechnol Adv 37:177–192.

9. Davies J, Wright GD. 1997. Bacterial resistance to aminoglycoside antibiotics. Trends Microbiol 5:234–240.

10. Schaenzer AJ, Wright GD. 2020. Antibiotic resistance by enzymatic modification of antibiotic targets. Trends Mol Med 26:768–782.

11. Ramirez MS, Tolmasky ME. 2010. Aminoglycoside modifying enzymes. Drug Resist Updat 13:151–171.

12. Shaw KJ, Rather PN, Hare RS, Miller GH. 1993. Molecular genetics of aminoglycoside resistance genes and familial relationships of the aminoglycoside-modifying enzymes. Microbiol Rev 57:138–163.

13. Wright GD. 1999. Aminoglycoside-modifying enzymes. Curr Opin Microbiol 2:499–503.

14. Wachino J, Shibayama K, Kurokawa H, Kimura K, Yamane K, Suzuki S, Shibata N, Ike Y, Arakawa Y. 2007. Novel plasmid-mediated 16S rRNA m1A1408 methyltransferase, NpmA, found in a clinically isolated *Escherichia coli* strain resistant to structurally diverse

aminoglycosides. Antimicrob Agents Chemother 51:4401–4409.

15. Macmaster R, Zelinskaya N, Savic M, Rankin CR, Conn GL. 2010. Structural insights into the function of aminoglycoside-resistance A1408 16S rRNA methyltransferases from antibiotic-producing and human pathogenic bacteria. Nucleic Acids Res 38:7791–7799.

16. Wachino J, Arakawa Y. 2012. Exogenously acquired 16S rRNA methyltransferases found in aminoglycoside-resistant pathogenic gram-negative bacteria: An update. Drug Resist Updat 15:133–148.

17. Aggen JB, Armstrong ES, Goldblum AA, Dozzo P, Linsell MS, Gliedt MJ, Hildebrandt DJ, Feeney LA, Kubo A, Matias RD, Lopez S, Gomez M, Wlasichuk KB, Diokno R, Miller GH, Moser HE. 2010. Synthesis and spectrum of the neoglycoside ACHN-490. Antimicrob Agents Chemother 54:4636–4642.

18. Armstrong ES, Miller GH. 2010. Combating evolution with intelligent design: the neoglycoside ACHN-490. Curr Opin Microbiol 13:565–573.

19. Cox G, Ejim L, Stogios PJ, Koteva K, Bordeleau E, Evdokimova E, Sieron AO, Savchenko A, Serio AW, Krause KM, Wright GD. 2018. Plazomicin retains antibiotic activity against most aminoglycoside modifying enzymes. ACS Infect Dis 4:980–987.

20. O'Connor S, Lam LKT, Jones ND, Chaney MO. 1976. Apramycin, a unique aminocyclitol antibiotic. J Org Chem 41:2087–2092.

21. Kang AD, Smith KP, Eliopoulos GM, Berg AH, McCoy C, Kirby JE. 2017. *In vitro* apramycin activity against multidrug-resistant *Acinetobacter baumannii* and *Pseudomonas aeruginosa*. Diagn Microbiol Infect Dis 88:188–191.

22. Meyer M, Freihofer P, Scherman M, Teague J, Lenaerts A, Böttger EC. 2014. *In vivo* efficacy of apramycin in murine infection models. Antimicrob Agents Chemother 58:6938–6941.

23. Hao M, Shi X, Lv J, Niu S, Cheng S, Du H, Yu F, Tang Y-W, Kreiswirth BN, Zhang H, Chen L. 2020. *In vitro* activity of apramycin against carbapenem-resistant and hypervirulent *Klebsiella pneumoniae* isolates. Front Microbiol 11:1–7.

24. Juhas M, Widlake E, Teo J, Huseby DL, Tyrrell JM, Polikanov YS, Ercan O, Petersson A, Cao S, Aboklaish AF, Rominski A, Crich D, Böttger EC, Walsh TR, Hughes D, Hobbie SN. 2019. *In vitro* activity of apramycin against multidrug-, carbapenem- and aminoglycoside-resistant *Enterobacteriaceae* and *Acinetobacter baumannii*. J Antimicrob Chemother 74:944–952.

25. Böttger EC, Crich D. 2020. Aminoglycosides: time for the resurrection of a neglected class of antibacterials? ACS Infect Dis 6:168–172.

780 26. Chaslus-Dancla E, Glupczynski Y, Gerbaud G, Lagorce M, Lafont JP, Courvalin P. 1989.
781 Detection of apramycin resistant *Enterobacteriaceae* in hospital isolates. FEMS Microbiol
782 Lett 61:261–265.

783 27. Magalhaes MLB, Blanchard JS. 2005. The kinetic mechanism of AAC(3)-IV
784 aminoglycoside acetyltransferase from *Escherichia coli* †. Biochemistry 44:16275–16283.

785 28. Davies J, O'Connor S. 1978. Enzymatic modification of aminoglycoside antibiotics: 3-*N*-
786 acetyltransferase with broad specificity that determines resistance to the novel
787 aminoglycoside apramycin. Antimicrob Agents Chemother 14:69–72.

788 29. Lovering AM, White LO, Reeves DS. 1987. AAC(1): a new aminoglycoside-acetylating
789 enzyme modifying the Cl aminogroup of apramycin. J Antimicrob Chemother 20:803–813.

790 30. Hedges RW, Shannon KP. 1984. Resistance to apramycin in *Escherichia coli* isolated from
791 animals: detection of a novel aminoglycoside-modifying enzyme. Microbiology 130:473–
792 482.

793 31. Feßler AT, Kadlec K, Schwarz S. 2011. Novel apramycin resistance gene *apmA* in bovine
794 and porcine methicillin-resistant *Staphylococcus aureus* ST398 isolates. Antimicrob Agents
795 Chemother 55:373–375.

796 32. Kadlec K, Feßler AT, Couto N, Pomba CF, Schwarz S. 2012. Unusual small plasmids
797 carrying the novel resistance genes *dfrK* or *apmA* isolated from methicillin-resistant or -
798 susceptible staphylococci. J Antimicrob Chemother 67:2342–2345.

799 33. Feßler AT, Zhao Q, Schoenfelder S, Kadlec K, Brenner Michael G, Wang Y, Ziebuhr W,
800 Shen J, Schwarz S. 2017. Complete sequence of a plasmid from a bovine methicillin-
801 resistant *Staphylococcus aureus* harbouring a novel *ica*-like gene cluster in addition to
802 antimicrobial and heavy metal resistance genes. Vet Microbiol 200:95–100.

803 34. Cox G, Sieron A, King AM, De Pascale G, Pawlowski AC, Koteva K, Wright GD. 2017. A
804 common platform for antibiotic dereplication and adjuvant discovery. Cell Chem Biol
805 24:98–109.

806 35. Eneva GI, Spassov SL, Haimova MA, Sandström J. 1992. Complete 1H and 13C NMR
807 assignments for apramycin, sisomicin and some N- and N,O-polyacetylated
808 aminoglycosides. Magn Reson Chem 30:841–846.

809 36. Stogios PJ, Kuhn ML, Evdokimova E, Courvalin P, Anderson WF, Savchenko A. 2014.
810 Potential for reduction of streptogramin A resistance revealed by structural analysis of
811 acetyltransferase VatA. Antimicrob Agents Chemother 58:7083–7092.

812 37. Sugantino M, Roderick SL. 2002. Crystal structure of Vat(D): an acetyltransferase that
813 inactivates streptogramin group A antibiotics † , ‡. Biochemistry 41:2209–2216.

38. Beaman TW, Sugantino M, Roderick SL. 1998. Structure of the hexapeptide xenobiotic acetyltransferase from *Pseudomonas aeruginosa*. Biochemistry 37:6689–6696.

39. White PA, Stokes H., Bunny KL, Hall RM. 1999. Characterisation of a chloramphenicol acetyltransferase determinant found in the chromosome of *Pseudomonas aeruginosa*. FEMS Microbiol Lett 175:27–35.

40. Bassenden A V., Rodionov D, Shi K, Berghuis AM. 2016. Structural analysis of the tobramycin and gentamicin clinical resistome reveals limitations for next-generation aminoglycoside design. ACS Chem Biol 11:1339–1346.

41. Alcock BP, Raphenya AR, Lau TT, Tsang KK, Bouchard M, Edalatmand A, Huynh W, Nguyen AL V., Cheng AA, Liu S, Min SY, Miroshnichenko A, Tran HK, Werfalli RE, Nasir JA, Oloni M, Speicher DJ, Florescu A, Singh B, Faltyn M, Hernandez-Koutoucheva A, Sharma AN, Bordeleau E, Pawlowski AC, Zubyk HL, Dooley D, Griffiths E, Maguire F, Winsor GL, Beiko RG, Brinkman FS, Hsiao WW, Domselaar G V, McArthur AG. 2020. CARD 2020: antibiotic resistome surveillance with the comprehensive antibiotic resistance database. Nucleic Acids Res 48:D517–D525.

42. Quirke JCK, Rajasekaran P, Sarpe VA, Sonousi A, Osinnii I, Gysin M, Haldimann K, Fang Q-J, Shcherbakov D, Hobbie SN, Sha S-H, Schacht J, Vasella A, Böttger EC, Crich D. 2020. Apralogs: apramycin 5-O-glycosides and ethers with improved antibacterial activity and ribosomal selectivity and reduced susceptibility to the aminoacyltransferase (3)-IV resistance determinant. J Am Chem Soc 142:530–544.

43. Matt T, Ng CL, Lang K, Sha S-H, Akbergenov R, Shcherbakov D, Meyer M, Duscha S, Xie J, Dubbaka SR, Perez-Fernandez D, Vasella A, Ramakrishnan V, Schacht J, Bottger EC. 2012. Dissociation of antibacterial activity and aminoglycoside ototoxicity in the 4-monosubstituted 2-deoxystreptamine apramycin. Proc Natl Acad Sci 109:10984–10989.

44. Vicens Q, Westhof E. 2003. RNA as a drug target: the case of aminoglycosides. ChemBioChem 4:1018–1023.

45. Han Q, Zhao Q, Fish S, Simonsen KB, Vourloumis D, Froelich JM, Wall D, Hermann T. 2005. Molecular recognition by glycoside pseudo base pairs and triples in an apramycin-RNA complex. Angew Chemie Int Ed 44:2694–2700.

46. Pfister P, Hobbie S, Vicens Q, Böttger EC, Westhof E. 2003. The molecular basis for A-site mutations conferring aminoglycoside resistance: relationship between ribosomal susceptibility and x-ray crystal structures. ChemBioChem 4:1078–1088.

47. Swiatlo E, Kocka FE. 1987. Inducible expression of an aminoglycoside-acetylating enzyme in *Providencia stuartii*. J Antimicrob Chemother 19:27–30.

48. Hegde SS, Javid-Majd F, Blanchard JS. 2001. Overexpression and mechanistic analysis of

chromosomally encoded aminoglycoside 2′-*N*-acetyltransferase (AAC(2′)-Ic) from *Mycobacterium tuberculosis*. J Biol Chem 276:45876–45881.

49. Fabre A, Oleastro M, Nunes A, Santos A, Sifré E, Ducournau A, Bénéjat L, Buissonnière A, Floch P, Mégraud F, Dubois V, Lehours P. 2018. Whole-genome sequence analysis of multidrug-resistant *Campylobacter* isolates: a focus on aminoglycoside resistance determinants. J Clin Microbiol 56:1–12.

50. Murray IA, Shaw W V. 1997. *O*-Acetyltransferases for chloramphenicol and other natural products. Antimicrob Agents Chemother 41:1–6.

51. Wybenga-Groot LE, Draker K ann, Wright GD, Berghuis AM. 1999. Crystal structure of an aminoglycoside 6'-*N*-acetyltransferase: defining the GCN5-related *N*-acetyltransferase superfamily fold. Structure 7:497–507.

52. Stogios PJ, Kuhn ML, Evdokimova E, Law M, Courvalin P, Savchenko A. 2017. Structural and biochemical characterization of *Acinetobacter* spp. aminoglycoside acetyltransferases highlights functional and evolutionary variation among antibiotic resistance enzymes. ACS Infect Dis 3:132–143.

53. Biswas T, Houghton JL, Garneau-Tsodikova S, Tsodikov O V. 2012. The structural basis for substrate versatility of chloramphenicol acetyltransferase CAT I. Protein Sci 21:520–530.

54. Morar M, Wright GD. 2010. The genomic enzymology of antibiotic resistance. Annu Rev Genet 44:25–51.

55. Xu Z, Stogios PJ, Quaile AT, Forsberg KJ, Patel S, Skarina T, Houliston S, Arrowsmith C, Dantas G, Savchenko A. 2017. Structural and functional survey of environmental aminoglycoside acetyltransferases reveals functionality of resistance enzymes. ACS Infect Dis 3:653–665.

56. Thoden JB, Reinhardt LA, Cook PD, Menden P, Cleland WW, Holden HM. 2012. Catalytic mechanism of perosamine *N*-acetyltransferase revealed by high-resolution x-ray crystallographic studies and kinetic analyses. Biochemistry 51:3433–3444.

57. Thoden JB, Cook PD, Schäffer C, Messner P, Holden HM. 2009. Structural and functional studies of QdtC: an *N*-acetyltransferase required for the biosynthesis of dTDP-3-acetamido-3,6-dideoxy-α- d-glucose † ‡. Biochemistry 48:2699–2709.

58. Craggs PD, Mouilleron S, Rejzek M, De Chiara C, Young RJ, Field RA, Argyrou A, De Carvalho LPS. 2018. The mechanism of acetyl transfer catalyzed by *Mycobacterium tuberculosis* GlmU. Biochemistry 57:3387–3401.

59. Draker K, Wright GD. 2004. Molecular mechanism of the *Enterococcal* aminoglycoside 6'-*N*-acetyltransferase': role of GNAT-conserved residues in the chemistry of antibiotic

inactivation †. Biochemistry 43:446–454.

60. Ho SN, Hunt HD, Horton RM, Pullen JK, Pease LR. 1989. Site-directed mutagenesis by overlap extension using the polymerase chain reaction. Gene 77:51–59.

61. CLSI. 2018. M07-A10: Methods for dilution antimicrobial susceptibility tests for bacteria that grow aerobically, 11th edition.

62. Delano WL. 2002. The PyMOL molecular graphics system. DeLano Scientific.

63. Armougom F, Moretti S, Poirot O, Audic S, Dumas P, Schaeli B, Keduas V, Notredame C. 2006. Expresso: automatic incorporation of structural information in multiple sequence alignments using 3D-Coffee. Nucleic Acids Res 34.

64. O'Sullivan O, Suhre K, Abergel C, Higgins DG, Notredame C. 2004. 3DCoffee: combining protein sequences and structures within multiple sequence alignments. J Mol Biol 340:385–395.

65. Poirot O, Suhre K, Abergel C, O'Toole E, Notredame C. 2004. 3DCoffee@igs: a web server for combining sequences and structures into a multiple sequence alignment. Nucleic Acids Res 32:W37–W40.

66. Di Tommaso P, Moretti S, Xenarios I, Orobitg M, Montanyola A, Chang J-M, Taly J-F, Notredame C. 2011. T-Coffee: a web server for the multiple sequence alignment of protein and RNA sequences using structural information and homology extension. Nucleic Acids Res 39:W13–W17.

67. Notredame C, Higgins DG, Heringa J. 2000. T-coffee: a novel method for fast and accurate multiple sequence alignment. J Mol Biol 302:205–217.

68. Eddy SR. 2020. HMMER v3.3.1 - biological sequence analysis using profile hidden Markov models.

69. Waterhouse AM, Procter JB, Martin DMA, Clamp M, Barton GJ. 2009. Jalview Version 2-a multiple sequence alignment editor and analysis workbench. Bioinformatics 25:1189–1191.

Supplementary information

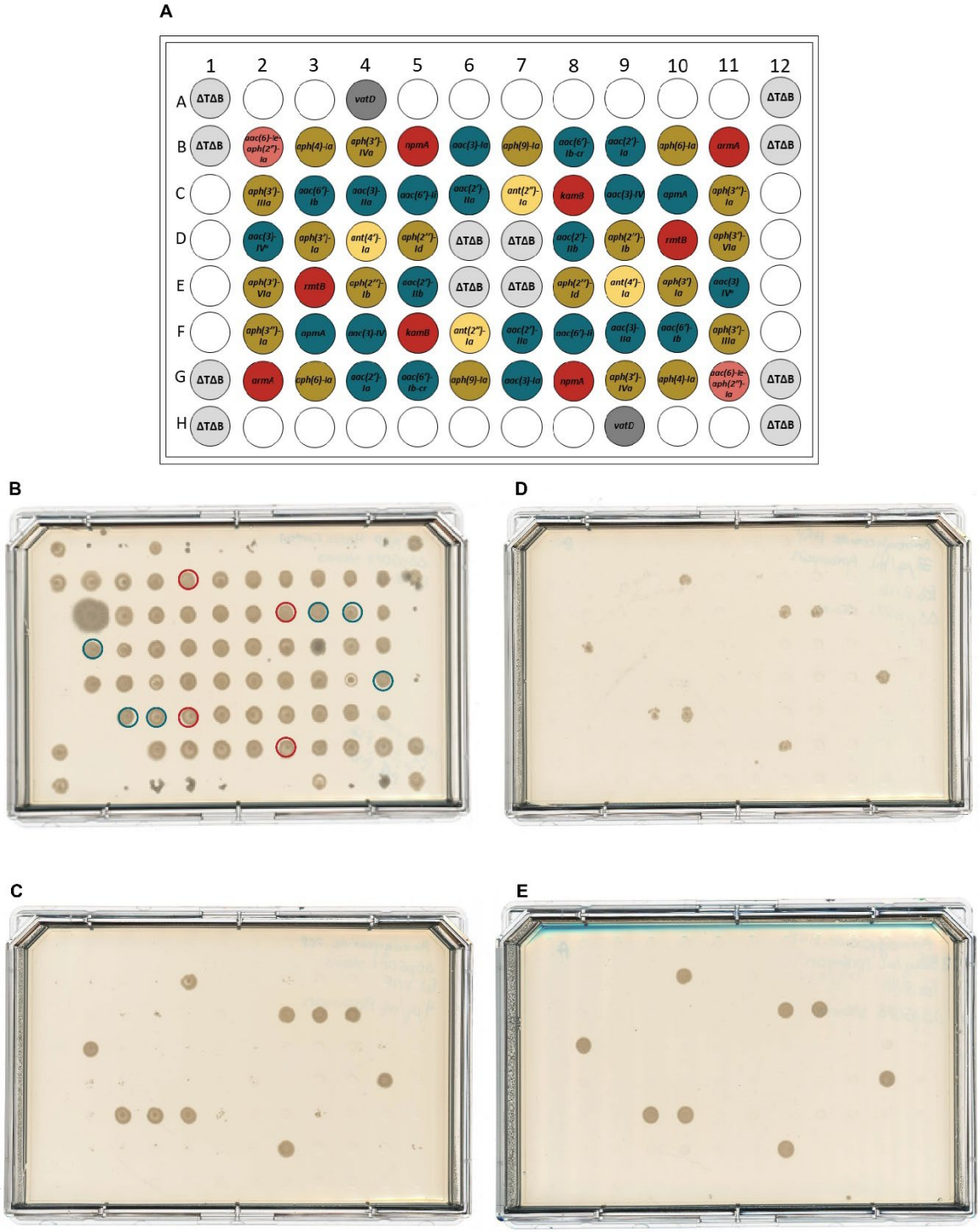

Figure S1. Apramycin resistance elements identified while screening within the aminoglycoside resistance library expressed in *E. coli* BW25113 Δ*tolC*Δ*bamB*. (A) Aminoglycoside resistance glycerol library layout. Color legend; *N*-acetyltransferase (blue), *O*-phosphotransferase (gold), *O*-nucleotidyltransferase (yellow), bifunctional acetyltransferase

(pink), 16S rRNA methyltransferase (red). Each gene was under the control of the P_{Bla} promoter. (B) Control growth of library on cation adjusted Mueller Hinton agar supplemented with no drug. Colony growth highlighted with a circle were those found to confer apramycin resistance. (C) 4 µg/mL apramycin (D) 32 µg/mL apramycin (E) 256 µg/mL apramycin.

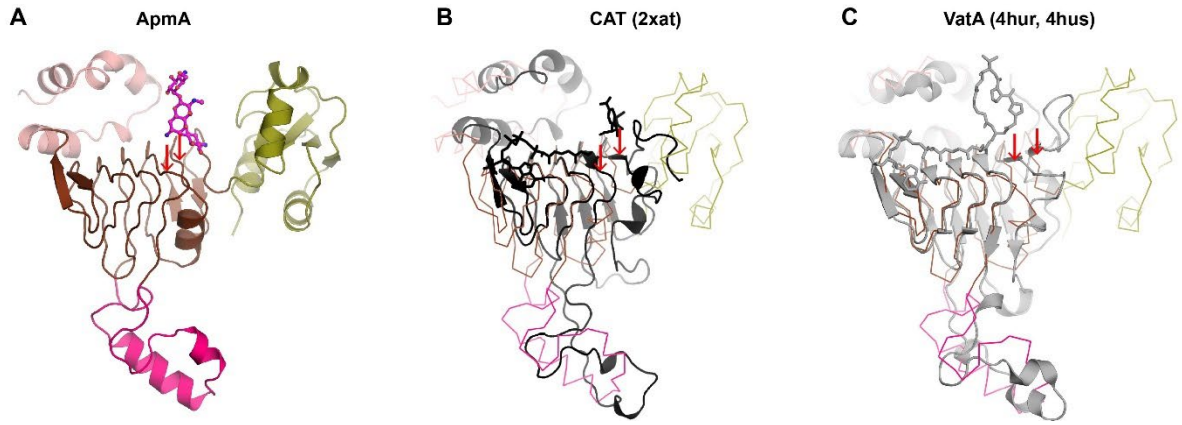

Figure S2. Impact of the N-terminal region on the substrate binding pocket of ApmA. Red arrows indicate the first two β-strands from the 7-stranded β-sheet of the LβH domain. (A) Superimpositions of ApmA in complex with apramycin (B) CAT (C) VatA.

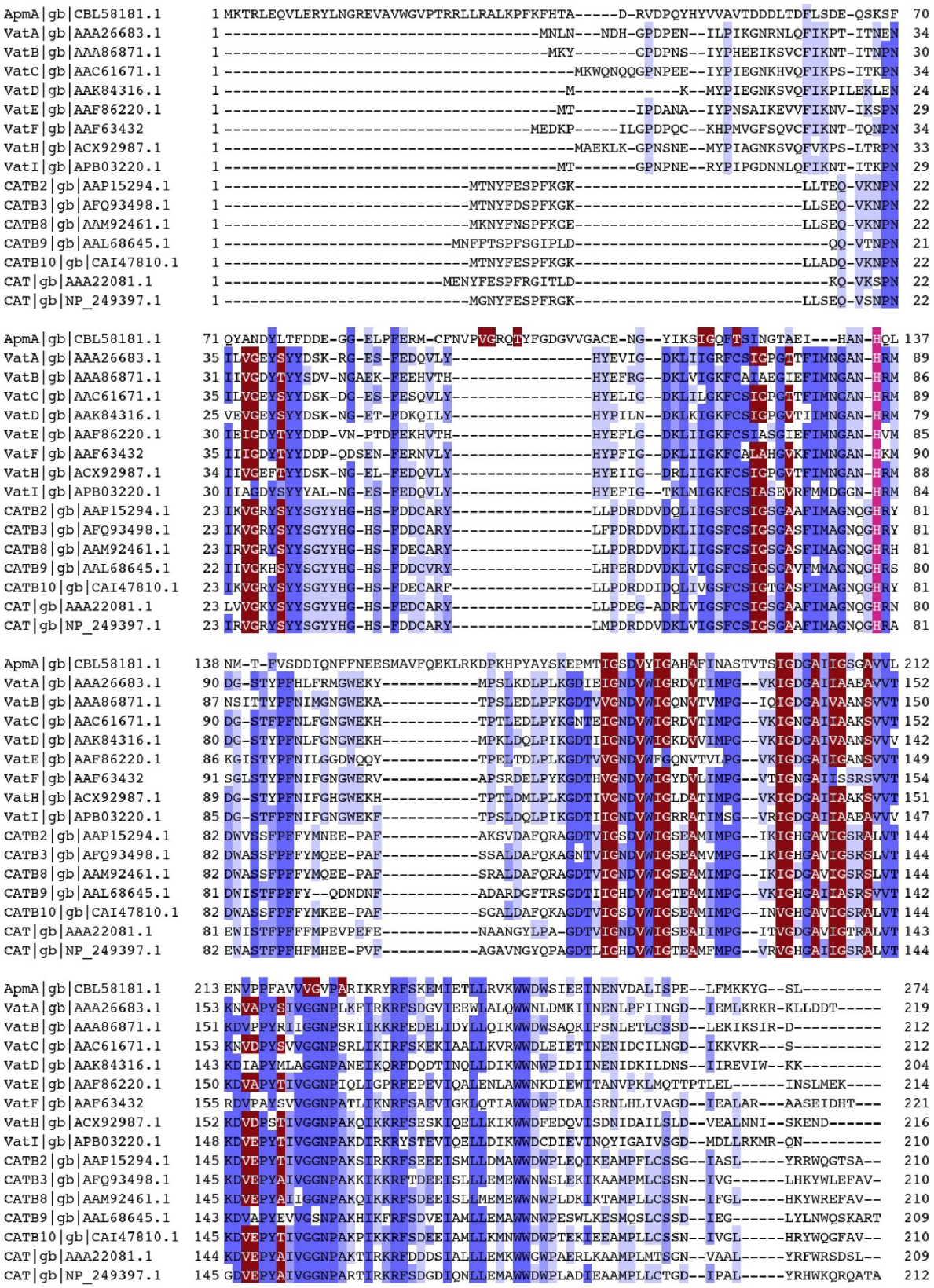
ApmA|gb|CBL58181.1
VatA|gb|AAA26683.1
VatB|gb|AAA86871.1
VatC|gb|AAC61671.1
VatD|gb|AAK84316.1
VatE|gb|AAF86220.1
VatF|gb|AAF63432
VatH|gb|ACX92987.1
VatI|gb|APB03220.1
CATB2|gb|AAP15294.1
CATB3|gb|AFQ93498.1
CATB8|gb|AAM92461.1
CATB9|gb|AAL68645.1
CATB10|gb|CAI47810.1
CAT|gb|AAA22081.1
CAT|gb|NP_249397.1

931 **Figure S3. Sequence relationship of ApmA to the LβH superfamily.** Full multiple sequence
932 alignment of ApmA with CATs and Vats obtained from the Comprehensive Antibiotic Resistance
933 Database. Amino acids are coloured based on percent identity. Traditional hexapeptide motif (i,
934 i+1 and i+4) of the LβH domain is highlighted in red. Conserved catalytic histidine of the XAT
935 subclass is highlighted in pink.

936

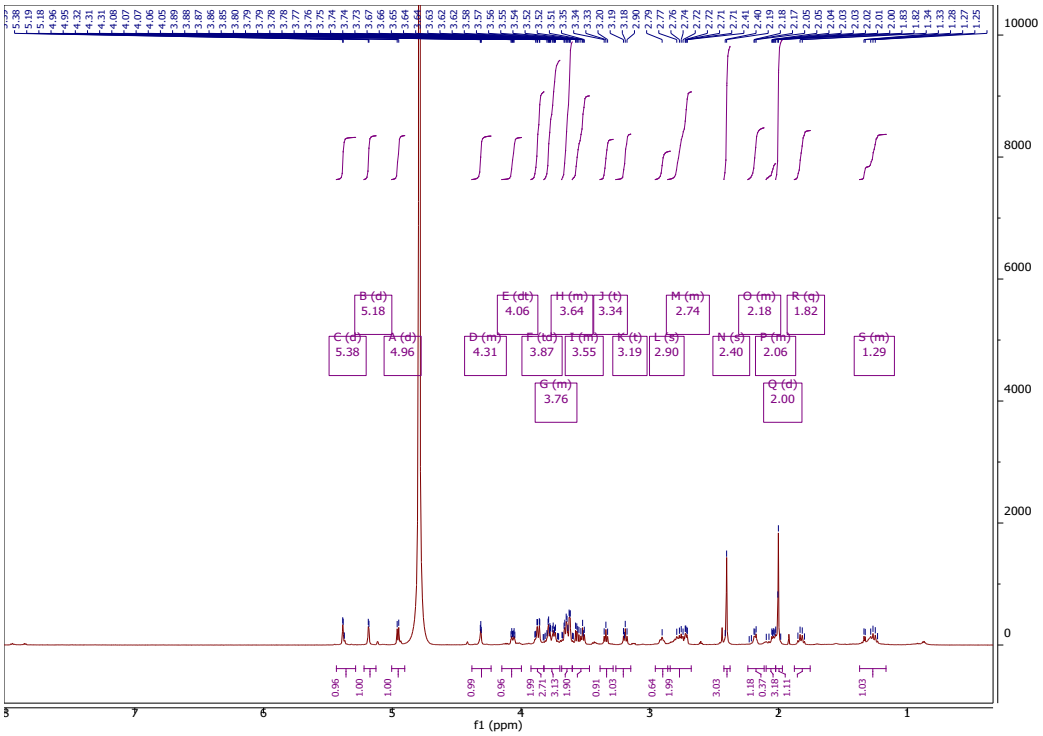

Figure S4. ^{1}H NMR for 2'-acetyl-apramycin.

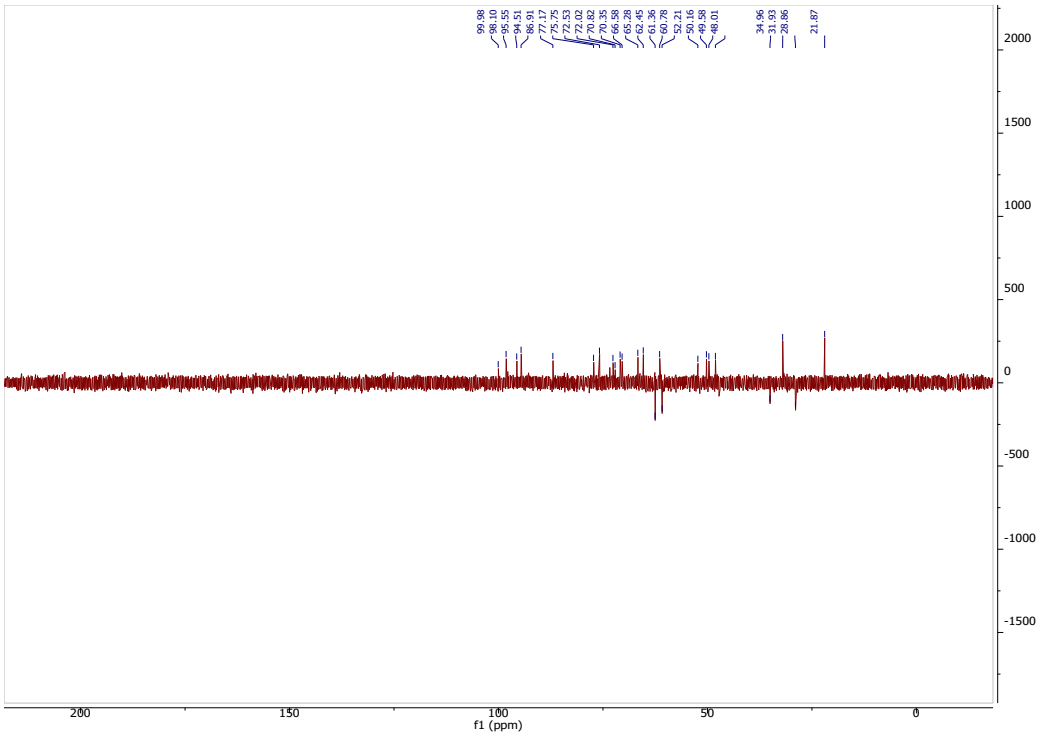

940

941 **Figure S5. ^{13}C NMR for 2'-acetyl-apramycin.**

942

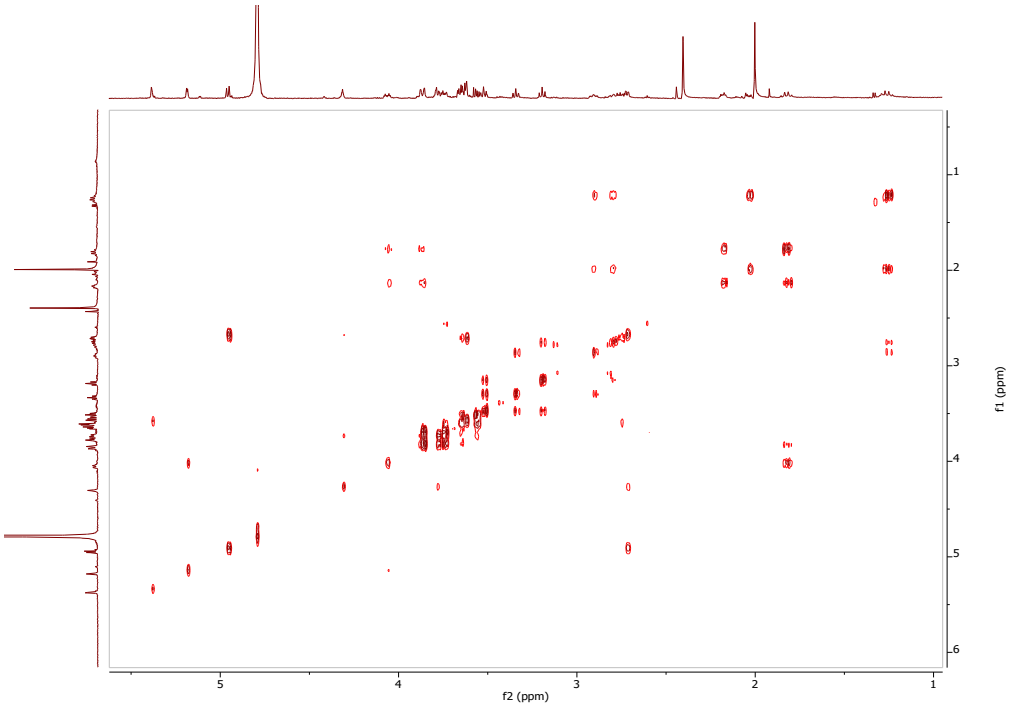

943

944 **Figure S6. ^{1}H-^{1}H COSY NMR for 2'-acetyl-apramycin.**

945

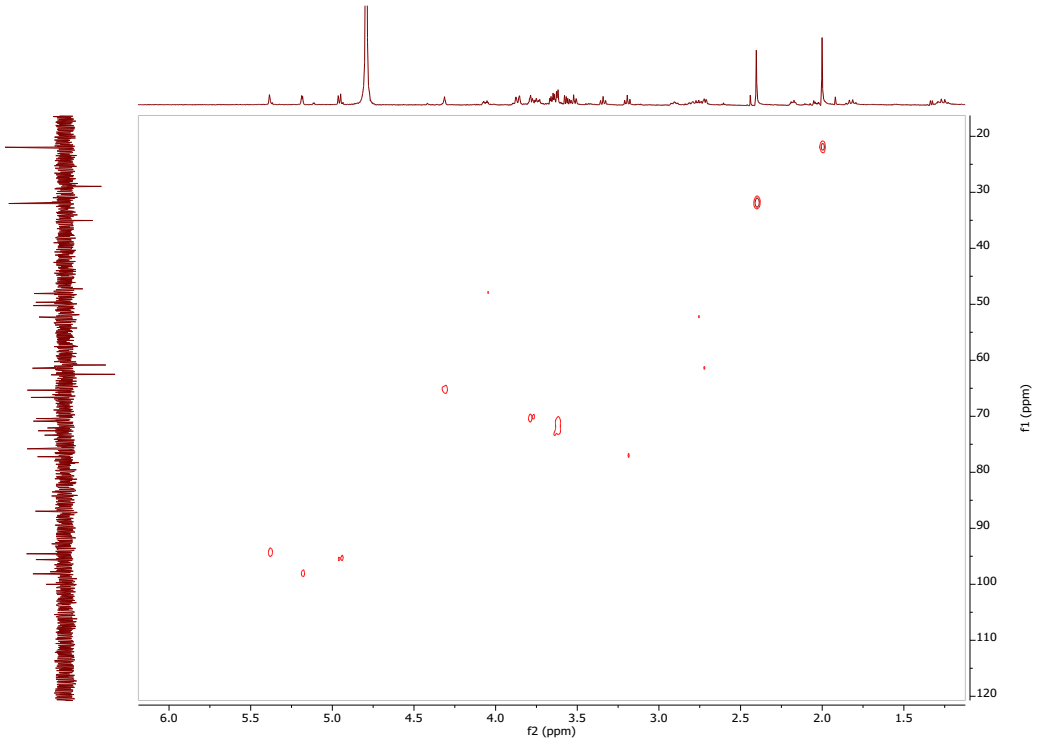

946

947 **Figure S7. ^{1}H-^{13}C HSQC for 2'-acetyl-apramycin.**

948

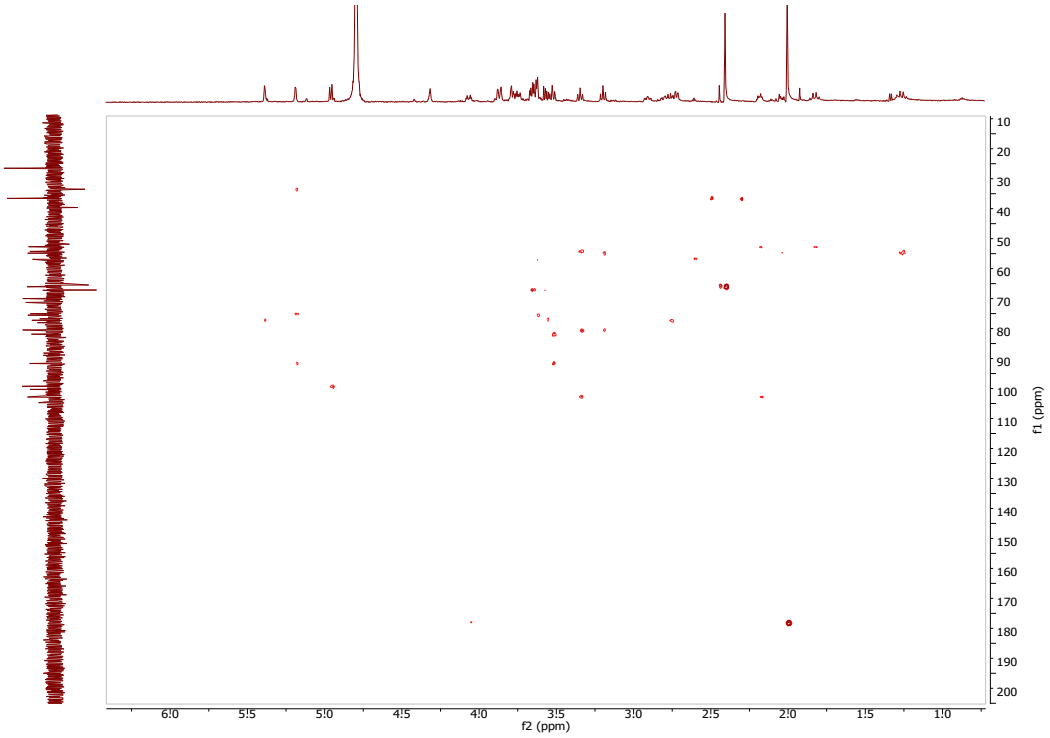

Figure S8. ^{1}H-^{13}C HMBC for 2'-acetyl-apramycin.

Chapter Three: Mechanistic plasticity in the antibiotic resistance acetyltransferase ApmA enables substrate promiscuity

Preface

The work presented in the following chapter is a manuscript in preparation for publication.

Bordeleau, E., Stogios, P. J., Evdokimova, E., Koteva, K., Savchenko, A., & Wright, G. D.

E.B. and G.D.W. conceived the study and designed the experiments. E.B. completed all antimicrobial susceptibility testing and wrote the published manuscript. Purification of ApmA and acetylated aminoglycosides was completed by E.B., K.K. completed spectroscopic characterization of acetylated aminoglycosides. P.J.S. solved all crystal structures and wrote the manuscript. E.B. completed structural analysis, protein engineering and steady-state kinetics. E.E. performed protein purification and crystallization. A.S. and G.D.W. oversaw the work and wrote the manuscript.

Abstract

Aminoglycoside antibiotics are a focus of next-generation design efforts to combat multidrug-resistant pathogens. The most significant barrier in new aminoglycoside development is the wide circulation of resistance genes responsible for drug and target modification. One candidate aminoglycoside that evades most of these resistance elements is apramycin. Nevertheless, the aminoglycoside acetyltransferase (AAC), ApmA, confers apramycin resistance. ApmA is found in a growing number of pathogens and is the first AAC reported to belong to the left-handed β-helix (LβH) protein superfamily. Here, we show that ApmA is capable of broad-spectrum aminoglycoside resistance with a molecular mechanism that diverges from other detoxifying enzymes of the LβH superfamily and canonical AACs. Antimicrobial susceptibility testing identified next-generation aminoglycosides susceptible to modification by ApmA along with drugs already critical in the clinic. We crystallized ApmA in complex with several aminoglycosides to comprehensively investigate the structural elements involved in substrate binding and catalysis. Using site-directed mutagenesis and steady-state kinetic studies, we find the role of the conserved active site histidine differs from other LβH enzymes and remarkably varies depending on the acetyl-accepting antibiotic substrate. This unusual flexibility in molecular mechanism demonstrates the unexpected plasticity of antibiotic resistance elements to co-opt protein catalysts in the evolution of drug detoxification and provides vital structural and mechanistic data to inform the future development of aminoglycoside antibiotics.

Introduction

Aminoglycosides (AGs) are polycationic amino sugar-based antibiotics first identified over 60 years ago that have excellent bactericidal activity in Gram negative and Gram positive pathogens. Widespread and genetically diverse resistance has diminished their impact, but they have found renewed interest in treating multidrug-resistant pathogens. The well-established pharmacokinetic-pharmacodynamic profiles and broad-spectrum antimicrobial activity of aminoglycosides make them attractive candidates for further development[1]. Most clinically used AGs consist of a 2-deoxystreptamine (2-DOS) ring core decorated with different sugars that define subclasses **(Extended Data Fig. 1)**. The positive charge generated by several amines gives AGs affinity for the negatively charged backbone of 16S rRNA[2]. Upon binding to the decoding center of the ribosome, AGs disrupt the proof-reading process of translation resulting in miscoding or inhibit translocation.

The molecular details of AG-ribosome interactions have informed the development of analogs with increased target selectivity and reduced toxicity[3]. These efforts have been complemented by investigations of AG resistance mechanisms reported during their decades of use. The AG-modifying enzymes (AMEs) capable of derivatizing amino or hydroxyl groups on the AG scaffold are the most significant contributors to clinical resistance. These enzymes fall into three subclasses: *O*-phosphotransferases, *O*-nucleotidyltransferases, and *N*-acetyltransferases (AACs). Modified AG-substituents can create a steric clash or disrupt fundamental interactions with the 16S rRNA, compromising the drug's antimicrobial activity. AAC-modified AGs also experience an overall reduction in positive charge that lowers their affinity for the rRNA backbone. Understanding these relationships and the interactions between modifying enzymes and

susceptible AGs provide vital information to guide the development of less resistance-prone analogs[4,5].

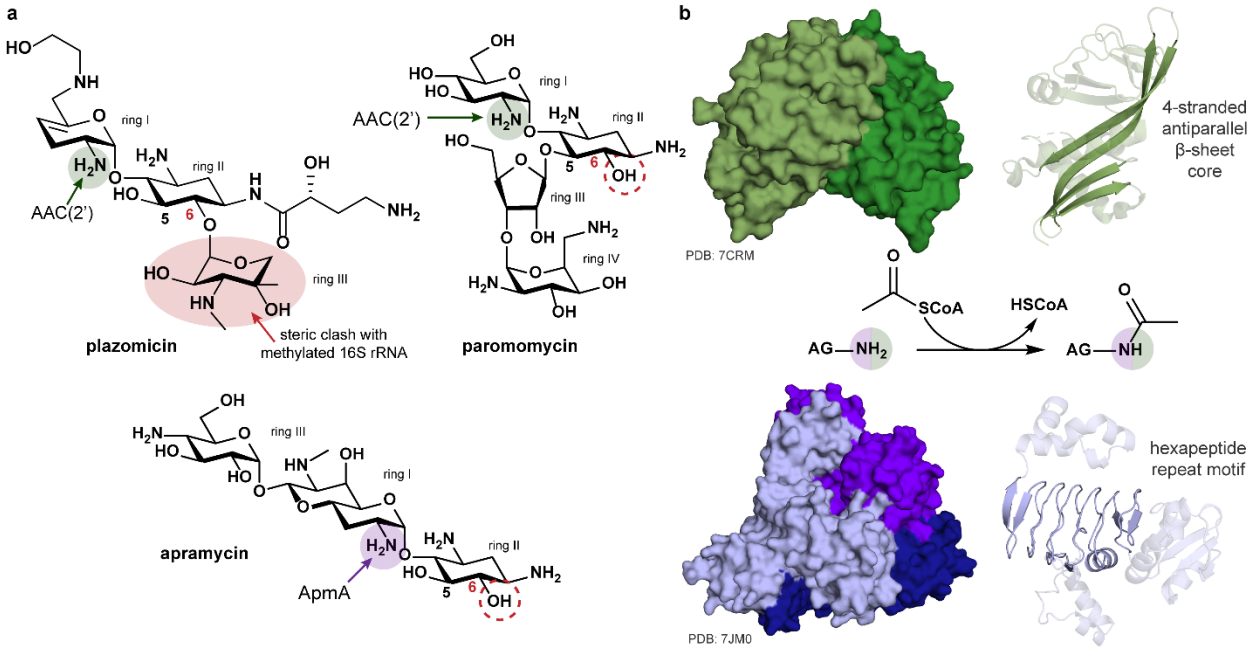

Figure 1. Next-generation AG scaffolds vulnerable to 2'-N-acetylation by proteins of two structurally distinct superfamilies. (a) Chemical structures of next-generation AG scaffolds. Apramycin and paromomycin lack substitution at C6 (highlighted by red circles), evading the action of 16S RMTases. Site of 2'-*N*-acetylation and is shaded green or purple for each structure. (b) AAC(2')-I belongs to the GNAT superfamily (top) and ApmA belongs to the LβH superfamily (bottom). Both enzymes utilize acetyl-CoA to modify N2' of AGs. Defining structural motifs are highlighted in structure of the single subunit.

Plazomicin is the most recent clinically approved next-generation AG, designed to evade the majority of AMEs **(Fig. 1a, Extended Data Fig. 1)**[6]. Plazomicin is a semi-synthetic derivative of the naturally occurring 4,6-disubstituted AG, sisomicin. The addition of an (S)-4-amino-2-hydroxybutyryl group on N1 and hydroxyethyl group on N6' protect against prevalent AAC(3) and AAC(6'), respectively[6]. Unfortunately, plazomicin remains susceptible to clinically relevant target modifying enzymes, 16S rRNA methyltransferases, that are increasingly common among multidrug resistant pathogens[7]. The methylation of A1405 of the 16S rRNA creates a steric clash

with ring III of the 4,6 disubstituted subclass. This liability has prompted the search for AGs whose structures and mode of action evade both AMEs and target modification mechanisms[8] **(Fig. 1a)**.

Paromomycin **(Fig. 1a)** is a naturally occurring 4,5-disubstituted AG with limited clinical usage due to this subclass's increased toxicity[9,10]. The substitution of ring III at C5 allows the antibiotic to retain activity against pathogens expressing 16S RMTases. Propylamycin is one of several new AG-derivatives designed to improve the properties of the 4,5-disubstituted subclass[11]. This semisynthetic derivative of paromomycin differs by the addition of a 4'-deoxy-4'-alkyl substituent **(Extended Data Fig. 1)**. This modification provides increased selectivity towards bacterial ribosomes and superior efficacy over paromomycin towards AG-resistant ESKAPE pathogens[11,12]. Apramycin **(Fig. 1a)** is another naturally occurring AG used in veterinary medicine. The unique monosubstitution at C4 with an octadiose element protects against clinically important 16S RMTases and the most common AMEs[8]. Apramycin is only susceptible to acetylation by AAC(3)-IV[13,14] and the recently investigated ApmA[15,16]. These AACs use acetyl-coenzyme A to modify primary amines and render apramycin inactive. While apramycin analogs that evade AAC(3)-IV have been reported[17], the 3D structure of ApmA has only been recently available to guide semi-synthesis[16].

ApmA is the first acetyltransferase of the AG resistome belonging to the left-hand beta-helix acyltransferase superfamily (LβH)[16], falling under the subclass of xenobiotic acetyltransferases (XATs)[18,19] **(Fig. 1b)**. Our previous investigation of ApmA found apramycin prone to acetylation at the N2' position, assigning ApmA as an AAC(2')[20]. In contrast, other known AAC(2') enzymes belong to the GCN5-*N*-acetyltransferase (GNAT) superfamily **(Fig. 1b)** and are chromosomally encoded by *Providencia stuartii*[21] and *Mycobacterium tuberculosis*[22]. The

report that plazomicin is susceptible to AAC(2')-Ia has prompted research into other isoforms of this GNAT enzyme[6,23,24].

Crystal structures of complexes of plazomicin and other susceptible AGs have provided the structural rationale for substrate specificity[23]. Structural and biochemical analyses of AMEs belonging to the GNAT superfamily describe a flexible active architecture supporting AG acetylation. The binding and orientation of substrates in the correct geometries for catalysis are more critical than conserved residues directly participating in acid/base chemistry[25]. Like these GNATs, our mutagenesis and cell-based assays with the LβH ApmA demonstrated that apramycin N2' acetylation does not require an active site base[16]. This finding was unexpected since other antibiotic resistance XATs that *O*-acetylate type A streptogramin and chloramphenicol antibiotics rely on an invariant His in this role[18,26]. ApmA, therefore, must have a distinct molecular mechanism of antibiotic inactivation. In this study, we employ a combination of protein function and cell-based assays, together with structural studies, to investigate the mechanism of AG modification by ApmA.

Results

ApmA can *N*-acetylate a range of aminoglycoside substrates to confer resistance

We previously established that ApmA is an *N*-acetyltransferase that modifies apramycin at the N2' position to confer high-level resistance[16]. To further investigate substrate specificity, we performed antimicrobial susceptibility testing with an expanded AG panel **(Extended Data Fig. 1)**. ApmA confers resistance to not only apramycin's unique chemical scaffold but also a broad spectrum of 4,5-DOS and 4,6-DOS AGs **(Table 1)**.

Table 1. Aminoglycoside susceptibility testing of *E. coli* BW25113 Δ*tolC*Δ*bamB* expressing apmA under the control of the P_{bla} promoter

Aminoglycoside		MIC (μg/mL)	
Structural subfamily	Name	No plasmid control	pGDP3:*apmA*
4-monosubstituted 2-DOS	apramycin	4	64
4,5-disubstituted 2-DOS	paromomycin	2	256
	neomycin	0.5	16
4,6-disubstituted 2-DOS	tobramycin	0.5	16
	gentamicin	0.25	2
	kanamycin A	2	2
	kanamycin B	1	64 – 128
	plazomicin	0.25	8-16
	amikacin	0.5	0.5
5-monosubstituted 2-DOS	hygromycin B	16-32	16
aminocyclitol	spectinomycin	8	8

Acetylation of paromomycin and kanamycin B resulted in the highest resistance levels, with the minimal inhibitory concentration (MIC) increasing 128-fold. No resistance was observed to kanamycin A, an antibiotic that differs from ApmA-susceptible kanamycin B by incorporation of a hydroxyl at the 2' position rather than a primary amine **(Extended Data Fig. 1)**. Amikacin, a first-generation semi-synthetic AG that also includes a hydroxyl at position 2', is also not

susceptible to ApmA **(Extended Data Fig. 1)**. Both observations suggest that, unlike other LβH acetyltransferases, ApmA is limited to *N*-acetylation of AG substrates. Like amikacin, the N1 position of plazomicin contains an (S)-4-amino-2-hydroxybutyrate substitution for evasion from a wide variety of AMEs. Additionally, plazomicin also has a hydroxyethyl group at position N6' to block the activity of clinically relevant AAC(6')s **(Extended Data Fig. 1)**. Despite these chemical changes, the N2' of plazomicin remains susceptible to modification by ApmA with a 32-fold increase in MIC **(Table 1)**.

We confirmed the regiospecificity of acetyl-transfer for three AGs, with representatives from the 4,5-DOS (neomycin[27,28], paromomycin) and 4,6-DOS (tobramycin[29]) subclasses. Each acetylated AG was produced *in vitro* with purified recombinant ApmA and purified to homogeneity. Consistent with our previous report for ApmA-inactivated apramycin, each of the AGs was acetylated at the 2' position of ring I. High-resolution electrospray ionization mass spectrometry (HR-ESI-MS) was consistent with monoacetylation (mass increase of 42.0 Da, [**Extended Data Table 2**]). The regiospecificity of acetylation was confirmed by a combination of one-and two-dimensional nuclear magnetic resonance spectroscopy of purified, ApmA-inactivated AG **(Table S1-S3, Fig. S1-S13)**.

We next probed ApmA's *in vitro* activity towards apramycin and paromomycin using steady-state kinetics **(Fig.2)**. The enzyme exhibited negative cooperativity towards both AGs as reflected by the Hill constants ($n < 1$) **(Fig. 2b)**. The sigmoidal steady-state kinetic curve indicates a decreased affinity for binding a second AG substrate after the first[30]. At first glance, this form of cooperative behavior for a detoxifying enzyme would not seem optimal to protect the host from antibiotics, i.e., the enzyme gets less active as antibiotic concentration increases. Further inspection of the traditional Michaelis-Menten and allosteric model fit with kinetic data for ApmA identifies

the advantage of this phenomenon **(Fig. 2b)**. At the lower concentrations of AG substrate, the rates are higher than they would otherwise be if ApmA did not exhibit this form of cooperative behavior. The benefit in the context of antibiotic resistance is that maximal AG inactivation is achieved at low concentrations of AG that are not yet overwhelming the defensive capacity of the cell[31].

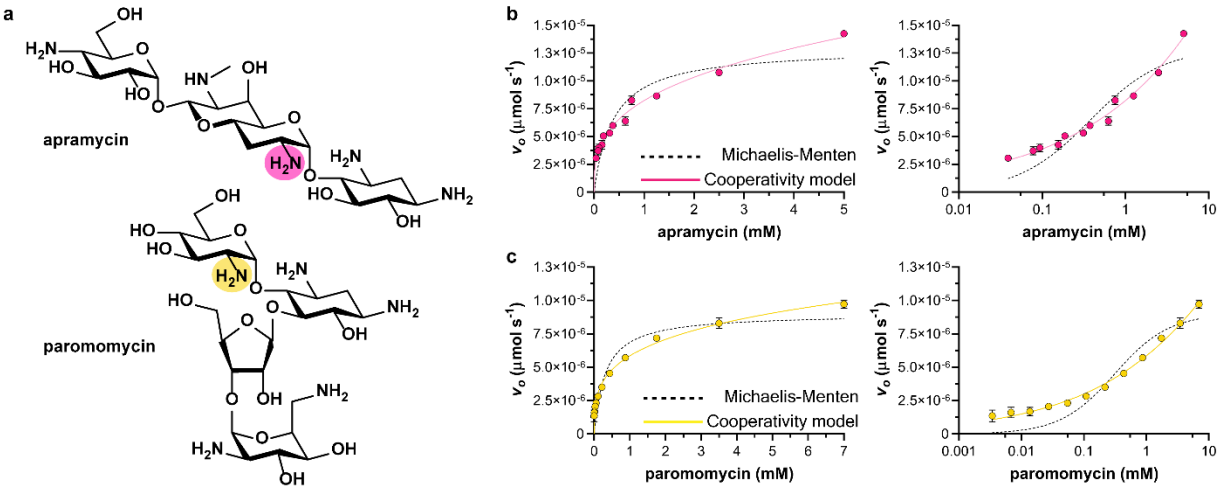

Figure 2. Kinetic activity of wild-type ApmA towards AGs. (a) Chemical structures of next-generation AG parent scaffolds apramycin and paromomycin. Site of ApmA-catalyzed acetylation is highlighted. (b) and (c) *In vitro* kinetics for apramycin and paromomycin respectively. Assays were both completed with 400 μM of acetyl-CoA. Apramycin and paromomycin kinetics were obtained using 150 nM and 250 nM wild-type ApmA respectively. Linear and semilogarithmic plots for velocity versus AG concentrations are shown for both substrates. The Michaelis-Menten model (dotted line) and allosteric sigmoidal model (solid coloured line) for cooperativity are shown to illustrate the best fit for both sets of data.

Structural analysis of aminoglycoside binding and promiscuity of ApmA

Crystal structures of ApmA bound with 4,5-DOS AGs (neomycin and paromomycin) and 4,6-DOS AGs (gentamicin, tobramycin, and kanamycin B) were determined to investigate the binding of AG substrates **(Fig. 3, Extended Data Fig. 2)**. Crystallographic statistics for all the structures are presented in **Supplemental Table 4**.

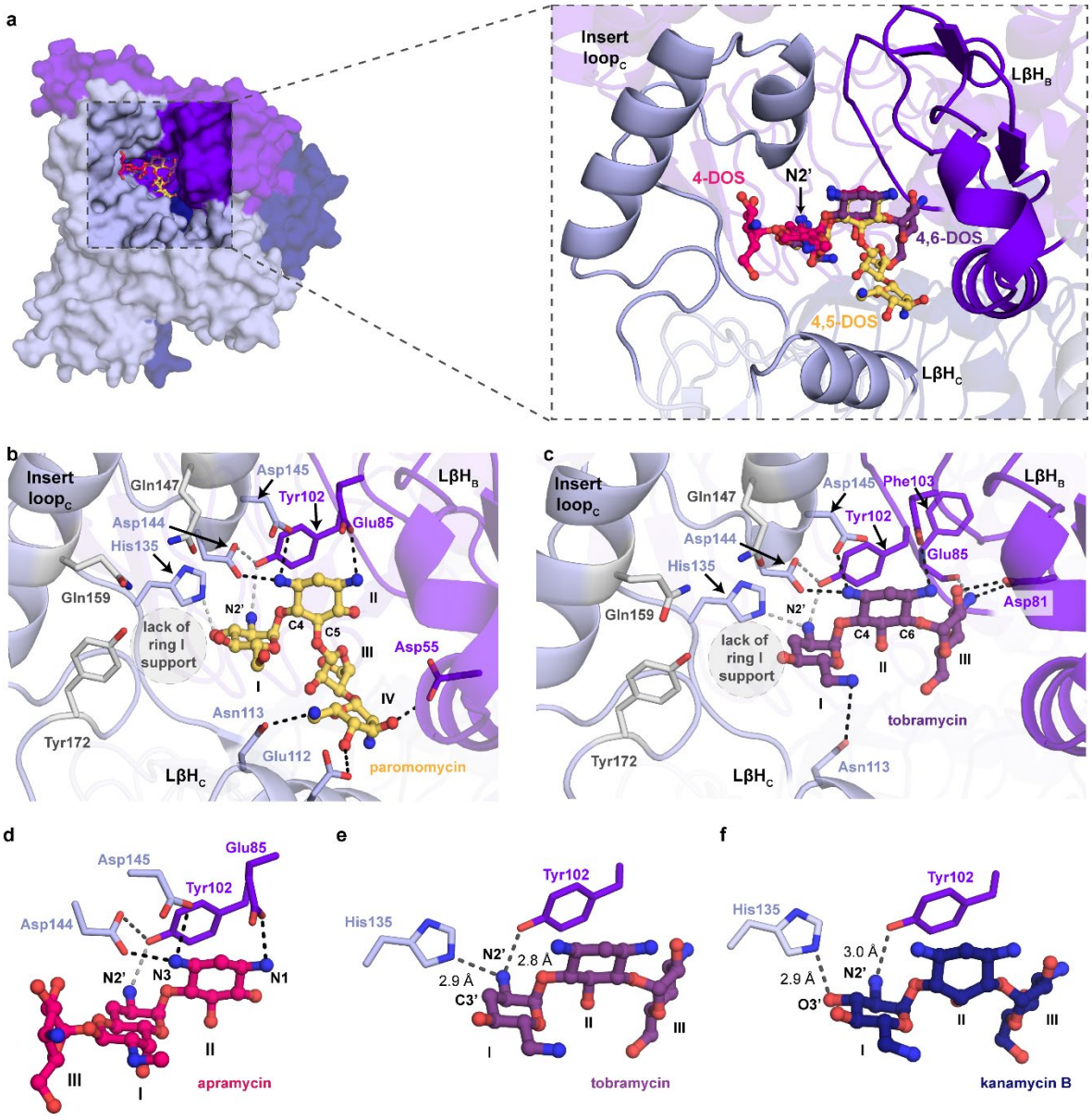

Figure 3. Breakdown of AG binding in the acetyl-acceptor pocket of ApmA. (a) Surface view of ApmA highlights the AG binding pocket. ApmA in complex with different AGs are superimposed onto ApmA in complex with apramycin (PDB 7JM2). AGs shown in crystal structure complex; apramycin (pink), paromomycin (PDB 7UUM, yellow) and tobramycin (PDB 7UUK, purple). A close view cartoon representation of the AG binding pocket shows different regions of chains directly interacting with substrates. The positioning of the N2' and 2-DOS ring of 4,5- and 4,6-DOS AGs are consistent with apramycin. (b and c) Amino acids implicated in binding AGs of different 2-DOS ring substitution pattern. Residues for binding of ring III for apramycin are shown in grey. AG representatives: paromomycin (b) and tobramycin (c) are shown in the acetyl-accepting binding pocket. Interactions within 4.0 Å are represented by dashed lines. Interactions between paromomycin and ApmA(chain B) were identified from a superimposed complex of ApmA•apramycin and ApmA•paromomycin. (d) Conserved network of interactions involved in the binding and positioning of N2' and 2-DOS ring of all ApmA substrates. (e) and (f) show

differences in AG binding based on lack of and presence of O3' group for tobramycin and kanamycin B (PDB 7UUL) respectively.

Positioning of the 2-DOS ring is conserved for all AG substrates investigated and consistent with our previously reported complex of ApmA with apramycin **(Fig. 3a)**. The negatively charged Asp144, Asp145, and Glu85 create an optimal environment for binding the positively charged N1 and N3 atoms on the 2-DOS ring. When ring III is substituted at C5 (e.g., neomycin, paromomycin), it extends in the direction of the N-terminal region but does not make any contacts with the binding pocket. For both 4,5-DOS AGs, ring IV interacts with Asp55 of the N-terminal region in addition to Asn133 and Glu112 of the LβH domain **(Fig. 3b)**. The substitution of ring III at C6 for tobramycin and kanamycin B creates interactions within the LβH domain to Asp81 and the backbone of Phe103 **(Fig. 3c, Extended Data Fig. 2a)**. Ring III of gentamicin only benefits from interactions with Asp81 **(Extended Data Fig. 2b)**. The specific interactions and conformations of AGs when bound by ApmA are comparable to those observed for GNATs of the AG resistome. It has been suggested that this conformation is the lowest energy conformer, and by evolving to bind the drugs in the same orientation, modifying enzymes can compete with the ribosomal target[32].

The same network of interactions involved in binding the N2' of all AG substrates includes the hydrogen bonds between amino acids of the LβH domain (Tyr102) and the insert loop region (Asp144) **(Fig. 3d)**. A lack of sugar rings branching from C4 in both 4,5- and 4,6-DOS AGs limits the interactions that can support positioning the N2' for acetylation **(Fig. 3b and 3c)**. Notably, the conserved His135 of LβH enzymes is only within hydrogen-bonding distance of the N2' when ApmA is in complex with either tobramycin, gentamicin, or apramycin. When ApmA is in complex with either kanamycin B or 4,5-DOS AGs, the O3' of these compounds is more likely to

interact with the Nε2 of the His135 imidazole group **(Fig. 3e and 3f)**. Interestingly, we found O3' containing AGs the more challenging substrates to produce crystals of ligand bound to ApmA.

Mutagenesis studies implicate residues involved in substrate binding and positioning

To identify residues that may play a substantial role in AG binding, we generated single amino acid substitutions at five positions in the active site of ApmA **(Fig. 4, Extended Data Table 2)**. Cell-based assays were used to survey changes in the AG susceptibility of *E. coli* BW25113 expressing ApmA mutants compared to the wildtype enzyme.

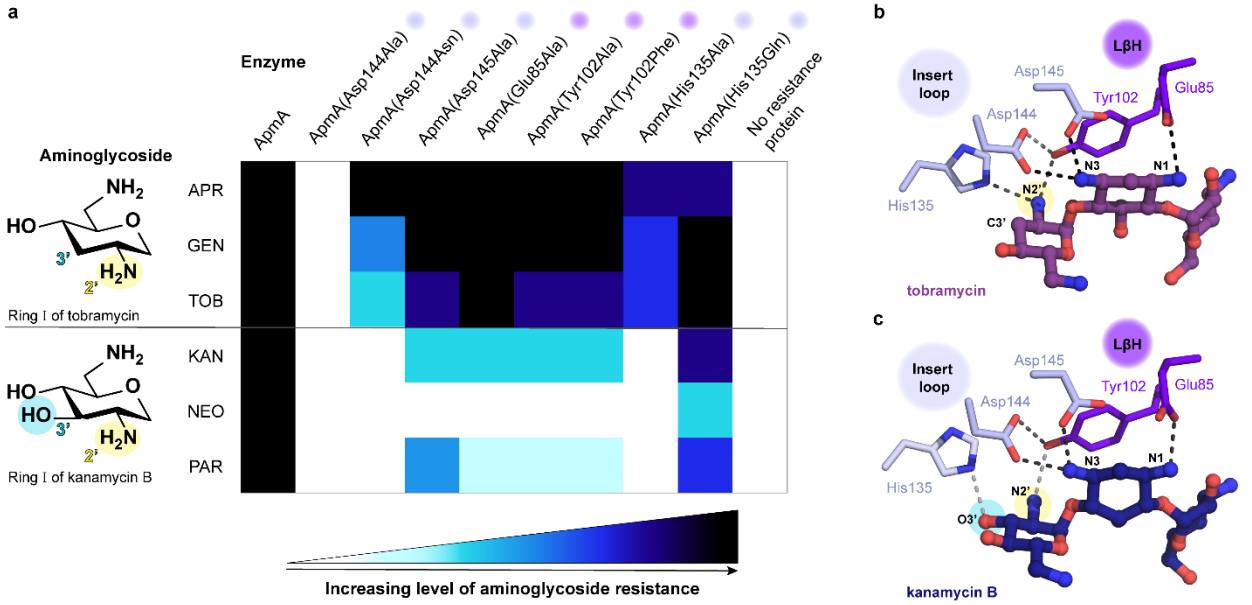

Figure 4. Aminoglycoside resistance conferred by wild-type ApmA and ApmA mutants. (a) Antimicrobial susceptibility testing was completed in *E. coli* BW25113 Δ*tolC*Δ*bamB* against structurally diverse AG substrates of ApmA. The reference point in the heat map is the MIC when wild-type ApmA is expressed. AGs are grouped together based on the absence (top) or presence (bottom) of 3' hydroxyl. Ring I of tobramycin and kanamycin B are shown for structural representation for group comparison. 4-monosubstituted AG subclass; APR (apramycin), 4,6-disubstituted AG subclass; TOB (tobramycin), GEN (gentamicin), KAN (kanamycin B), 4,5-disubsituted AG subclass; NEO (neomycin), PAR (paromomycin). (b) and (c) Active site residues targeted for mutagenesis studies for ligand bound structures of tobramycin (b) and kanamycin B (c). Positions 2' and 3'are highlighted as shown for Ring I in panel A.

Only the substitution of Asp144 with Ala caused *E. coli* to become susceptible to all the AGs tested. Furthermore, expression of ApmA(Asp144Ala) was the only mutant to impact the MIC of apramycin significantly. The other mutants constructed did not alter apramycin's MIC outside a 2-fold range when the wildtype protein was expressed. The Asp144Asn mutant was then produced to supplement the hydrogen bonding potential between the AG and ApmA. When expressed in *E. coli*, the Asn substitution restored activity sufficiently to provide an equivalent resistance level to apramycin to the wildtype protein. However, ApmA(Asp144Asn) resistance was diminished or abolished towards all other AGs tested. Mutation of the acidic residues Glu85 and Asp145 that interact with the 2-DOS ring had minimal effect on resistance towards 4,6-DOS AGs. In contrast, these mutations compromised activity and increased susceptibility to 4,5-DOS AGs and kanamycin B.

Replacement of Tyr102 with Ala or Phe significantly increased the susceptibility of *E. coli* to 4,5-DOS AGs, and the MIC of kanamycin B was reduced 8-fold. These findings indicate that maintaining an aromatic ring for structural stability is not as crucial as the hydrogen bonding potential of the phenolic hydroxyl for the activity of ApmA with select substrates.

The evidence reveals contrasting salt bridging and hydrogen bonding requirements that depend on the AG substrate. Apramycin's rings I and III provide contacts within the binding pocket of ApmA surrounding the 2'-NH_2 to be acetylated. Alteration of these residues, except for Asp144, does not significantly compromise the acetylation of apramycin in cells **(Fig. 4a)**. However, acetylation of disubstituted AGs is more sensitive to the substitution of any of these binding site residues. These findings imply that correctly positioning the core 2-DOS ring for disubstituted AGs is critical in orienting the N2' for acetylation and other nearby residues required for optimal catalysis.

The interactions between sugars substituted from C5 or C6 of the 2-DOS ring and ApmA are the dominant elements for binding and orientation of the prime ring I for acetylation. Their importance results from a lack of direct contacts within the insert loop region of ApmA's LβH domain to provide flanking support for orienting the N2' **(Fig. 3b and 3c)**. There is a conserved network of interactions through Asp144 and Tyr102 that help to position N2' of all AGs for acetylation and bind ring II 3-NH_2 **(Fig. 3d)**. The amide side chain of Asp144Asn has reduced hydrogen bonding capacity, with any interactions formed dependent on the functional group's rotamer conformation. The carbonyl is either available to bridge a network with Tyr102 and the N2' or be an electron acceptor for the AG's N3 **(Extended Data Fig. 3)**. For O3' containing AG substrates, the impact of a Tyr102 substitution is compounded by the difference in interactions with His135. AG substrates that lack an O3' (apramycin, tobramycin, and gentamicin) benefit from hydrogen bonding between His135 and the N2' to orient the functional group **(Fig. 4b)**. Conversely, for O3' containing AGs (kanamycin B, neomycin, paromomycin), His135 is closer to the O3', creating a dependence on Tyr102 for orienting the N2' for acetylation **(Fig. 4c)**.

The active site His of ApmA breaks its traditional role in LβH enzymes

The ApmA His135Ala mutation does not significantly impact resistance to apramycin[16]. This result implies that His135 is unlikely to act as an active site base, contrary to its role for other XATs[18,26]. When we tested this mutant against our expanded AG panel, we observed that the His135Ala substitution provided the most variability in AG susceptibility. The changes in MIC observed for tobramycin and gentamicin were within 4-fold, indicating significant retention of AG-modifying activity **(Fig. 4a)**. In contrast, *E. coli* expressing this mutant was susceptible to kanamycin B and 4,5-DOS AGs. The significance of this residue in the molecular mechanism of XATs prompted us to verify the AG-susceptibility phenotypes correlated to the trends observed *in*

vitro. Acetyltransferase activity was assessed for the wildtype and His135Ala mutant with AGs spanning each structural subclass **(Extended Data Fig. 4a and 4b)**.

Consistent with the wildtype enzyme, we did not observe *in vitro* modification of kanamycin A, verifying that ApmA cannot perform *O*-acetylation. Kanamycin B and paromomycin were both poor substrates. In contrast, tobramycin, differing from kanamycin B only by a single hydroxyl group at the O3' position, was modified, albeit at a 4-fold decreased level **(Extended Data Fig. 4a and 4b)**. Without His135, Tyr102 is the sole residue available to orient the N2' of tobramycin. The His135Ala mutant did not affect apramycin modification, and kinetic analysis verified that the mutant retains negative cooperativity **(Fig. 5a and b, Extended Data Fig 4a and 4b)**. These results support our observation that disubstituted AGs rely more on active site residues for binding and positioning.

The His135Gln mutant conserves the imidazole ring's hydrogen bonding potential but cannot participate in acid/base catalysis. If the histidine's role in binding substrates is more critical than acid/base catalytic potential, we predicted that expression of the His135Gln mutant should confer a comparable resistance level to the wildtype protein. Resistance was moderately recovered for most of the AGs tested compared to His135Ala **(Fig. 4a)**. As the best O3'-containing substrate for the wild-type enzyme **(Extended Data Fig. 4a)**, paromomycin was selected as a representative substrate for *in vitro* assessment with ApmA(His135Gln). Consistent with the resistance phenotypes, the enzyme was active towards the 4,5-DOS AG and retained negative cooperativity kinetics **(Fig. 5c and 5d)**. The expression of the His135Gln mutant generated wildtype levels of kanamycin B and tobramycin resistance **(Fig. 4a)**. Taken together, the *in vitro* kinetics and cell-based data indicate a dependence on the presence of a hydrogen-bonding acceptor at position 135, rather than an acid/base, for the acetylation of O3' containing AGs.

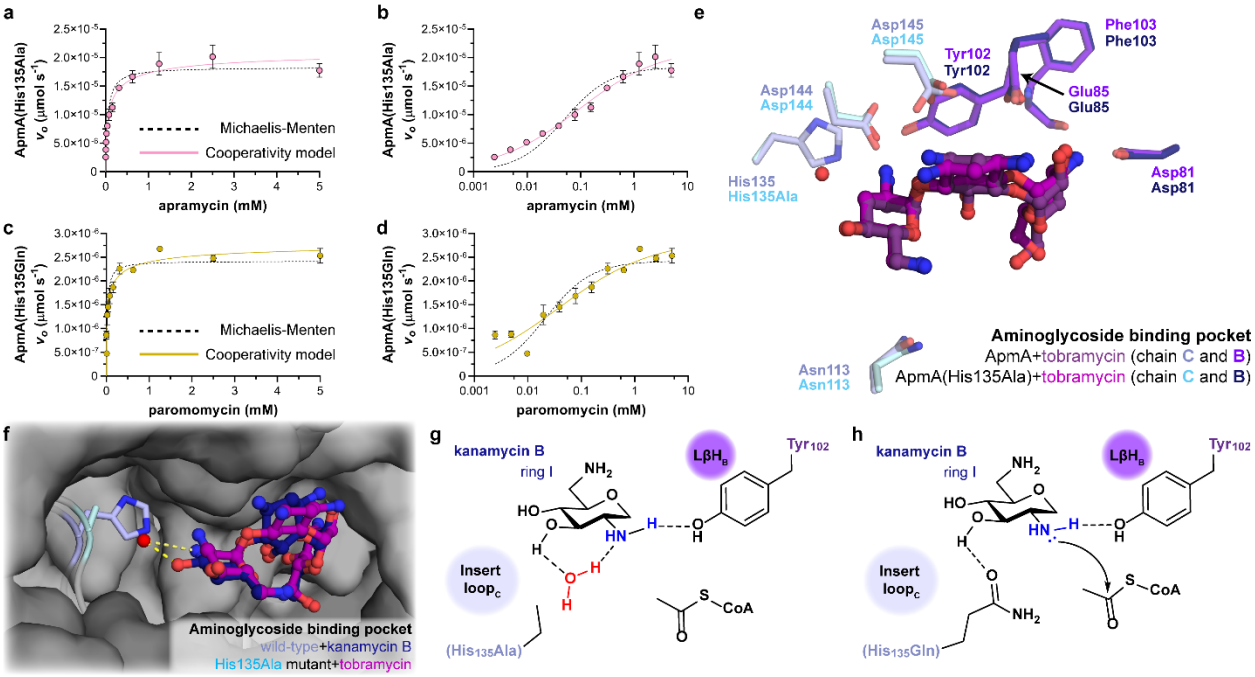

Figure 5. Proposed role for active site His135 in the acetylation of O3' containing aminoglycosides. (a) and (b) *In vitro* kinetics for ApmA(His135Ala) with apramycin. (c and d) *In vitro* kinetics for ApmA(His135Gln) with paromomycin. Assays were both completed with 400 µM of acetyl-CoA. Apramycin kinetics were obtained using 300 nM of ApmA(His135Ala). Paromomycin kinetics were obtained with 250 nM ApmA(His135Gln). Linear and semilogarithmic plots for velocity versus AG concentrations are shown for both substrates. **(e) and (f)** ApmA(His135Ala)•tobramycin•coenzyme A complex superimposed with ApmA•tobramycin complex (e) ApmA•kanamycin B complex (f). (f) Cross-section of the active site is shown to reveal the histidine and alanine at position 135 of wild-type and His135Ala mutant respectively. The red sphere represents the observed density for a water molecule in the active site of the His135Ala mutant. Yellow dashes highlight proposed intermolecular hydrogen bonds. (g) and (h) Proposed molecular mechanism of ApmA. Ring I of kanamycin B is shown to highlight the network of intermolecular interactions within the active site of ApmA that influences the acetylation of O3' containing AGs.

We determined the structure of ApmA(His135Ala) in complex with tobramycin and coenzyme A to investigate changes within the AG binding pocket that account for these observations **(Fig. 5e, Supplemental Table 4)**. Side chain interactions remained consistent for both ligands, assuming near-identical conformations when bound to the wildtype enzyme **(Fig. 5e)**. In the binding pocket of tobramycin, the alanine substitution created enough space for

positioning a water molecule where the imidazole side chain of His135 would have been located **(Fig. 5e and 5f)**.

We propose that residue 135 in the wildtype enzyme and His135Gln mutant spatially prevent a water molecule from interfering and assists in the prime ring I alignment due to side chain interactions with the O3'.Without an imidazole or amide functionality, this water molecule mediates a new set of hydrogen bonds between the N2' and O3' **(Fig. 5g and 5h)**. By sequestering the N2' unoccupied electrons, the nucleophilicity of this functional group is reduced, and acetylation will not occur. For 4,6-disubstituted substrates that lack an O3', the activity of the two variants suffers minimally from a lack of hydrogen bonding side chain at position 135 when alanine is introduced. The free electrons of the N2' for these substrates remain available for nucleophilic addition to the carbonyl functional group of acetyl-CoA **(Fig. 5e)**. Activity towards apramycin *in vitro* **(Fig. 2a, Extended Data Fig. 4a, and 4b)** and cell-based assays **(Fig. 4a)** exhibited no significant difference, which we attribute to the unique 4-DOS monosubstitution. Interactions between ring III of apramycin and the insert loop region optimize support for ring I and N2' positioning **(Extended Data Fig. 4c).** In contrast, O3'-lacking substrates rely on Tyr102 to position N2' for catalysis **(Extended Data Fig. 4d)**.

We hypothesize that the lack of 2'-*O*-acetylating activity is due to the interaction between His135 and O3'. In cell-based assays, both kanamycin A and amikacin are O2' containing substrates that retain activity towards *E. coli* expressing ApmA **(Table 1)**. Our *in vitro* kinetic studies further demonstrated that ApmA does not modify kanamycin A but is active towards the N2' containing kanamycin B **(Extended Data Fig. 4a)**. Moreover, we found plazomicin susceptible to modification in our cell-based assays, demonstrating the tolerance of ApmA to accommodate the N1-(S)-4-amino-2-hydroxybutyrate substituent of amikacin in the binding

pocket **(Table 1)**. If His135 is positioned closer to the O3' of kanamycin A and amikacin, as seen for kanamycin B, the residue would be unavailable to participate in the required acid-base catalysis.

Discussion

The acquisition and spread of antibiotic modification resistance mechanisms present challenges in developing new drug scaffolds. The informed design of next-generation AGs requires knowledge of the structural and biochemical diversity in the broader resistome. Here, we expand the functional definition of ApmA from an apramycin 2'-*N*-acetylating enzyme to an AAC(2') capable of high-level, broad-spectrum AG resistance. The AG promiscuity of ApmA jeopardizes next-generation scaffolds and the traditional AGs currently relied upon in the clinic. Tobramycin is an effective therapy for treating chronic *Pseudomonas aeruginosa* infections in cystic fibrosis patients[2,33]. While mobilization of *apmA* has the potential to compromise the efficacy of these antibiotics, these AGs could select for *apmA* before next-generation AGs are introduced. Our comprehensive structural and biochemical analysis uncovers the molecular determinants of substrate specificity and *N*-acetylating activity for the first XAT identified in the AG resistome[16]. This information can be leveraged to develop analogs less prone to resistance or inhibitors of ApmA.

Even though ApmA exhibits the conserved active site architecture of XATs to facilitate *O*-acetylation, we show that this enzyme cannot carry out this activity to confer AG resistance. The structural diversity of ApmA substrates allowed us to provide a detailed rationale for these active site residues' varying roles in AG binding and acetylation. We attribute the strikingly different resistance phenotypes for ApmA(His135) variants to the site of modification on the molecule. Previously studied GNATs, AAC(3), and AAC(6') enzymes show similar consequences across substrates studied upon mutation of suspect residues involved in AG catalysis[34,35]. The primary amines susceptible to these AMEs exhibit nearly the same chemical environment across all AG subclasses. Unique to substrates of AAC(2') is the presence or absence of an O3' neighboring the

site of acetylation. This difference in the immediate chemical environment for the N2' can influence its behavior.

The participation of water molecules in AG orientation and binding is precedented in interactions with 16S rRNA[2,36]. Studies utilizing x-ray crystallography and NMR have all produced structural data for AG-ribosomal complexes that have aided in understanding these relationships[5,37-39]. Water molecules bridge important intramolecular hydrogen bonds between the N2' of ring I and O5' of ring II for 4,6 disubstituted AGs[2]. These interactions assist in establishing the correct orientation that optimizes target recognition and binding by the antibiotics. Water-mediated hydrogen bonds facilitate a third of the interactions between functional groups of AG sugars and the RNA[5]. While studied to a lesser extent, structural studies of AAC(2')-Ic have found similar interactions in the binding and positioning ring I of AGs for acetylation[40]. Literature describing the underlying 2'-*N*-acetylating activity for AAC(2') was last addressed 20 years ago[40]. More recently, attention returned to probe substrate specificity determinants of AAC(2') isoforms[23,24]. Our study demonstrates the intricacies behind these interactions that can be applied to the alternative roles that active site residues can play in binding or catalysis.

Previous kinetic characterizations completed by our group of AAC(6')-I and AAC(3)-I isoforms have found that these GNATs exhibit positive cooperativity ($n > 1$) towards AG substrates[41,42]. This form of cooperative behavior reflects an increased affinity for substrates upon binding, resulting in faster rates at the higher concentrations of substrate[30]. This relationship supports our earlier studies with AAC(6')-Ii, which reported a positive correlation between MIC and k_{cat}, the rate observed at saturating AG concentrations that would be overwhelming the cell[43]. Consequently, these proteins are susceptible to small environmental changes, as reflected in the steepness of their sigmoidal curve[30]. This behavior benefits the defensive capacity of the cell in

the event there is a sudden influx of AGs. In contrast, the LβH AG-detoxifying enzyme ApmA exhibits the opposite cooperative relationship to its antibiotic substrate. Our report of negative cooperativity for ApmA is the first example of such a mechanism in AG resistance but not unprecedented for other drug inactivating enzymes. Early investigations of chloramphenicol acetyltransferases (CAT_{III}) also found negative cooperativity towards their antibiotic substrate[44,45]. Beyond antibiotic resistance are similar examples among other members of the LβH superfamily. Negative cooperativity has been reported for serine acetyltransferase (SAT[46]) and NodL[47], an acetyltransferase for oligosaccharides of *Rhizobium leguminosarum*.

Characterization of ApmA provides further evidence for the depths of mechanistic diversity in the AG resistome necessary to guide future investigations and understand the evolution of this AG-modifying function within the LβH superfamily.

Methods

Site-directed mutagenesis

PCR site-directed mutagenesis by primer extension was performed to introduce nucleotide substitutions in *apmA*. The pGDP3:*apmA* construct was used as a template with the mutagenic primers listed in **Supplementary Table 4** to generate *apmA* mutants (for susceptibility testing and *in vitro* enzyme kinetics). The ApmA His135Ala mutant (for crystallography) was generated using Quickchange site-directed mutagenesis using the *apmA* gene in the vector pMCGS53.

Antimicrobial susceptibility testing

AG susceptibility testing of *E. coli* BW25113 Δ*tolC* Δ*bamB* expressing wildtype *apmA* and *apmA* mutants was completed following the methods described in PMID 33563840.

In vitro enzyme kinetics and spectroscopic characterization of ApmA-catalyzed acetylated aminoglycosides

ApmA wildtype, His135Ala and His135Gln proteins were purified as described in PMID 33563840. AG acetylation catalyzed by ApmA wildtype and mutant enzymes was monitored by the detection of thiols from released CoA with the chromogenic reagent 5,5-dithio-bis(2-nitrobenzoic acid) (DTNB) at 412 nm. All kinetic assays were carried out in 96-well plates with a final reaction volume of 300 µL, 50 mM HEPES (pH 7.5) and 1 mM DTNB dissolved in ethanol (final ethanol concentration maintained at 5 %). All reactions were initiated by adding AG substrate. GraphPad Prism Version 9.3.0 was used for all kinetic data analysis. Kinetic data were fit with equation (1) for Michaelis-Menten kinetics and equation (2) for an Allosteric sigmoidal model. Nonlinear regression model comparisons were completed using the Extra sum-of-fit F test method (P value < 0.05).

equation (1) $v = V_{max}*[S]/(K_m + [S])$

equation (2) $v = V_{max}*[S]^h/(K' + [S]^h)$

where v is the initial velocity, V_{max} is the maximal velocity, [S] is the concentration of AG substrate, K_m and K' is the substrate concentration at half maximal velocity and h is the Hill coefficient. Characterization of acetylated AGs was completed following procedures outlined in PMID 33563840.

Crystallization, data collection, structure determination and analysis

ApmA wildtype and His135Ala proteins were purified as described in PMID 33563840. All crystals were grown at room temperature using the vapor diffusion sitting drop method with 0.5 µl of protein solution mixed with 0.5 µl of reservoir solution. Crystals were grown by co-crystallization using the following reservoir solutions: ApmA plus paromomycin complex - 0.2 M lithium sulfate, 0.1 M Tris pH 8.5, 23% (w/v) PEG3350 and 14 mM paromomycin; ApmA plus neomycin complex - 0.2 M lithium sulfate, 0.1 M Tris pH 8.5, 23% (w/v) PEG3350 and 10 mM neomycin; ApmA plus gentamicin complex - 0.2 M calcium chloride dihydrate, 16% (w/v) PEG3350 and 2.5 mM gentamicin; ApmA plus tobramycin complex - 0.2 M calcium chloride, 20% (w/v) PEG3350 and 5 mM tobramycin; ApmA plus kanamycin B complex - 0.2 M lithium sulfate, 0.1 M Tris pH 8.5, 25% (w/v) PEG3350 and 5 mM kanamycin B; ApmA H135A mutant plus tobramycin complex -0.1 M sodium acetate pH 4.5, 10% (w/v) PEG 10K and 2mM tobramycin. Crystals were cryoprotected with Paratone-N oil, 25% (w/v) ethylene glycol or 25% (w/v) MPD, depending on the crystal. Diffraction data were collected at the Advanced Photon Source, Argonne National Laboratory, beamline 21-ID or at a home source Rigaku Micromax 007-HF rotating anode. All data were processed by HKL-3000 and all structures were solved by

Molecular Replacement using the ApmA apoenzyme structure (PDB 7JM0). Structure refinement was performed using Phenix.refine plus manual building with Coot. The presence of substrate molecules was identified by building into the Fo-Fc difference density after the initial rounds of refinement. Ligand-bound structures of ApmA were visualized in PyMol to identify potential residues involved in substrate binding and catalysis. Candidates were defined as amino acids within 4.0 Å of AG functional groups. Structures have been deposited to the Protein Databank under accession codes 7UUJ, 7UUK, 7UUL, 7UUM, 7UUN and 7UUO.

Acknowledgments

This work used the Centre for Microbial Chemical Biology core facility at McMaster University for antibiotic susceptibility testing. We thank Jurek Osipiuk and Karolina Michalska at the Structural Biology Center, Advanced Photon Source, Argonne National Laboratory for x-ray diffraction data collection. Crystal structures solved in this work were funded in whole or in part with U.S. federal funds from the National Institute of Allergy and Infectious Diseases, National Institutes of Health, Department of Health and Human Services, under contract No. HHSN272201700060C (Center for Structural Genomics of Infectious Diseases (CSGID); http://csgid.org). This research was funded by a Canadian Institutes of Health Research grant (FRN-148463), the Ontario Research Fund, and a Canada Research Chair to G.D.W.

References

1. Bottger, E.C. & Crich, D. Aminoglycosides: time for the resurrection of a neglected class of antibacterials? *ACS Infect Dis* **6**, 168-172 (2020).
2. Vicens, Q. & Westhof, E. RNA as a drug target: the case of aminoglycosides. *Chembiochem* **4**, 1018-23 (2003).
3. Matt, T. et al. Dissociation of antibacterial activity and aminoglycoside ototoxicity in the 4-monosubstituted 2-deoxystreptamine apramycin. *Proc Natl Acad Sci U S A* **109**, 10984-9 (2012).
4. Zárate, S.G. et al. Overcoming aminoglycoside enzymatic resistance: design of novel antibiotics and inhibitors. *Molecules* **23**(2018).
5. Pfister, P., Hobbie, S., Vicens, Q., Bottger, E.C. & Westhof, E. The molecular basis for A-site mutations conferring aminoglycoside resistance: relationship between ribosomal susceptibility and X-ray crystal structures. *Chembiochem* **4**, 1078-88 (2003).
6. Cox, G. et al. Plazomicin retains antibiotic activity against most aminoglycoside modifying enzymes. *ACS Infect Dis* **4**, 980-987 (2018).
7. Doi, Y., Wachino, J.I. & Arakawa, Y. Aminoglycoside resistance: the emergence of acquired 16S ribosomal RNA methyltransferases. *Infect Dis Clin North Am* **30**, 523-537 (2016).
8. Juhas, M. et al. *In vitro* activity of apramycin against multidrug-, carbapenem- and aminoglycoside-resistant Enterobacteriaceae and *Acinetobacter baumannii*. *J Antimicrob Chemother* **74**, 944-952 (2019).
9. Hu, Y., Liu, L., Zhang, X., Feng, Y. & Zong, Z. *In vitro* activity of neomycin, streptomycin, paromomycin and apramycin against carbapenem-resistant Enterobacteriaceae clinical strains. *Front Microbiol* **8**, 2275 (2017).
10. Ishikawa, M. et al. Lower ototoxicity and absence of hidden hearing loss point to gentamicin C1a and apramycin as promising antibiotics for clinical use. *Sci Rep* **9**, 1-15 (2019).
11. Matsushita, T. et al. Design, multigram synthesis, and *in vitro* and *in vivo* evaluation of propylamycin: a semisynthetic 4,5-deoxystreptamine class aminoglycoside for the treatment of drug-resistant Enterobacteriaceae and other Gram-negative pathogens. *J Am Chem Soc* **141**, 5051-5061 (2019).
12. Sati, G.C. et al. Modification at the 2'-position of the 4,5-series of 2-deoxystreptamine aminoglycoside antibiotics to resist aminoglycoside modifying enzymes and increase ribosomal target selectivity. *ACS Infect Dis* **5**, 1718-1730 (2019).

13. Plattner, M., Gysin, M., Haldimann, K., Becker, K. & Hobbie, S.N. Epidemiologic, phenotypic, and structural characterization of aminoglycoside-resistance gene *aac(3)-IV*. *Int J Mol Sci* **21**, 6133 (2020).

14. Magalhaes, M.L. & Blanchard, J.S. The kinetic mechanism of AAC(3)-IV aminoglycoside acetyltransferase from *Escherichia coli*. *Biochemistry* **44**, 16275-83 (2005).

15. Fessler, A.T., Kadlec, K. & Schwarz, S. Novel apramycin resistance gene apmA in bovine and porcine methicillin-resistant *Staphylococcus aureus* ST398 isolates. *Antimicrob Agents Chemother* **55**, 373-5 (2011).

16. Bordeleau, E. et al. ApmA is a unique aminoglycoside antibiotic acetyltransferase that inactivates apramycin. *mBio* **12**, e02705-20 (2021).

17. Quirke, J.C.K. et al. Apralogs: apramycin 5-*O*-glycosides and ethers with improved antibacterial activity and ribosomal selectivity and reduced susceptibility to the aminoacyltranserferase (3)-IV resistance determinant. *J Am Chem Soc* **142**, 530-544 (2020).

18. Stogios, P.J. et al. Potential for reduction of streptogramin A resistance revealed by structural analysis of acetyltransferase VatA. *Antimicrob Agents Chemother* **58**, 7083-92 (2014).

19. Beaman, T.W., Sugantino, M. & Roderick, S.L. Structure of the hexapeptide xenobiotic acetyltransferase from *Pseudomonas aeruginosa*. *Biochemistry* **37**, 6689-96 (1998).

20. Shaw, K.J., Rather, P.N., Hare, R.S. & Miller, G.H. Molecular genetics of aminoglycoside resistance genes and familial relationships of the aminoglycoside-modifying enzymes. *Microbiol Rev* **57**, 138-63 (1993).

21. Franklin, K. & Clarke, A.J. Overexpression and characterization of the chromosomal aminoglycoside 2'-*N*-acetyltransferase of *Providencia stuartii*. *Antimicrob Agents Chemother* **45**, 2238-44 (2001).

22. Hegde, S.S., Javid-Majd, F. & Blanchard, J.S. Overexpression and mechanistic analysis of chromosomally encoded aminoglycoside 2'-*N*-acetyltransferase (AAC(2')-Ic) from *Mycobacterium tuberculosis*. *J Biol Chem* **276**, 45876-81 (2001).

23. Bassenden, A.V. et al. Structural and phylogenetic analyses of resistance to next-generation aminoglycosides conferred by AAC(2') enzymes. *Sci Rep* **11**, 11614 (2021).

24. Jeong, C.S. et al. Structural and biochemical analyses of an aminoglycoside 2'-*N*-acetyltransferase from *Mycolicibacterium smegmatis*. *Sci Rep* **10**, 21503 (2020).

25. Draker, K.A. & Wright, G.D. Molecular mechanism of the enterococcal aminoglycoside 6'-*N*-acetyltransferase: role of GNAT-conserved residues in the chemistry of antibiotic inactivation. *Biochemistry* **43**, 446-54 (2004).

26. Murray, I.A. & Shaw, W.V. *O*-Acetyltransferases for chloramphenicol and other natural products. *Antimicrob Agents Chemother* **41**, 1-6 (1997).

27. Botto, R.E. & Coxon, B. Two-dimensional proton J-resolved NMR spectroscopy of neomycin B. *Journal of Carbohydrate Chemistry* **3**, 545-563 (1984).

28. Hanessian, S., Takamoto, T., Massé, R. & Patil, G. Aminoglycoside antibiotics: chemical conversion of neomycin B, paromomycin, and lividomycin B into bioactive pseudosaccharides. *Canadian Journal of Chemistry* **56**, 1482-1491 (1978).

29. Eneva, G.I., Spassov, S.L., Haimova, M.A. & Sandström, J. Complete 1H and 13C NMR assignments for apramycin, sisomicin and some *N*-and *N*, *O*-polyacetylated aminoglycosides. *Magnetic resonance in chemistry* **30**, 841-846 (1992).

30. Koshland, D.E. Protein shape and biological control. *Scientific American* **229**, 52-67 (1973).

31. Radika, K. & Northrop, D.B. Correlation of antibiotic resistance with Vmax/Km ratio of enzymatic modification of aminoglycosides by kanamycin acetyltransferase. *Antimicrob Agents Chemother* **25**, 479-82 (1984).

32. Bassenden, A.V., Rodionov, D., Shi, K. & Berghuis, A.M. Structural analysis of the tobramycin and gentamicin clinical resistome reveals limitations for next-generation aminoglycoside design. *ACS Chem Biol* **11**, 1339-46 (2016).

33. Fiel, S.B. & Roesch, E.A. The use of tobramycin for *Pseudomonas aeruginosa*: a review. *Expert Rev Respir Med*, 1-7 (2022).

34. Draker, K.A., Northrop, D.B. & Wright, G.D. Kinetic mechanism of the GC*N*5-related chromosomal aminoglycoside acetyltransferase AAC(6')-Ii from *Enterococcus faecium*: evidence of dimer subunit cooperativity. *Biochemistry* **42**, 6565-74 (2003).

35. Boehr, D.D., Jenkins, S.I. & Wright, G.D. The molecular basis of the expansive substrate specificity of the antibiotic resistance enzyme aminoglycoside acetyltransferase-6'-aminoglycoside phosphotransferase-2". The role of Asp-99 as an active site base important for acetyl transfer. *J Biol Chem* **278**, 12873-80 (2003).

36. Han, Q. et al. Molecular recognition by glycoside pseudo base pairs and triples in an apramycin-RNA complex. *Angew Chem Int Ed Engl* **44**, 2694-2700 (2005).

37. Golkar, T. et al. Structural basis for plazomicin antibiotic action and resistance. *Commun Biol* **4**, 729 (2021).

38. Walter, F., Vicens, Q. & Westhof, E. Aminoglycoside-RNA interactions. *Curr Opin Chem Biol* **3**, 694-704 (1999).

39. Lynch, S.R. & Puglisi, J.D. Structural origins of aminoglycoside specificity for prokaryotic ribosomes. *J Mol Biol* **306**, 1037-58 (2001).

40. Vetting, M.W., Hegde, S.S., Javid-Majd, F., Blanchard, J.S. & Roderick, S.L. Aminoglycoside 2'-*N*-acetyltransferase from *Mycobacterium tuberculosis* in complex with coenzyme A and aminoglycoside substrates. *Nat Struct Biol* **9**, 653-8 (2002).

41. Xu, Z. et al. Structural and functional survey of environmental aminoglycoside acetyltransferases reveals functionality of resistance enzymes. *ACS Infect Dis* **3**, 653-665 (2017).

42. Stogios, P.J. et al. Structural and biochemical characterization of *Acinetobacter* spp. aminoglycoside acetyltransferases highlights functional and evolutionary variation among antibiotic resistance enzymes. *ACS Infect Dis* **3**, 132-143 (2017).

43. Wright, G.D. & Ladak, P. Overexpression and characterization of the chromosomal aminoglycoside 6'-*N*-acetyltransferase from *Enterococcus faecium*. *Antimicrob Agents Chemother* **41**, 956-60 (1997).

44. Lewendon, A., Murray, I.A., Shaw, W.V., Gibbs, M.R. & Leslie, A.G. Replacement of catalytic histidine-195 of chloramphenicol acetyltransferase: evidence for a general base role for glutamate. *Biochemistry* **33**, 1944-50 (1994).

45. Ellis, J., Bagshaw, C.R. & Shaw, W.V. Substrate binding to chloramphenicol acetyltransferase: evidence for negative cooperativity from equilibrium and kinetic constants for binary and ternary complexes. *Biochemistry* **30**, 10806-13 (1991).

46. Hindson, V.J. & Shaw, W.V. Random-order ternary complex reaction mechanism of serine acetyltransferase from *Escherichia coli*. *Biochemistry* **42**, 3113-9 (2003).

47. Hindson, V.J., Dunn, S.O., Rowe, A.J. & Shaw, W.V. Kinetic and hydrodynamic studies of the NodL *O*-acetyl transferase of *Rhizobium leguminosarum*: a random-order ternary complex mechanism for acetyl transfer by a roughly spherical trimeric protein. *Biochim Biophys Acta* **1479**, 203-13 (2000).

Extended data

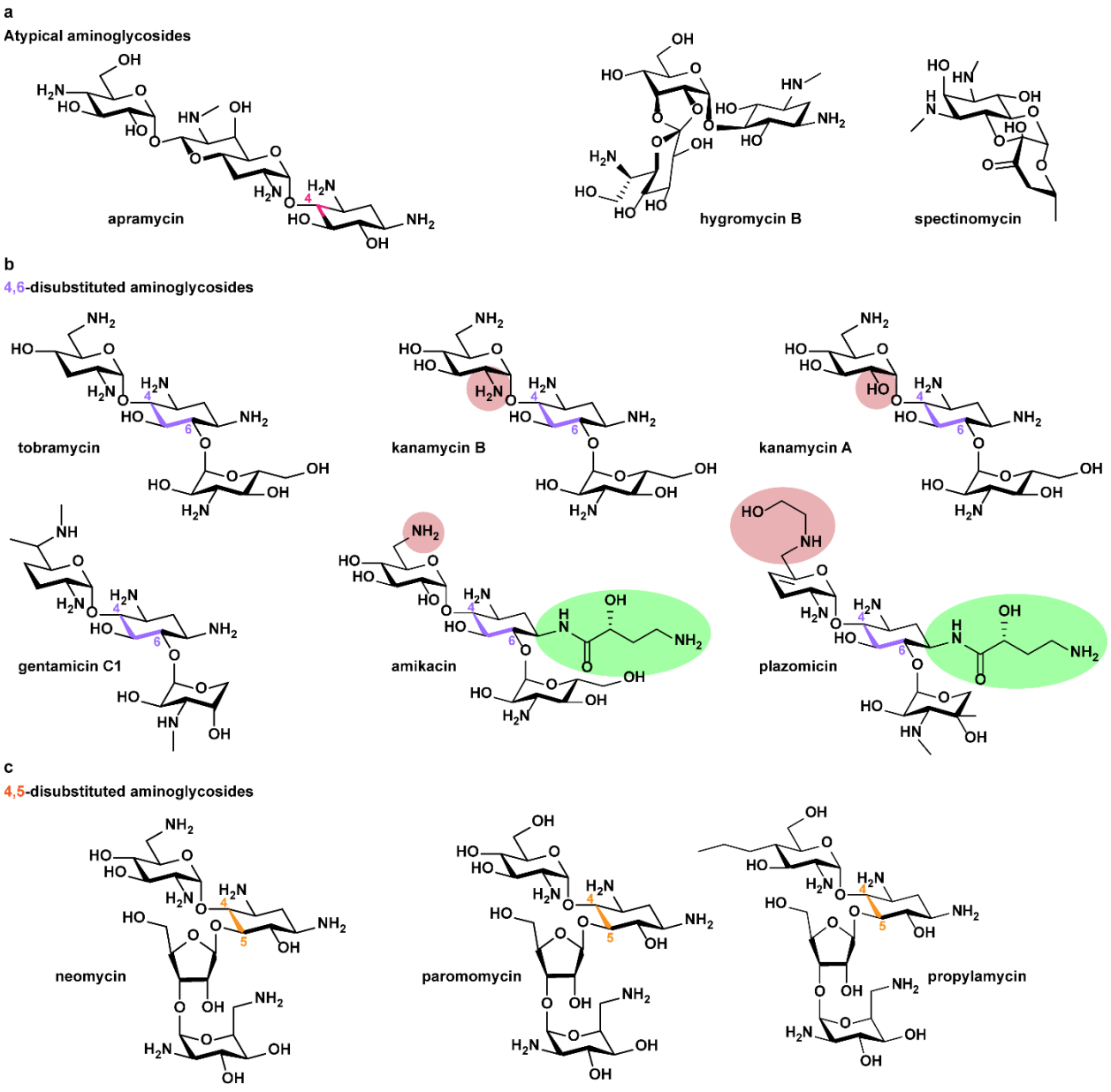

Extended Data Fig. 1. Chemical Structures of AGs referenced in our study and used for antimicrobial susceptibility testing. AGs are group according to structural subclass with carbons coloured to distinguish substitution pattern of 2-DOS ring when present. (a) atypical subclass. (b) 4,6-disubstituted AGs. Kanamycin A and B differ at the 2' position highlighted in red. Amikacin and plazomicin differ at the N6' position (red highlight) but both contain the same substituent at N1. (c) 4,5-disubstituted AGs.

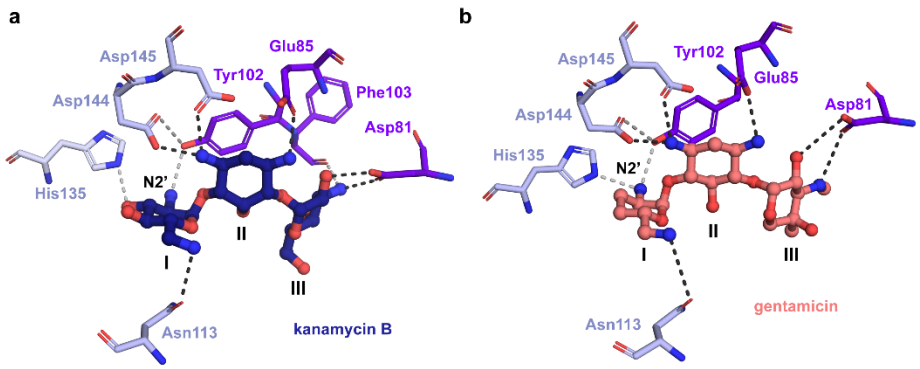

Extended Data Fig. 2. Additional ligand bound crystal structure complexes. Amino acids implicated in binding AGs of different 2-DOS substitution pattern AGs are shown. (a) kanamycin B. (b) gentamicin

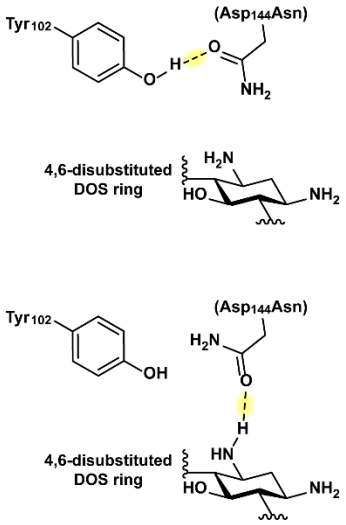

Extended Data Fig. 3. Chemical line representation of Asp144Asn substitution impact on AG binding to ApmA.

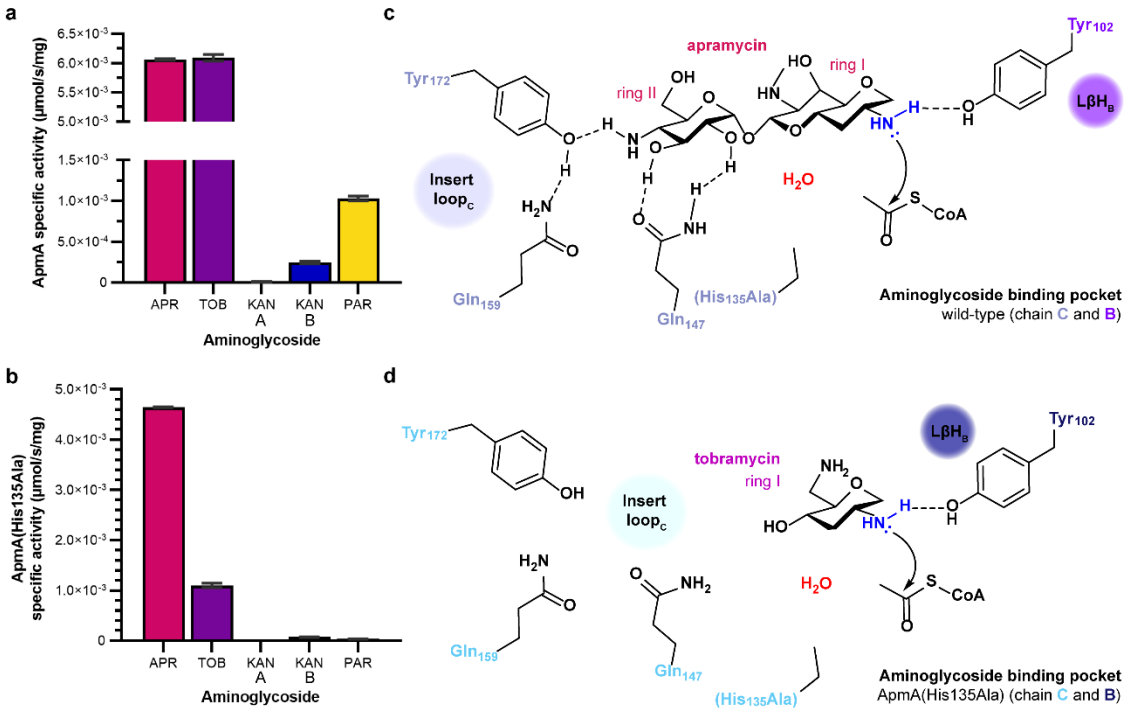

Extended Data Fig. 4. Specific activities for (a) ApmA-mediated acetylation and (b) ApmA(His135Ala)-mediated acetylation of AGs were determined *in vitro* with 1 M AG substrate, 100 µM acetyl-CoA. (c) Chemical line drawing representation of apramycin acetylation mediated by His135Ala mutant. **(d)** Chemical line drawing representation of tobramycin acetylation mediated by His135Ala mutant.

Extended Data Table 1. HR-ESI-MS analysis of ApmA-catalyzed acetylated aminoglycosides in positive ion mode

Modified Aminoglycoside	Molecular formula	Exact mass [M + H]	
		Calculated	Observed
acetyl-neomycin	$C_{25}H_{49}N_6O_{14}$	657.3307	657.3300
acetyl-paromomycin	$C_{25}H_{48}N_5O_{15}$	658.3143	658.3126
acetyl-tobramycin	$C_{20}H_{39}N_5O_{10}$	510.2770	510.2777

Extended Data Table 2. Aminoglycoside susceptibility testing of *E. coli* BW25113 Δ*tolC*Δ*bamB* expressing *apmA* and *apmA* mutants under the control of the P_{bla} promoter

apmA mutant	Aminoglycoside MIC (μg/mL)					
	apramycin	gentamicin	tobramycin	kanamycin B	neomycin	paromomycin
wild-type	64 (4)	2 (0.25)	16 (0.5)	64 – 128 (1)	16 (0.5)	256 (2)
Asp144Ala	4	0.25	0.5	0.5	0.5	1 – 2
Asp144Asn	64	0.25 – 0.5	1	0.5	0.5	1
Asp145Ala	32 – 64	2	8 – 16	8	0.5	32
Glu85Ala	32 – 64	2	8 – 16	8 – 16	0.5 – 1	8 – 16
Tyr102Ala	64	2	8 – 16	4 – 8	0.5 – 1	4 – 8
Ty102Phe	64	2	8 – 16	8	0.5	4 – 8
His135Ala	32 – 64	0.5 – 1	4	0.5	0.5 – 1	2
His135Gln	64	2	16 – 32	64	1	64

Supplementary information

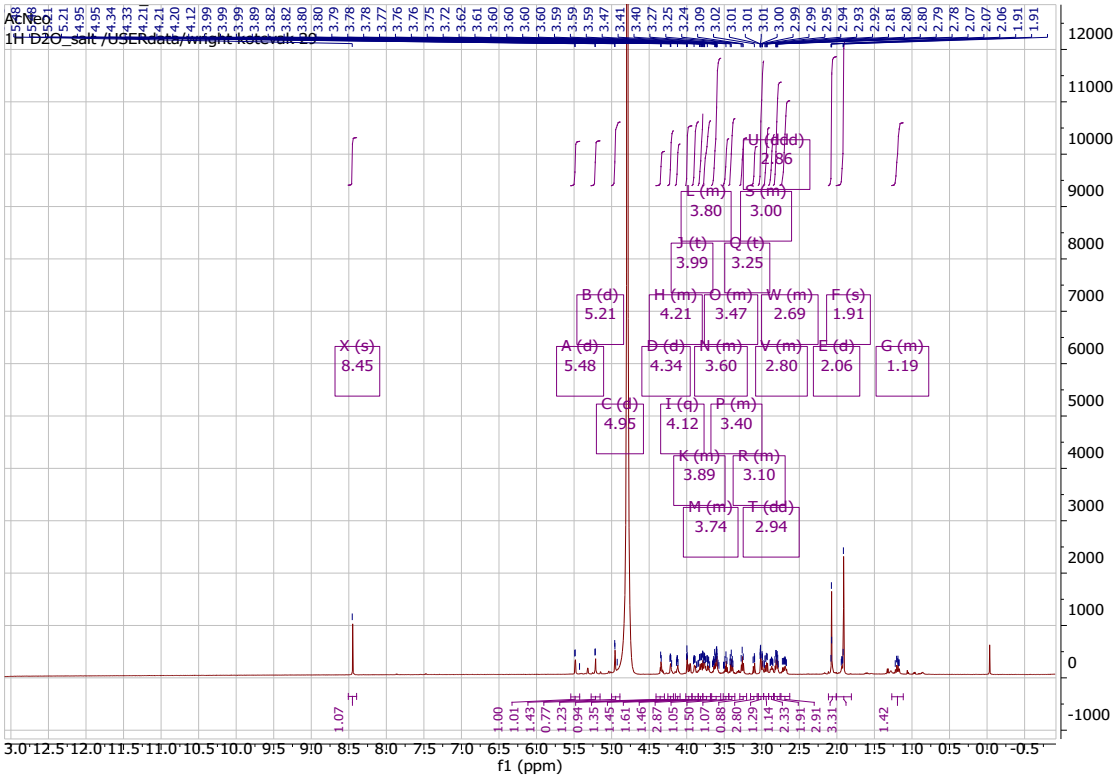

Figure S1. ^{1}H-NMR spectra for 2'-acetyl-neomycin.

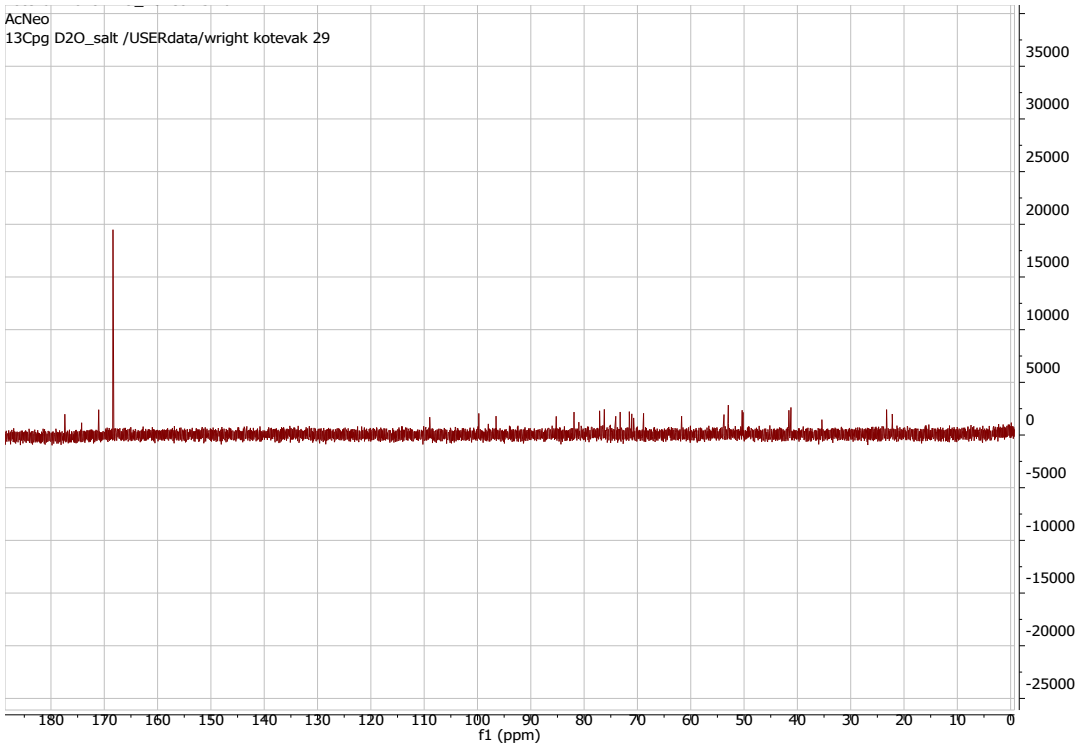

Figure S2. ^{13}C-NMR spectra for 2'-acetyl-neomycin.

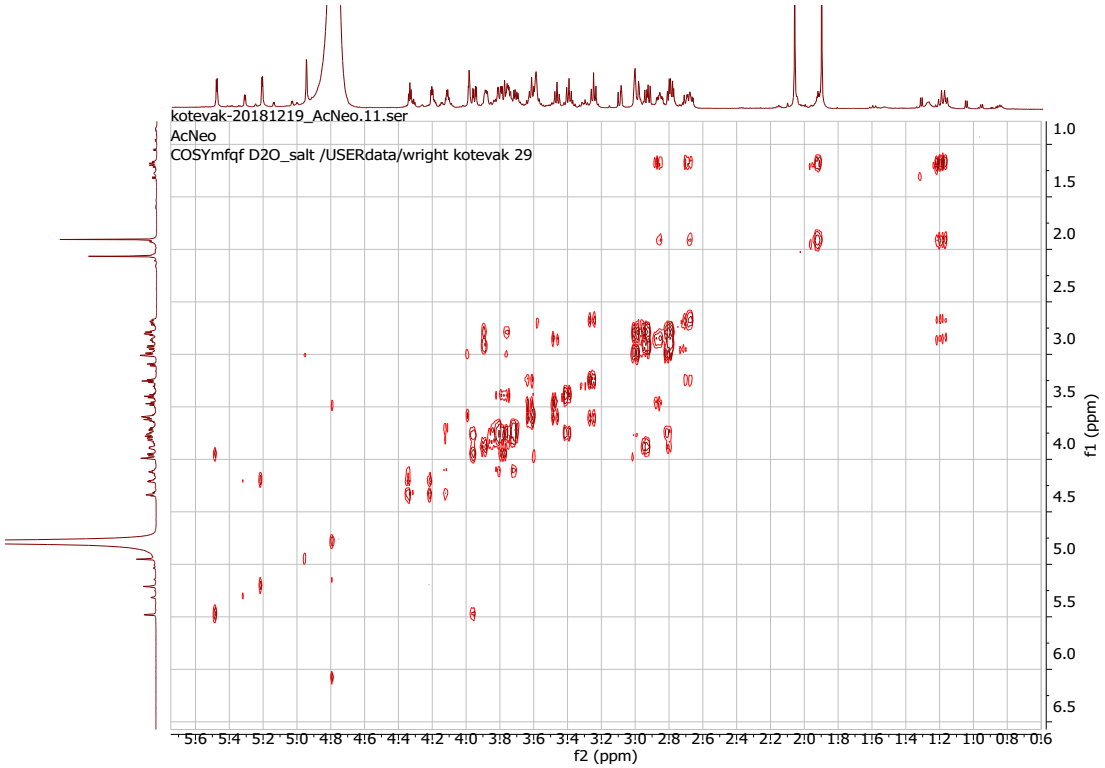

Figure S3. ^{1}H-^{1}H-COSY spectra for 2'-acetyl-neomycin.

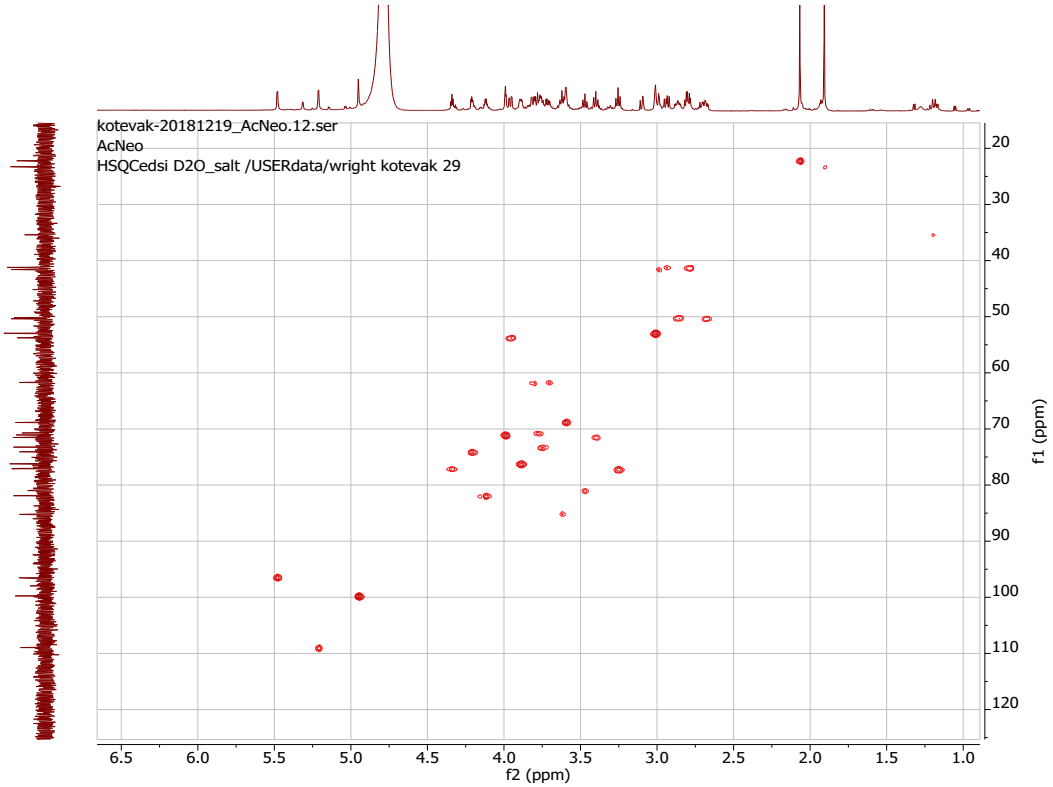

Figure S4. ^{1}H-^{13}C-HSQC spectra for 2'-acetyl-neomycin.

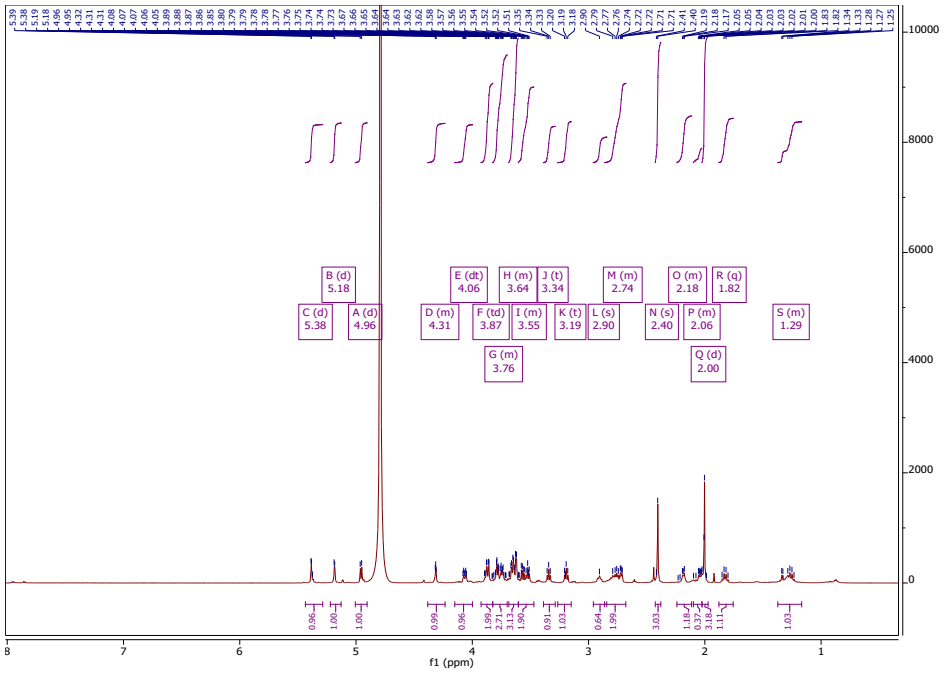

Figure S5. ^{1}H-NMR spectra for 2'-acetyl-paromomycin.

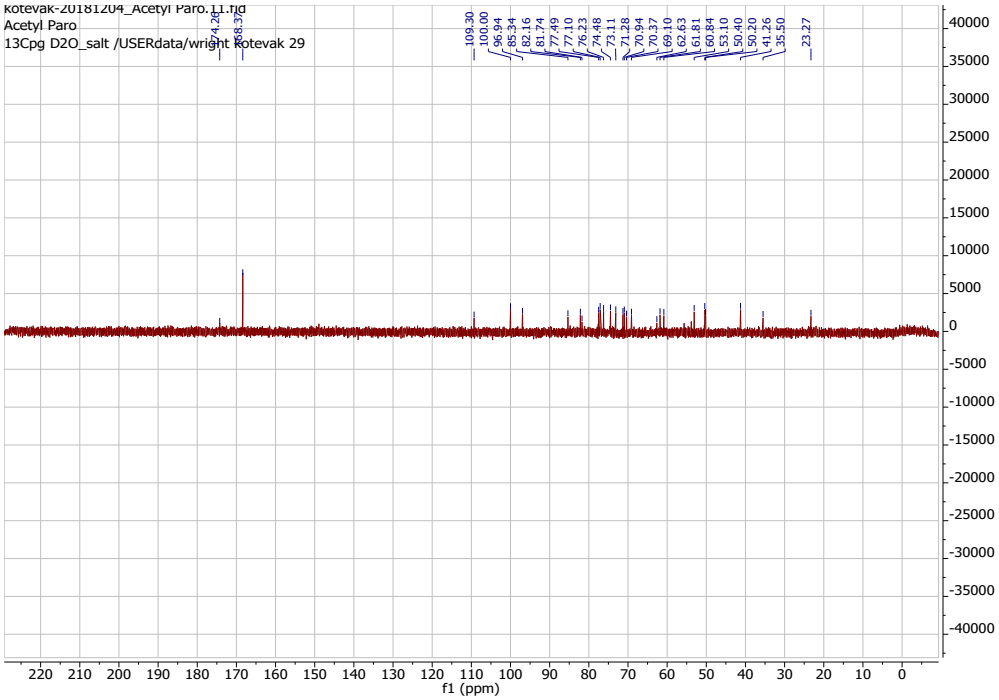

Figure S6. ^{13}C- NMR (Dept-135) spectra for 2'-acetyl-paromomycin.

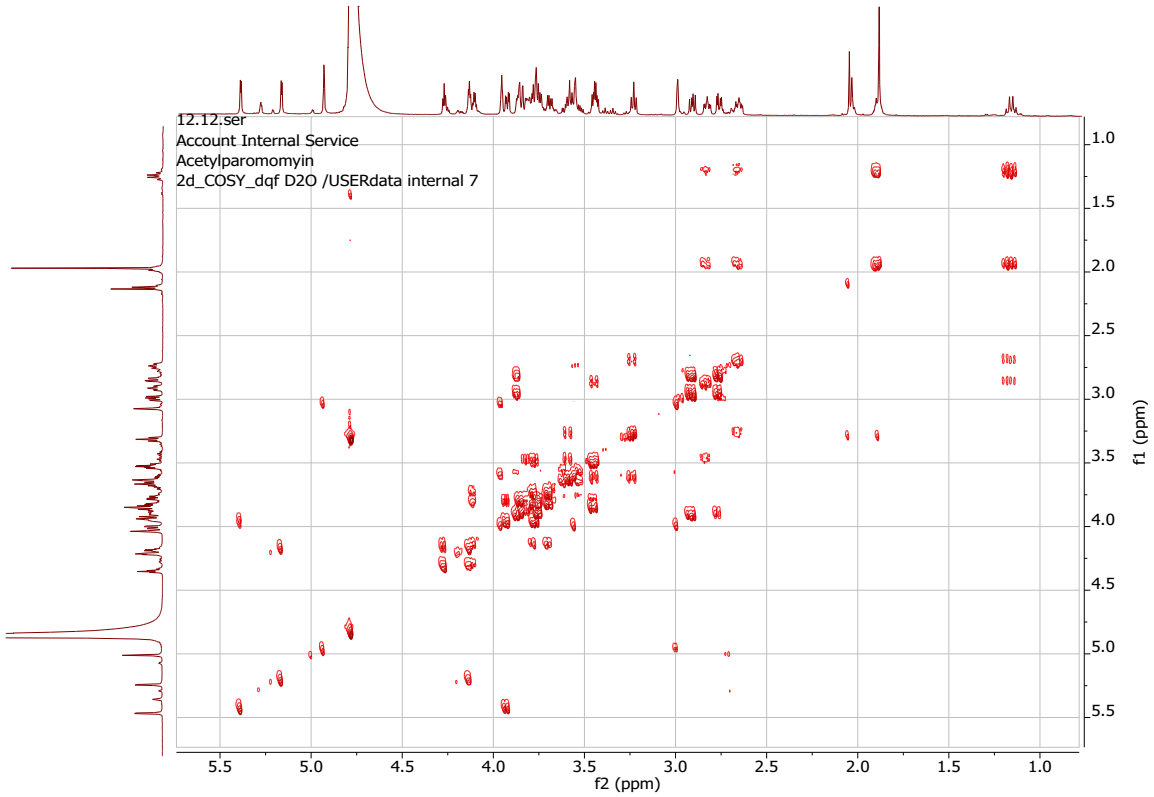

Figure S7. ^{1}H-^{1}H-COSY spectra for 2'-acetyl-paromomycin.

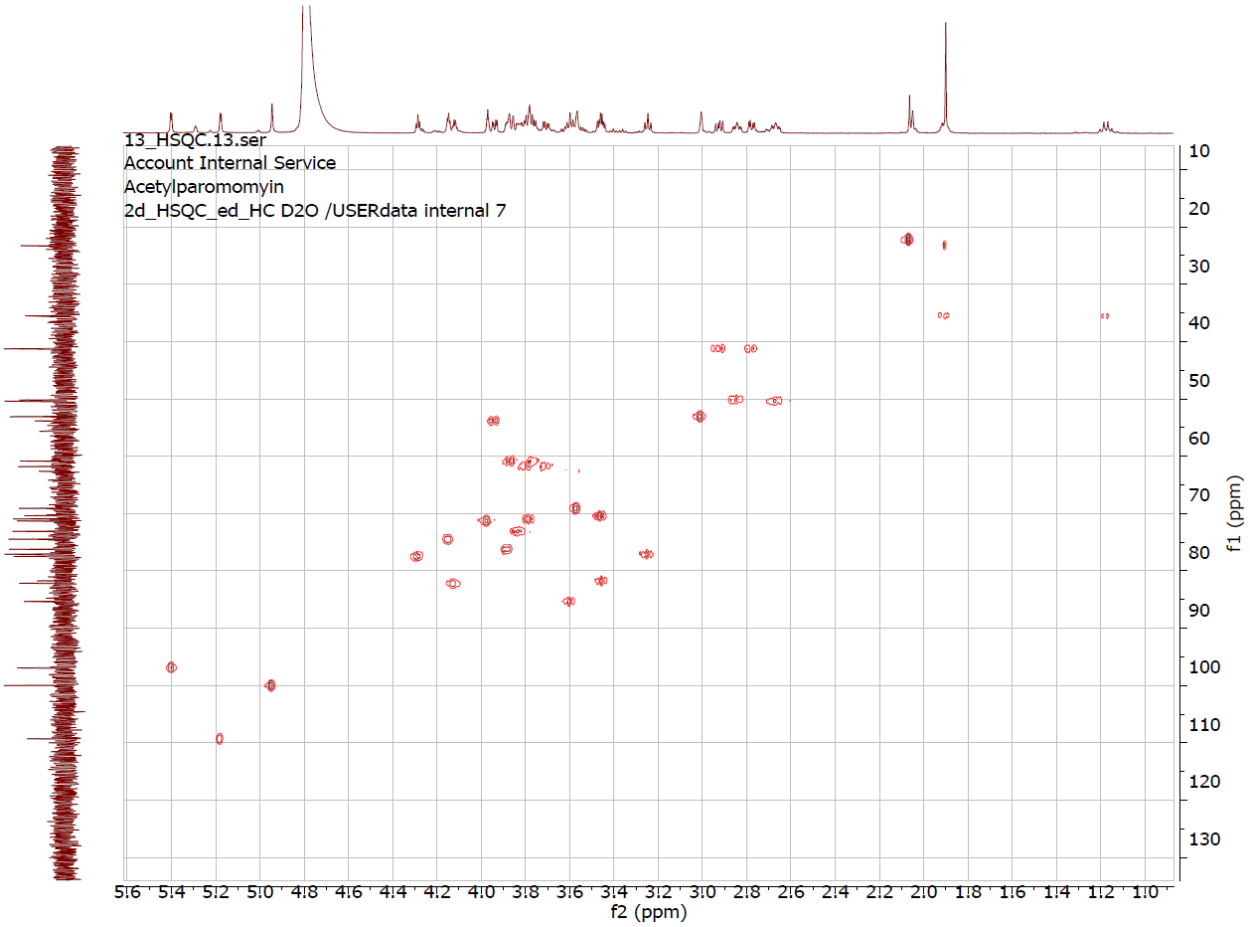

Figure S8. ^{1}H-^{13}C-HSQC spectra for 2'-acetyl-paromomycin.

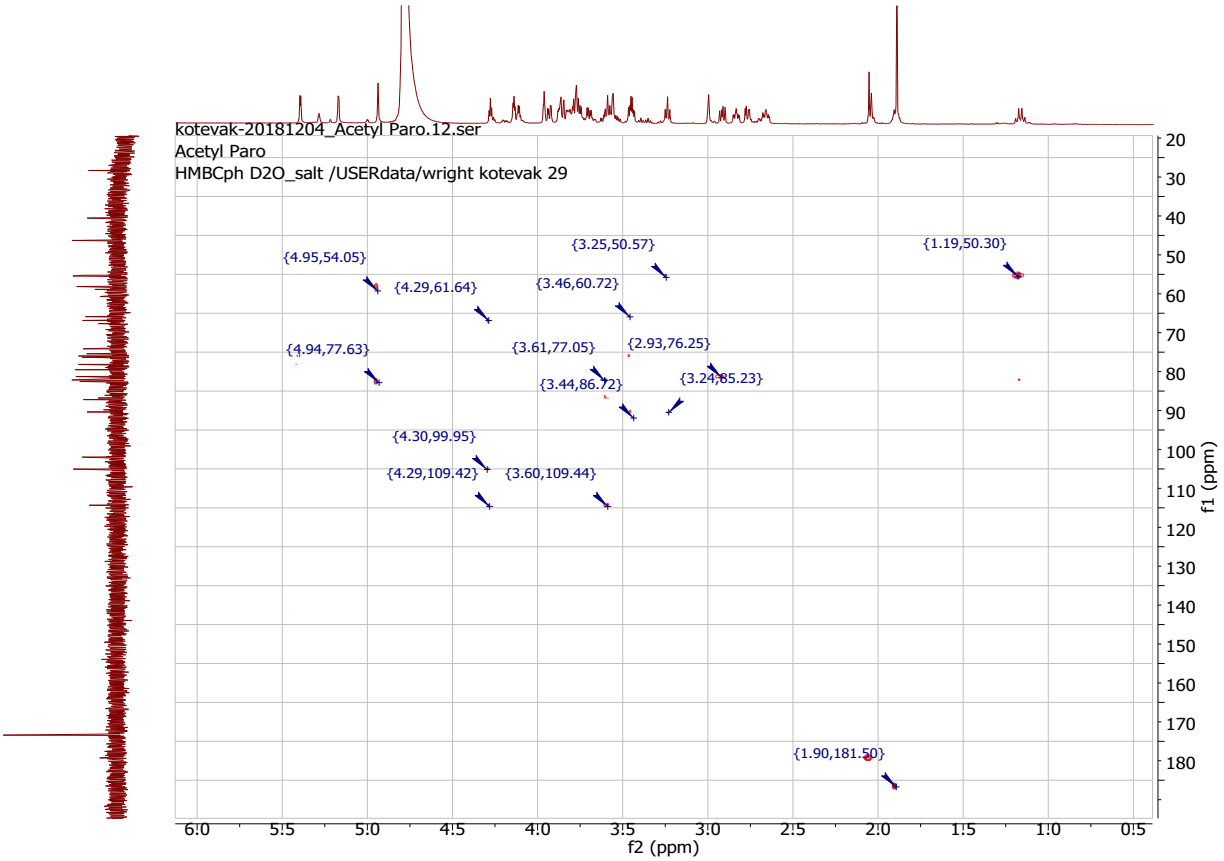

Figure S9. ^{1}H-^{13}C- HMBC spectra for 2'-acetyl-paromomycin.

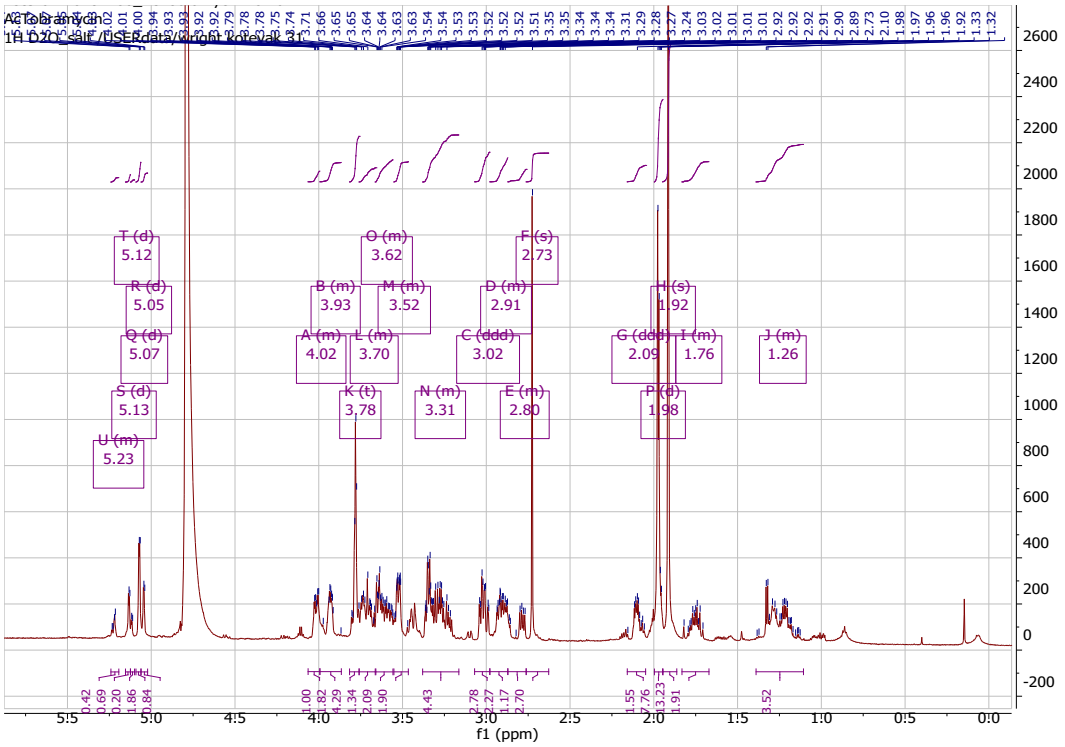

Figure S10. ^{1}H-NMR spectra for 2'-acetyl-tobramycin.

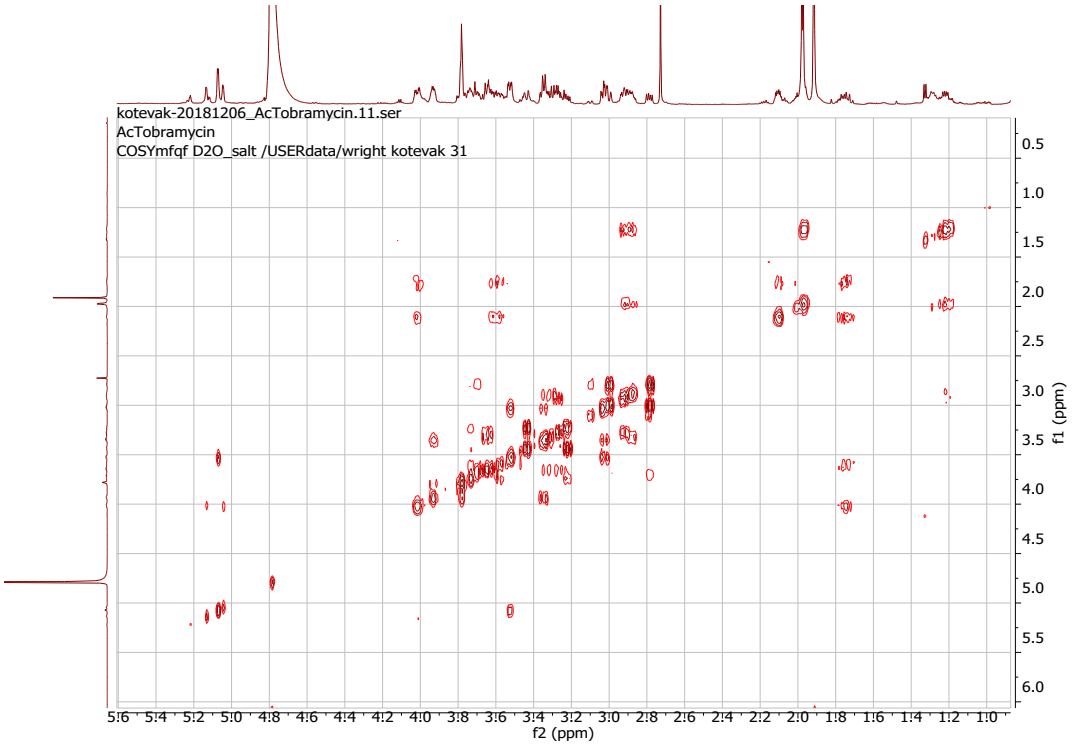

Figure S11. ^{1}H-^{1}H-COSY spectra for 2'-acetyl-tobramycin.

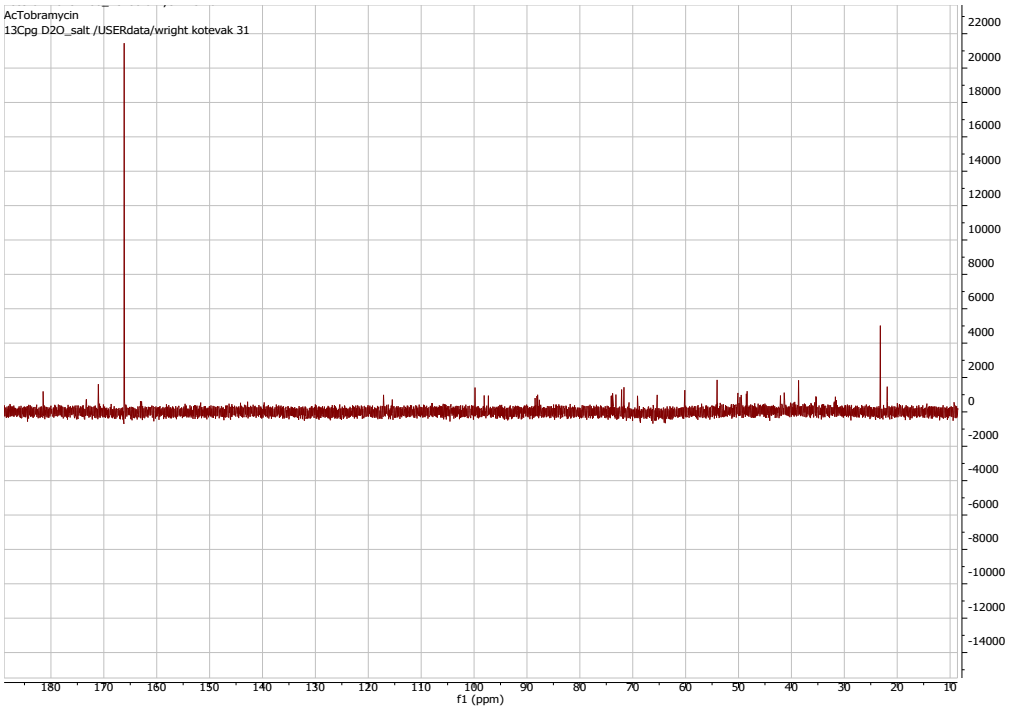

Figure S12. ^{13}C NMR spectra for 2'-acetyl-tobramycin.

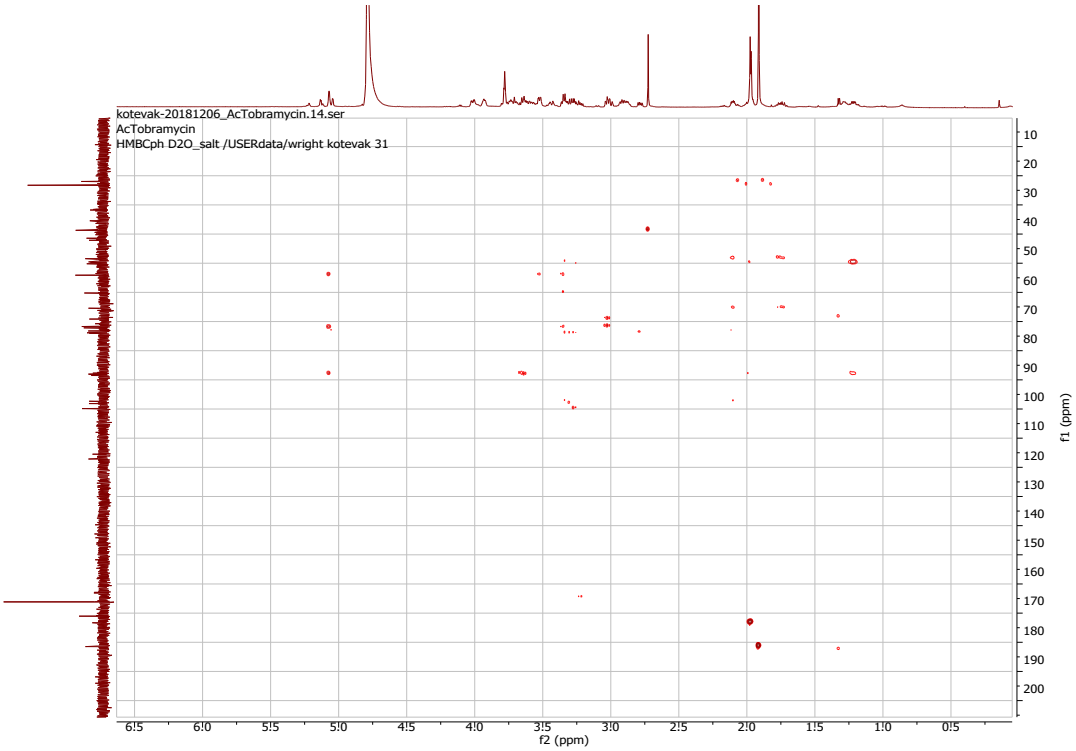

Figure S13. ^{1}H-^{13}C-HMBC spectra for 2'-acetyl-tobramycin.

1627 **Table S1. NMR Assignments for 2'-acetyl-neomycin**

	Neomycin standard		Acetyl-neomycin			
Carbon Number	^{1}H (ppm)[27,28]	^{13}C (ppm)[27,28]	^{1}H (ppm)	^{13}C (ppm)	COSY H #	HMBC C to # H
1	2.72	51.2	2.69 (m, 1H)	50.38	2, 6	2
2	1.95 1.20	36.5	1.92 (m, 1H) 1.19 (m, 1H)	35.65	1,3	
3	2.89	51.2	2.86 (ddd, *J* = 12.5, 9.4, 4.1 Hz, 1H)	50.20	2,4	
4	3.46	83.2	3.47(t, *J* = 9.2 Hz, 1H)	81.14	3,5	
5	3.68	82.4	3.62 (m, 1H)	85.27	4,6	4
6	3.26	78.4	3.25(t, *J* = 9.5 Hz, 1H)	77.11	5,1	5, 2
1'	5.45	100.3	5.48 (d, *J* = 3.8 Hz, 1H)	96.63	2'	
2'	**2.74**	**56.4**	**3.96 (dd, *J* = 10.7, 3.7 Hz, 1H)**	**53.98**	**1',3'**	
2'-NH-CO-**CH$_3$**			**1.91 (s, 3H)**	23.27		
2'-NH-**CO**-CH$_3$			NA	181.18		2' (CO-<u>CH$_3$</u>)
3'	3.61	74.1	3.77 (m, 1H)	70.76	3', 4'	4',1'
4'	3.33	72.2	3.40 (m, 1H)	71.55		6'
5'	3.77	74.1	3.74 (m, 1H)	73.28	6'	1', 4', 6'
6'	3.00 2.82	42.6	2.99 (m, 1H) 2.83(m,1H)	41.66	5'	4'
1"	5.37	109.2	5.18 (m, 1H)	109.00	2"	3", 5
2"	4.29	74.1	4.21 (m, 1H)	74.26	1", 3"	
3"	4.43	77.0	4.34 (t, *J* = 5.1 Hz, 1H)	77.18	2", 4"	1''', 5''
4"	4.14	85.1	4.13 (m, 1H)	82.16	3", 5"	
5"	3.88 3.73	62.3	3.82 (m, 1H) 3.70 (m, 1H)	61.67	4"	3"
1'''	4.96	99.8	4.94 (d, *J* = 1.9 Hz, 1H)	99.86	2'''	3"
2'''	3.02	53.7	3.01(m, 1H)	53.14	1''', 2'''	1''', 4'''
3'''	4.02	71.6	3.99 (t, *J* = 3.2 Hz, 1H)	71.14	2''', 4'''	1'''
4'''	3.64	69.4	3.59(m, 1H)	68.88		6'''
5'''	3.91	77.0	3.88 (m, 1H)	76.22	6'''	6'''
6'''	2.97 2.83	42.1	2.92(dd, *J* = 13.5, 8.7 Hz, 1H) 2.77 (dt, *J* = 13.7, 5.0 Hz, 1H)	41.22	5'''	

1628

Table S2. NMR assignments of 2'-acetyl-paromomycin

Carbon Number	Acetyl-paromomycin			
	^{1}H (ppm)	^{13}C (ppm)	COSY H #	HMBC C to # H
1	2.67 (m, 1H)	50.58	2, 6	2
2	1.92 (m, 1H)	35.50	1,3	
	1.17 (q, *J* = 12.5 Hz, 1H)			
3	2.87 (ddd, *J* = 13.0, 9.4, 4.0 Hz, 1H)	50.20	2,4	
4	3.46 (m, 1H)	81.74	3,5	
5	3.60 (m, 1H)	85.58	4,6	
6	3.24 (t, *J* = 9.5 Hz, 1H)	77.10	5,1	5
1'	5.40 (d, *J* = 3.7 Hz, 1H)	96.94	2'	
2'	**3.94 (dd, *J* = 10.7, 3.7 Hz, 1H)**	54.03	1',3'	
2'-NH-CO-CH$_3$	1.90 (s, 3H)	23.27		
2'-NH-CO-CH$_3$	na	181.5		2' (CO-CH$_3$)
3'	3.78 (m, 1H)	71.02	3', 4'	
4'	3.46 (m, 1H)	81.57	4'.5'	
5'	3.60	85.47	4', 6'	
6'	**3.81 (m, 1H)**	**62.63**	5'	
	3.71(m,1H)			
1"	5.18 (m, 1H)	109.30	2"	3"
2"	4.15 (m, 1H)	74.48	1", 3"	
3"	4.28 (t, *J* = 5.1 Hz, 1H)	77.49	2", 4"	1'''
4"	4.13 (m, 1H)	82.16	3", 5"	
5"	**3.92 (m, 1H)**	**61.02**	4"	3"
	3.83 (m, 1H)			
1'''	4.94 (d, *J* = 1.9 Hz, 1H)	100.00	2'''	3"
2'''	3.01(m, 1H)	53.14	1''', 2'''	
3'''	3.97 (t, *J* = 3.2 Hz, 1H)	**54.02**	2''', 4'''	1'''
4'''	3.76 (m, 1H)		3''', 5'''	
5'''	3.88 (m, 1H)	76.29	4''', 6'''	6'''
6'''	2.77 (dt, *J* = 13.7, 5.0 Hz, 1H)	41.26	5'''	
	2.92 (dd, *J* = 13.5, 8.7 Hz, 1H)			

1632 **Table S3. NMR assignments of 2'-acetyl-tobramycin**

	Tobramycin		Acetyl-tobramycin			
Carbon Number	^{1}H (ppm)[29]	^{13}C (ppm)[29]	^{1}H (ppm)	^{13}C (ppm)	COSY H #	HMBC C to # H
1	2.90	50.4	2.90 (m, 1H)	50.28	2	
2	1.23 1.96	35.5	1.21 (m, 1H) 1.98 (m, 1H)	35.47	1,3	
3	2.90	49.2	2.90 (m, 1H)	49.85	2,4	2,
4	3.33	86.5	3.30 (m, 1H)	88.32	3,5	2,
5	3.64	74.5	3.68 (m, 1H)	74.18	4,6	
6	3.25	88.1	3.30 (m, 1H)	88.66	5	1'',2, 5
1'	5.16	99.7	5.13 (dd, *J* = 11.2, 3.7 Hz, 1H)	97.37	2'	
2'	**2.90**	49.4	**4.03 (m, 1H)**	49.0	1',3'	3'
2'-NH-CO-CH$_3$			**1.91 (s, 3H)**	23.40		
2'-NH-CO-CH$_3$				181.5		**NH-CO-CH$_3$**
3'	1.61 2.03	34.9	1.80 (m,1H) 2.13 (m,1H)	31.71	2',4'	
4'	3.54	66.2	3.63	65.64	3',5'	3'
5'	3.58	73.7	3.71	73.78	4',6'	3', 6'
6'	2.73 2.97	41.6	2.79 (dd, *J* = 13.7, 7.3 Hz, 1H) 3.00 (m,1H)	41.36	5'	
1''	5.05	100.0	5.06 (dd, *J* = 19.0, 3.7 Hz, 1H)	99.81	2''	4''
2''	3.51	71.8	3.53 (m, 1H)	71.88	1'',3''	3''
3''	3.01	54.2	3.03 (m, 1H)	54.21	2'',4''	1'', 2'', 3''
4''	3.33	69.3	3.37 (m, 1H)	69.25	3'',5''	3''
5''	3.92	72.1	3.95 (m, 1H)	72.48	4'',6''	
6''	3.77	60.3	3.78 (t, *J* = 3.7 Hz, 2H)	60.36	5''	

1633

1634 **Table S4. Crystallographic statistics for aminoglycoside•ApmA complexes**

Structure	ApmA•gentamicin	ApmA•tobramycin	ApmA•kanamycin B•CoA
PDB code	7UUJ	7UUK	7UUL
Data collection			
Space group	$P2_12_12_1$	$P2_12_12_1$	$P2_12_12_1$
Cell dimensions			
a, *b*, *c* (Å)	60.8, 107.1, 137.1	62.1, 107.4, 135.0	101.1, 131.7, 157.9
α, β, γ, (°)	90, 90, 90	90, 90, 90	90, 90, 90
Resolution, Å	30.00 – 1.78	30.00 – 2.82	29.47 – 2.26
R_{merge}[a]	0.074 (0.807)*	0.158 (0.702)	0.085 (0.888)
R_{pim}[b]	0.032 (0.376)	0.078 (0.389)	0.034 (0.436)
$CC_{1/2}$	0.999 (0.878)	0.996 (0.655)	0.999 (0.889)
$I / \sigma(I)$	19.1 (1.0)	5.9 (1.0)	22.2 (1.30)
Completeness, %	96.2 (91.0)	96.4 (93.7)	99.4 (9.4)
Redundancy	6.1 (5.0)	5.0 (4.1)	6.9 (4.8)
Refinement			
Resolution, Å	29.85 – 1.78	29.85 – 2.82	29.47 – 2.26
No. unique reflections: working, test	83017, 1983	21441, 1072	96912, 3281
R_{work}/R_{free}[c]	17.3/22.1 (31.7/36.9)	19.9/25.4 (27.3/33.1)	17.3/23.2 (27.5/27.3)
No. atoms			
Protein	6607	6616	13217

Aminoglycoside	93	96	198
Coenzyme A	N/A	N/A	240
Solvent	19	3	86
Water	851	196	1900
B-factors			
Protein	33.1	44.9	37.9
Aminoglycoside	36.2	34.4	32.2
Coenzyme A	N/A	N/A	43.2
Solvent	50.1	53.5	50.0
Water	42.1	39.0	42.6
R.m.s. deviations			
Bond lengths, Å	0.011	0.004	0.012
Bond angles, °	1.110	0.660	1.419
Ramachandran plot			
Favored, %	98.2	96.9	97.7
Allowed, %	1.8	3.1	2.3
Outliers, %	0	0	0

1635

Structure	**ApmA•paromomycin•CoA**	**ApmA•neomycin**	**ApmA(H135A)•tobramycin•CoA**
PDB code	7UUM	7UUN	7UUO
Data collection			
Space group	$P4_332$	$P4_332$	P3
Unit cell			
a, *b, c* (Å)	133.7, 133.7, 133.7	133.6, 133.6, 133.6	108.3, 108.3, 87.7
α, β, γ, (°)	90, 90, 90	90, 90, 90	90, 90, 120

Resolution, Å	50.00 – 2.74	40.90 – 2.83	30.0 – 2.65
R_{merge}	0.197 (1.791)*	0.102 (4.877)	0.144 (1.610)
R_{pim}	0.036 (0.548)	0.016 (0.770)	0.052 (0.605)
$CC_{1/2}$	1.00 (0.527)	1.00 (0.924)	0.998 (0.638)
$I / \sigma(I)$	20.2 (1.3)	54.3 (1.1)	16.7 (1.43)
Completeness, %	100 (100)	99.9 (100)	99.9 (99.9)
Redundancy	30.1 (13.2)	40.9 (40.5)	8.1 (7.5)
Refinement			
Resolution, Å	35.75 – 2.74	24.80 – 2.83	29.45 – 2.65
No. unique reflections:	10423, 940	9940, 786	32941, 1614
working, test			
R_{work}/ R-free	22.4/24.9 (33.7/30.3)	21.3/25.0 (36.3/41.3)	28.8/32.8 (37.0/41.2)
No. atoms,			
Protein	2194	2185	6536
Aminoglycoside	42	42	96
Coenzyme A	48	N/A	48
Solvent	6	4	4
Water	54	92	24
B-factors			
Protein	46.9	82.5	115.6
Aminoglycoside	49.5	87.5	89.4
Coenzyme A	75.2	N/A	150.1
Solvent	40.1	85.4	57.0
Water	37.0	60.1	63.4

R.m.s. deviations			
Bond lengths, Å	0.003	0.005	0.007
Bond angles, °	0.725	0.885	1.082
Ramachandran plot			
Favored, %	97.7	95.9	94.5
Allowed, %	3.3	4.1	5.5
Outliers, %	0	0	0

[a] $R_{merge} = \Sigma_{hkl}\Sigma_j|I_{hkl,j} - \langle I_{hkl}\rangle|/\Sigma_{hkl}\Sigma_j I_{hk,j}$, where $I_{hkl,j}$ and $\langle I_{hk,j}\rangle$ are the *j*th and mean measurement of the intensity of reflection *j*.

[b] $R_{pim} = \Sigma_{hkl}\sqrt{(n/n-1)}\ \Sigma^{n}_{j=1}|I_{hkl,j} - \langle I_{hkl}\rangle|/\Sigma_{hkl}\Sigma_j I_{hk,j}$

[c] $R = \Sigma|F_p^{obs} - F_p^{calc}|/\Sigma F_p^{obs}$, where F_p^{obs} and F_p^{calc} are the observed and calculated structure factor amplitudes, respectively.

N/A = not applicable.

Table S5 Primers for generating *apmA* mutants

Mutation	Oligonucleotide sequence[a]
H135A	5'-AGAGATCCATGCGAAC**GCT**CAGTTAAACATGACCTTTG-3'
H135Q	5'-AGAGATCCATGCGAAC**CAG**CAGTTAAACATGACCTTTG-3'
Y102A	5'-TGGCAGGCAAACG**GCT**TTTGGAGACGGTGTC-3'
Y102F	5'-TGGCAGGCAAACG**TTT**TTTGGAGACGGTGTCG-3'
D144A	5'-ATGACCTTTGTAAGC**GCC**GATATTCAAAACTTCTTCAACG-3'
D144N	5'-ATGACCTTTGTAAGC**AAC**GATATTCAAAACTTCTTCAACG-3'
D145A	5'-ATGACCTTTGTAAGCGAC**GCG**ATTCAAAACTTCTTC-3'
E85A	5'-TTGACGACGAGGGAGGC**GCA**CTTCCGTTTGAACG-3'
N/A (FWD plasmid primer)	5'-CGTACGCATATGAAAACCAG ACTTGAACAAGTTTTAGAACGTTATCTCAAC-3'
N/A (REV plasmid primer)	5'-ATCCGCCTCGAGTTACAAACTCCCGTAC TTTTTCATAAATAGTTCAGGTGATATAAGC-3'

Notes: a. Bolded nucleotides represent change in codon for the desired amino acid substitution. Underlined nucleotides indicate the addition of restriction enzyme sites required for cloning each *apmA* mutant into the pGDP3 vector.

Chapter Four: Structural and molecular rationale for the diversification of resistance mediated by the Antibiotic_NAT family

Preface

The work presented in the following chapter has been published in *Communications Biology – Nature*.

Stogios, P.J., Bordeleau, E., Xu, Z. *et al.* Structural and molecular rationale for the diversification of resistance mediated by the Antibiotic_NAT family. *Commun Biol* **5**, 263 (2022). https://doi.org/10.1038/s42003-022-03219-w

EB completed all antibiotic susceptibility testing, prepared figures, and wrote the manuscript. PJS solved all crystal structures, completed sequence and structural analyses, prepared figures, and wrote the manuscript. ZX performed protein purification and characterization. TS performed protein purification and crystallization. EE performed protein purification and crystallization. SC performed cloning. LTD performed FMG, sequence analysis and prepared figures. AWD and SP performed FMG. GD, GDW and AS oversaw the work and wrote the manuscript.

Abstract

The environmental microbiome harbors a vast repertoire of antibiotic resistance genes (ARGs) which can serve as evolutionary predecessors for ARGs found in pathogenic bacteria, or can be directly mobilized to pathogens in the presence of selection pressures. Thus, ARGs from benign environmental bacteria are an important resource for understanding clinically relevant resistance. Here, we conduct a comprehensive functional analysis of the Antibiotic_NAT family of aminoglycoside acetyltransferases. We determined a pan-family antibiogram of 21 Antibiotic_NAT enzymes, including 8 derived from clinical isolates and 13 from environmental metagenomic samples. We find that environment-derived representatives confer high-level, broad-spectrum resistance, including against the atypical aminoglycoside apramycin, and that a metagenome-derived gene likely is ancestral to an *aac(3)* gene found in clinical isolates. Through crystallographic analysis, we rationalize the molecular basis for diversification of substrate specificity across the family. This work provides critical data on the molecular mechanism underpinning resistance to established and emergent aminoglycoside antibiotics and broadens our understanding of ARGs in the environment.

Introduction

Antibiotic resistance is a global crisis that threatens every class of clinically deployed antibiotic [1]. Antibiotic resistance genes (ARGs) isolated from bacteria that cause life-threatening disease can often be traced to environmental microbial communities (reviewed in [2–4]). To understand the sources of antibiotic resistance, the identification of links connecting ARGs in the clinic with those in the environment, characterization of their horizontal transfer, evolution, and biochemical/molecular properties are focuses of continuing research (reviewed in [4] and [5]). For example, the *mcr* family of plasmid-borne colistin resistance genes is thought to originate from chromosomal genes found in various *Moraxella* and *Aeromonas* species [6–8]. The family of extended-spectrum β-lactamase $bla_{\text{CTX-M}}$ genes found on plasmids of Gram-negative pathogens has been traced to the chromosomal genes of various *Kluyvera* species that are only rarely pathogenic[9]. Given the regular exchange of genetic material harboring ARGs between microbial species, more research is required to understand the breadth and depth of the global resistome, including such aspects as the scope of resistance mechanisms, the specificity and efficiency of ARG products in conferring resistance, and their potential to be mobilized and transferred to pathogens. This comprehensive data is critical for tackling the antibiotic resistance crisis[5,10].

Aminoglycosides (AGs) (**Figure 1**) are widely used to treat infections caused both by Gram-positive and Gram-negative bacteria due to their broad-spectrum activity[11]. Toxicity and resistance are significant problems complicating the use of this class of drugs; nonetheless, they retain value for treating multi-drug and extensively-drug resistant Gram-negative pathogens causing serious infections[12]. Canonical AGs are characterized by a core 2-deoxystreptamine ring with substitutions at the 4- and 6- or 4- and 5- positions. Non-canonical AGs possess variations on the 2-deoxystreptamine core such as streptomycin, or apramycin which contains a fourth ring

structure fused to 2-deoxystreptamine. Apramycin is currently used in veterinary medicine[13,14], and with the notable exceptions of *aac3-IV* and the emerging resistance determinant *apmA* [15,16], few ARGs confer resistance to apramycin, prompting excitement for broader deployment in medicine [17–21].

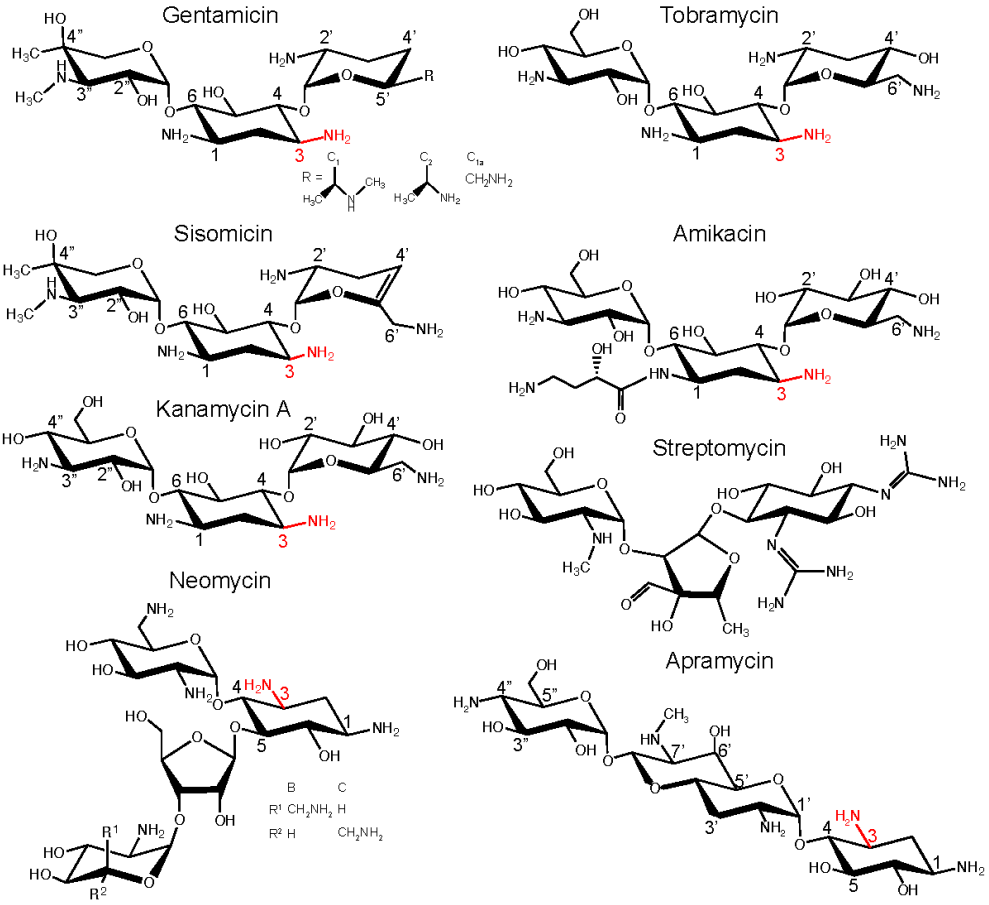

Figure 1. Chemical structures of aminoglycosides. The 3-amino group is highlighted in red.

AG resistance is primarily conferred by three classes of aminoglycoside-modifying enzymes (AMEs): phosphotransferases (APHs), nucleotidylyltransferases (ANTs), and acetyltransferases (AACs)[22]. AMEs permanently alter the AG substrate, preventing them from binding to their target, the A-site of the 16S rRNA in the bacterial ribosome. AMEs are widely disseminated in pathogens. Current research focuses on their specificity, mechanisms, and

inhibition by small molecules to fortify the design of next-generation AG against resistance, as exemplified by the development of plazomicin and apramycin analogs (apralogs, [23–25]).

Previously, we identified 27 AACs in grassland soils microbial communities using a functional metagenomics (FMG) approach [26,27]. These AACs belonged to two sequence and structurally distinct acetyltransferase families - GNAT (GCN5-related *N*-acetyltransferase) and Antibiotic_NAT. These families are distinct in sequence length (approx. 120 residues for GNAT and approx. 220 residues for Antibiotic_NAT) and are classified distinctly by sequence databases (Antibiotic_NAT in Pfam: family Antibiotic_NAT (PF02522), clan Antibiotic_NAT (CL0627) vs GNAT: Acetyltransf_1 (PF00583), Clan Acetyltrans (CL0257) and by structural databases (Antibiotic_NAT in SCOP: Class = Alpha and beta proteins (a/b), Fold = TTHA0583/YokD-like, Superfamily = TTHA0583/YokD-like, Family Aminoglycoside 3-N-acetyltransferase-like vs GNAT: Class Alpha and beta proteins (a+b), Fold: Acyl-CoA N-acyltransferases (Nat), Superfamily: Acyl-CoA N-acyltransferases (Nat), Family: N-acetyltransferase, NAT). Furthermore, the distinction between these two families is reflected in the divergence in the topology of the β-sheet core of each fold, where the Antibiotic_NAT family is centered on a 3-stranded parallel β-sheet while the GNAT family is centered on a 4-stranded antiparallel β-sheet. Finally, the two families utilize distinct enzymatic mechanisms, with Antibiotic_NAT utilizing a catalytic histidine/glutamate dyad [28] while GNAT utilizes a catalytic tyrosine and glutamate pair [29]. For GNAT AACs, we showed that many environment derived ARGs, which we called meta-AACs for metagenomic AACs, possess resistance activity, acetylation efficiency, and structural properties comparable to AMEs derived from drug resistant clinical species[24,26]. Our research established that GNAT meta-AACs include all the qualities necessary to cause high-level resistance if mobilized and transferred to human pathogens.

In contrast to the GNAT family, less is known about the biochemical, structural, and molecular features of the Antibiotic_NAT family. There are approximately 50 of this family members identified[26] and many are highly disseminated in Gram-negative pathogens[30], including AAC(3)-II, AAC(3)-III, and AAC(3)-IVa. The AAC(3)-IIa enzyme possesses narrow AG specificity as it is active only against 4,6-disubstituted compounds, while AAC(3)-IIIa is strongly promiscuous due to its activity against a broad range of 4,5- and 4,6-disubstituted AGs [28,31] . The AAC(3)-IVa enzyme was also shown to be promiscuous against a broad range of 4,5- and 4,6-disubstituted AGs as well as against apramycin[15]. There have been no studies describing the enzymatic characteristics of environment-derived members of this family and no comprehensive family-wide analysis to understand their diversification of structure and function.

Several members of the Antibiotic_NAT family have been structurally characterized, including AAC(3)-IIIb and AAC(3)-VIa [28,32] (note: these were erroneously assigned as members of the GNAT family of AAC enzymes in these publications). Other structurally characterized members of this family include FrbF from *Streptomyces rubellomurinus*[33], YokD from *Bacillus subtilis,* and BA2930 from *Bacillus anthracis*[34], none of which possess activity against AGs.

Here, we report a comprehensive structural and functional analysis of the aminoglycoside-resistance spectrum conferred by Antibiotic_NAT family enzymes through characterization of 13 environment-derived enzymes and 8 derived from clinical isolates. This analysis shows that many confer high-level, broad-spectrum aminoglycoside resistance, and five environment-derived enzymes confer apramycin resistance. Crystallographic analysis of various family members, including meta-AAC0038, AAC(3)-IVa, AAC(3)-IIb, and AAC(3)-Xa, allowed the construction of a molecular model explaining the diversification of substrate specificity in this ARG family.

Results

The Antibiotic_NAT family sequences branch into four distinct clades, with all but one including environment-derived members

Identification of new members of the Antibiotic_NAT family through antibiotic selections of soil metagenomic libraries[35] prompted a revisit of the sequence diversity of this family. Comparative sequence analysis of the family, including these 14 enzymes derived from environmental microbial communities, 12 Antibiotic_NAT enzymes originating from pathogenic strains, and 25 additional representatives identified by BLAST searches of Genbank, confirmed the presence of conserved sequence motifs typical of Antibiotic_NAT enzymes (**Supplementary Figure 1**). This analysis also identified highly variable regions that correspond to residues 62-95, 110-117, 127-142, and 190-212 in meta-AAC0038, along with a variable C-terminal region (**Supplementary Figure 1**). The TxΦHΦAE (where Φ=a hydrophobic residue) sequence motif was previously proposed to contain key catalytic residues of this family [28,32,33] . The glutamate residue in this motif interacts with the histidine serving to increase the basicity of latter residue. The histidine extracts a proton from the AG 3-*N*-amine group, activating it for nucleophilic attack on the acetyl-CoA carbonyl group [28,32,33]. The threonine in this motif is thought to stabilize the tetrahedral intermediate. Similar sequence signatures (residues Thr165-Glu171 in meta-AAC0038, **Supplementary Figure 1**) were identified in all analyzed members of this family, with His and Glu (His168 and Glu171 in meta-AAC0038) along with two glycine residues (Gly122 and Gly158 in metaAAC0038), completely conserved. This motif's threonine (Thr165 in meta-AAC0038) is also conserved in all but one of the analyzed sequences where it is substituted by a chemically similar serine (**Supplementary Figure 1**) [28,32,33].

Bayesian reconstruction of the phylogeny of the Antibiotic_NAT family revealed four main clades (Groups 1 through 4, **Figure 2**). Enzymes identified by our metagenomic sampling

were distributed among all the clades except for Group 2, which exclusively contains sequences derived from *Actinomycetes*. Several meta-AACs such as meta-AAC0038, meta-AAC0016, and meta-AAC0043 appear to be paralogs of AAC(3)-III, AAC(3)-IVa, and AAC(3)-IIa, respectively.

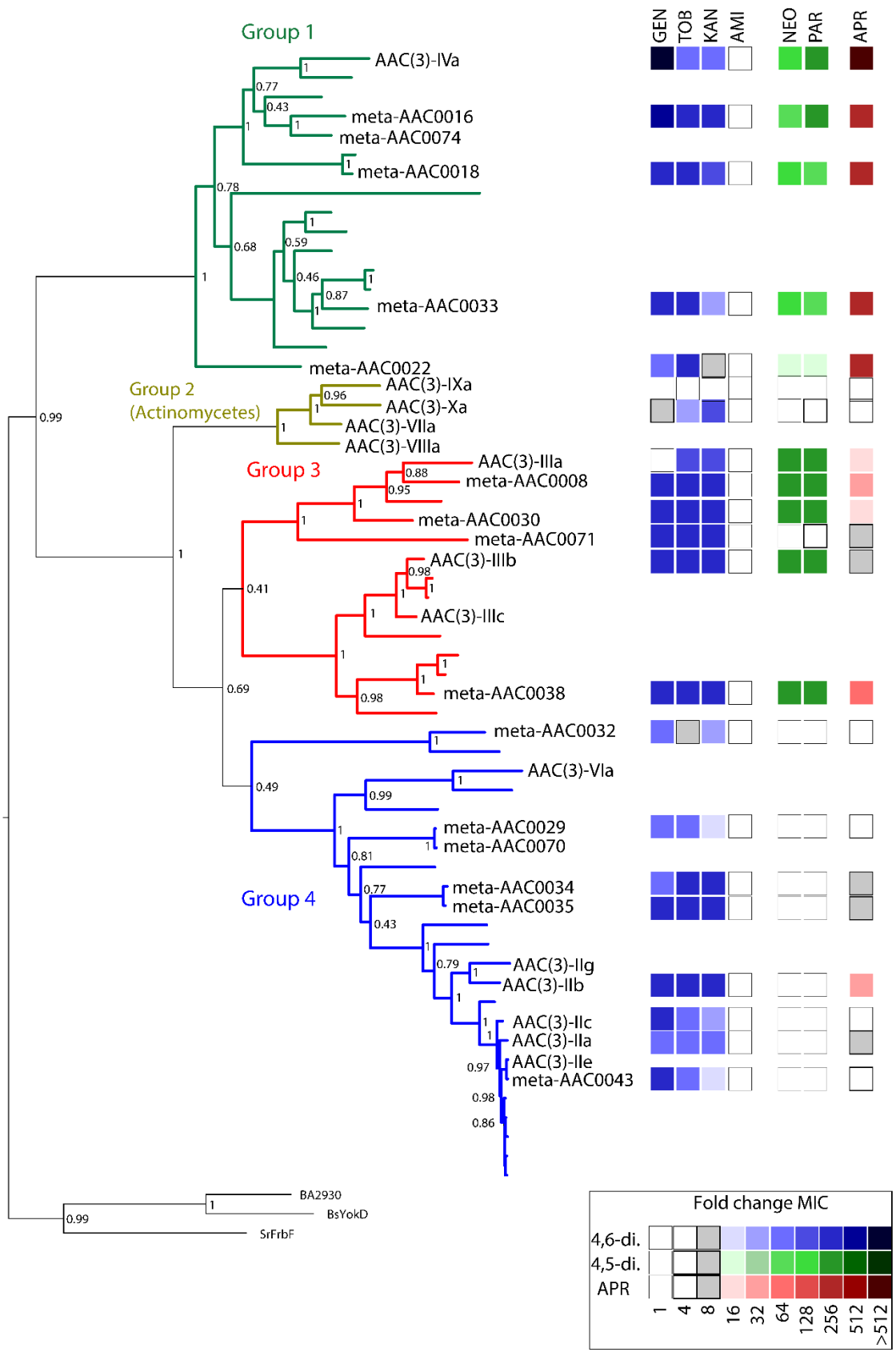
GEN
TOB
KAN
AMI
NEO
PAR
APR
Group 1
AAC(3)-IVa
meta-AAC0016
meta-AAC0074
meta-AAC0018
meta-AAC0033
meta-AAC0022
Group 2
(Actinomycetes)
AAC(3)-IXa
AAC(3)-Xa
AAC(3)-VIIa
AAC(3)-VIIIa
Group 3
AAC(3)-IIIa
meta-AAC0008
meta-AAC0030
meta-AAC0071
AAC(3)-IIIb
AAC(3)-IIIc
meta-AAC0038
meta-AAC0032
AAC(3)-VIa
meta-AAC0029
meta-AAC0070
Group 4
meta-AAC0034
meta-AAC0035
AAC(3)-IIg
AAC(3)-IIb
AAC(3)-IIc
AAC(3)-IIa
AAC(3)-IIe
meta-AAC0043
BA2930
BsYokD
SrFrbF
Fold change MIC
4,6-di.
4,5-di.
APR
1
4
8
16
32
64
128
256
512
>512

1800

Figure 2. Family-wide antibiotic susceptibility mapped onto phylogenetic reconstruction of Antibiotic_NAT family. The four main groups are separately colored. Sequence names are only shown for meta-AAC, clinical isolates of AAC(3) enzymes, and outgroup members with Antibiotic_NAT fold but with no activity against aminoglycosides (FrbF, YokD, and BA2930); other sequences not labeled are hits from BLAST search of NCBI nr database. Node labels are Bayesian probability values. Right side represents a heatmap of AG susceptibility (fold change MIC relative to control strain containing no resistance element), with key shown at bottom right, full data in **Supplementary Table 1**.

Pan-family antimicrobial susceptibility testing aligns substrate specificity with phylogeny

To comprehensively characterize the spectrum and degree of resistance conferred by Antibiotic_NAT family members, we tested the antimicrobial susceptibility of *E. coli* individually harboring the 21 different genes coding for Antibiotic_NAT enzymes on the pGDP3 plasmid[36]. The results (**Figure 2** and **Supplementary Table 1**) show that the spectrum and degree of AG resistance correlate with the phylogenetic clustering. Group 1 members including AAC(3)-IVa and four meta-AACs confer the broadest spectrum and highest degree of resistance to 4,6- and 4,5-disubstituted AGs, consistent with previous studies on AAC(3)-IVa[15], and confer high-level resistance to apramycin. We found that the Group 2 member AAC(3)-Xa, derived from an Actinomycetes, is limited in its AG specificity to the 4,6-disubstituted AGs kanamycin and tobramycin; the only other Group 2 member tested in our host *E. coli* was AAC(3)-IXa did not convey any detectable AG resistance. Group 3 enzymes including AAC(3)-IIIb and four meta-AACs confer resistance to 4,6- and 4,5-disubstituted AGs, consistent with previous data reported for AAC(3)-III enzymes[28,31]; meta-AAC0038 is the lone member of this family that confers resistance to apramycin. Group 4 members are restricted in activity to 4,6-disubstituted AGs, including AAC(3)-IIb/IIc and six meta-AAC enzymes, which is reflective of reports on the resistance profile of AAC(3)-VIa[32,37]; AAC(3)-IIb also confers low-level apramycin resistance.

Notably, each meta-AAC confers AG resistance, with many demonstrating broad-spectrum and high-level resistance, including against apramycin (meta-AAC0016, meta-AAC0018, meta-AAC0033, meta-AAC0030, and meta-AAC0038).

Crystal structures of meta-AAC0038, AAC(3)-IVa, AAC(3)-IIb, and AAC(3)-Xa enzymes show that the variation in the minor subdomain is responsible for diversity in activity against AGs

We undertook a structural genomics campaign to understand the structural basis of the evident diversification of substrate specificity across the Antibiotic_NAT family, with particular interest in the broadly active Group 1 and meta-AAC enzymes. We solved crystal structures of the AAC(3)-IVa, AAC(3)-IIb, AAC(3)-Xa, and meta-AAC0038 enzymes, including ligand-bound states of AAC(3)-IVa and meta-AAC0038. Crystallographic statistics for all determined structures are shown in **Table 1**.

The fold typical of the Antibiotic_NAT family is evident in all structures, composed of 13 α-helices and 8 β-strands (**Figure 3A**), and determined structures superpose with pairwise RMSD's 0.8-1.0 Å between 197 to 266 matching Cα atoms. Notably, the primary sequence most conserved across the family representatives (**Supplementary Figure 1**) belong to what we defined as a major subdomain in the Antibiotic_NAT fold (**Figure 3B**). In contrast, the variable sequence regions identified by our comparative analysis (see above) constitute a minor subdomain (**Figure 3B**). According to this distinction, the major subdomain is centered on a 7-stranded antiparallel β-sheet with a bundle of 5 α-helices arranged on one face of the sheet, with a second bundle of 4 α-helices arranged on the other face of the sheet. The minor subdomain is characterized by four main structural variations that are subfamily-specific, which we called inserts 1 to 4. Insert 1 (**Figure 3B**) forms an extended loop structure of variable length, while adopting a helical structure in AAC(3)-Xa, meta-AAC0038, and AAC(3)-IIb but not in AAC(3)-IVa. Insert 2 forms a short turn

between two α-helices, which most closely impacts the AG binding site. Insert 3 forms a two-stranded antiparallel β-sheet while corresponding to a short α-helix found only in AAC(3)-IIb structure. Finally, insert 4 is a C-terminal extension to the major subdomain unique to AAC(3)-IVa and forms an α-helix and a C3H1 Zn^{2+} binding site. Altogether, this global structural analysis reflects that the minor domain is the principal source of structural diversity among members of this family. A negatively charged cleft is formed in the region between the minor and major subdomains in each structure, with the deepest section formed primarily by the minor subdomain. As will be discussed in detail later, this cleft harbors the AG binding site.

The Antibiotic_NAT enzymes also diversify in their oligomerization state. The meta-AAC0038 adopt dimeric structure with buried surface of ~900 $Å^2$ per subunit (**Figure 3**). This enzyme also forms dimer in solution according to the size exclusion chromatography (not shown). In contrast, the AAC(3)-Xa enzyme exists as a monomer in solution despite forming a dimer in crystal lattice (**Figure 3**). AAC(3)-IVa also adopted a dimeric structure (**Figure 3**) both in crystal and in solution, in line with previous reports on its oligomeric state[15], but the arrangement of the two chains in this enzyme differed from that of the meta-AAC0038 dimer. The buried surface area between subunits of the AAC(3)-IVa dimer (~650 $Å^2$) was formed nearly exclusively through interactions between the major subdomains of the two monomers of this enzyme. Finally, AAC(3)-IIb was monomeric both in the crystal structure or in solution (not shown).

1871 **Table 1. X-ray crystallographic statistics.**

Structure	**Meta-AAC0038^{H29A} apoenzyme**	**Meta-AAC0038^{H168A}•AcCoA**	**Meta-AAC0038^{H168A}•CoA**	**Meta-AAC0038^{H168A}•apramycin•CoA**
PDB code	6MMZ	6MN0	5HT0	7KES
Data collection				
Space group	C2	C2	C2	$P3_12_1$
Cell dimensions				
a, *b*, *c* (Å)	105.8, 158.1, 143.4	108.1, 159.6, 143.3	107.02, 159.50, 146.22	127.77, 127.77, 94.65
α, β, γ, (°)	90, 94.9, 90	90, 94.6, 90	90, 94.7, 90	90, 90, 120
Resolution, Å	25.00 – 3.30	25.00 – 2.40	25.0 – 2.75	30.0 – 2.36
R_{merge}[a]	0.268 (0.743)*	0.094 (0.372)	0.074 (0.440)	0.091 (1.427)
R_{pim}	0.142 (0.395)	0.062 (0.249)	0.085 (0.251)	0.031 (0.505)
$CC_{1/2}$	0.809*	0.949	0.968	0.601
I / σ(I)	6.3 (2.3)	10.75 (2.09)	17.76 (3.19)	21.87 (1.0)
Completeness, %	99.4 (99.9)	99.9 (100)	96.7 (90.4)	100 (100)
Redundancy	4.6 (4.6)	3.3 (3.2)	4.0 (3.7)	9.9 (8.8)
Refinement				
Resolution, Å	19.75 – 3.30	24.93 – 2.39	24.97 – 2.75	29.19 – 2.36
No. unique reflections: working, test	35122, 1646	94715, 1996	60061, 2021	36879, 1846
R_{work}/R_{free}[b]	20.4/26.1 (29.6/38.9)	17.8/20.8 (23.1/28.9)	20.4/23.3 (31.3/30.8)	19.1/22.8 (29.6/34.7)
No. atoms, molecules				
Protein	11977, 6	12033, 6	12016, 6	3992, 2
Aminoglycoside	N/A	N/A	N/A	73, 2
Acetyl-CoA/CoA	N/A	306, 6	288, 6	96, 2
Solvent	104	236	105	25
Water	104	1706	343	170
B-factors				
Protein	59.2	32.9	54.1	70.9
Aminoglycoside	N/A	N/A	N/A	129.0
Acetyl-CoA/CoA	N/A	33.1	52.9	61.9

Structure	Meta-AAC0038^{H29A} apoenzyme	Meta-AAC0038^{H168A}•AcCoA	Meta-AAC0038^{H168A}•CoA	Meta-AAC0038^{H168A}•apramycin•CoA
Solvent	96.2	71.4	108.2	100.5
Water	20.4	43.4	47.7	64.2
R.m.s. deviations				
Bond lengths, Å	0.002	0.005	0.014	0.005
Bond angles, °	0.552	1.770	1.827	1.337

1872

Structure	AAC(3)-IVa apoenzyme	AAC(3)-IVa^{H154A}•APR	AAC(3)-IVa^{H154A}•GEN	AAC(3)-IIb	AAC(3)-Xa
PDB code	6MN3	6MN4	6MN5	7LAO	7LAP
Data collection					
Space group	C2	$P2_12_12_1$	$P2_12_12_1$	$P2_12_12_1$	$P6_322$
Unit cell					
a, *b*, *c* (Å)	114.2, 55.3, 94.3	77.6, 103.5, 264.9	77.6, 131.9, 266.9	43.2, 61.4, 112.0	161.5, 161.5, 138.7
α, β, γ, (°)	90, 102.6, 90	90, 90, 90	90, 90, 90	90, 90, 90	90, 90, 120
Resolution, Å	30.00 – 2.39	30.00 – 2.80	40.0 – 2.58	40.0 – 1.92	50.0 – 2.04
R_{merge}[a]	0.141 (0.997)	0.183 (1.771)	0.086 (0.542)	0.080 (0.332)	0.098 (1.074)
R_{pim}	0.080 (0.572)	0.063 (0.613)	0.048 (0.371)	0.037 (0.159)	0.024 (0.396)
$CC_{1/2}$	0.524	0.776	0.703	0.524	0.593
I / σ(I)	9.98 (1.25)	12.77 (1.40)	14.08 (1.08)	26.19 (3.13)	31.42 (1.08)
Completeness, %	98.8 (99.9)	95.2 (97.1)	95.7 (82.0)	95.8 (79.8)	99.5 (92.9)
Redundancy	3.9 (3.9)	9.0 (8.9)	3.7 (2.5)	5.4 (4.7)	17.2 (6.6)
Refinement					
Resolution, Å	30 – 2.39	29.33 – 2.80	38.4 – 2.58	35.32 – 1.92	49.39 – 2.04
No. unique reflections: working, test	22587, 1129	63643, 3627	83240, 2000	22528, 2167	66736, 3279
R-factor/free *R*-factor[b]	18.2/22.8 (27.1/32.2)	26.1/32.1 (35.3/41.1)	18.7/22.1 (26.8/28.1)	18.0/22.9 (23.6/29.4)	16.5/19.8 (28.7/31.5)
No. refined atoms, molecules					
Protein					
Aminoglycoside	3921, 2	11564, 6	11824, 6	2045, 1	4421, 2

Structure	**AAC(3)-IVa apoenzyme**	**AAC(3)-IVa^{H154A}•APR**	**AAC(3)-IVa^{H154A}•GEN**	**AAC(3)-IIb**	**AAC(3)-Xa**
Acetyl-CoA/CoA	N/A	186, 5	186, 6	N/A	N/A
Solvent	N/A	N/A	N/A	N/A	N/A
Water	3	5	422	17	58
	176	330	519	211	678
B-factors					
Protein	48.7	90.4	91.2	50.8	53.1
Aminoglycoside	N/A	111.0	142.9	N/A	N/A
Acetyl-CoA/CoA	N/A	N/A	N/A	N/A	N/A
Solvent	53.3	86.7	98.0	70.3	105.8
Water	39.6	61.4	72.6	45.7	63.2
r.m.s.d.					
Bond lengths, Å	0.004	0.006	0.006	0.014	0.012
Bond angles, °	0.803	1.071	0.879	1.260	1.118

*All values in brackets and all $CC_{1/2}$ values refer to highest resolution shells.

[a] $R_{merge} = \Sigma_{hkl}\Sigma_j|I_{hkl,j} - \langle I_{hkl}\rangle|/\Sigma_{hkl}\Sigma_j I_{hk,j}$, where $I_{hkl,j}$ and $\langle I_{hkl}\rangle$ are the *j*th and mean measurement of the intensity of reflection *j*.

[b] $R_{pim} = \Sigma_{hkl}\sqrt{(n/n-1)}\ \Sigma^{n}_{j=1}|I_{hkl,j} - \langle I_{hkl}\rangle|/\Sigma_{hkl}\Sigma_j I_{hk,j}$

[c] value refers to highest resolution shell.

[d] $R = \Sigma|F_p^{obs} - F_p^{calc}|/\Sigma F_p^{obs}$, where F_p^{obs} and F_p^{calc} are the observed and calculated structure factor amplitudes, respectively.

ND = not determined

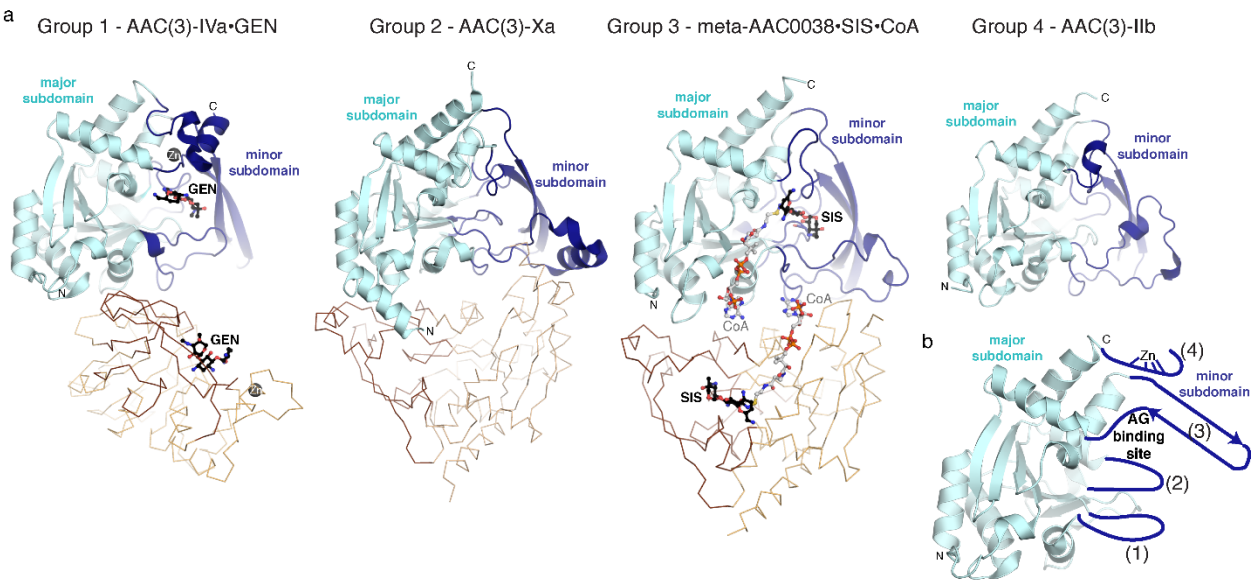

Figure 3. Structures of AAC(3)-IVa, AAC(3)-Xa, meta-AAC0038, and AAC(3)-IIb. a) As representatives of groups 1 through 4, respectively. The conserved major subdomain of the Antibiotic_NAT fold is colored in cyan; the variable minor subdomain is colored in dark blue. Zn^{2+} ion bound to AAC(3)-IVa is shown as a dark grey sphere. Ligands bound to AAC(3)-IVa and meta-AAC0038 are shown in sticks and labeled. b) Schematic of structural variations in the minor subdomain as insertions or extensions to the major subdomain, numbered 1 through 4.

Structural analysis of the group 1 enzyme AAC(3)-IVa suggests a mechanism for broad specificity against AG substrates

To understand the structural basis of the highly promiscuous nature of group 1 Antibiotic_NAT enzymes, we pursued structural characterization of AAC(3)-IVa representative of this clade in complex with AG substrates. To increase the chances of capturing substrate-bound enzyme complex we used catalytically impaired His154Ala mutant of AAC(3)-IVa.

Using this strategy, we were able to determine the crystal structures of AAC(3)-IVa enzyme in complex with gentamicin or apramycin to 2.6 and 2.8 Å, respectively. In both complex structures, the electron density corresponding to the AG molecule localized to the cleft between major and minor subdomains of the enzyme. Most of the AG substrate interactions with the protein are mediated by amino acid sidechains from the minor subdomain (**Figure 4A, 4B, 4C**). For the AG substrate in both structures, the 3-*N* group is positioned close to residue 154 and proximal to

the presumed location of the thiol of CoA. We observe similar substrate orientation in the crystal structures of meta-AAC0038 enzyme complexes, described below, suggesting a common active site topology for this family.

In the complex structures, the gentamicin molecule spans across enzyme's minor subdomain while the apramycin molecule is twisted nearly 90° relative to gentamicin. This difference is reflected in the rotation of the 2-deoxystreptamine rings of each compound being rotated (**Figure 4B**). The 2-deoxystreptamine/II ring of apramycin stacks against the sidechain of Trp63, and its rotation positioned the central and III rings more into the minor subdomain cleft and towards Asp67. Notably, these two residues are contributed from the much shorter hairpin connecting the α4 and α5 helices compared to the equivalent region in the other enzymes we crystallized. Additionally, Glu185 appears to be a critical residue for interactions with gentamicin and apramycin as it positions the 2-deoxystreptamine ring for modification through interactions with the 1-*N* of gentamicin or the 5-hydroxyl of apramycin. Interestingly, Cys190, which is just N-terminal to the Zn^{2+} binding site, interacts with the 3-*N* of gentamicin. Finally, the C-terminal extension of AAC(3)-IVa corresponding to residues 236-257 contributes to the interactions with both gentamicin and apramycin via Glu249 side chain.

We identified a Zn^{2+} ion binding site in the C-terminal extension of AAC(3)-IVa structure. This feature may be of only structural significance since neither this ion nor the sidechains of its cysteine and histidine ligands formed any interactions with the AGs. The binding of Zn^{2+} could stabilize this region and allow for orientation of the Glu249 residue for AG recognition. The Zn^{2+}-binding residues are fully conserved across Antibiotic_NAT Group 1 representatives.

The analysis of the AAC(3)-IVa•gentamicin complex allowed to propose a mechanism for this enzyme's ability to recognize 4,5-disubstituted AGs. In the complex structure, gentamicin's

5-OH pointed out of enzyme's active site. If similarly oriented, 4,5-disubstituted AGs would not cause a steric clash with this enzyme's active site. Collectively, these observations show that AGs can adopt multiple bound orientations facilitated by the dramatic structural changes in the minor subdomain of AAC(3)-IVa, thereby supporting broad substrate specificity for AG modification.

The meta-AAC0038 enzyme active site's molecular architecture allows for activity against 4,5 and 4,6-disubstituted AGs

Our data presented above demonstrated that the environmental metagenome-derived meta-AAC0038 enzyme can confer high and broad resistance to AGs including to the atypical AG - apramycin when expressed in *E. coli*. Using the catalytically inactive His168Ala mutant of this enzyme, we were able to determine the crystal structures of ternary meta-AAC0038^{H168A}•apramycin•CoA and the binary meta-AAC0038^{H168A}•acetyl-CoA complexes.

In line with the previously discussed Antibiotic_NAT enzyme structures, meta-AAC0038 accommodated the substrates in the negatively charged cleft formed by the minor subdomain, with the 3-*N* group of apramycin located within 2.6 Å of the sulfhydryl group of CoA (**Figure 4C**). Notably, the I and III rings of apramycin were positioned out from the active site cleft and did not form interactions with the enzyme except for hydrogen bonds with the Asp94 and Asp162 sidechains. The ability to retain this AG molecule in the active site via very few contacts could explain the activity of meta-AAC0038 on this substrate resulting in the low-level resistance to apramycin which was not detected for the other representatives of Group 3 Antibiotic_NAT enzymes.

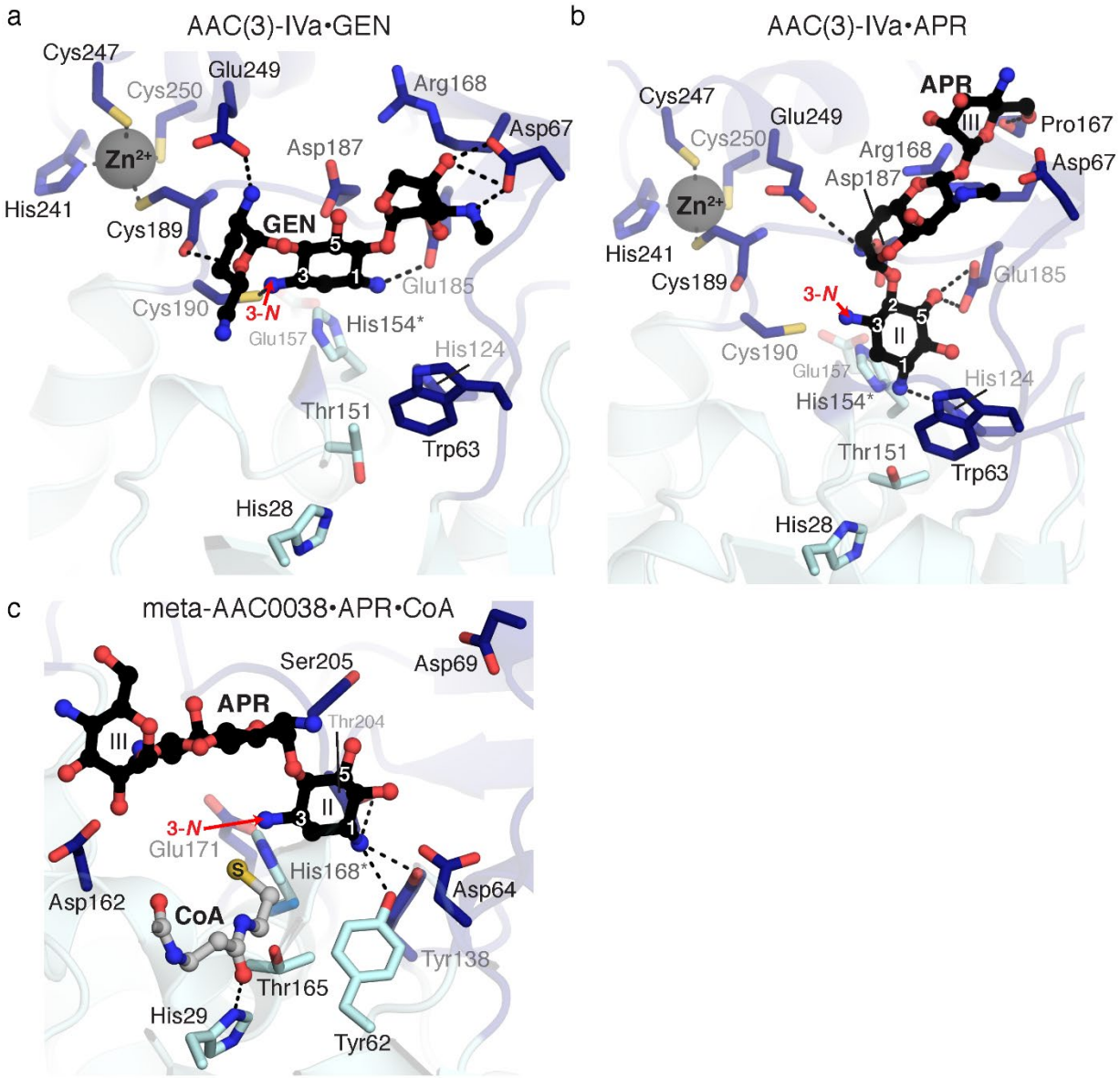

Figure 4. Details of molecular recognition of aminoglycosides by meta-AAC0038 and AAC(3)-IVa. a) From solved crystal structures, active sites of AAC(3)-IVa^{H154A} and gentamicin, b) AAC(3)-IVa^{H154A} and apramycin, c) meta-AAC0038^{H168A} and apramycin and CoA. Dashes indicate hydrogen bonds. Since each protein was crystallized with inactive mutants, His168Ala of His154A mutations for meta-AAC0038 and AAC(3)-IVa, respectively, these sidechains shown in this figure are from the apoenzyme structures and indicated with asterisks. Residues colored in dark and light blue are from the major and minor subdomains of the two enzymes, respectively. Acetylation sites (3-*N* groups) are labeled with red arrows.

AAC(3)-IIIb, another group 3 enzyme, has been previously characterized in detail for its interactions with 4,6- and 4,5-disubstituted AGs[28]. The meta-AAC0038 and AAC(3)-IIIb structures superimpose with RMSD 0.54 Å across 219 Cα atoms, share all the minor subdomain

structural elements, and show complete conservation of AG binding residues (**Fig. 4C**). However, the position corresponding to Glu223 in AAC(3)-IIIb is occupied by Asp213 in meta-AAC0038. Glu223 is positioned at the ring I binding site of apramycin, which may impact the ability of AAC(3)-IIIb to accommodate this AG as a substrate.

The group 4 enzyme AAC(3)-IIb harbors a restricted active site

The crystal structure of AAC(3)-IIb represents the first molecular image of enzymes with AAC(3)-II activity. Its structure superimposes with RMSD 0.7 Å over 221 Cα atoms with the previously characterized AAC(3)-VIa structure[32], consistent with our phylogenetic analysis placing both these enzymes in the group 4 of the Antibiotic_NAT family. Similarly to the AAC(3)-VIa enzyme[32], the minor subdomain loop of AAC(3)-IIb contains the conserved Asn208, which is predicted to clash with substituents at position 5 of the AG substrate, thereby explaining the lack of activity toward 4,5-disubstituted AGs. Other notable amino acids in the active site of AAC(3)-IIa that may restrict the size and positioning of AG substrates include Tyr66, positioned near the binding location of the double prime ring (**Figure 1**), and Phe97, positioned near the central 2-deoxystreptamine ring. Altogether, AAC(3)-IIb – like AAC(3)-VIa – harbors a more restricted active site, consistent with its limited AG specificity.

AAC(3)-Xa also harbors a restricted AG binding site

As indicated by our AG susceptibility testing, the activity of AAC(3)-Xa is limited to tobramycin and kanamycin (**Figure 2**). To rationalize this strict specificity, we modeled the position of kanamycin into the active site of the apoenzyme structure based on the position of gentamicin bound to AAC(3)-IVa. This analysis suggested that gentamicin would not be

accommodated due to the Tyr79 and Asp130 residues, which would clash with the 4”-OH group or the methylated 3”-amine of the corresponding AG substrate, respectively. This model also provides a hypothesis for the inability of this enzyme to confer resistance to 4,5-disubstituted AGs, as the 5-substituents would clash with Glu220 of the enzyme. Based on comparative analysis of the AAC(3)-Xa and AAC(3)-IVa•apramycin complex structures, Tyr79 would also introduce a steric clash with this AG in the AAC(3)-Xa active site. Notably, Tyr79, Asp130, Glu220, and adjacent active site residues are highly conserved in Antibiotic_NAT Group 2 (**Supplementary Figure 1**), suggesting these are critical determinants for restricting the specificity of these enzymes.

Genetic elements adjacent to meta-AACs suggest possible mobilization mechanisms

To investigate the potential for lateral transfer of meta-AACs, we searched for mobile genetic elements (MGEs) on the AAC-encoding contigs. Of the genes recovered through FMG, only one - *meta-AAC0043* - is syntenic with multiple MGEs. This sequence is co-localized on our phylogeny (**Figure 1**) with *aac(3)-IIe*, suggesting a close evolutionary relationship. This finding is in line with the observation that all 28 gentamicin-selected FMG contigs annotated with a gene encoding an AAC(3)-II family enzyme were syntenic with at least one MGE. Worryingly, this contig shows extremely high similarity to sequences found in both chromosomes and plasmids of pathogens like *E. coli, K. pneumoniae, C. freundii,* and *V. cholerae* (**Figure 5**). Taken together, our analysis demonstrates that representatives of Antibiotic_NAT family encoded by environmental microbiome can be directly mobilized across taxonomic boundaries to convey resistance in clinically important bacterial species.

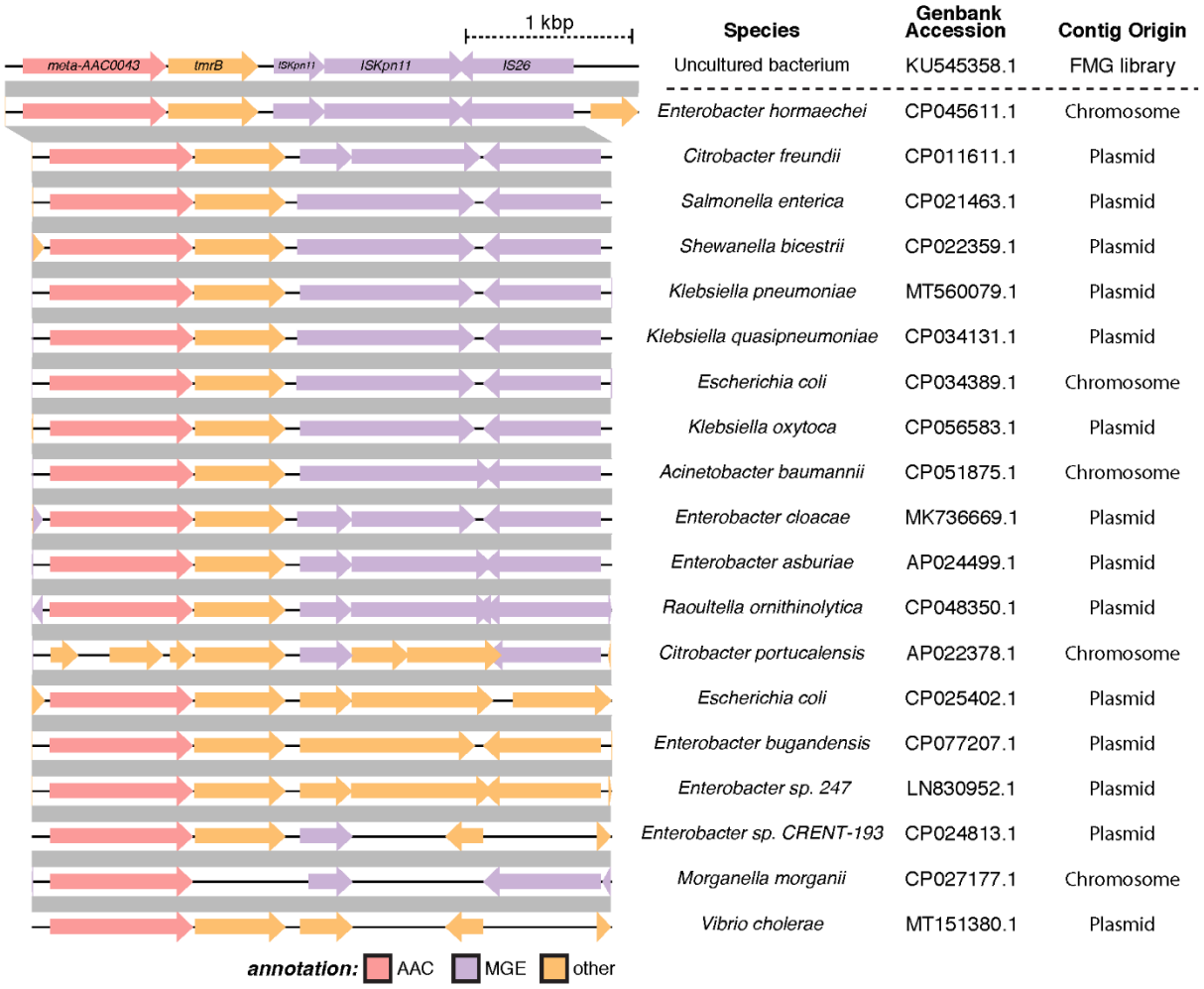

Species	Genbank Accession	Contig Origin
Uncultured bacterium	KU545358.1	FMG library
Enterobacter hormaechei	CP045611.1	Chromosome
Citrobacter freundii	CP011611.1	Plasmid
Salmonella enterica	CP021463.1	Plasmid
Shewanella bicestrii	CP022359.1	Plasmid
Klebsiella pneumoniae	MT560079.1	Plasmid
Klebsiella quasipneumoniae	CP034131.1	Plasmid
Escherichia coli	CP034389.1	Chromosome
Klebsiella oxytoca	CP056583.1	Plasmid
Acinetobacter baumannii	CP051875.1	Chromosome
Enterobacter cloacae	MK736669.1	Plasmid
Enterobacter asburiae	AP024499.1	Plasmid
Raoultella ornithinolytica	CP048350.1	Plasmid
Citrobacter portucalensis	AP022378.1	Chromosome
Escherichia coli	CP025402.1	Plasmid
Enterobacter bugandensis	CP077207.1	Plasmid
Enterobacter sp. 247	LN830952.1	Plasmid
Enterobacter sp. CRENT-193	CP024813.1	Plasmid
Morganella morganii	CP027177.1	Chromosome
Vibrio cholerae	MT151380.1	Plasmid

Figure 5: Synteny of meta-AAC0043 with mobile genetic elements. The contig containing meta-AAC0043 was queried against the NCBI nucleotide database and filtered for highly similar sequences, revealing the presence of similar sequences in a hugely diverse set of taxa. A representative set of similar genomic segments are shown, with grey bars indicating blastn percent identity >= 99.5%. Many of these matches are from plasmid sequences, and almost all of them contain ORFs annotated as MGEs (e.g., transposons, insertion sequences, etc.). FMG = functional metagenomic library.

Discussion

The realization that environmental microbial communities are important reservoirs of ARGs provides keys to understanding the emergence of antibiotic resistance in pathogenic species. For most ARG families, the evolution, transferability, and molecular/structural basis for the activity of their environmental relatives has not been well characterized. Given that antibiotic use in agricultural and other anthropogenic settings represents a significant proportion of global antibiotic deployment, it is vital to understand the scope and breadth of resistance in the broader global resistome, which may select for the evolution and transfer of ARGs. This knowledge is critical to protecting the potency of our current antibiotic arsenal and designing antibiotics that are less susceptible to ARGs.

In this study, we follow on our previous identification of multiple Antibiotic_NAT family members in soil-derived metagenomic libraries[35] through detailed structural and functional analysis. Firstly, the phylogenetic reconstruction of this family that we calculated was linked to a comprehensive study of the substrate specificity profiles of the four main clades, represented by the AAC(3)-IV, AAC(3)-VII/VIII/IX/X, AAC(3)-III, and AAC(3)-II/IV enzymes. Secondly, with the additional crystal structures described in this study and comparison to previously-available structural information, we conclusively show that this division is reflected in differences in activity against AG substrates and in structural diversification localized to the minor subdomain of the Antibiotic_NAT fold. Given that the minor subdomain is much less conserved between Antibiotic_NAT family members, the deficit in molecular information about variations in this subdomain that would allow for better understanding of the role of individual amino acids in this region for substrate specificity necessitated and inspired our structural investigation into additional representatives of this family. Thirdly, we show that environment-derived enzymes of this family, which previously have not been characterized for molecular determinants behind their activity

against antibiotic substrates, possess resistance-conferring activities comparable to and sometimes exceeding those activities of their counterparts derived from clinical isolates. Fourthly, we show that numerous members of this family inactivate apramycin, an atypical AG that is increasingly being considered for clinical deployment and for which little has been known about possible resistance determinants.

Our structural data includes the crystal structure of AAC(3)-IVa enzyme which is the first molecular image of Group 1 Antibiotic_NAT enzymes. Our extensive structural and functional characterization demonstrates that this enzyme mediates broad-spectrum AG resistance, including to 4,5-, 4,6-disubstituted AGs and the atypical AG apramycin by evolving a more spacious active site. This is achieved by a C-terminal extension and modifications the structure and residue composition of the α4-α5 hairpin of the minor subdomain of the enzyme which allow for broad spectrum of AG recognition. The role of the Zn^{2+}-binding site in the mechanism of action of AAC(3)-IVa and Group 1 enzymes is the subject of ongoing investigation. After the structures of AAC(3)-IVa•gentamicin and AAC(3)-IVa•apramycin were publicly available in the PDB, another group performed structure-guided mutagenesis on the enzyme[38]. This analysis confirmed the Glu185 and Asp187 residues' important roles for interactions with AG substrates, and the role of Asp67 residue in specificity for gentamicin recognition. This group also generated a double mutant Cys247Ser/Cys250Ser, which abrogated resistance to both gentamicin and apramycin, suggesting that Zn^{2+}-binding is necessary for substrate recognition. However, since no evidence for the effect of these two mutations on overall stability of this enzyme was provided, the direct effect of Zn^{2+} binding on interaction with AG substrates remains unclear.

According to our sequence analysis the Group 1 members meta-AAC0022, meta-AAC0033, meta-AAC0016, and meta-AAC0018 also share the C-terminal extension, the Zn^{2+}-

binding residues, and the shorter sequence corresponding to the α4-α5 hairpin. Thus, we hypothesis that these enzymes are likely to be active against the wide range of AGs including apramycin.

Antibiotic_NAT Group 3 members showed a high degree of promiscuity, including activity toward the 4,5- and 4,6-disubstituted AGs. Notably, the meta-AAC0038 enzyme was also active against apramycin which inspired our structural analysis of this activity. According to our meta-AAC0038-apramycin complex structure, binding of apramycin to this enzyme differed from its interactions to AAC(3)-IVa. Meta-AAC0038 demonstrated activity analogous to AAC(3)-IIIb and AAC(3)-IIIc enzymes, which belonged to the same clade. Other environment-derived members, including meta-AAC0008, meta-AAC0030, and meta-AAC0071, were similarly active against 4,5- and 4,6-disubstituted AGs.

Representatives of Antibiotic_NAT Groups 2 and 4 were the most restricted in their specificity, and this was reflected in more constrained and smaller active sites, as revealed by the structures of AAC(3)-IIb and AAC(3)-Xa. The environment-derived enzymes of Group 4, including meta-AAC0032, meta-AAC0029, meta-AAC0034, meta-AAC0035, and meta-AAC0043, likewise conferred resistance only to kanamycin and tobramycin. The crystal structure of AAC(3)-IIb features an active site highly like that in AAC(3)-VIa, consistent with the 4,6-disubstituted specificity of Group 4 enzymes.

Additionally, our study expanded the repertoire of AMEs active against apramycin to include six environment-derived enzymes, with the Group 1 members meta-AAC0016, meta-AAC0018, meta-AAC0033, and meta-AAC0022 conferring high-level apramycin resistance. The presence of these enzymes in environmental microbial species may be provoked by widespread

apramycin use in agriculture settings. As apramycin is deployed in the clinic, it is important to be mindful of possible further dissemination of these ARGs.

Our analysis of lateral gene transfer signatures in the genetic vicinity of meta-AAC genes indicates that these genes show low potential for mobilization, for the most part, with the notable exception of *meta-AAC0043*. This conclusion is corroborated by the separation of meta-AAC and AAC(3) enzyme sequences in each group within our phylogenetic reconstruction, except for the close clustering of meta-AAC0008 with AAC(3)-IIIa (67% identical at the protein level) and meta-AAC0043 with AAC(3)-IIc (96% identical). While no MGEs were identified in the contig containing the *meta-AAC0008* gene, multiple MGEs were present in the contig harboring *meta-AAC0043*. This proximity strongly suggests that *meta-AAC0043* has mobilized into pathogens, manifesting in the enzyme AAC(3)-IIe, conferring resistance to 4,6-disubstituted AGs. This precedent suggests that with further FMG sampling, additional meta-AAC genes may be identified which represent environmental sources of clinically relevant Antibiotic_NAT genes.

The metagenomic, structural, and functional data presented in this study establishes key molecular insights into the molecular basis for AG recognition by all four clades of the Antibiotic_NAT family. This provides deeper understanding of primary sequence signatures important for AG resistance profile conferred by corresponding enzymes. Our observation that environmental members of this family can confer broad, high-level AG resistance and have already mobilized into pathogenic species warrants surveillance and FMG sampling to detect new connections between ARGs in the clinic and the environment.

Acknowledgments

This work made use of the Centre for Microbial Chemical Biology core facility at McMaster University for antibiotic susceptibility testing. We thank Rosa Di Leo for cloning, and Zdzislaw Wawrzak and Karolina Michalska, Argonne National Laboratory, for x-ray diffraction data collection. This project has been funded in whole or in part with Federal funds from the National Institute of Allergy and Infectious Diseases, National Institutes of Health (NIH), Department of Health and Human Services, under Contract numbers HHSN272201200026C and HHSN272201700060C. This research was supported by the Ontario Research Fund Research Excellence (ORF-RE) Grant No. RE07-048 (to G.D.W. and A.S.) and a Canadian Institutes of Health Research grant (FRN-148463) and a Canada Research Chair to G.D.W. This work is supported in part by an award to G. Dantas through the National Institute of Allergy and Infectious Diseases of the National Institutes of Health (U01 AI123394). A.W. D'Souza received support from the National Research Service Award-Medical Scientist grant to Washington University (T32 GM007200), and the Institutional Program Unifying Population and Laboratory-Based Sciences Burroughs Welcome Fund grant to Washington University. The content is solely the responsibility of the authors and does not necessarily represent the official views of the funding agencies.

Competing interests

The authors declare no competing interests.

Data availability statement

The data generated in this study are available in Supplementary Data 1 (MIC data), Protein Databank (crystal structures) under accession codes 5HT0, 6MMZ, 6MN0, 7KES, 6MN3, 6MN4,

6MN5, 7LAO, and 7LAP, or NCBI Database (i.e. FMG sampling) with accession codes indicated in Fig. 5.

Methods

Sequence analysis and phylogenetic reconstruction

Previously identified members of the Antibiotic_NAT family from functional selections of soil metagenomes[35] were aligned with clinically isolated AAC(3) enzyme sequences and homologs in Genbank identified by BLAST. Sequence alignment was performed using the Clustal Omega server (EMBL-EBI). The phylogenetic reconstruction was generated from the sequence alignment by MrBayes[39] (with gamma-distributed rates across sites, rate matrix=mixed, 1000000 generations for mcmc) and visualized by using FigTree v1.4.2.

Antibiotic susceptibility testing

Environmental and clinical Antibiotic_NAT sequences were cloned into the low copy plasmid pGDP3. Expression levels of each gene were controlled by the strong, constitutive promoter P_{bla}. Aminoglycoside susceptibility testing was completed in technical triplicate, single colony dilution replicated across three rows of the same microtiter plate, with our hyperpermeable, efflux-deficient strain *E. coli* BW25113 Δ*tolC*Δ*bamB* following the Clinical and Laboratory Standards Institute (CLSI) protocols for the microbroth dilution method[40]. *E. coli* was cultured in a cation-adjusted Mueller Hinton broth (CAMHB) arrayed in a 96-well format. The plates were incubated for 18 hrs at 37 °C. A Labcyte Echo 550 and Thermo Combi nL was used for dispensing the antibiotics and a Formulatrix Tempest for culture dispensing.

Protein Purification

E.coli BL21(DE3) Gold was used for *meta-AAC0038* and *aac(3)-IVa* overexpression. 3 mL overnight culture was diluted into 1 L LB media containing selection antibiotic ampicillin and

grew at 37°C with shaking. The cell culture was induced with IPTG at 17 °C once the OD_{600} reached 0.6-0.8. Cell pellets were collected by centrifugation at 7000 g. Ni-NTA affinity chromatography was used for protein purification. Cells were resuspended in binding buffer [100 mM HEPES pH 7.5, 500 mM NaCl, 5 mM imidazole, and 5% glycerol (v/v)], lysed with a sonicator. Then insoluble cell debris was removed by centrifugation at 30000 g. The soluble cell lysate fraction was loaded on a 4 mL Ni-NTA column (QIAGEN) pre-equilibrated with binding buffer, washed with 250 mL washing buffer [100 mM HEPES pH 7.5, 500 mM NaCl, 30 mM imidazole, and 5% glycerol (v/v)], and N-terminal His6-tagged protein was eluted with elution buffer [100 mM HEPES pH 7.5, 500 mM NaCl, 250 mM imidazole and 5% glycerol (v/v)]. The His6-tagged proteins were then subjected to overnight TEV cleavage using 50μg of TEV per mg of His6-tagged protein in binding buffer and dialyzed overnight against the binding buffer. The His-tag and TEV were removed by rerunning the protein over the Ni-NTA column. The tag-free protein was then dialyzed in crystallization buffer (50 mM HEPES pH 7.5, 500 mM NaCl) overnight, and the purity of the protein was analyzed by SDS-polyacrylamide gel electrophoresis.

Crystallization and Structure Determination

The meta-AAC0038 apoenzyme crystal was grown at room temperature using the vapor diffusion sitting drop method solution containing 20 mg/mL protein, 2.5 M ammonium sulfate, 0.1 M Bis-Tris propane pH 7, and 10 mM gentamicin. For the AG-bound structures of meta-AAC0038 and AAC(3)-IVa, we utilized the catalytically inactive mutants His168Ala and His154Ala. The meta-AAC0038^{H168A}-apramycin-CoA complex was co-crystallized from solution containing 20 mg/mL protein, 20% PEG 3350, 50 mM ADA pH 7, 10 mM apramycin. The AAC(3)-IVa apoenzyme was crystallized as selenomethionine-derivative from a solution containing 30 mg/mL

protein, 0.2 M magnesium chloride, 0.1 M Tris pH 8.8, and 25% PEG3350. The AAC(3)-IVa^{H154A}-apramycin complex was co-crystallized from a solution containing 0.1 M Hepes pH 7.6, 30% PEG 1K, and 2.5 mM apramycin; the AAC(3)-IVa^{H154A}-apramycin complex was co-crystallized from a solution containing 0.1 M Hepes pH 7.5, 30% PEG 1K and 1 mM gentamicin.

Diffraction data at 100K were collected at a home source Rigaku Micromax 007-HF/R-Axis IV system, at beamline 21-ID-G of the Life Sciences Collaborative Access Team at the Advanced Photon Source (MAR CCD detector with 300 mm plate), or beamline 19-ID of the Structural Biology Center of the Advanced Photon Source, Argonne National Laboratory. All diffraction data were processed using HKL3000[41]. For meta-AAC0038, the apoenzyme structure was solved by Molecular Replacement (MR), using the structure of YokD[34] and the CCP4 online server Balbes program. The apramycin complex structure was used solved by MR using the apoenzyme model. For AAC(3)-IVa, the apoenzyme structure was solved by MR using the structure of FrbF (PDB 3SMA)[33] and the CCP4 online server MoRDa program, and the AG bound structures were solved by MR using the apoenzyme model.

All model building and refinement were performed using Phenix.refine [42] and Coot[43]. Atomic coordinates have been deposited in the Protein Data Bank with accession codes 5HT0, 6MMZ, 6MN0, 7KES, 6MN3, 6MN4, 6MN5, 7LAO, and 7LAP. Dimerization interfaces were determined using the PDBePISA server[44]. Structural homologs were identified in the PDB using the Dali-lite server[45] or the PDBeFold server[46].

References

1. World Health Organization (WHO). Antimicrobial resistance: global report on surveillance. (2014).
2. Surette, M. D. & Wright, G. D. Lessons from the Environmental Antibiotic Resistome. *Annu. Rev. Microbiol.* **71**, 309–329 (2017).
3. Finley, R. L. *et al.* The scourge of antibiotic resistance: The important role of the environment. *Clin. Infect. Dis.* **57**, 704–710 (2013).
4. Peterson, E. & Kaur, P. Antibiotic resistance mechanisms in Bacteria: Relationships Between Resistance Determinants of Antibiotic Producers, Environmental Bacteria, and Clinical Pathogens. *Front. Microbiol.* **9**, 243 (2018).
5. Crofts, T. S., Gasparrini, A. J. & Dantas, G. Next-generation approaches to understand and combat the antibiotic resistome. *Nat. Rev. Microbiol.* **67**, 7–434 (2017).
6. Stogios, P. J. *et al.* Substrate Recognition by a Colistin Resistance Enzyme from *Moraxella catarrhalis*. *ACS Chem. Biol.* **13**, (2018).
7. Kieffer, N., Nordmann, P. & Poirel, L. *Moraxella* Species as Potential Sources of MCR-Like Polymyxin Resistance Determinants. *Antimicrob. Agents Chemother.* **61**, e00129--17 (2017).
8. W, Y. *et al.* Novel Plasmid-Mediated Colistin Resistance Gene *mcr-3* in *Escherichia coli*. *MBio* **8**, (2017).
9. Zhao, W.-H. & Hu, Z.-Q. Epidemiology and genetics of CTX-M extended-spectrum β-lactamases in Gram-negative bacteria. *Crit. Rev. Microbiol.* **39**, 79–101 (2013).
10. Wright, G. D. Solving the Antibiotic Crisis. *ACS Infect. Dis.* **1**, 80–84 (2015).
11. Fosso, M. Y., Li, Y. & Garneau-Tsodikova, S. New trends in aminoglycosides use. *Medchemcomm* **5**, 1075–1091 (2014).
12. Jackson, J., Chen, C. & Buising, K. Aminoglycosides: how should we use them in the 21st century? *Curr. Opin. Infect. Dis.* **26**, 516–525 (2013).
13. Zhang, A. *et al.* Characterization of Resistance Patterns and Detection of Apramycin Resistance Genes in *Escherichia coli* Isolated from Chicken Feces and Houseflies after Apramycin Administration. *Front. Microbiol.* **9**, 261 (2018).
14. KM, B., TS, E., TR, C., KJ, G. & DJ, N. Characterization of antimicrobial resistant *Salmonella Kinshasa* from dairy calves in Texas. *Lett. Appl. Microbiol.* **38**, 140–145 (2004).
15. Magalhães, M. L. B. & Blanchard, J. S. The kinetic mechanism of AAC3-IV aminoglycoside acetyltransferase from *Escherichia coli*. *Biochemistry* **44**, 16275–16283 (2005).

16. Kadlec, K., Fessler, A. T., Hauschild, T. & Schwarz, S. Novel and uncommon antimicrobial resistance genes in livestock-associated methicillin-resistant *Staphylococcus aureus*. *Clin. Microbiol. Infect.* **18**, 745–755 (2012).

17. AD, K. *et al.* Invitro Apramycin Activity against multidrug-resistant *Acinetobacter baumannii* and *Pseudomonas aeruginosa*. *Diagn. Microbiol. Infect. Dis.* **88**, 188–191 (2017).

18. DM, L. *et al.* Activity of aminoglycosides, including ACHN-490, against carbapenem-resistant *Enterobacteriaceae* isolates. *J. Antimicrob. Chemother.* **66**, 48–53 (2011).

19. Juhas, M. *et al.* In vitro activity of apramycin against multidrug-, carbapenem- and aminoglycoside-resistant *Enterobacteriaceae* and *Acinetobacter baumannii*. *J. Antimicrob. Chemother.* **45**, 568 (2019).

20. M, H. *et al.* In vitro Activity of Apramycin Against Carbapenem-Resistant and Hypervirulent *Klebsiella pneumoniae* Isolates. *Front. Microbiol.* **11**, (2020).

21. S, R. *et al.* Evaluation of apramycin against spectinomycin-resistant and -susceptible strains of *Neisseria gonorrhoeae*. *J. Antimicrob. Chemother.* **74**, 1311–1316 (2019).

22. Ramirez, M. S. & Tolmasky, M. E. Aminoglycoside modifying enzymes. *Drug Resist. Updat.* **13**, 151–171 (2010).

23. Cox, G. *et al.* Plazomicin Retains Antibiotic Activity against Most Aminoglycoside Modifying Enzymes. *ACS Infect. Dis.* **4**, (2018).

24. Becker, B. & Cooper, M. A. Aminoglycoside antibiotics in the 21st century. *ACS Chem. Biol.* **8**, 105–115 (2013).

25. JCK, Q. *et al.* Apralogs: Apramycin 5- O-Glycosides and Ethers with Improved Antibacterial Activity and Ribosomal Selectivity and Reduced Susceptibility to the Aminoacyltranserferase (3)-IV Resistance Determinant. *J. Am. Chem. Soc.* **142**, 530–544 (2020).

26. Xu, Z. *et al.* Structural and Functional Survey of Environmental Aminoglycoside Acetyltransferases Reveals Functionality of Resistance Enzymes. *ACS Infect. Dis.* **3**, 653–665 (2017).

27. Forsberg, K. J. *et al.* The shared antibiotic resistome of soil bacteria and human pathogens. *Sci. (New York, NY)* **337**, 1107–1111 (2012).

28. Kumar, P., Selvaraj, B., Serpersu, E. H. & Cuneo, M. J. Encoding of Promiscuity in an Aminoglycoside Acetyltransferase. *J. Med. Chem.* **61**, 10218–10227 (2018).

29. Baumgartner, J. T. *et al.* Gcn5-Related N- Acetyltransferases (GNATs) With a Catalytic Serine Residue Can Play Ping-Pong Too. *Front. Mol. Biosci.* **8**, (2021).

30. Vakulenko, S. B. & Mobashery, S. Versatility of Aminoglycosides and Prospects for Their Future. *Clin. Microbiol. Rev.* **16**, 430–450 (2003).

31. Norris, A. L. & Serpersu, E. H. Ligand promiscuity through the eyes of the aminoglycoside N3 acetyltransferase IIa. *Protein Sci.* **22**, 916–928 (2013).

32. Kumar, P., Serpersu, E. H. & Cuneo, M. J. A low-barrier hydrogen bond mediates antibiotic resistance in a noncanonical catalytic triad. *Sci. Adv.* **4**, eaas8667 (2018).

33. Bae, B., Cobb, R. E., DeSieno, M. A., Zhao, H. & Nair, S. K. New N-acetyltransferase fold in the structure and mechanism of the phosphonate biosynthetic enzyme FrbF. *J. Biol. Chem.* **286**, 36132–36141 (2011).

34. Klimecka, M. M. *et al.* Structural analysis of a putative aminoglycoside N-acetyltransferase from *Bacillus anthracis*. *J. Mol. Biol.* **410**, 411–423 (2011).

35. Forsberg, K. J. *et al.* Bacterial phylogeny structures soil resistomes across habitats. *Nature* **509**, 612–616 (2014).

36. Cox, G. *et al.* A Common Platform for Antibiotic Dereplication and Adjuvant Discovery. *Cell Chem. Biol.* **24**, 98–109 (2017).

37. P, K. *et al.* Low-Barrier and Canonical Hydrogen Bonds Modulate Activity and Specificity of a Catalytic Triad. *Angew. Chem. Int. Ed. Engl.* **58**, 16260–16266 (2019).

38. Plattner, M., Gysin, M., Haldimann, K., Becker, K. & Hobbie, S. N. Epidemiologic, phenotypic, and structural characterization of aminoglycoside-resistance gene *Aac(3)-IV*. *Int. J. Mol. Sci.* **21**, 1–11 (2020).

39. Ronquist, F. & Huelsenbeck, J. P. MrBayes 3: Bayesian phylogenetic inference under mixed models. *Bioinformatics* **19**, 1572–1574 (2003).

40. M07: Dilution AST for Aerobically Grown Bacteria - CLSI. https://clsi.org/standards/products/microbiology/documents/m07/.

41. Minor, W., Cymborowski, M., Otwinowski, Z. & Chruszcz, M. HKL-3000: the integration of data reduction and structure solution--from diffraction images to an initial model in minutes. *Acta Crystallogr. Sect. D, Biol. Crystallogr.* **62**, 859–866 (2006).

42. Adams, P. D. *et al.* PHENIX: A comprehensive Python-based system for macromolecular structure solution. *Acta Crystallogr. Sect. D Biol. Crystallogr.* **66**, 213–221 (2010).

43. Emsley, P., Lohkamp, B., Scott, W. G. & Cowtan, K. Features and development of Coot. *Acta Crystallogr. Sect. D, Biol. Crystallogr.* **66**, 486–501 (2010).

44. Krissinel, E. & Henrick, K. Inference of macromolecular assemblies from crystalline state. *J. Mol. Biol.* **372**, 774–797 (2007).

45. L, H. & P, R. Dali server: conservation mapping in 3D. *Nucleic Acids Res.* **38**, (2010).

46. E, K. & K, H. Secondary-structure matching (SSM), a new tool for fast protein structure alignment in three dimensions. *Acta Crystallogr. D. Biol. Crystallogr.* **60**, 2256–2268 (2004).

Supplemental information

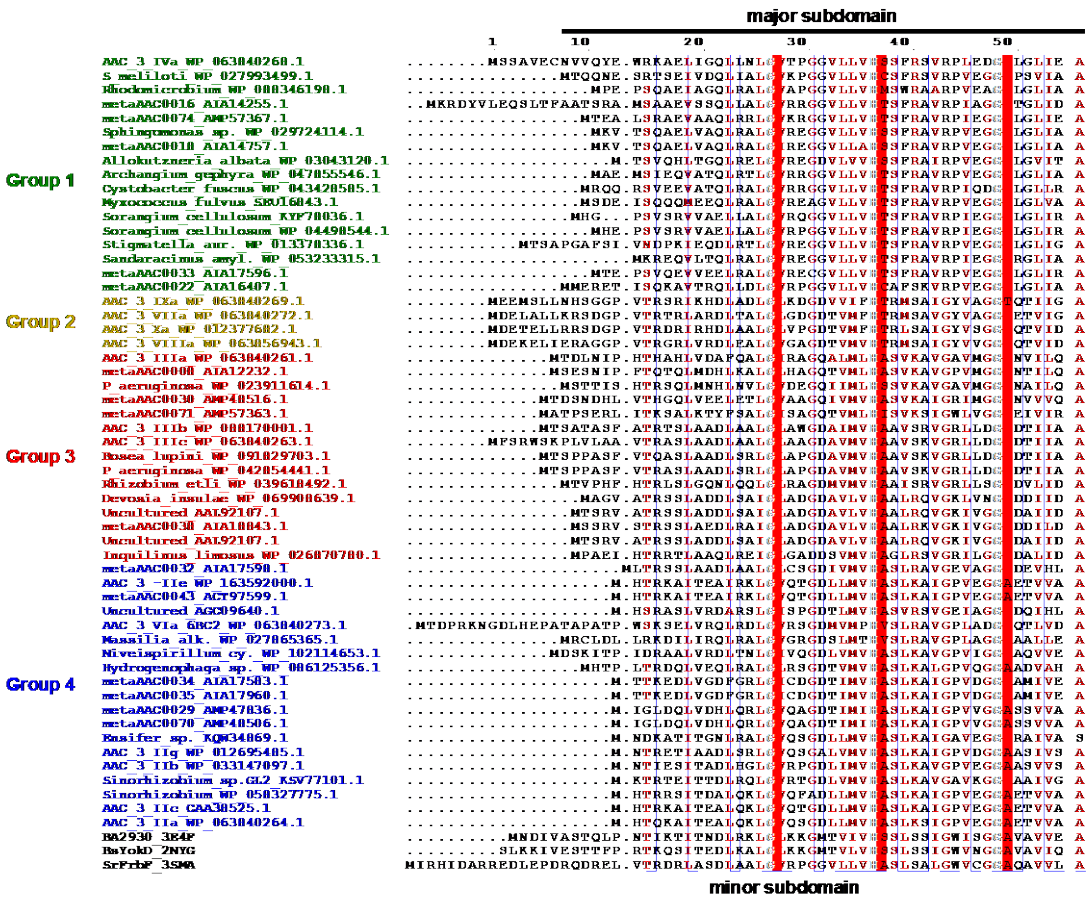
major subdomain
minor subdomain
Group 1
Group 2
Group 3
Group 4

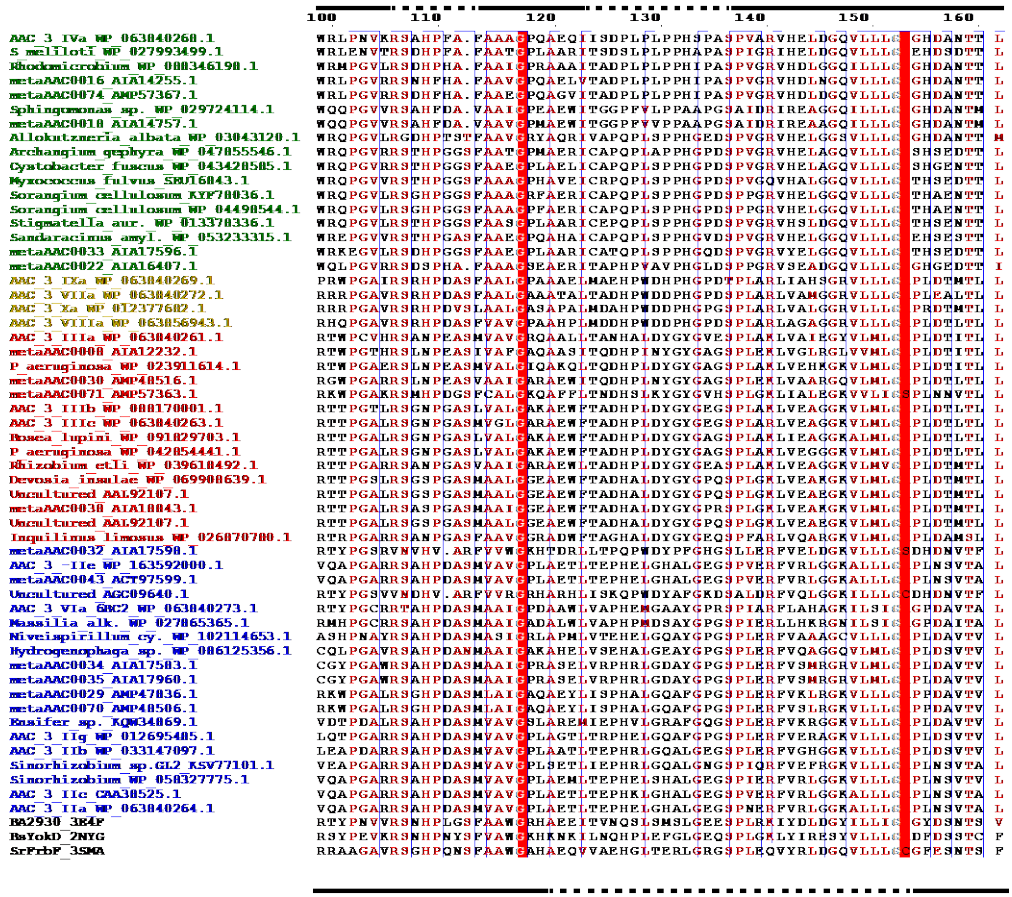

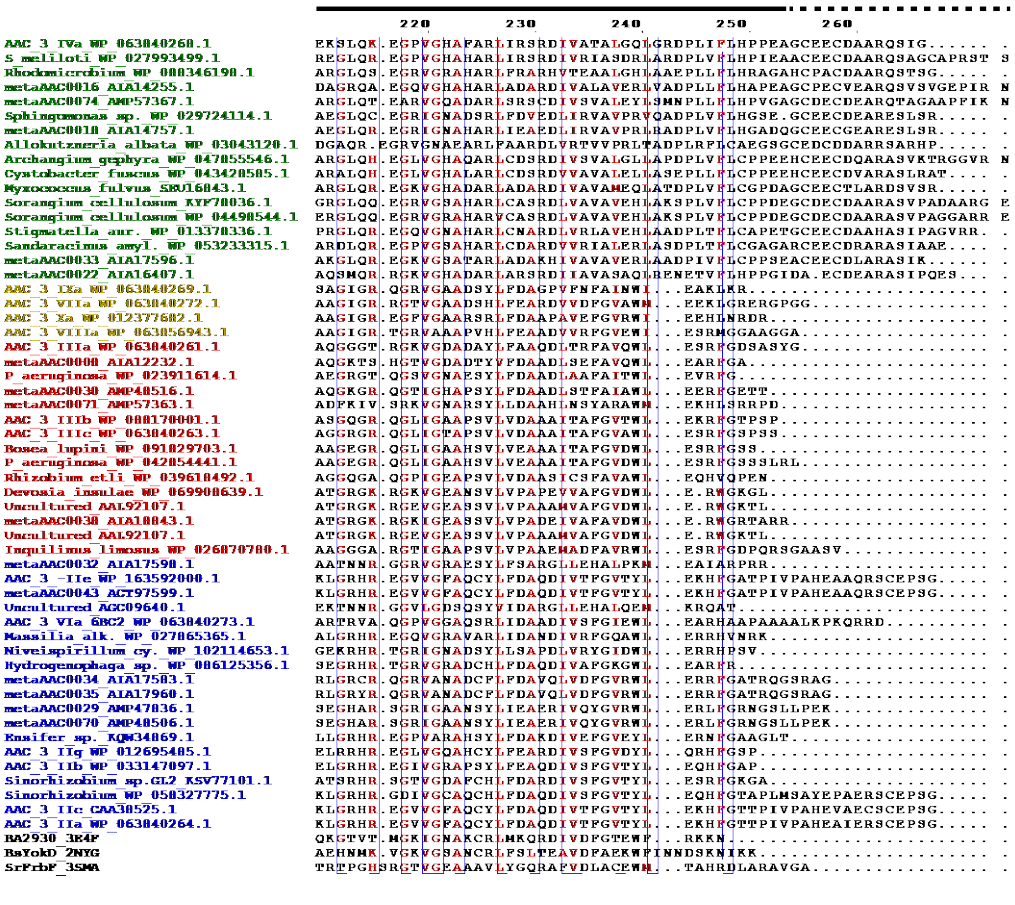

Supplementary Figure 1. Sequence alignment of the Antibiotic_NAT family. Sequences are grouped and shaded according to phylogenetic reconstruction in Figure 1. Includes meta-AAC's, AAC(3) enzymes from clinical isolates, and sequences identified through BLAST searches of NCBI. Darker color or shading of amino acids indicates higher conservation. Major and minor subdomains are indicated with solid and dashed black lines, respectively, above the sequence alignment.

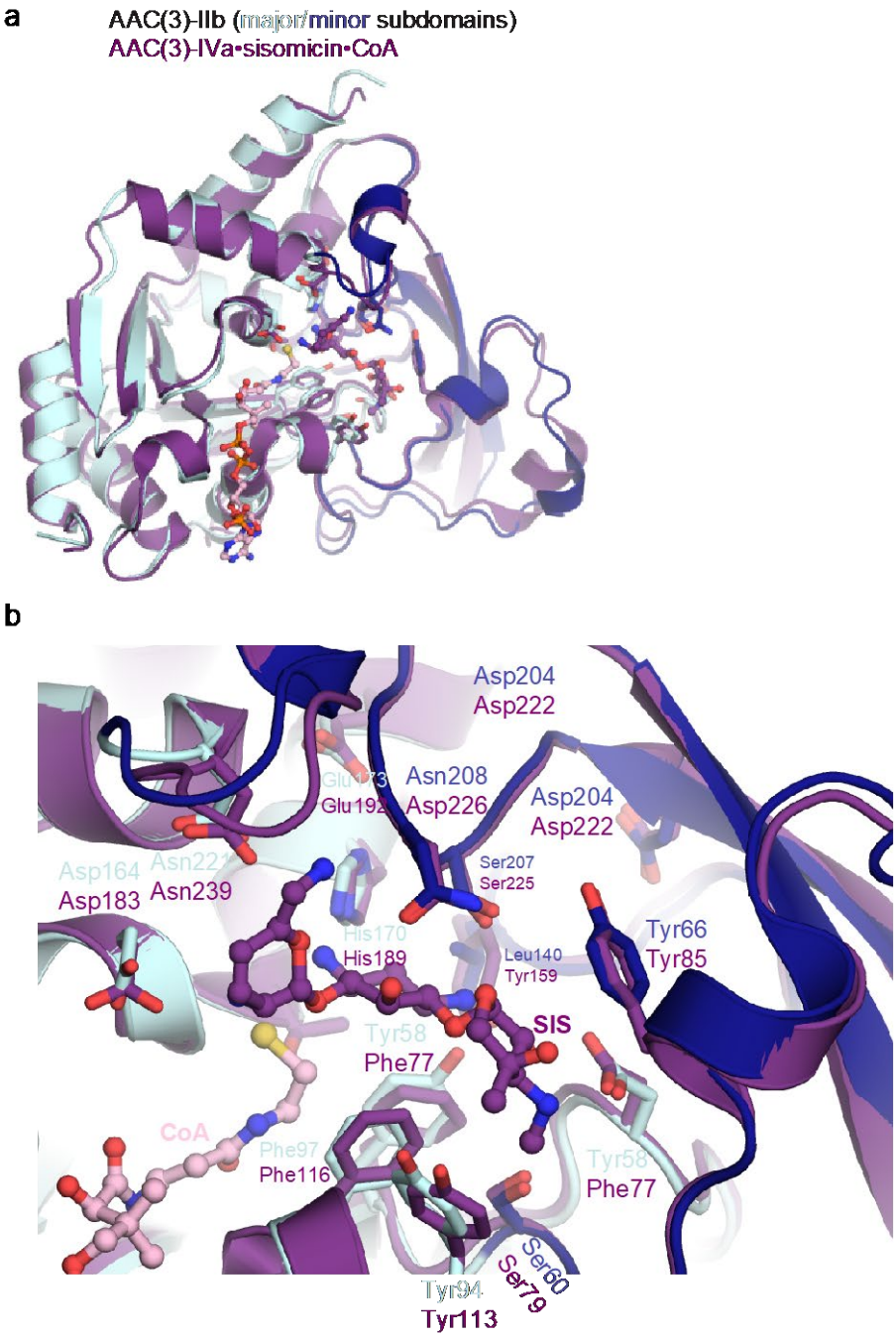

Supplementary Figure 2. Structural analysis of Group 4 AAC(3)-IIb vs. AAC(3)-VIa. a) Superposition of overall structures. b) Zoom of active sites, sisomicin and CoA are shown in ball-and-stick representation.

Supplementary Table 1. Aminoglycoside susceptibility of E. coli harboring Antibiotic_NAT genes. *E. coli* BW25113 Δ*tolC*Δ*bamB* expressing individual Antibiotic_NAT genes under the control of the P_{bla} promoter in vector pGDP3. Shown are MIC values in µg/mL grouped and coloured as in **Figure 2**. Raw data used to derive this table is shown in **Supplementary Data 1.**

Group 1

	Control	Meta-AAC0016	Meta-AAC0018	HMB0022	HMB00033	AAC(3)-IVa
APR	4	> 256	> 256	> 256	> 256	> 512
TOB	0.5	> 256	> 256	> 256	> 256	≥ 64
GEN	0.25-0.5	≥ 256	128-256	64	≥ 256	> 512
KAN	2	128-256	64-128	8	32	64
AMI	1-2	1-2	1	1-2	1	1
NEO	1	64	128	8-16	64-128	64-128
PAR	2	> 256	128	16	64-128	128-256

Group 2

	AAC(3)-VIIa	AAC(3)-VIIIa	AAC(3)-IXa	AAC(3)-Xa
APR	ND	ND	4	2-4
TOB	ND	ND	≤ 0.5	16-32
GEN	ND	ND	≤ 0.5	8
KAN	ND	ND	2	64-128
AMI	ND	ND	1	1
NEO	ND	ND	1	1
PAR	ND	ND	2	4

Group 3

	Meta-AAC0008	Meta-AAC0030	Meta-AAC0038	Meta-AAC0071	AAC(3)-IIIa	AAC(3)-IIIc	AAC(3)-IIIb
APR	16-32	16	32-64	4-8	8-16	ND	8
TOB	> 256	> 256	> 256	> 256	> 256	ND	> 256
GEN	> 256	> 256	> 256	> 256	> 256	ND	> 256
KAN	> 256	> 256	> 256	> 256	> 256	ND	> 256
AMI	1	1-2	1-2	1-2	1	ND	0.5 – 1
NEO	> 256	64-128	256	1	128-256	ND	256
PAR	> 256	> 256	> 256	4	> 256	ND	> 256

Group 4

	Meta-AAC0029	Meta-AAC0032	Meta-AAC0035	Meta-AAC0043	Meta-AAC0070	AAC(3)-IIa	AAC(3)-IIb	AAC(3)-IIc	AAC(3)-VIa	Meta-AAC0034
APR	4	2-4	8	4	ND	8	16-32	2	4	8
TOB	64	4-8	> 256	32-64	ND	> 64	> 256	64 - 128	8	> 256
GEN	> 64	64	> 256	≥ 256	ND	> 64	> 256	> 256	≥ 256	> 64
KAN	16	16-32	≥ 256	16	ND	>64	> 256	32	16	> 256
AMI	0.5-1	1-2	1	1-2	ND	2	1	0.5-1	1-2	1-2
NEO	≤ 1	1	1	1	ND	1	0.5-1	0.5-1	≤ 1	≤ 1
PAR	1	2	2	2-4	ND	2-4	1-2	0.5-1	2	1

ND = No data.

Supplementary Data 1. Raw data for MIC experiments. Raw data from excel document provided as images, reproduced for presentation in thesis.

Please read the notes below for how to navigate the supplemental data presented in this document

This document is an extended record for our antimicrobial susceptibility testing data; *E. coli* BW25113 Δ*tolC* Δ*bamB* expressing individual Antibiotic_NAT genes under the control of the P_{bla} promoter in vector pGDP3.

The summary table below presents all minimal inhibitory concentration values obtained in this study. The Antibiotic_NAT proteins are coloured and listed in this table in the order they appear in the phylogeny from Figure 2 in the main text.

Tabs 2 - 5 contain raw data for antimicrobial susceptibility testing. Each tab contains the data for individual clades, organized and color coded according to phylogeny presented in Figure 2 of main text.

Supplemental Table 1 Extended: Aminoglycoside susceptibility of *E. coli* harboring Antibiotic_NAT genes

Structural subclass of aminoglycoside	Antibiotic name	MIC (μg/mL)					
		No Vector Control	AAC(3)-IVa	meta-AAC00016	meta-AAC00018	meta-AAC00033	meta-AAC0022
4-monosubsituted	Apramycin	4	> 512	> 256	> 256	> 256	> 256
4,6-disubsituted	Tobramycin	0.5	≥ 64	> 256	> 256	> 256	> 256
	Gentamicin	0.25-0.5	> 512	≥ 256	128-256	≥ 256	64
	Kanamycin	2	64	128-256	64-128	32	8
	Amikacin	1-2	1	1-2	1	1	1-2
4,5-disubstituted	Neomycin	1	64-128	64	128	64-128	8-16
	Paromomycin	2	128-256	> 256	128	64-128	16

Legend:

* Structural subclass refers to the substitution pattern of sugars from 2-deoxystreptamine ring core of the aminoglycoside
* Phylogeny colour code: Clade 1 | Clade 2 | Clade 3 | Clade 4

Structural subclass of aminoglycoside	Antibiotic name	MIC (μg/mL)						
		AAC(3)-IXa	AAC(3)-Xa	AAC(3)-VIIa	AAC(3)-VIIIa	AAC(3)-IIIa	meta-AAC00008	meta-AAC0030
4-monosubsituted	Apramycin	4	2-4	ND	ND	8-16	16-32	16
4,6-disubsituted	Tobramycin	≤ 0.5	16-32	ND	ND	> 256	> 256	> 256
	Gentamicin	≤ 0.5	8	ND	ND	> 256	> 256	> 256
	Kanamycin	2	64-128	ND	ND	> 256	> 256	> 256
	Amikacin	1	1	ND	ND	1	1	1-2
4,5-disubstituted	Neomycin	1	1	ND	ND	128-256	> 256	64-128
	Paromomycin	2	4	ND	ND	> 256	> 256	> 256

Structural subclass of aminoglycoside	Antibiotic name	MIC (μg/mL)				
		AAC(3)-IIIc	meta-AAC00038	meta-AAC00032	AAC(3)-VIa	meta-AAC0029
4-monosubsituted	Apramycin	ND	32-64	2-4	4	4
4,6-disubsituted	Tobramycin	ND	> 256	4-8	8	64
	Gentamicin	ND	> 256	64	≥ 256	> 64
	Kanamycin	ND	> 256	16-32	16	16
	Amikacin	ND	1-2	1-2	1-2	0.5-1
4,5-disubstituted	Neomycin	ND	256	1	≤ 1	≤ 1
	Paromomycin	ND	> 256	2	2	1

Structural subclass of aminoglycoside	Antibiotic name	MIC (μg/mL)						
		meta-AAC0070	meta-AAC00034	meta-AAC00035	AAC(3)-IIb	AAC(3)-IIc	AAC(3)-IIa	meta-AAC0043
4-monosubsituted	Apramycin	ND	8	8	16-32	2	8	4
4,6-disubsituted	Tobramycin	ND	>256	> 256	> 256	64 - 128	> 64	32-64
	Gentamicin	ND	> 64	> 256	> 256	> 256	> 64	≥ 256
	Kanamycin	ND	> 256	≥ 256	> 256	32	> 64	16
	Amikacin	ND	1-2	1	1	0.5-1	2	1-2
4,5-disubstituted	Neomycin	ND	≤ 1	1	0.5-1	0.5-1	1	1
	Paromomycin	ND	1	2	1-2	0.5-1	2-4	2-4

No vector control

	0	Media	0.125	0.25	0.5	1	2	4	8	16	32	64	MIC (ug/mL)
Neomycin	0.576	0.043	0.523	0.475	0.279	0.042	0.044	0.041	0.041	0.041	0.043	0.042	1
	0.609	0.043	0.491	0.503	0.267	0.044	0.044	0.043	0.041	0.041	0.042	0.041	1
	0.477	0.041	0.466	0.523	0.241	0.094	0.045	0.042	0.041	0.042	0.044	0.043	1
Paromomycin	0.682	0.04	0.625	0.566	0.45	0.239	0.042	0.045	0.041	0.04	0.04	0.042	2
	0.671	0.04	0.58	0.602	0.437	0.243	0.043	0.043	0.041	0.04	0.041	0.042	2
	0.66	0.041	0.656	0.626	0.452	0.226	0.066	0.046	0.043	0.041	0.045	0.043	2

	0	Media	0.125	0.25	0.5	1	2	4	8	16	32	64	MIC (ug/mL)
Tobramycin	0.533	0.045	0.436	0.232	0.042	0.042	0.043	0.044	0.044	0.042	0.046	0.042	0.5
	0.588	0.048	0.444	0.279	0.076	0.059	0.052	0.045	0.041	0.042	0.045	0.043	0.5
	0.471	0.044	0.406	0.248	0.089	0.087	0.051	0.045	0.041	0.041	0.041	0.042	0.5
Kanamycin	0.616	0.044	0.611	0.547	0.421	0.209	0.041	0.041	0.041	0.042	0.041	0.044	2
	0.607	0.041	0.538	0.618	0.400	0.208	0.042	0.042	0.041	0.040	0.041	0.041	2
	0.645	0.040	0.564	0.583	0.400	0.171	0.043	0.042	0.042	0.041	0.042	0.042	2

	0	Media	0.125	0.25	0.5	1	2	4	8	16	32	64	MIC (ug/mL)
Apramycin	0.563	0.041	0.515	0.490	0.494	0.408	0.235	0.042	0.041	0.041	0.041	0.041	4
	0.580	0.041	0.518	0.555	0.510	0.443	0.232	0.041	0.043	0.042	0.040	0.041	4
	0.462	0.040	0.457	0.641	0.437	0.435	0.232	0.042	0.041	0.042	0.041	0.041	4
Gentamicin	0.649	0.040	0.390	0.226	0.067	0.043	0.042	0.042	0.045	0.042	0.040	0.042	0.5
	0.625	0.040	0.372	0.225	0.046	0.045	0.045	0.045	0.041	0.042	0.040	0.042	0.5
	0.654	0.040	0.407	0.220	0.042	0.044	0.041	0.041	0.043	0.041	0.041	0.041	0.5

	0	Media	0.125	0.25	0.5	1	2	4	8	16	32	64	MIC (ug/mL)
Amikacin	0.563	0.04	0.534	0.498	0.33	0.043	0.042	0.044	0.041	0.041	0.04	0.041	1
	0.597	0.041	0.536	0.48	0.32	0.218	0.042	0.042	0.041	0.041	0.041	0.041	2
	0.477	0.041	0.473	0.503	0.306	0.079	0.049	0.045	0.045	0.045	0.041	0.044	1

2342

AAC(3)-IVa

	0	Media	0.125	0.25	0.5	1	2	4	8	16	32	64	MIC (µg/mL)
Gentamicin	1.097	0.039	1.156	1.146	1.109	1.047	1.068	1.085	1.105	1.046	1.135	1.178	> 64
	1.101	0.038	1.192	1.059	1.105	1.078	1.082	1.055	1.121	1.184	1.234	1.207	> 64
	1.161	0.038	1.183	1.165	1.095	1.071	1.076	1.105	1.05	1.153	1.241	1.08	> 64

	0	0.5	1	2	4	8	16	32	64	128	256	512	MIC (ug/mL)
Gentamicin	0.670	0.657	0.635	0.665	0.633	0.645	0.664	0.623	0.609	0.598	0.366	0.156	> 512
	0.655	0.655	0.635	0.640	0.652	0.623	0.623	0.627	0.621	0.583	0.364	0.150	> 512
	0.658	0.658	0.630	0.652	0.621	0.617	0.613	0.637	0.631	0.645	0.350	0.151	> 512

	0	Media	0.5	1	2	4	8	16	32	64	128	256	(MIC µg/mL)
Apramycin	1.206	0.043	1.275	1.212	1.174	1.182	1.199	1.314	1.255	1.296	1.18	1.24	> 256
	1.39	0.039	1.343	1.379	1.2	1.391	1.356	1.152	1.341	1.293	1.33	1.226	> 256
	1.316	0.039	1.288	1.256	1.234	1.23	1.239	1.25	1.262	1.308	1.296	1.176	> 256

	0	0.5	1	2	4	8	16	32	64	128	256	512	(MIC µg/mL)
Apramycin	0.6714	0.6155	0.6276	0.6213	0.633	0.6356	0.6327	0.6395	0.6294	0.6335	0.6288	0.7443	> 512
	0.6228	0.6294	0.6133	0.637	0.6353	0.6453	0.6412	0.6426	0.6461	0.635	0.6374	0.7319	> 512
	0.6588	0.6319	0.6554	0.646	0.6652	0.6506	0.6551	0.6479	0.6515	0.6468	0.6495	0.7328	> 512

	0	Media	0.125	0.25	0.5	1	2	4	8	16	32	64	MIC (µg/mL)
Tobramycin	1.168	0.04	1.165	1.109	1.095	1.06	1.144	1.079	1.065	1.114	1.047	1.164	> 64
	1.148	0.039	1.139	1.124	1.115	1.139	1.131	1.138	1.12	1.185	1.193	1.15	> 64
	1.168	0.038	1.149	1.169	1.124	1.125	1.181	1.191	1.208	1.219	1.221	1.132	> 64

	0	Media	0.5	1	2	4	8	16	32	64	128	256	MIC (µg/mL)
Kanamycin A	1.032	0.039	1.018	1.006	0.994	1.002	1.002	0.997	0.742	0.042	0.042	0.043	64
	1.076	0.04	1.01	0.997	0.981	0.986	0.998	0.984	0.712	0.041	0.04	0.058	64
	1.083	0.04	1.023	1.025	1.018	1.012	1.014	0.989	0.788	0.06	0.04	0.042	64

	0	Media	0.25	0.5	1	2	4	8	16	32	64	128	MIC (µg/mL)
Amikacin	0.62	0.044	0.359	0.222	0.052	0.044	0.042	0.042	0.042	0.042	0.045	0.053	1
	0.453	0.044	0.34	0.266	0.047	0.042	0.041	0.042	0.044	0.042	0.045	0.051	1
	0.473	0.044	0.364	0.278	0.041	0.042	0.043	0.044	0.061	0.043	0.043	0.047	1

	0	Media	0.5	1	2	4	8	16	32	64	128	256	MIC (µg/mL)
Neomycin	1.073	0.039	1.084	1.117	1.117	1.21	1.102	1.077	0.117	0.512	0.039	0.04	128
	1.117	0.038	1.176	1.105	1.149	1.155	1.144	1.076	0.158	0.04	0.04	0.04	64
	1.145	0.037	1.153	1.071	1.133	1.152	1.168	1.087	0.716	0.041	0.042	0.042	64

	0	Media	0.5	1	2	4	8	16	32	64	128	256	MIC (µg/mL)
Paromomycin	1.161	0.039	1.176	1.195	1.159	1.12	1.194	1.128	1.109	1.203	0.037	0.074	128
	1.126	0.035	1.171	1.14	1.084	1.057	1.044	1.076	1.1	1.157	0.048	0.04	128
	1.139	0.036	1.142	1.132	1.118	1.094	1.117	1.094	1.107	1.043	0.352	0.042	256

2343

meta-AAC0016

	0	Media	256	128	64	32	16	8	4	2	1	0.5	MIC (µg/mL)
Apramycin	1.172	0.035	1.141	1.126	1.123	1.116	1.124	1.116	1.093	1.123	1.128	1.14	> 256
	1.138	0.035	1.099	1.079	1.065	1.061	1.059	1.056	1.052	1.064	1.074	1.088	> 256
	1.131	0.036	1.087	1.056	1.043	1.038	1.038	1.038	1.055	1.055	1.064	1.086	> 256

	0	Media	0.5	1	2	4	8	16	32	64	128	256	MIC (µg/mL)
Gentamicin	1.122	0.037	1.068	1.047	1.04	1.042	1.041	1.036	1.045	1.054	1.036	0.07	256
	1.118	0.039	1.096	1.051	1.05	1.046	1.049	1.045	1.057	1.066	1.032	0.143	> 256
	1.143	0.04	1.107	1.087	1.071	1.065	1.063	1.065	1.071	1.092	1.091	0.069	256

	0	Media	0.5	1	2	4	8	16	32	64	128	256	MIC (µg/mL)
Kanamycin A	1.186	0.04	1.151	1.124	1.114	1.12	1.124	1.122	1.146	0.536	0.062	0.041	128
	1.15	0.039	1.111	1.095	1.085	1.073	1.079	1.09	1.109	0.404	0.062	0.043	128
	1.137	0.04	1.091	1.08	1.058	1.051	1.052	1.063	1.069	0.468	0.137	0.043	256
Tobramycin	1.133	0.043	1.097	1.068	1.061	1.039	1.053	1.062	1.076	1.113	1.114	0.526	> 256
	1.153	0.043	1.119	1.097	1.101	1.085	1.081	1.093	1.092	1.105	1.095	0.43	> 256
	1.182	0.043	1.121	1.129	1.108	1.1	1.123	1.105	1.104	1.123	1.141	0.896	> 256

	0	Media	0.5	1	2	4	8	16	32	64	128	256	MIC (µg/mL)
Neomycin	1.17	0.04	1.155	1.13	1.123	1.134	1.146	1.146	1.156	0.092	0.059	0.058	64
	1.163	0.04	1.129	1.108	1.095	1.078	1.105	1.119	1.16	0.09	0.058	0.047	64
	1.143	0.041	1.101	1.095	1.082	1.079	1.084	1.092	1.088	0.081	0.058	0.091	64
Paromomycin	1.144	0.044	1.108	1.091	1.075	1.07	1.065	1.075	1.09	1.113	1.125	1.11	> 256
	1.144	0.043	1.109	1.091	1.095	1.091	1.087	1.088	1.09	1.095	1.102	1.089	> 256
	1.154	0.045	1.139	1.111	1.107	1.115	1.105	1.107	1.108	1.114	1.118	1.115	> 256

	0	Media	0.5	1	2	4	8	16	32	64	128	256	MIC (µg/mL)
Amikacin	1.182	0.043	1.155	0.074	0.068	0.043	0.042	0.043	0.042	0.042	0.045	0.043	1
	1.185	0.04	1.125	0.072	0.062	0.049	0.043	0.042	0.043	0.044	0.045	0.043	1
	1.185	0.042	1.116	0.254	0.059	0.046	0.044	0.043	0.044	0.043	0.043	0.042	2

2344

meta-AAC0018

	0	Media	0.5	1	2	4	8	16	32	64	128	256	MIC (µg/mL)
Kanamycin	1.018	0.038	0.979	0.963	0.968	0.995	0.995	0.979	0.778	0.041	0.042	0.046	64
	1.022	0.039	0.992	0.958	0.987	0.988	0.967	0.943	0.778	0.165	0.04	0.044	128
	1.065	0.039	1.009	0.994	0.996	0.977	0.966	0.845	0.708	0.159	0.061	0.057	128

	0	Media	0.5	1	2	4	8	16	32	64	128	256	MIC (µg/mL)
Apramycin	1.067	0.037	1.039	1.014	1.006	1.024	0.994	0.999	1.002	1.008	0.996	1.015	> 256
	1.047	0.037	1.013	0.991	0.989	0.96	0.973	0.98	0.974	0.993	0.986	0.999	> 256
	1.036	0.039	1.005	0.968	0.969	0.97	0.991	0.97	0.996	1.028	0.977	0.983	> 256
Gentamicin	1.041	0.039	1.008	0.978	0.97	0.959	0.97	0.969	0.966	0.455	0.042	0.043	128
	1.049	0.04	1.016	0.994	0.987	0.973	0.977	0.981	0.965	0.522	0.058	0.043	128
	1.063	0.04	1.042	1.019	1.013	0.982	0.986	0.989	0.949	0.393	0.168	0.041	256

	0	Media	0.5	1	2	4	8	16	32	64	128	256	MIC (µg/mL)
Tobramycin	0.549	0.039	1.032	1.02	1.006	0.994	0.998	0.995	0.979	0.965	0.916	0.575	> 256
	1.05	0.037	1.036	1.019	1.008	0.994	0.989	0.994	0.989	0.969	0.906	0.509	> 256
	1.043	0.038	1.026	1.011	1.022	0.999	0.994	1.017	0.978	0.974	0.913	0.543	> 256
Amikacin	1.03	0.579	0.262	0.042	0.042	0.04	0.077	0.042	0.042	0.041	0.04	0.042	1
	1.037	0.04	0.052	0.041	0.04	0.04	0.041	0.1	0.04	0.039	0.04	0.041	≤ 0.5
	1.057	0.041	0.041	0.041	0.04	0.04	0.041	0.041	0.039	0.039	0.04	0.042	≤ 0.5

	0	Media	0.5	1	2	4	8	16	32	64	128	256	MIC (µg/mL)
Neomycin	1.029	0.038	1.033	1.015	0.992	0.985	0.929	0.888	0.536	0.139	0.051	0.049	128
	1.062	0.037	1.006	0.991	1.077	0.971	0.948	0.902	0.544	0.14	0.06	0.064	128
	1.051	0.038	1.005	0.969	0.962	0.943	0.931	0.894	0.57	0.153	0.062	0.056	128
Paromomycin	1.023	0.038	1.003	0.98	0.97	0.954	0.948	0.784	0.372	0.157	0.04	0.057	128
	1.037	0.039	1.007	0.991	0.987	0.963	0.965	0.839	0.372	0.173	0.04	0.059	128
	1.034	0.04	1.026	1.009	0.993	0.964	0.946	0.801	0.359	0.133	0.043	0.041	128

2345

meta-AAC0033

	0	Media	0.5	1	2	4	8	16	32	64	128	256	MIC (µg/mL)
Tobramycin	0.4	0.04	0.405	0.404	0.39	0.381	0.366	0.363	0.362	0.358	0.341	0.29	> 256
	0.397	0.04	0.4	0.408	0.384	0.379	0.362	0.365	0.363	0.359	0.34	0.305	> 256
	0.407	0.04	0.4	0.449	0.384	0.382	0.377	0.384	0.368	0.36	0.339	0.297	> 256
Amikacin	0.408	0.04	0.228	0.042	0.043	0.04	0.04	0.042	0.04	0.04	0.04	0.041	1
	0.417	0.039	0.229	0.144	0.041	0.043	0.04	0.068	0.074	0.078	0.039	0.041	2
	0.41	0.04	0.229	0.142	0.041	0.041	0.041	0.041	0.04	0.039	0.041	0.042	2

	0	Media	0.5	1	2	4	8	16	32	64	128	256	MIC (µg/mL)
Neomycin	0.377	0.04	0.388	0.359	0.356	0.352	0.316	0.245	0.194	0.041	0.066	0.044	64
	0.378	0.04	0.392	0.374	0.388	0.353	0.303	0.241	0.197	0.102	0.041	0.045	128
	0.389	0.039	0.377	0.369	0.365	0.353	0.3	0.244	0.202	0.062	0.041	0.066	64
Paromomycin	0.361	0.041	0.401	0.375	0.356	0.341	0.268	0.246	0.193	0.048	0.042	0.062	64
	0.404	0.298	0.411	0.384	0.369	0.352	0.295	0.251	0.189	0.084	0.04	0.041	128
	0.406	0.04	0.381	0.385	0.361	0.357	0.306	0.252	0.193	0.09	0.04	0.04	128

	0	Media	0.125	0.25	0.5	1	2	4	8	16	32	64	MIC (µg/mL)
Kanamycin	0.475	0.043	0.495	0.483	0.513	0.485	0.496	0.458	0.370	0.150	0.042	0.044	32
	0.485	0.045	0.493	0.413	0.494	0.402	0.549	0.369	0.386	0.166	0.046	0.049	32
	0.519	0.043	0.538	0.521	0.527	0.502	0.503	0.490	0.403	0.175	0.042	0.044	32

	0	Media	0.5	1	2	4	8	16	32	64	128	256	MIC (µg/mL)
Apramycin	0.436	0.041	0.413	0.421	0.416	0.41	0.403	0.381	0.387	0.378	0.369	0.292	> 256
	0.407	0.04	0.415	0.399	0.404	0.408	0.395	0.378	0.389	0.376	0.36	0.29	> 256
	0.41	0.04	0.413	0.408	0.412	0.405	0.387	0.382	0.377	0.422	0.392	0.336	> 256
Gentamicin	0.416	0.042	0.441	0.439	0.414	0.399	0.384	0.383	0.373	0.297	0.221	0.043	256
	0.412	0.04	0.479	0.438	0.43	0.424	0.389	0.384	0.375	0.311	0.225	0.082	256
	0.416	0.043	0.412	0.447	0.411	0.417	0.404	0.403	0.379	0.298	0.247	0.1	> 256

2346

meta-AAC0022

	0	Media	0.5	1	2	4	8	16	32	64	128	256	MIC (µg/mL)
Tobramycin	0.44	0.039	0.441	0.401	0.405	0.402	0.42	0.408	0.42	0.401	0.322	0.217	> 256
	0.438	0.039	0.433	0.397	0.411	0.406	0.446	0.415	0.655	0.421	0.331	0.217	> 256
	0.449	0.04	0.436	0.416	0.425	0.428	0.451	0.658	0.606	0.49	0.34	0.221	> 256
Amikacin	0.455	0.04	0.213	0.048	0.04	0.04	0.04	0.04	0.041	0.039	0.04	0.04	1
	0.446	0.04	0.196	0.041	0.04	0.04	0.04	0.041	0.04	0.039	0.039	0.04	1
	0.457	0.043	0.204	0.157	0.04	0.04	0.04	0.04	0.04	0.04	0.039	0.041	2

	0	Media	0.5	1	2	4	8	16	32	64	128	256	MIC (µg/mL)
Apramycin	0.413	0.04	0.446	0.391	0.424	0.412	0.405	0.392	0.404	0.402	0.376	0.253	> 256
	0.421	0.269	0.444	0.425	0.425	0.416	0.427	0.405	0.399	0.402	0.489	0.259	> 256
	0.405	0.041	0.43	0.395	0.4	0.398	0.401	0.397	0.41	0.403	0.37	0.252	> 256
Gentamicin	0.396	0.04	0.418	0.402	0.397	0.385	0.379	0.326	0.211	0.043	0.041	0.041	64
	0.415	0.039	0.42	0.405	0.452	0.396	0.386	0.33	0.217	0.063	0.04	0.041	64
	0.425	0.333	0.424	0.419	0.4	0.418	0.391	0.335	0.212	0.04	0.043	0.042	64

	0	Media	0.5	1	2	4	8	16	32	64	128	256	MIC (µg/mL)
Kanamycin	0.395	0.04	0.414	0.4	0.335	0.197	0.086	0.045	0.042	0.04	0.039	0.046	8
	0.389	0.039	0.407	0.391	0.326	0.201	0.048	0.041	0.04	0.039	0.04	0.04	8
	0.406	0.048	0.411	0.429	0.347	0.206	0.043	0.042	0.04	0.04	0.039	0.041	8

	256	128	64	32	16	8	4	2	1	0.5	Media	0	MIC (µg/mL)
Paromomycin	0.043	0.044	0.048	0.043	0.05	0.172	0.242	0.334	0.389	0.412	0.042	0.408	16
	0.051	0.051	0.045	0.046	0.072	0.182	0.232	0.361	0.405	0.416	0.042	0.426	16
	0.042	0.044	0.046	0.047	0.047	0.18	0.247	0.326	0.41	0.375	0.042	0.402	16

	32	16	8	4	2	1	0.5	0.25	0.125	0.0625	Media	0	MIC (µg/mL)
Neomycin	0.044	0.049	0.121	0.217	0.343	0.371	0.42	0.381	0.4	0.409	0.042	0.399	16
	0.047	0.042	0.116	0.237	0.345	0.391	0.406	0.413	0.438	0.404	0.042	0.47	16
	0.046	0.046	0.044	0.222	0.344	0.345	0.377	0.342	0.393	0.365	0.043	0.397	8

2347

2348

AAC(3)-IX

	0	Media	0.5	1	2	4	8	16	32	64	128	256	MIC (μg/mL)
Amikacin	0.923	0.041	0.607	0.041	0.042	0.043	0.041	0.041	0.052	0.041	0.041	0.043	1
	0.911	0.041	0.602	0.068	0.066	0.068	0.067	0.041	0.041	0.068	0.042	0.061	1
	0.911	0.041	0.592	0.042	0.041	0.067	0.041	0.042	0.047	0.041	0.07	0.063	1

	0	Media	0.5	1	2	4	8	16	32	64	128	256	MIC (μg/mL)
Apramycin	0.893	0.041	0.886	0.77	0.428	0.047	0.041	0.041	0.041	0.041	0.041	0.042	4
	0.878	0.041	0.976	0.762	0.481	0.041	0.041	0.105	0.105	0.043	0.125	0.055	4
	0.905	0.042	1.002	0.822	0.526	0.049	0.075	0.077	0.043	0.042	0.095	0.046	4
Gentamicin	0.909	0.043	0.058	0.079	0.14	0.041	0.042	0.114	0.147	0.042	0.195	0.07	≤ 0.5
	0.937	0.048	0.055	0.043	0.042	0.041	0.042	0.042	0.042	0.052	0.042	0.043	≤ 0.5
	0.945	0.042	0.071	0.061	0.063	0.077	0.041	0.075	0.073	0.042	0.062	0.074	≤ 0.5

	0	Media	0.5	1	2	4	8	16	32	64	128	256	MIC (μg/mL)
Neomycin	0.903	0.041	0.396	0.045	0.041	0.041	0.044	0.044	0.041	0.041	0.041	0.048	1
	0.903	0.041	0.366	0.041	0.057	0.041	0.042	0.041	0.042	0.041	0.042	0.042	1
	0.898	0.041	0.437	0.079	0.07	0.072	0.042	0.042	0.077	0.042	0.087	0.042	1
Paromomycin	0.914	0.041	0.737	0.418	0.044	0.041	0.041	0.041	0.041	0.067	0.055	0.041	2
	0.913	0.041	0.773	0.452	0.059	0.051	0.155	0.11	0.073	0.041	0.078	0.059	2
	0.929	0.041	0.776	0.458	0.076	0.069	0.068	0.08	0.064	0.041	0.079	0.07	2

	0	Media	0.5	1	2	4	8	16	32	64	128	256	MIC (μg/mL)
Tobramycin	0.926	0.041	0.043	0.041	0.041	0.042	0.044	0.042	0.041	0.041	0.041	0.041	≤ 0.5
	0.911	0.041	0.041	0.042	0.041	0.041	0.042	0.041	0.041	0.041	0.042	0.042	≤ 0.5
	0.903	0.041	0.041	0.087	0.096	0.089	0.097	0.045	0.042	0.096	0.089	0.045	≤ 0.5
Kanamycin	1.067	0.041	0.799	0.444	0.041	0.06	0.042	0.045	0.042	0.041	0.041	0.043	2
	0.91	0.041	0.741	0.342	0.087	0.09	0.08	0.096	0.074	0.084	0.074	0.041	2
	0.946	0.051	0.747	0.408	0.08	0.072	0.082	0.042	0.042	0.041	0.042	0.041	2

AAC(3)-X

	0	Media	256	128	64	32	16	8	4	2	1	0.5	MIC (μg/mL)
Apramycin	1.16	0.04	0.041	0.04	0.039	0.04	0.043	0.042	0.041	0.063	1.134	1.229	2
	1.127	0.039	0.039	0.039	0.039	0.041	0.041	0.042	0.044	0.072	1.103	1.18	2
	1.12	0.042	0.041	0.041	0.041	0.041	0.042	0.042	0.042	0.199	1.128	1.224	4
	0	Media	0.5	1	2	4	8	16	32	64	128	256	MIC (μg/mL)
Gentamicin	1.103	0.04	1.048	1.035	1.032	0.166	0.046	0.043	0.043	0.042	0.043	0.043	8
	1.098	0.043	1.026	1.016	1.021	0.532	0.067	0.043	0.043	0.042	0.043	0.043	8
	1.077	0.043	1.024	1.018	1.043	0.563	0.049	0.047	0.042	0.042	0.042	0.044	8

	0	Media	0.5	1	2	4	8	16	32	64	128	256	MIC (μg/mL)
Kanamycin A	1.133	0.037	1.083	1.064	1.052	1.063	1.059	1.069	0.831	0.061	0.044	0.039	64
	1.133	0.037	1.044	1.02	1.004	1.055	1.016	1.037	0.932	0.044	0.042	0.041	64
	1.108	0.04	1.026	0.995	0.982	0.988	1.002	1.045	0.91	0.175	0.043	0.042	128
Tobramycin	1.074	0.038	1.009	0.982	0.972	0.981	0.955	0.062	0.041	0.041	0.041	0.042	16
	1.078	0.039	1.011	0.991	0.991	0.99	0.964	0.086	0.041	0.044	0.045	0.043	16
	1.043	0.04	1	0.991	0.996	0.989	0.989	0.103	0.041	0.039	0.04	0.043	32

	0	Media	0.5	1	2	4	8	16	32	64	128	256	MIC (μg/mL)
Neomycin	1.238	0.038	1.202	0.042	0.04	0.041	0.042	0.043	0.042	0.042	0.042	0.044	1
	1.179	0.039	1.145	0.043	0.04	0.039	0.042	0.043	0.043	0.042	0.042	0.042	1
	1.179	0.039	1.119	0.044	0.04	0.04	0.042	0.042	0.043	0.041	0.05	0.041	1
Paromomycin	1.149	0.041	1.1	1.092	1.049	0.05	0.043	0.042	0.043	0.042	0.041	0.041	4
	1.136	0.041	1.109	1.1	0.967	0.054	0.042	0.042	0.041	0.042	0.042	0.041	4
	1.14	0.042	1.103	1.098	0.823	0.045	0.043	0.042	0.04	0.04	0.04	0.044	4

	0	Media	0.5	1	2	4	8	16	32	64	128	256	MIC (μg/mL)
Amikacin	1.169	0.039	0.239	0.042	0.039	0.043	0.042	0.042	0.077	0.043	0.042	0.041	1
	1.141	0.039	0.104	0.049	0.039	0.039	0.042	0.042	0.042	0.041	0.041	0.041	1
	1.133	0.041	0.441	0.041	0.041	0.04	0.042	0.042	0.041	0.041	0.042	0.046	1

AAC(3)-IIIa

	0	Media	0.5	1	2	4	8	16	32	64	128	256	MIC (µg/mL)
Amikacin	0.724	0.444	0.443	0.039	0.078	0.082	0.078	0.082	0.076	0.076	0.085	0.038	1
	0.725	0.039	0.448	0.086	0.087	0.082	0.073	0.055	0.076	0.039	0.039	0.039	1
	0.753	0.044	0.467	0.08	0.087	0.077	0.039	0.04	0.082	0.039	0.084	0.08	1

	0	Media	0.5	1	2	4	8	16	32	64	128	256	MIC (µg/mL)
Apramycin	0.724	0.034	0.69	0.691	0.676	0.601	0.093	0.078	0.038	0.038	0.037	0.036	8
	0.759	0.034	0.666	0.68	0.716	0.562	0.229	0.137	0.117	0.062	0.036	0.037	16
	0.752	0.21	0.703	0.682	0.691	0.596	0.204	0.092	0.091	0.036	0.115	0.113	8
Gentamicin	0.754	0.041	0.708	0.701	0.663	0.69	0.677	0.659	0.714	0.747	0.692	0.608	> 256
	0.725	0.035	0.697	0.677	0.677	0.68	0.683	0.672	0.66	0.666	0.642	0.583	> 256
	0.746	0.036	0.747	0.684	0.702	0.663	0.669	0.687	0.657	0.714	0.64	0.6	> 256

	0	Media	0.5	1	2	4	8	16	32	64	128	256	MIC (µg/mL)
Neomycin	0.825	0.04	0.782	0.731	0.707	0.776	0.634	0.706	0.622	0.482	0.047	0.061	128
	0.745	0.04	0.725	0.713	0.696	0.663	0.649	0.648	0.608	0.425	0.122	0.104	256
	0.739	0.039	0.753	0.732	0.704	0.693	0.736	0.68	0.79	0.365	0.100	0.077	256
Paromomycin	0.754	0.039	0.743	0.733	0.697	0.733	0.719	0.703	0.716	0.738	0.738	0.698	> 256
	0.737	0.041	0.706	0.692	0.689	0.673	0.672	0.671	0.673	0.679	0.687	0.71	> 256
	0.762	0.041	0.724	0.707	0.726	0.747	0.735	0.685	0.689	0.7	0.737	0.749	> 256

	0	Media	0.5	1	2	4	8	16	32	64	128	256	MIC (µg/mL)
Tobramycin	0.705	0.035	0.707	0.709	0.703	0.718	0.708	0.717	0.714	0.707	0.696	0.694	> 256
	0.791	0.035	0.699	0.654	0.695	0.696	0.775	0.649	0.707	0.64	0.686	0.754	> 256
	0.717	0.036	0.669	0.658	0.648	0.744	0.657	0.705	0.648	0.705	0.645	0.667	> 256
Kanamycin	0.706	0.036	0.68	0.667	0.665	0.672	0.659	0.657	0.655	0.658	0.662	0.681	> 256
	0.811	0.038	0.706	0.703	0.691	0.666	0.684	0.688	0.685	0.687	0.676	0.768	> 256
	0.738	0.039	0.759	0.685	0.744	0.698	0.674	0.727	0.666	0.695	0.761	0.756	> 256

meta-AAC0008

	0	Media	0.5	1	2	4	8	16	32	64	128	256	MIC (µg/mL)
Gentamicin	0.721	0.053	0.724	0.719	0.7	0.711	0.713	0.713	0.729	0.722	0.87	0.471	> 256
	0.832	0.039	0.724	0.729	0.712	0.755	0.715	0.719	0.736	0.722	0.807	0.511	> 256
	0.727	0.04	0.733	0.717	0.718	0.727	0.708	0.718	0.732	0.735	0.725	0.526	> 256

	0	Media	0.5	1	2	4	8	16	32	64	128	256	MIC (µg/mL)
Neomycin	0.732	0.036	0.729	0.719	0.696	0.757	0.691	0.681	0.672	0.665	0.485	0.186	> 256
	0.723	0.036	0.719	0.709	0.719	0.684	0.687	0.681	0.672	0.648	0.513	0.185	> 256
	0.734	0.604	0.732	0.713	0.695	0.719	0.691	0.694	0.656	0.666	0.598	0.29	> 256
Paromomycin	0.765	0.04	0.733	0.742	0.728	0.724	0.728	0.731	0.728	0.735	0.754	0.741	> 256
	0.735	0.038	0.748	0.749	0.727	0.718	0.726	0.729	0.739	0.723	0.749	0.719	> 256
	0.743	0.038	0.744	0.73	0.737	0.733	0.733	0.73	0.712	0.722	0.732	0.743	> 256

	0	Media	0.5	1	2	4	8	16	32	64	128	256	MIC (µg/mL)
Kanamycin	0.744	0.037	0.715	0.722	0.708	0.721	0.717	0.73	0.754	0.776	0.809	0.74	> 256
	0.725	0.037	0.716	0.718	0.701	0.706	0.702	0.729	0.746	0.74	0.834	0.727	> 256
	0.79	0.04	0.752	0.726	0.716	0.708	0.719	0.725	0.737	0.782	0.895	0.899	> 256
Tobramycin	0.758	0.042	0.728	0.719	0.715	0.703	0.73	0.704	0.713	0.726	0.839	0.865	> 256
	0.834	0.04	0.74	0.767	0.793	0.785	0.793	0.707	0.719	0.69	0.789	0.817	> 256
	0.741	0.04	0.748	0.731	0.728	0.722	0.744	0.714	0.719	0.73	0.825	0.858	> 256

	0	Media	0.125	0.25	0.5	1	2	4	8	16	32	64	MIC (ug/mL)
Amikacin	0.5	0.043	0.493	0.436	0.297	0.074	0.042	0.051	0.041	0.041	0.042	0.042	1
	0.467	0.761	0.511	0.448	0.268	0.12	0.042	0.041	0.042	0.041	0.042	0.041	1
	0.487	0.041	0.556	0.476	0.329	0.042	0.043	0.044	0.042	0.042	0.046	0.043	1

	0	Media	0.125	0.25	0.5	1	2	4	8	16	32	64	MIC (ug/mL)
Apramycin	0.429	0.043	0.437	0.416	0.416	0.412	0.400	0.369	0.330	0.115	0.059	0.042	32
	0.440	0.041	0.463	0.423	0.429	0.419	0.451	0.373	0.331	0.056	0.042	0.041	16
	0.489	0.041	0.492	0.506	0.467	0.452	0.473	0.411	0.396	0.157	0.043	0.042	32

meta-AAC0030

	0	Media	0.5	1	2	4	8	16	32	64	128	256	MIC (µg/mL)
Gentamicin	0.731	0.039	0.705	0.688	0.675	0.676	0.677	0.672	0.671	0.665	0.647	0.584	> 256
	0.73	0.039	0.7	0.69	0.677	0.674	0.671	0.673	0.672	0.68	0.647	0.607	> 256
	0.729	0.041	0.701	0.692	0.681	0.674	0.677	0.673	0.681	0.664	0.657	0.618	> 256

	0	Media	0.5	1	2	4	8	16	32	64	128	256	MIC (µg/mL)
Neomycin	0.413	0.039	0.422	0.394	0.395	0.392	0.382	0.324	0.228	0.055	0.042	0.041	64
	0.419	0.04	0.449	0.462	0.437	0.474	0.408	0.333	0.235	0.063	0.042	0.04	64
	0.423	0.04	0.458	0.441	0.456	0.454	0.385	0.342	0.229	0.137	0.04	0.043	128
Paromomycin	0.415	0.04	0.411	0.433	0.422	0.4	0.391	0.448	0.404	0.405	0.395	0.398	> 256
	0.411	0.041	0.425	0.413	0.427	0.416	0.421	0.425	0.442	0.41	0.413	0.379	> 256
	0.412	0.039	0.437	0.41	0.422	0.46	0.437	0.455	0.449	0.41	0.422	0.36	> 256

	0	Media	0.5	1	2	4	8	16	32	64	128	256	MIC (µg/mL)
Kanamycin	0.738	0.04	0.71	0.694	0.688	0.697	0.677	0.686	0.686	0.679	0.68	0.69	> 256
	0.728	0.04	0.704	0.696	0.688	0.687	0.686	0.687	0.683	0.689	0.69	0.696	> 256
	0.738	0.042	0.711	0.695	0.686	0.684	0.683	0.688	0.681	0.69	0.687	0.696	> 256
Tobramycin	0.739	0.461	0.712	0.688	0.692	0.704	0.677	0.658	0.66	0.667	0.681	0.677	> 256
	0.737	0.043	0.714	0.694	0.691	0.678	0.691	0.665	0.669	0.67	0.678	0.679	> 256
	0.746	0.044	0.739	0.717	0.693	0.683	0.681	0.672	0.67	0.677	0.681	0.681	> 256

	0	Media	0.125	0.25	0.5	1	2	4	8	16	32	64	MIC (ug/mL)
Apramycin	0.428	0.040	0.400	0.393	0.393	0.393	0.350	0.296	0.191	0.041	0.041	0.041	16
	0.452	0.040	0.438	0.400	0.408	0.381	0.395	0.297	0.183	0.043	0.041	0.041	16
	0.456	0.042	0.512	0.433	0.426	0.415	0.420	0.346	0.193	0.042	0.043	0.045	16

	0	Media	0.125	0.25	0.5	1	2	4	8	16	32	64	MIC (ug/mL)
Amikacin	0.443	0.042	0.428	0.38	0.315	0.092	0.044	0.042	0.045	0.04	0.067	0.041	1
	0.458	0.041	0.426	0.39	0.309	0.116	0.043	0.041	0.041	0.041	0.041	0.041	2
	0.459	0.04	0.429	0.416	0.353	0.081	0.043	0.041	0.041	0.041	0.042	0.041	1

2354

meta-AAC0071

	0	Media	256	128	64	32	16	8	4	2	1	0.5	MIC (µg/mL)
Apramycin	1.292	0.037	0.037	0.038	0.037	0.039	0.039	0.04	0.16	1.232	1.219	1.225	8
	1.279	0.037	0.038	0.037	0.037	0.037	0.04	0.04	0.082	1.204	1.181	1.179	4
	1.274	0.038	0.038	0.037	0.037	0.036	0.039	0.04	0.281	1.152	1.168	1.186	8

	0	Media	0.5	1	2	4	8	16	32	64	128	256	MIC (µg/mL)
Gentamicin	1.272	0.039	1.264	1.23	1.225	1.206	1.211	1.222	1.212	1.186	1.178	0.451	> 256
	1.279	0.042	1.238	1.202	1.191	1.198	1.183	1.184	1.182	1.186	1.215	0.533	> 256
	1.271	0.044	1.239	1.229	1.208	1.219	1.208	1.214	1.219	1.227	1.254	0.671	> 256

	0	Media	0.5	1	2	4	8	16	32	64	128	256	MIC (µg/mL)
Kanamycin A	1.3	0.039	1.277	1.258	1.246	1.239	1.235	1.224	1.224	1.217	1.219	1.238	> 256
	1.289	0.039	1.236	1.204	1.185	1.171	1.173	1.173	1.17	1.166	1.172	1.192	> 256
	1.273	0.04	1.207	1.177	1.15	1.137	1.141	1.142	1.146	1.148	1.156	1.186	> 256
Tobramycin	1.261	0.04	1.198	1.171	1.149	1.145	1.138	1.14	1.147	1.151	1.146	1.188	> 256
	1.259	0.042	1.226	1.194	1.187	1.174	1.165	1.171	1.16	1.163	1.172	1.207	> 256
	1.278	0.044	1.242	1.224	1.235	1.208	1.212	1.215	1.214	1.226	1.23	1.27	> 256

	0	Media	0.5	1	2	4	8	16	32	64	128	256	MIC (µg/mL)
Neomycin	1.316	0.042	0.696	0.04	0.039	0.043	0.042	0.042	0.041	0.041	0.041	0.041	1
	1.292	0.039	0.845	0.04	0.039	0.039	0.043	0.042	0.042	0.042	0.045	0.041	1
	1.285	0.04	0.283	0.04	0.041	0.041	0.042	0.042	0.042	0.042	0.042	0.044	1
Paromomycin	1.279	0.041	1.282	1.266	0.219	0.041	0.042	0.043	0.042	0.043	0.043	0.058	4
	1.277	0.042	1.275	1.254	0.175	0.042	0.042	0.042	0.042	0.042	0.042	0.044	4
	1.306	0.042	1.282	1.278	0.372	0.042	0.042	0.042	0.043	0.042	0.042	0.043	4

	0	Media	0.5	1	2	4	8	16	32	64	128	256	MIC (µg/mL)
Amikacin	1.33	0.038	1.266	0.039	0.039	0.041	0.043	0.044	0.044	0.042	0.041	0.045	1
	1.294	0.038	1.246	0.04	0.039	0.039	0.041	0.041	0.041	0.042	0.042	0.041	1
	1.307	0.039	1.271	0.251	0.04	0.04	0.042	0.041	0.041	0.04	0.042	0.043	2

2355

AAC(3)-IIIb

	0	Media	0.25	0.5	1	2	4	8	16	32	64	128	MIC (µg/mL)
Apramycin	0.38	0.043	0.399	0.406	0.39	0.37	0.215	0.052	0.048	0.044	0.042	0.045	8
	0.388	0.043	0.403	0.395	0.396	0.354	0.212	0.046	0.044	0.051	0.044	0.045	8
	0.401	0.042	0.404	0.399	0.381	0.347	0.207	0.044	0.064	0.043	0.043	0.043	8

	0	Media	0.5	1	2	4	8	16	32	64	128	256	MIC (µg/mL)
Gentamicin	1.04	0.042	0.992	0.95	0.932	0.919	0.895	0.877	0.881	0.878	0.819	0.657	> 256
	1.071	0.044	0.978	0.952	0.946	0.928	0.901	0.881	0.869	0.862	0.773	0.648	> 256
	1.032	0.044	0.969	0.963	0.943	0.928	0.905	0.884	0.883	0.848	0.795	0.588	> 256

	0	Media	0.5	1	2	4	8	16	32	64	128	256	MIC (µg/mL)
Paromomycin	0.426	0.045	0.451	0.407	0.386	0.402	0.425	0.417	0.401	0.486	0.431	0.347	> 256
	0.402	0.043	0.42	0.394	0.394	0.396	0.408	0.406	0.408	0.407	0.404	0.343	> 256
	0.42	0.044	0.421	0.513	0.391	0.493	0.438	0.499	0.429	0.499	0.456	0.373	> 256

	0	Media	0.5	1	2	4	8	16	32	64	128	256	MIC (µg/mL)
Kanamycin A	0.445	0.039	0.441	0.416	0.478	0.455	0.439	0.451	0.485	0.414	0.418	0.465	> 256
	0.486	0.039	0.426	0.412	0.386	0.4	0.385	0.4	0.384	0.396	0.466	0.408	> 256
	0.524	0.04	0.513	0.416	0.391	0.468	0.392	0.397	0.384	0.44	0.379	0.432	> 256

	0	Media	0.25	0.5	1	2	4	8	16	32	64	128	MIC (µg/mL)
Amikacin	0.413	0.042	0.235	0.17	0.044	0.045	0.045	0.044	0.043	0.043	0.046	0.043	1
	0.424	0.041	0.239	0.082	0.041	0.042	0.044	0.044	0.049	0.042	0.043	0.042	0.5
	0.426	0.041	0.24	0.07	0.041	0.042	0.042	0.044	0.042	0.04	0.043	0.043	0.5

	0	Media	0.5	1	2	4	8	16	32	64	128	256	MIC (µg/mL)
Neomycin	1.067	0.039	1.023	0.997	0.984	0.975	0.968	0.953	0.926	0.925	0.751	0.042	256
	1.069	0.04	1.027	1	0.998	0.972	0.959	0.959	0.943	0.93	0.678	0.043	256
	1.05	0.041	1.024	1	1.007	0.963	0.956	0.946	0.935	0.907	0.552	0.042	256

	0	Media	0.5	1	2	4	8	16	32	64	128	256	MIC (µg/mL)
Tobramycin	1.042	0.04	1.002	0.974	0.959	0.946	0.927	0.911	0.892	0.88	0.872	0.867	> 256
	1.054	0.04	0.997	0.966	0.954	0.943	0.923	0.917	0.894	0.881	0.872	0.865	> 256
	1.041	0.042	0.999	0.962	0.951	0.932	0.914	0.89	0.899	0.905	0.875	0.891	> 256

2356

meta-AAC0038

	0	Media	0.5	1	2	4	8	16	32	64	128	256	MIC (µg/mL)
Gentamicin	0.918	0.04	0.835	0.983	0.798	0.764	0.747	0.733	0.751	0.762	0.777	0.723	> 256
	0.975	0.042	0.83	0.811	0.794	0.769	0.78	0.757	0.76	0.777	0.788	0.706	> 256
	0.904	0.043	0.832	0.852	0.975	0.771	0.761	0.767	0.77	0.777	0.791	0.739	> 256

	0	Media	0.5	1	2	4	8	16	32	64	128	256	MIC (µg/mL)
Neomycin	0.963	0.04	0.888	0.844	0.832	0.793	0.949	0.743	0.727	0.674	0.289	0.047	256
	0.94	0.053	0.883	0.871	0.82	0.769	0.756	0.746	0.713	0.645	0.274	0.043	256
	1.063	0.044	0.851	0.814	0.833	0.934	0.969	0.714	0.701	0.656	0.269	0.043	256
Paromomycin	1.055	0.042	0.866	0.827	0.784	0.793	0.789	0.787	0.731	0.736	0.741	0.694	> 256
	1.057	0.043	0.859	0.842	0.792	0.783	0.759	0.736	0.723	0.717	0.711	0.683	> 256
	0.917	0.043	0.836	0.796	0.787	0.783	0.78	0.735	0.731	0.732	0.717	0.702	> 256

	0	Media	0.5	1	2	4	8	16	32	64	128	256	MIC (µg/mL)
Kanamycin	0.904	0.04	0.837	0.809	0.791	0.78	0.773	0.764	0.78	0.762	0.785	0.794	> 256
	0.891	0.04	0.83	0.812	0.781	0.771	0.765	0.772	0.777	0.803	0.805	0.819	> 256
	0.894	0.041	0.847	0.818	0.784	0.78	0.765	0.756	0.777	0.776	0.787	0.793	> 256
Tobramycin	0.916	0.669	0.815	0.786	0.913	0.809	0.755	0.774	0.76	0.757	0.778	0.921	> 256
	0.876	0.043	0.834	0.876	0.769	0.772	0.754	0.766	0.77	0.757	0.76	0.79	> 256
	0.897	0.045	0.855	0.798	0.774	0.753	0.752	0.745	0.753	0.764	0.812	0.8	> 256

	0	Media	0.25	0.5	1	2	4	8	16	32	64	128	MIC (µg/mL)
Amikacin	0.426	0.043	0.354	0.238	0.199	0.043	0.042	0.042	0.041	0.042	0.041	0.043	2
	0.428	0.042	0.35	0.235	0.042	0.041	0.041	0.042	0.042	0.042	0.041	0.045	1
	0.431	0.042	0.377	0.195	0.042	0.041	0.041	0.043	0.042	0.042	0.042	0.044	1

	0	Media	0.125	0.25	0.5	1	2	4	8	16	32	64	MIC (ug/mL)
Apramycin	0.432	0.038	0.396	0.336	0.346	0.346	0.330	0.326	0.239	0.165	0.039	0.041	32
	0.426	0.037	0.464	0.479	0.375	0.401	0.339	0.333	0.254	0.147	0.037	0.038	32
	0.379	0.040	0.435	0.398	0.396	0.362	0.353	0.320	0.236	0.139	0.119	0.040	64

2357

2358

meta-AAC0032

	0	Media	0.5	1	2	4	8	16	32	64	128	256	MIC (µg/mL)
Kanamycin	0.464	0.055	0.942	1.003	0.984	0.899	0.295	0.04	0.039	0.04	0.041	0.071	16
	1.028	0.045	0.972	0.955	0.947	0.853	0.433	0.209	0.04	0.045	0.04	0.044	32
	1.017	0.038	0.957	0.937	0.942	0.882	0.412	0.044	0.056	0.039	0.039	0.039	16

	0	Media	0.5	1	2	4	8	16	32	64	128	256	MIC (µg/mL)
Apramycin	0.422	0.037	0.903	0.545	0.203	0.037	0.039	0.04	0.041	0.04	0.04	0.051	4
	0.989	0.038	0.874	0.542	0.039	0.037	0.04	0.041	0.041	0.041	0.04	0.042	2
	0.998	0.038	0.869	0.547	0.217	0.041	0.041	0.041	0.041	0.04	0.041	0.051	4
Gentamicin	0.988	0.039	0.972	0.975	0.999	0.955	0.806	0.277	0.228	0.041	0.042	0.077	64
	0.976	0.045	0.976	0.966	0.958	0.96	0.811	0.278	0.138	0.042	0.043	0.042	64
	1.002	0.042	0.988	0.971	0.991	0.957	0.834	0.272	0.142	0.042	0.041	0.043	64

	0	Media	0.5	1	2	4	8	16	32	64	128	256	MIC (µg/mL)
Neomycin	1.062	0.037	0.342	0.039	0.037	0.041	0.039	0.04	0.041	0.039	0.039	0.052	1
	1.048	0.037	0.277	0.039	0.037	0.037	0.039	0.041	0.04	0.041	0.043	0.042	1
	1.042	0.039	0.338	0.071	0.039	0.037	0.04	0.041	0.04	0.04	0.052	0.074	1
Paromomycin	1.041	0.039	0.525	0.041	0.04	0.04	0.04	0.041	0.042	0.04	0.041	0.084	1
	1.064	0.041	0.538	0.216	0.041	0.041	0.041	0.04	0.041	0.04	0.041	0.084	2
	1.101	0.041	0.576	0.225	0.041	0.04	0.04	0.041	0.04	0.04	0.047	0.075	2

	0	Media	0.5	1	2	4	8	16	32	64	128	256	MIC (µg/mL)
Tobramycin	1.084	0.037	0.995	0.572	0.18	0.038	0.04	0.04	0.039	0.044	0.039	0.041	4
	1.063	0.038	0.982	0.594	0.185	0.154	0.041	0.041	0.041	0.04	0.04	0.042	8
	1.056	0.038	0.98	0.585	0.203	0.04	0.041	0.041	0.04	0.039	0.042	0.041	4
Amikacin	1.068	0.04	0.405	0.384	0.045	0.04	0.041	0.041	0.04	0.04	0.043	0.041	2
	1.054	0.04	0.415	0.049	0.04	0.042	0.04	0.04	0.04	0.04	0.04	0.043	1
	1.09	0.042	0.438	0.042	0.044	0.04	0.041	0.047	0.04	0.039	0.039	0.043	1

2359

AAC(3)-VIa

	0	Media	0.5	1	2	4	8	16	32	64	128	256	MIC (µg/mL)
Amikacin	0.931	0.046	0.661	0.294	0.042	0.075	0.042	0.042	0.042	0.042	0.044	0.042	2
	0.941	0.041	0.416	0.07	0.042	0.042	0.042	0.042	0.088	0.046	0.042	0.043	1
	0.953	0.042	0.398	0.042	0.042	0.043	0.043	0.043	0.043	0.043	0.043	0.042	1

	0	Media	0.5	1	2	4	8	16	32	64	128	256	MIC (µg/mL)
Apramycin	0.914	0.042	0.901	0.739	0.43	0.044	0.05	0.042	0.041	0.052	0.041	0.041	4
	0.909	0.041	0.866	0.717	0.458	0.041	0.043	0.041	0.041	0.042	0.043	0.041	4
	0.941	0.043	0.896	0.752	0.483	0.041	0.041	0.041	0.049	0.041	0.05	0.134	4
Gentamicin	0.917	0.041	0.955	0.9	0.917	0.895	0.897	0.859	0.732	0.323	0.183	0.101	> 256
	0.909	0.043	0.92	0.888	0.888	0.867	0.883	0.857	0.745	0.325	0.126	0.043	256
	0.968	0.042	0.938	0.969	0.942	0.939	0.885	0.876	0.809	0.382	0.124	0.048	256

	0	Media	0.5	1	2	4	8	16	32	64	128	256	MIC (µg/mL)
Neomycin	0.915	0.043	0.046	0.044	0.041	0.043	0.041	0.042	0.041	0.041	0.041	0.042	≤ 0.5
	0.913	0.041	0.047	0.042	0.066	0.042	0.069	0.042	0.041	0.045	0.042	0.041	≤ 0.5
	0.915	0.041	0.078	0.042	0.041	0.041	0.042	0.042	0.042	0.042	0.044	0.042	≤ 0.5
Paromomycin	0.944	0.041	0.727	0.32	0.043	0.073	0.041	0.042	0.042	0.042	0.041	0.078	2
	0.926	0.041	0.709	0.327	0.041	0.041	0.041	0.041	0.042	0.041	0.041	0.043	2
	0.925	0.041	0.699	0.344	0.045	0.045	0.043	0.041	0.041	0.041	0.043	0.042	2

	0	Media	0.5	1	2	4	8	16	32	64	128	256	MIC (µg/mL)
Tobramycin	0.919	0.041	0.897	0.833	0.615	0.19	0.087	0.041	0.042	0.041	0.044	0.043	8
	0.919	0.041	0.899	0.819	0.602	0.191	0.084	0.041	0.041	0.069	0.043	0.042	8
	0.923	0.041	0.904	0.807	0.593	0.192	0.083	0.041	0.042	0.082	0.042	0.042	8
Kanamycin	0.92	0.041	0.878	0.832	0.739	0.33	0.135	0.041	0.041	0.041	0.041	0.042	16
	0.904	0.041	0.886	0.833	0.727	0.326	0.136	0.044	0.041	0.043	0.041	0.043	16
	0.995	0.041	0.892	0.859	0.747	0.341	0.135	0.041	0.041	0.041	0.041	0.044	16

2360

meta-AAC0029

	0	Media	0.5	1	2	4	8	16	32	64	128	256	MIC (µg/mL)
Neomycin	1.066	0.037	0.051	0.038	0.037	0.042	0.039	0.039	0.04	0.04	0.04	0.041	≤ 0.5
	1.063	0.797	0.349	0.038	0.037	0.037	0.04	0.04	0.041	0.041	0.042	0.04	1
	1.057	0.039	0.042	0.039	0.04	0.038	0.04	0.04	0.042	0.041	0.041	0.043	≤ 0.5
Paromomycin	1.064	0.039	0.399	0.04	0.044	0.04	0.04	0.041	0.041	0.042	0.041	0.042	1
	1.078	0.042	0.355	0.074	0.041	0.041	0.041	0.04	0.041	0.04	0.04	0.042	1
	1.102	0.041	0.375	0.046	0.041	0.04	0.041	0.041	0.041	0.044	0.041	0.043	1

	0	Media	0.125	0.25	0.5	1	2	4	8	16	32	64	MIC (ug/mL)
Amikacin	0.544	0.042	0.495	0.307	0.075	0.046	0.042	0.042	0.042	0.041	0.049	0.044	0.5
	0.542	0.042	0.448	0.339	0.211	0.043	0.042	0.041	0.043	0.042	0.041	0.041	1
	0.464	0.04	0.444	0.336	0.114	0.041	0.042	0.051	0.086	0.152	0.097	0.169	1

	0	Media	0.125	0.25	0.5	1	2	4	8	16	32	64	MIC (ug/mL)
Apramycin	0.464	0.040	0.436	0.443	0.393	0.305	0.204	0.042	0.041	0.041	0.041	0.041	4
	0.424	0.041	0.433	0.491	0.422	0.360	0.197	0.043	0.044	0.043	0.041	0.042	4
	0.416	0.040	0.415	0.511	0.376	0.303	0.193	0.046	0.041	0.041	0.056	0.041	4
Gentamicin	0.537	0.041	0.536	0.498	0.502	0.513	0.489	0.532	0.526	0.575	0.566	0.596	> 64
	0.478	0.040	0.496	0.577	0.513	0.541	0.484	0.562	0.538	0.580	0.452	0.610	> 64
	0.504	0.040	0.526	0.497	0.530	0.543	0.563	0.577	0.556	0.577	0.581	0.547	> 64

	0	Media	0.125	0.25	0.5	1	2	4	8	16	32	64	MIC (ug/mL)
Tobramycin	0.435	0.043	0.422	0.460	0.423	0.473	0.397	0.401	0.303	0.227	0.146	0.042	64
	0.445	0.042	0.467	0.498	0.482	0.553	0.429	0.471	0.333	0.244	0.143	0.053	64
	0.412	0.046	0.415	0.530	0.421	0.510	0.394	0.484	0.294	0.234	0.139	0.041	64
Kanamycin	0.518	0.041	0.508	0.528	0.595	0.481	0.383	0.246	0.153	0.040	0.041	0.041	16
	0.495	0.042	0.466	0.565	0.484	0.532	0.370	0.319	0.160	0.042	0.040	0.042	16
	0.502	0.043	0.553	0.501	0.507	0.455	0.427	0.241	0.150	0.041	0.041	0.042	16

2361

meta-AAC0034

	0	Media	0.5	1	2	4	8	16	32	64	128	256	MIC (µg/mL)
Tobramycin	0.414	0.04	0.401	0.392	0.406	0.414	0.405	0.419	0.379	0.346	0.299	0.246	> 256
	0.42	0.041	0.407	0.409	0.41	0.396	0.396	0.397	0.39	0.354	0.314	0.242	> 256
	0.456	0.043	0.418	0.435	0.431	0.404	0.398	0.386	0.381	0.362	0.299	0.246	> 256
Amikacin	0.43	0.039	0.209	0.044	0.043	0.057	0.042	0.042	0.041	0.058	0.039	0.04	1
	0.641	0.039	0.21	0.1	0.04	0.04	0.094	0.041	0.041	0.039	0.039	0.04	2
	0.49	0.04	0.24	0.084	0.078	0.04	0.04	0.08	0.04	0.039	0.04	0.041	1

	0	Media	0.5	1	2	4	8	16	32	64	128	256	MIC (µg/mL)
Neomycin	0.988	0.038	0.047	0.039	0.037	0.04	0.039	0.039	0.039	0.053	0.052	0.049	≤ 0.5
	1.013	0.037	0.36	0.038	0.098	0.037	0.04	0.04	0.048	0.043	0.043	0.041	1
	1.017	0.039	0.044	0.041	0.039	0.039	0.04	0.04	0.04	0.063	0.06	0.042	≤ 0.5
Paromomycin	1.031	0.039	0.506	0.043	0.214	0.04	0.04	0.04	0.043	0.043	0.149	0.057	1
	1.026	0.043	0.479	0.045	0.043	0.04	0.04	0.04	0.04	0.04	0.04	0.043	1
	1.052	0.042	0.506	0.052	0.043	0.041	0.042	0.043	0.042	0.045	0.05	0.043	1

	0	Media	0.5	1	2	4	8	16	32	64	128	256	MIC (µg/mL)
Kanamycin	0.453	0.039	0.432	0.444	0.411	0.387	0.383	0.379	0.364	0.326	0.262	0.179	> 256
	0.469	0.039	0.438	0.407	0.394	0.403	0.387	0.392	0.378	0.342	0.273	0.187	> 256
	0.471	0.04	0.442	0.43	0.398	0.404	0.393	0.424	0.373	0.337	0.28	0.41	> 256

	0	Media	0.125	0.25	0.5	1	2	4	8	16	32	64	MIC (ug/mL)
Apramycin	0.577	0.041	0.647	0.526	0.541	0.465	0.399	0.177	0.044	0.042	0.041	0.042	8
	0.559	0.042	0.609	0.608	0.554	0.520	0.356	0.182	0.043	0.042	0.041	0.041	8
	0.586	0.042	0.645	0.636	0.575	0.521	0.389	0.195	0.042	0.041	0.043	0.046	8
Gentamicin	0.697	0.042	0.727	0.706	0.672	0.619	0.661	0.618	0.684	0.648	0.660	0.606	> 64
	0.675	0.040	0.698	0.612	0.707	0.558	0.649	0.537	0.681	0.497	0.627	0.458	> 64
	0.627	0.041	0.643	0.695	0.607	0.635	0.598	0.660	0.605	0.630	0.587	0.606	> 64

2362

meta-AAC0035

	0	Media	256	128	64	32	16	8	4	2	1	0.5	MIC (µg/mL)
Apramycin	1.292	0.037	0.037	0.037	0.036	0.038	0.039	0.041	0.581	1.184	1.2	1.231	8
	1.24	0.037	0.037	0.038	0.036	0.036	0.039	0.041	0.64	1.171	1.182	1.2	8
	1.227	0.037	0.037	0.051	0.037	0.035	0.04	0.105	0.564	1.159	1.163	1.186	8
	0	Media	0.5	1	2	4	8	16	32	64	128	256	MIC (µg/mL)
Gentamicin	1.238	0.037	1.262	1.258	1.271	1.272	1.259	1.254	1.244	1.223	1.196	1.216	> 256
	1.228	0.039	1.241	1.239	1.247	1.242	1.236	1.232	1.23	1.214	1.208	1.218	> 256
	1.262	0.038	1.26	1.251	1.261	1.279	1.27	1.27	1.263	1.257	1.259	1.281	> 256
	0	Media	0.5	1	2	4	8	16	32	64	128	256	MIC (µg/mL)
Kanamycin A	1.318	0.036	1.288	1.27	1.252	1.225	1.224	1.204	1.186	1.169	1.119	0.039	256
	1.264	0.036	1.263	1.226	1.199	1.196	1.188	1.186	1.182	1.164	1.126	0.246	> 256
	1.264	0.036	1.254	1.202	1.171	1.16	1.154	1.159	1.2	1.2	1.106	0.04	256
Tobramycin	1.263	0.037	1.238	1.195	1.162	1.16	1.173	1.16	1.182	1.202	1.211	0.271	> 256
	1.274	0.039	1.267	1.23	1.207	1.196	1.199	1.204	1.22	1.222	1.207	0.252	> 256
	1.309	0.04	1.306	1.28	1.263	1.253	1.258	1.251	1.247	1.258	1.247	0.535	> 256
	0	Media	0.5	1	2	4	8	16	32	64	128	256	MIC (µg/mL)
Neomycin	1.326	0.039	0.919	0.039	0.039	0.038	0.044	0.041	0.041	0.041	0.042	0.041	1
	1.302	0.04	0.75	0.043	0.039	0.041	0.042	0.043	0.043	0.102	0.042	0.043	1
	1.284	0.04	0.396	0.041	0.041	0.04	0.044	0.044	0.043	0.045	0.042	0.044	1
Paromomycin	1.294	0.041	1.197	0.911	0.043	0.042	0.042	0.042	0.041	0.042	0.042	0.043	2
	1.299	0.041	1.214	1.015	0.096	0.042	0.042	0.042	0.042	0.041	0.042	0.043	2
	1.302	0.042	1.258	1.037	0.044	0.042	0.042	0.041	0.043	0.041	0.042	0.044	2
	0	Media	0.5	1	2	4	8	16	32	64	128	256	MIC (µg/mL)
Amikacin	1.348	0.04	1.245	0.048	0.056	0.039	0.042	0.042	0.042	0.041	0.042	0.042	1
	1.335	0.039	1.215	0.042	0.04	0.039	0.045	0.043	0.042	0.042	0.046	0.046	1
	1.3	0.04	1.218	0.059	0.042	0.042	0.043	0.043	0.042	0.041	0.042	0.045	1

2363

AAC(3)-IIb

	0	Media	0.5	1	2	4	8	16	32	64	128	256	MIC (µg/mL)
Tobramycin	1.056	0.041	0.996	0.962	0.933	0.908	0.886	0.868	0.845	0.825	0.808	0.792	> 256
	1.033	0.04	0.989	0.948	0.937	0.94	0.875	0.861	0.832	0.831	0.793	0.746	> 256
	1.03	0.044	0.969	0.936	0.924	0.926	0.865	0.864	0.866	0.807	0.793	0.726	> 256
Gentamicin	1.021	0.04	0.961	0.927	0.902	0.883	0.869	0.898	0.847	0.817	0.803	0.821	> 256
	0.984	0.043	0.929	0.915	1.054	0.873	1.032	0.837	0.853	0.824	0.813	0.817	> 256
	0.987	0.043	0.955	0.899	0.879	0.87	0.854	0.853	0.824	0.807	0.815	0.938	> 256
	0	Media	0.5	1	2	4	8	16	32	64	128	256	MIC (µg/mL)
Kanamycin	0.49	0.039	0.467	0.436	0.433	0.418	0.413	0.397	0.371	0.303	0.222	0.144	> 256
	0.461	0.039	0.459	0.434	0.437	0.415	0.413	0.395	0.361	0.3	0.216	0.141	> 256
	0.503	0.039	0.474	0.444	0.447	0.417	0.408	0.401	0.376	0.352	0.212	0.146	> 256
	0	Media	0.25	0.5	1	2	4	8	16	32	64	128	MIC (µg/mL)
Apramycin	0.518	0.043	0.543	0.482	0.511	0.475	0.355	0.193	0.042	0.042	0.043	0.043	16
	0.547	0.042	0.531	0.468	0.514	0.429	0.345	0.186	0.141	0.043	0.041	0.046	32
	0.551	0.042	0.514	0.517	0.486	0.452	0.357	0.189	0.043	0.041	0.044	0.043	16
	0	Media	0.25	0.5	1	2	4	8	16	32	64	128	MIC (µg/mL)
Amikacin	0.526	0.042	0.377	0.180	0.042	0.049	0.044	0.045	0.044	0.041	0.044	0.041	1
	0.480	0.051	0.361	0.220	0.043	0.049	0.041	0.043	0.043	0.043	0.041	0.041	1
	0.535	0.045	0.418	0.122	0.041	0.041	0.042	0.045	0.043	0.043	0.048	0.043	1
	0	Media	0.0625	0.125	0.25	0.5	1	2	4	8	16	32	MIC (µg/mL)
Neomycin	0.586	0.043	0.535	0.468	0.362	0.044	0.041	0.044	0.049	0.046	0.043	0.046	0.5
	0.518	0.042	0.502	0.471	0.381	0.084	0.045	0.045	0.044	0.043	0.048	0.066	0.5
	0.563	0.044	0.537	0.483	0.379	0.204	0.042	0.044	0.045	0.044	0.056	0.05	1
	0	Media	0.5	1	2	4	8	16	32	64	128	256	MIC (µg/mL)
Paromomycin	0.516	0.043	0.269	0.077	0.049	0.042	0.048	0.042	0.05	0.044	0.046	0.048	1
	0.506	0.042	0.326	0.219	0.046	0.044	0.037	0.038	0.043	0.043	0.051	0.04	2
	0.537	0.042	0.334	0.045	0.046	0.046	0.037	0.18	0.045	0.042	0.034	0.033	1

2364

AAC(3)-IIc

	0	Media	0.5	1	2	4	8	16	32	64	128	256	MIC (µg/mL)
Tobramycin	1.137	0.039	0.937	0.901	0.884	0.809	0.742	0.607	0.278	0.076	0.041	0.041	64
	1.083	0.04	0.974	0.959	0.983	0.839	0.795	0.598	0.248	0.16	0.042	0.042	128
	1.092	0.045	0.965	0.924	0.967	0.925	0.774	0.597	0.258	0.049	0.042	0.043	64
Gentamicin	0.999	0.043	0.972	0.955	0.933	0.954	0.863	0.852	0.857	0.814	0.725	0.69	> 256
	1.007	0.044	0.949	0.908	0.874	0.988	0.849	0.831	0.821	0.785	0.711	0.812	> 256
	1.107	0.044	1.052	0.878	0.836	0.834	0.814	0.794	0.77	0.747	0.843	0.73	> 256

	0	Media	0.5	1	2	4	8	16	32	64	128	256	MIC (µg/mL)
Kanamycin	0.773	0.041	0.808	0.75	0.662	0.381	0.216	0.147	0.04	0.04	0.04	0.041	32
	0.743	0.04	0.797	0.779	0.627	0.491	0.215	0.151	0.041	0.041	0.039	0.04	32
	0.549	0.04	0.482	0.439	0.426	0.303	0.217	0.154	0.04	0.039	0.04	0.042	32

	0	Media	0.25	0.5	1	2	4	8	16	32	64	128	(MIC µg/mL)
Apramycin	0.587	0.043	0.516	0.408	0.239	0.041	0.043	0.041	0.041	0.041	0.042	0.042	2
	0.536	0.043	0.450	0.366	0.226	0.051	0.044	0.044	0.042	0.041	0.041	0.042	2
	0.522	0.042	0.470	0.384	0.228	0.044	0.069	0.043	0.042	0.041	0.041	0.044	2

	0	Media	0.5	1	2	4	8	16	32	64	128	256	MIC (µg/mL)
Paromomycin	1.024	0.042	0.257	0.132	0.042	0.040	0.041	0.041	0.041	0.039	0.038	0.036	2
	0.580	0.040	0.251	0.050	0.041	0.041	0.039	0.043	0.043	0.043	0.045	0.047	1
	0.606	0.042	0.270	0.043	0.042	0.042	0.042	0.043	0.041	0.043	0.043	0.048	1

	0	Media	0.0625	0.125	0.25	0.5	1	2	4	8	16	32	MIC (µg/mL)
Neomycin	0.891	0.042	0.620	0.484	0.293	0.041	0.042	0.042	0.041	0.043	0.040	0.041	0.5
	0.571	0.043	0.483	0.477	0.312	0.043	0.063	0.042	0.044	0.045	0.041	0.043	0.5
	0.642	0.043	0.537	0.496	0.321	0.140	0.042	0.042	0.043	0.041	0.042	0.043	1

	0	Media	0.25	0.5	1	2	4	8	16	32	64	128	MIC (µg/mL)
Amikacin	0.597	0.042	0.335	0.153	0.044	0.042	0.041	0.041	0.041	0.041	0.041	0.041	1
	0.518	0.042	0.292	0.176	0.047	0.042	0.044	0.041	0.041	0.043	0.035	0.041	1
	0.526	0.042	0.284	0.095	0.043	0.075	0.043	0.040	0.042	0.040	0.038	0.042	0.5

2365

AAC(3)-IIa

	0	Media	0.5	1	2	4	8	16	32	64	128	256	MIC (µg/mL)
Paromomycin	1.054	0.037	1.061	0.54	0.506	0.04	0.039	0.041	0.038	0.038	0.035	0.037	4
	1.057	0.035	1.068	0.572	0.616	0.034	0.038	0.04	0.04	0.036	0.037	0.042	4
	1.092	0.036	1.067	0.51	0.035	0.035	0.038	0.039	0.038	0.039	0.038	0.038	2

	0	Media	0.5	1	2	4	8	16	32	64	128	256	MIC (µg/mL)
Neomycin	1.154	0.039	0.933	0.039	0.039	0.042	0.039	0.039	0.039	0.04	0.038	0.04	1
	1.122	0.037	0.822	0.039	0.051	0.038	0.039	0.039	0.039	0.039	0.057	0.039	1
	1.131	0.037	0.926	0.037	0.037	0.036	0.039	0.039	0.039	0.039	0.04	0.045	1

	0	Media	0.125	0.25	0.5	1	2	4	8	16	32	64	MIC (µg/mL)
Amikacin	1.208	0.038	1.273	1.187	0.721	0.812	0.043	0.043	0.04	0.041	0.038	0.039	2
	1.315	0.037	1.305	1.253	0.731	0.78	0.04	0.04	0.039	0.039	0.04	0.04	2
	1.318	0.037	1.292	1.232	0.755	0.816	0.042	0.041	0.041	0.042	0.042	0.041	2

	0	Media	0.125	0.25	0.5	1	2	4	8	16	32	64	MIC (µg/mL)
Kanamycin	1.165	0.04	1.27	1.238	1.215	1.217	1.218	1.182	1.191	0.976	0.633	0.526	> 64
	1.262	0.039	1.394	1.407	1.226	1.295	1.463	1.006	1.206	1.012	0.653	0.21	> 64
	1.317	0.039	1.368	1.259	1.313	1.287	1.257	1.277	1.232	1.133	0.686	0.407	> 64

	0	Media	0.125	0.25	0.5	1	2	4	8	16	32	64	MIC (µg/mL)
Tobramycin	1.095	0.04	1.191	1.244	1.215	1.247	1.256	1.219	1.21	1.252	1.065	0.711	> 64
	1.281	0.038	1.323	1.365	1.382	1.361	1.38	1.382	1.346	1.374	1.279	0.879	> 64
	1.308	0.038	1.337	1.303	1.282	1.297	1.3	1.323	1.315	1.421	1.316	0.92	> 64

	0	Media	0.125	0.25	0.5	1	2	4	8	16	32	64	MIC (µg/mL)
Gentamicin	1.135	0.046	1.228	1.24	1.044	1.186	1.232	1.238	1.256	1.169	1.28	1.185	> 64
	1.213	0.039	1.292	1.294	1.263	1.257	1.282	1.274	1.29	1.303	1.32	1.281	> 64
	1.203	0.037	1.295	1.309	1.291	1.248	1.295	1.308	1.296	1.341	1.369	1.341	> 64

	0	Media	0.5	1	2	4	8	16	32	64	128	256	MIC (µg/mL)
Apramycin	1.106	0.04	1.144	1.246	0.957	0.604	0.041	0.045	0.04	0.039	0.038	0.041	8
	1.271	0.038	1.315	1.263	0.966	0.623	0.042	0.041	0.041	0.042	0.06	0.041	8
	1.117	0.038	1.311	1.264	0.999	0.607	0.041	0.042	0.041	0.045	0.042	0.041	8

2366

meta-AAC0043

	0	Media	256	128	64	32	16	8	4	2	1	0.5	MIC (µg/mL)
Apramycin	1.348	0.052	0.037	0.038	0.039	0.037	0.04	0.042	0.04	1.008	1.137	1.261	4
	1.307	0.037	0.042	0.037	0.037	0.04	0.04	0.049	0.04	1.002	1.091	1.203	4
	1.303	0.038	0.039	0.039	0.038	0.037	0.04	0.062	0.066	0.97	1.077	1.199	4
	0	Media	0.5	1	2	4	8	16	32	64	128	256	MIC (µg/mL)
Gentamicin	1.315	0.045	1.273	1.249	1.212	1.194	1.171	1.151	1.095	0.977	0.631	0.09	256
	1.297	0.041	1.263	1.241	1.215	1.237	1.18	1.175	1.136	0.985	0.629	0.101	> 256
	1.319	0.041	1.276	1.256	1.251	1.245	1.267	1.206	1.156	1.027	0.604	0.12	> 256

	0	Media	0.5	1	2	4	8	16	32	64	128	256	MIC (µg/mL)
Kanamycin A	1.346	0.038	1.343	1.2	1.139	1.006	0.239	0.04	0.039	0.039	0.041	0.043	16
	1.325	0.037	1.224	1.178	1.113	0.967	0.19	0.041	0.04	0.039	0.039	0.04	16
	1.321	0.039	1.218	1.154	1.105	0.95	0.172	0.079	0.041	0.04	0.041	0.042	16
Tobramycin	1.306	0.038	1.202	1.142	1.095	0.997	0.717	0.128	0.041	0.041	0.042	0.043	32
	1.311	0.041	1.235	1.165	1.112	0.938	0.637	0.122	0.041	0.04	0.042	0.045	32
	1.331	0.041	1.268	1.256	1.204	0.987	0.63	0.128	0.117	0.04	0.045	0.042	64

	0	Media	0.5	1	2	4	8	16	32	64	128	256	MIC (µg/mL)
Neomycin	1.38	0.039	0.576	0.039	0.039	0.038	0.043	0.043	0.041	0.041	0.042	0.042	1
	1.351	0.04	0.458	0.041	0.04	0.04	0.044	0.043	0.043	0.044	0.047	0.051	1
	1.349	0.046	0.043	0.041	0.041	0.04	0.045	0.045	0.044	0.041	0.043	0.048	≤ 0.5
Paromomycin	1.373	0.04	1.278	0.918	0.044	0.043	0.043	0.044	0.042	0.043	0.042	0.042	2
	1.339	0.041	1.282	0.998	0.043	0.042	0.043	0.049	0.042	0.048	0.041	0.042	2
	1.362	0.042	1.311	0.95	0.099	0.041	0.043	0.042	0.041	0.04	0.041	0.076	4

	0	Media	0.5	1	2	4	8	16	32	64	128	256	MIC (µg/mL)
Amikacin	1.381	0.068	0.996	0.042	0.041	0.043	0.043	0.048	0.058	0.059	0.043	0.049	1
	1.361	0.038	0.994	0.05	0.044	0.042	0.051	0.052	0.056	0.058	0.049	0.06	1
	1.383	0.057	1.066	0.289	0.044	0.04	0.042	0.046	0.053	0.052	0.05	0.042	2

Chapter Five: Discussion and future directions

Discussion and future directions

ApmA's unique AG resistance profile warrants the classification of this enzyme to be AAC(2')-IIIa **(Fig. 1)**. The isoform refers to the GenBank protein sequence identifier WP_032494221, the sequence under investigation in Chapters 2 and 3 of this thesis. The sequence for *apmA* was originally identified on a multiresistance resistant plasmid from a bovine methicillin-resistant *Staphylococcus aureus* (MRSA) ST398 isolate[78,79]. There is also a second sequence for *apmA* (GenBank identifier WP_015059965), reported in 2012 as the sole resistance element of a smaller plasmid originating in an MRSA ST398 isolate from a swine breeding pen[80]. While our reports are the first characterization of an LβH acetyltransferase involved in AG detoxification, they are not the first for the modification of sugar-based compounds.

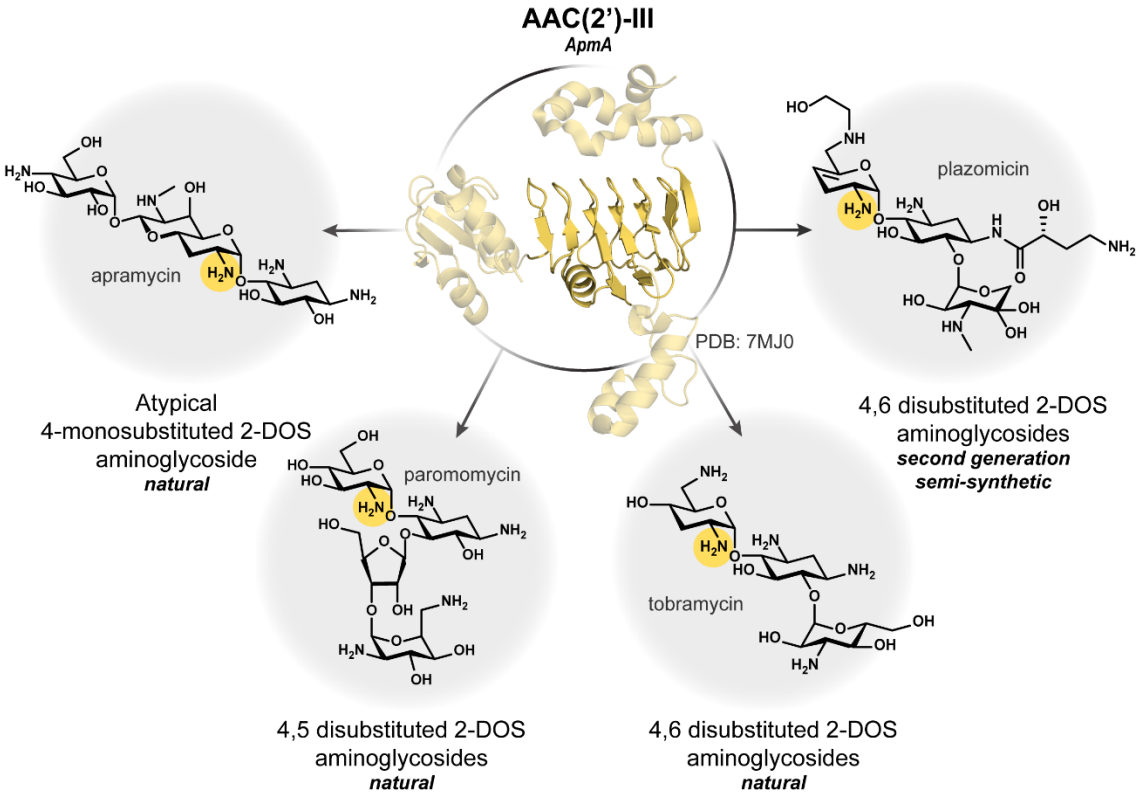

Figure 1. ApmA substrate specificity spans across each AG structural subclass.

The LβH superfamily is primarily involved in *N*- or *O*-acetylating nucleotide-linked sugars in the biosynthesis of outer membrane components for Gram-negative bacteria[81-83] or the S-layer glycoprotein glycans produced by Gram-positive bacteria[84,85]. Ligand-bound crystal structure complexes are available for many of these enzymes with their respective acetyl-accepting substrate[82]. The structural data from crystallographic analyses has informed protein engineering and *in vitro* steady-state kinetics to identify key residues involved in catalysis and substrate positioning[86]. The conserved active site histidine, in sequence and structure, is the defining feature for these enzymes. Conclusions to the residue's chemical significance are usually drawn as to determine if the histidine is essential as a general base irrespective of an *N*- or *O*-acetylation mechanism. Residues deemed not essential in the active site are loosely described important for substrate binding or positioning[84,86].

Unique to our evaluation of ApmA-mediated acetylation, is the structural diversity of susceptible substrates. This allowed us to explore the chemistries governing substrate binding, positioning and subsequent acetylation in greater detail. We present an alternate significance for the histidine, attributing the flexibility in its role of AG-modification resulting from the immediate chemical environment for acetylation. These findings widen the scope of future investigations within the LβH superfamily beyond the current notion that histidine is only conserved for the necessity to act as a general base. The lessons from this work can also be applied for future biochemical investigations of AAC(2') from the GNAT superfamily.

Interdisciplinary approaches are key to continue challenging our current perspectives on the biochemistry underlying these enzyme-mediated reactions. Our characterization of ApmA can now be leveraged to identify other LβH acetyltransferases with AG-acetylating activity or their potential to do so. Towards this goal, future investigations will need to fill the gap in the

bioinformatics component of our genomic enzymology study. This will involve evaluating the genetic context of *apmA* in greater detail and curation of homologous protein sequences to study where ApmA falls in the phylogeny. These relationships can be used in the reconstruction of ancestral protein sequences to capture the functional diversity within the LβH superfamily.

Chapter 4 of this thesis incorporates bioinformatic approaches to map structural-functional relationships to the phylogeny of Antibiotic_NAT AACs. Our characterization of the Antibiotic_NAT family produced molecular determinants from representative crystal structures across 4 clades of AAC(3)s to rationalize substrate specificity. We show Antibiotic_NAT sequences originating in the clinic or environment is distributed throughout the phylogeny. One of these clades includes all known AAC(3)s identified in biosynthetic gene clusters of AGs. The expanded substrate specificity seen towards apramycin in different clades, highlights the depth of diversity that remains to be identified in the AG resistome. Together, the phylogeny and functional data presented serves as a foundation moving forward to investigating the evolution of AG-acetylation within this protein family **(Fig. 2)**.

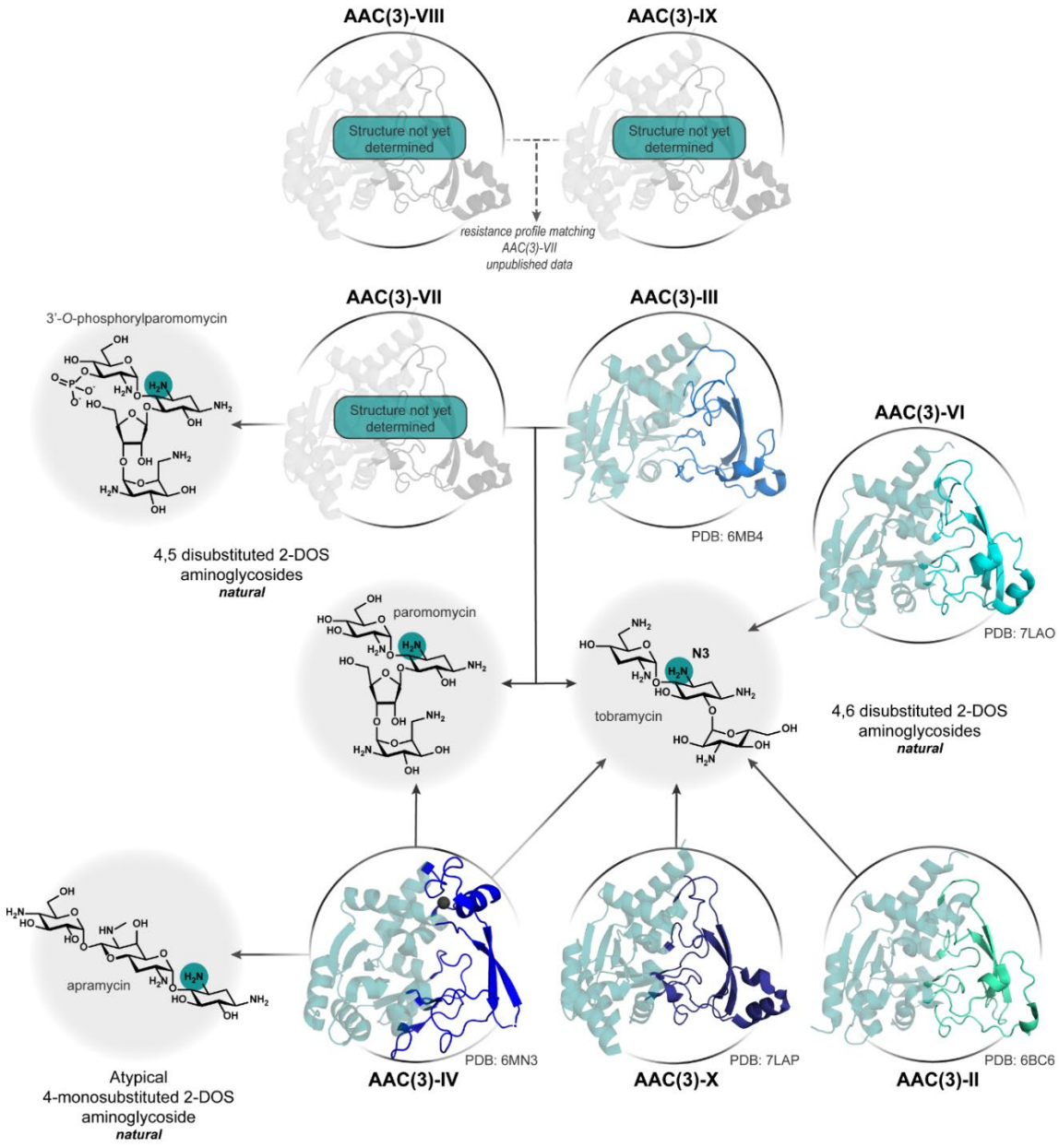

Figure 2. Antibiotic_NAT family exhibits several iterations in the minor domain to permit the 3-N-acetylation of various structurally distinct AGs. Major domain is coloured consistent across each structure shown. The minor domain, responsible for AG binding is shown in a different colour in each structure. Gaps in structural information are indicated. Representatives of susceptible AGs are shown, those selected are substrates shared by indicated AAC(3)s.

There have been extensive investigations into the underlying chemical mechanisms of some AAC(3) Antibiotic_NATs[87], however, there is still much to learn. The most notable member of the Antibiotic_NAT family is AAC(3)-IV. As the first AAC identified to confer resistance to apramycin,[88,89] we found it belonged within a clade distinct from other clinically relevant

Antibiotic_NAT AAC(3)s. The structural data obtained for this enzyme also revealed a Zn^{2+} binding site. Our structural data can be combined with previously published steady-state kinetics[23] for AAC(3)-IV to fill in the gaps remaining for the chemical mechanism. The structural uniqueness observed with AAC(3)-IV creates an opportunity to gain insight into alternate physiological roles members of this clade possess. Is the Zn^{2+} important solely for protein folding and structural integrity? Is there a secondary function for these enzymes that requires the Zn^{2+} or is it important for AG recognition? Pursing further characterization of such enzymes can be used to broaden the search of additional sequences involved in AG detoxification or other antibiotic classes. Opportunity for future work also exists within the clade of AAC(3)s identified in biosynthetic gene clusters of AG-producing *Streptomyces sp.* Like the GNAT superfamily, very little structural information exists for these enzymes. As we learn more about the biosynthesis of AGs, we must leverage the knowledge to investigate how these chemistries are adapted or evolve for antibiotic resistance.

Concluding remarks

I want to use this opportunity to unify the decades of quality research investigating the sequence-structure-function relationships of the three protein families involved in AG acetylation. The information presented in the introductory chapter will serve as the first section in a literature review of the AACs. The second and third section of the review will discuss where the research started, what we have learned and where the research is needed for the Antibiotic_NAT and ApmA-like AACs respectively. The lessons from each section will inform future investigations into the evolution of AG-acetylating activity within each protein family. As these mechanisms continue to evolve, genomic enzymology-based studies will continue to inform AG development, stewardship, and surveillance for resistance mechanisms in different environments.

References

1. Wright, G.D. Bacterial resistance to antibiotics: enzymatic degradation and modification. *Advanced drug delivery reviews* **57**, 1451-1470 (2005).

2. Serio, A.W., Magalhães, M.L., Blanchard, J.S. & Connolly, L.E. Aminoglycosides: mechanisms of action and resistance. in *Antimicrobial drug resistance* 213-229 (Springer, 2017).

3. Becker, K. et al. Efficacy of EBL-1003 (apramycin) against *Acinetobacter baumannii* lung infections in mice. *Clinical Microbiology and Infection* **27**, 1315-1321 (2021).

4. Lubriks, D. et al. Synthesis and Antibacterial Activity of Propylamycin Derivatives Functionalized at the 5"- and Other Positions with a View to Overcoming Resistance Due to Aminoglycoside Modifying Enzymes. *ACS Infect Dis* **7**, 2413-2424 (2021).

5. Pirrone, M.G., Hobbie, S.N., Vasella, A., Bottger, E.C. & Crich, D. Influence of ring size in conformationally restricted ring I analogs of paromomycin on antiribosomal and antibacterial activity. *RSC Med Chem* **12**, 1585-1591 (2021).

6. Armstrong, E.S. & Miller, G.H. Combating evolution with intelligent design: the neoglycoside ACHN-490. *Curr Opin Microbiol* **13**, 565-73 (2010).

7. Favrot, L., Blanchard, J.S. & Vergnolle, O. Bacterial GC*N*5-related *N*-acetyltransferases: from resistance to regulation. *Biochemistry* **55**, 989-1002 (2016).

8. Xie, L., Zeng, J., Luo, H., Pan, W. & Xie, J. The Roles of Bacterial GC*N*5-Related *N*-acetyltransferases. *Critical Reviews in Eukaryotic Gene Expression* **24**, 77-87 (2014).

9. Okamoto, S. & Suzuki, Y. Chloramphenicol-, dihydrostreptomycin-, and kanamycin-inactivating enzymes from multiple drug-resistant *Escherichia coli* carrying episome 'R'. *Nature* **208**, 1301-3 (1965).

10. Shaw, K.J., Rather, P.N., Hare, R.S. & Miller, G.H. Molecular genetics of aminoglycoside resistance genes and familial relationships of the aminoglycoside-modifying enzymes. *Microbiol Rev* **57**, 138-63 (1993).

11. Davies, J. & Kagan, S.A. What is the mechanism of plasmid-determined resistance to aminoglycoside antibiotics? in *R-Factors: Their Properties and Possible Control* 207-219 (Springer, 1977).

12. Mitsuhashi, S. Proposal for a rational nomenclature for phenotype, genotype, and aminoglycoside-aminocyclitol modifying enzymes. in *Drug-Inactivating Enzymes and Antibiotic Resistance* (ed. S. Mitsuhashi, L.R., V. Krčméry) 115-119 (Avicenum and Springer-Verlag, Czechoslovak Medical Press, Prague and Berlin, Heidelberg, New York, 1975).

13. Novick, R.P. et al. Uniform nomenclature for bacterial plasmids: a proposal. *Bacteriological reviews* **40**, 168-189 (1976).

14. Vanhoof, R., Hannecart-Pokorni, E. & Content, J. Nomenclature of genes encoding aminoglycoside-modifying enzymes. *Antimicrob Agents Chemother* **42**, 483 (1998).

15. Sunada, A., Nakajima, M., Ikeda, Y., Kondo, S. & Hotta, K. Enzymatic 1-*N*-acetylation of paromomycin by an actinomycete strain #8 with multiple aminoglycoside resistance and paromomycin sensitivity. *J Antibiot (Tokyo)* **52**, 809-14 (1999).

16. Lovering, A.M., White, L.O. & Reeves, D.S. AAC(1): a new aminoglycoside-acetylating enzyme modifying the Cl aminogroup of apramycin. *J Antimicrob Chemother* **20**, 803-13 (1987).

17. Gomez-Luis, R., Vergara, Y., Lopez, L., Castillo, J. & Rubio, M. 1-*N*-aminoglycoside acetyltransferase [AAC (1)] in clinical isolates of *Campylobacter* spp. in *Interscience Conference on Antimicrobial Agents and Chemotherapy* (1999).

18. Burckhardt, R.M. & Escalante-Semerena, J.C. Small-molecule acetylation by GC*N*5-related N-acetyltransferases in bacteria. *Microbiology and Molecular Biology Reviews* **84**, e00090-19 (2020).

19. Ramirez, M.S. & Tolmasky, M.E. Aminoglycoside modifying enzymes. *Drug Resistance Updates* **13**, 151-171 (2010).

20. Juhas, M. et al. *In vitro* activity of apramycin against multidrug-, carbapenem- and aminoglycoside-resistant Enterobacteriaceae and *Acinetobacter baumannii*. *J Antimicrob Chemother* **74**, 944-952 (2019).

21. Elbourne, L.D. & Hall, R.M. Gene cassette encoding a 3-*N*-aminoglycoside acetyltransferase in a chromosomal integron. *Antimicrob Agents Chemother* **50**, 2270-1 (2006).

22. Galimand, M. et al. AAC(3)-XI, a new aminoglycoside 3-*N*-acetyltransferase from *Corynebacterium striatum*. *Antimicrobial Agents and Chemotherapy* **59**, 5647-5653 (2015).

23. Magalhaes, M.L. & Blanchard, J.S. The kinetic mechanism of AAC(3)-IV aminoglycoside acetyltransferase from *Escherichia coli*. *Biochemistry* **44**, 16275-83 (2005).

24. Hegde, S.S., Javid-Majd, F. & Blanchard, J.S. Overexpression and mechanistic analysis of chromosomally encoded aminoglycoside 2'-*N*-acetyltransferase (AAC(2')-Ic) from *Mycobacterium tuberculosis*. *J Biol Chem* **276**, 45876-81 (2001).

25. Aínsa, J.A. et al. Aminoglycoside 2′-*N*-acetyltransferase genes are universally present in mycobacteria: characterization of the *aac(2')-Ic* gene from *Mycobacterium tuberculosis*

and the *aac(2')-Id* gene from *Mycobacterium smegmatis*. *Molecular Microbiology* **24**, 431-441 (1997).

26. Wright, G.D. & Ladak, P. Overexpression and characterization of the chromosomal aminoglycoside 6'-*N*-acetyltransferase from *Enterococcus faecium*. *Antimicrob Agents Chemother* **41**, 956-60 (1997).

27. Wolf, E. et al. Crystal structure of a GC*N*5-related *N*-acetyltransferase: *Serratia marcescens* aminoglycoside 3-*N*-acetyltransferase. *Cell* **94**, 439-449 (1998).

28. Xu, Z. et al. Structural and functional survey of environmental aminoglycoside acetyltransferases reveals functionality of resistance enzymes. *ACS Infect Dis* **3**, 653-665 (2017).

29. Popov, G., Evdokimova, E., Stogios, P.J. & Savchenko, A. Structure of the full-length *Serratia marcescens* acetyltransferase AAC(3)-Ia in complex with coenzyme A. *Protein Science* **29**, 803-808 (2020).

30. Brzezinska, M., Benveniste, R., Davies, J., Daniels, P.J. & Weinstein, J. Gentamicin resistance in strains of Pseudomonas aeruginosa mediated by enzymic N-acetylation of the deoxystreptamine moiety. *Biochemistry* **11**, 761-766 (1972).

31. Davies, J. & Benveniste, R. Enzymatic acetylation of aminoglycoside antibiotics by *Excherichia coli* carrying an R factor. *Biochemistry* **10**, 1787-1796 (1971).

32. Phillips, I., King, A. & Shannon, K. Prevalence and mechanisms of aminoglycoside resistance. a ten-year study. *Am J Med* **80**, 48-55 (1986).

33. Maxwell, A., Ghate, V., Aranjani, J. & Lewis, S. Breaking the barriers for the delivery of amikacin: Challenges, strategies, and opportunities. *Life Sci* **284**, 119883 (2021).

34. Kawaguchi, H., Naito, T., Nakagawa, S. & Fujisawa, K.-I. BB-K8, a new semisynthetic aminoglycoside antibiotic. *The Journal of Antibiotics* **25**, 695-708 (1972).

35. Ahmed, A.M. New aminoglycoside acetyltransferase gene, *aac(3)-Id*, in a class 1 integron from a multiresistant strain of *Vibrio fluvialis* isolated from an infant aged 6 months. *Journal of Antimicrobial Chemotherapy* **53**, 947-951 (2004).

36. Doublet, B.T., Weill, F.O.-X., Fabre, L., Chaslus-Dancla, E. & Cloeckaert, A. Variant *Salmonella* genomic island 1 antibiotic resistance gene cluster containing a novel 3′-*N*-aminoglycoside acetyltransferase gene cassette, *aac(3)-Id*, in *Salmonella enterica* serovar Newport. *Antimicrobial Agents and Chemotherapy* **48**, 3806-3812 (2004).

37. Riccio, M.L. et al. Novel 3-*N*-aminoglycoside acetyltransferase gene, *aac(3)-Ic*, from a *Pseudomonas aeruginosa* integron. *Antimicrobial Agents and Chemotherapy* **47**, 1746-1748 (2003).

38. Levings, R.S., Partridge, S.R., Lightfoot, D., Hall, R.M. & Djordjevic, S.P. New integron-associated gene cassette encoding a 3-*N*-aminoglycoside acetyltransferase. *Antimicrobial Agents and Chemotherapy* **49**, 1238-1241 (2005).

39. Forsberg, K.J. et al. Bacterial phylogeny structures soil resistomes across habitats. *Nature* **509**, 612-616 (2014).

40. Meyer, J.F. & Wiedemann, B. Characterization of aminoglycoside 6'-*N*-acetyltrasferases [AAC(6')] from Gram-negative bacteria and *Streptomyces kanamyceticus*. *Journal of Antimicrobial Chemotherapy* **15**, 271-282 (1985).

41. Mana, H.A. et al. Low-level amikacin resistance induced by AAC(6')-Ib and AAC(6')-Ib-cr in extended-spectrum beta-lactamase (ESBL)-producing Enterobacterales isolated from urine in children. *J Glob Antimicrob Resist* **26**, 42-44 (2021).

42. Haldorsen, B.C., Simonsen, G.S., Sundsfjord, A., Samuelsen, O. & Norwegian Study Group on Aminoglycoside, R. Increased prevalence of aminoglycoside resistance in clinical isolates of *Escherichia coli* and *Klebsiella* spp. in Norway is associated with the acquisition of AAC(3)-II and AAC(6')-Ib. *Diagn Microbiol Infect Dis* **78**, 66-9 (2014).

43. Robicsek, A. et al. Fluoroquinolone-modifying enzyme: a new adaptation of a common aminoglycoside acetyltransferase. *Nat Med* **12**, 83-8 (2006).

44. Kim, C., Villegas-Estrada, A., Hesek, D. & Mobashery, S. Mechanistic characterization of the bifunctional aminoglycoside-modifying enzyme AAC(3)-Ib/AAC(6‘)-Ib‘ from *Pseudomonas aeruginosa*. *Biochemistry* **46**, 5270-5282 (2007).

45. Kim, C., Hesek, D., Zajíček, J., Vakulenko, S.B. & Mobashery, S. Characterization of the bifunctional aminoglycoside-modifying enzyme ANT(3’’)-Ii/AAC(6‘)-IId from *Serratia marcescens*. *Biochemistry* **45**, 8368-8377 (2006).

46. Boehr, D.D., Daigle, D.M. & Wright, G.D. Domain-domain interactions in the aminoglycoside antibiotic resistance enzyme AAC(6')-APH(2"). *Biochemistry* **43**, 9846-55 (2004).

47. Boehr, D.D., Jenkins, S.I. & Wright, G.D. The molecular basis of the expansive substrate specificity of the antibiotic resistance enzyme aminoglycoside acetyltransferase-6'-aminoglycoside phosphotransferase-2". The role of Asp-99 as an active site base important for acetyl transfer. *J Biol Chem* **278**, 12873-80 (2003).

48. Daigle, D.M., Hughes, D.W. & Wright, G.D. Prodigious substrate specificity of AAC(6′)-APH(2″), an aminoglycoside antibiotic resistance determinant in enterococci and staphylococci. *Chemistry & Biology* **6**, 99-110 (1999).

49. Costa, Y., Galimand, M., Leclercq, R., Duval, J. & Courvalin, P. Characterization of the chromosomal *aac(6')-Ii* gene specific for *Enterococcus faecium*. *Antimicrobial agents and chemotherapy* **37**, 1896-1903 (1993).

50. Magnet, S., Lambert, T., Courvalin, P. & Blanchard, J.S. Kinetic and mutagenic characterization of the chromosomally encoded Salmonella enterica AAC(6')-Iy aminoglycoside *N*-acetyltransferase. *Biochemistry* **40**, 3700-9 (2001).

51. Draker, K.A. & Wright, G.D. Molecular mechanism of the enterococcal aminoglycoside 6'-*N*-acetyltransferase: role of GNAT-conserved residues in the chemistry of antibiotic inactivation. *Biochemistry* **43**, 446-54 (2004).

52. Wybenga-Groot, L.E., Draker, K., Wright, G.D. & Berghuis, A.M. Crystal structure of an aminoglycoside 6'-*N*-acetyltransferase: defining the GC*N*5-related *N*-acetyltransferase superfamily fold. *Structure* **7**, 497-507 (1999).

53. Vetting, M.W., Magnet, S., Nieves, E., Roderick, S.L. & Blanchard, J.S. A bacterial acetyltransferase capable of regioselective *N*-acetylation of antibiotics and histones. **11**, 565-573 (2004).

54. Stogios, P.J. et al. Structural and biochemical characterization of *Acinetobacter* spp. aminoglycoside acetyltransferases highlights functional and evolutionary variation among antibiotic resistance enzymes. *ACS Infect Dis* **3**, 132-143 (2017).

55. Draker, K.A., Northrop, D.B. & Wright, G.D. Kinetic mechanism of the GC*N*5-related chromosomal aminoglycoside acetyltransferase AAC(6')-Ii from *Enterococcus faecium*: evidence of dimer subunit cooperativity. *Biochemistry* **42**, 6565-74 (2003).

56. Vetting, M.W. et al. Mechanistic and structural analysis of aminoglycoside *N*-acetyltransferase AAC(6')-Ib and its bifunctional, fluoroquinolone-active AAC(6')-Ib-cr variant. *Biochemistry* **47**, 9825-35 (2008).

57. Aggen, J.B. et al. Synthesis and spectrum of the neoglycoside ACHN-490. *Antimicrob Agents Chemother* **54**, 4636-42 (2010).

58. Cox, G. et al. Plazomicin retains antibiotic activity against most aminoglycoside modifying enzymes. *ACS Infect Dis* **4**, 980-987 (2018).

59. Yamaguchi, M., Mitsuhashi, S., Kobayashi, F. & Zenda, H. A 2'-*N*-acetylating enzyme of aminoglycosides. *The Journal of Antibiotics* **27**, 507-515 (1974).

60. Rather, P., Orosz, E., Shaw, K., Hare, R. & Miller, G. Characterization and transcriptional regulation of the 2'-*N*-acetyltransferase gene from *Providencia stuartii*. *Journal of bacteriology* **175**, 6492-6498 (1993).

61. Franklin, K. & Clarke, A.J. Overexpression and characterization of the chromosomal aminoglycoside 2'-*N*-acetyltransferase of *Providencia stuartii*. *Antimicrob Agents Chemother* **45**, 2238-44 (2001).

62. Vetting, M.W., Hegde, S.S., Javid-Majd, F., Blanchard, J.S. & Roderick, S.L. Aminoglycoside 2'-*N*-acetyltransferase from *Mycobacterium tuberculosis* in complex with coenzyme A and aminoglycoside substrates. *Nat Struct Biol* **9**, 653-8 (2002).

63. Ainsa, J.A., Martin, C., Gicquel, B. & Gomez-Lus, R. Characterization of the chromosomal aminoglycoside 2'-*N*-acetyltransferase gene from *Mycobacterium fortuitum*. *Antimicrobial agents and chemotherapy* **40**, 2350-2355 (1996).

64. Jeong, C.S. et al. Structural and biochemical analyses of an aminoglycoside 2'-*N*-acetyltransferase from *Mycolicibacterium smegmatis*. *Sci Rep* **10**, 21503 (2020).

65. Payie, K.G. & Clarke, A.J. Characterization of gentamicin 2'-*N*-acetyltransferase from *Providencia stuartii*: its use of peptidoglycan metabolites for acetylation of both aminoglycosides and peptidoglycan. *Journal of Bacteriology* **179**, 4106-4114 (1997).

66. Bassenden, A.V. et al. Structural and phylogenetic analyses of resistance to next-generation aminoglycosides conferred by AAC(2') enzymes. *Sci Rep* **11**, 11614 (2021).

67. Golkar, T. et al. Structural basis for plazomicin antibiotic action and resistance. *Commun Biol* **4**, 729 (2021).

68. Umezawa, H. et al. A new antibiotic, kasugamycin. *The Journal of Antibiotics, Series A* **18**, 101-103 (1965).

69. Zhang, Y. et al. The context of the ribosome binding site in mRNAs defines specificity of action of kasugamycin, an inhibitor of translation initiation. *Proc Natl Acad Sci U S A* **119**, e2118553119 (2022).

70. Schuwirth, B.S. et al. Structural analysis of kasugamycin inhibition of translation. *Nature Structural & Molecular Biology* **13**, 879-886 (2006).

71. Yoshii, A., Moriyama, H. & Fukuhara, T. The novel kasugamycin 2'-*N*-acetyltransferase gene aac(2')-IIa, carried by the IncP island, confers kasugamycin resistance to rice-pathogenic bacteria. *Appl Environ Microbiol* **78**, 5555-64 (2012).

72. Yoshii, A. et al. Two types of genetic carrier, the IncP genomic island and the novel IncP-1β plasmid, for the *aac(2')-IIa* gene that confers kasugamycin resistance in *Acidovorax avenae* ssp. *avenae*. *Molecular Plant Pathology* **16**, 288-300 (2015).

73. Pawlowski, A.C. et al. A diverse intrinsic antibiotic resistome from a cave bacterium. *Nature Communications* **7**, 13803 (2016).

74. Kasuga, K. et al. Heterologous production of kasugamycin, an aminoglycoside antibiotic from *Streptomyces kasugaensis*, in *Streptomyces lividans* and *Rhodococcus erythropolis* L-88 by constitutive expression of the biosynthetic gene cluster. *Applied Microbiology and Biotechnology* **101**, 4259-4268 (2017).

75. Rattinam, R. et al. KasQ an Epimerase Primes the Biosynthesis of Aminoglycoside Antibiotic Kasugamycin and KasF/H Acetyltransferases Inactivate Its Activity. *Biomedicines* **10**, 212 (2022).

76. Smith, C.A., Toth, M., Weiss, T.M., Frase, H. & Vakulenko, S.B. Structure of the bifunctional aminoglycoside-resistance enzyme AAC(6′)-Ie-APH(2″)-Ia revealed by crystallographic and small-angle X-ray scattering analysis. *Acta Crystallographica Section D Biological Crystallography* **70**, 2754-2764 (2014).

77. Hannecart-Pokorni, E. et al. Characterization of the 6'-*N*-aminoglycoside acetyltransferase gene *aac(6')-Im* [corrected] associated with a sulI-type integron. *Antimicrobial Agents and Chemotherapy* **41**, 314-318 (1997).

78. Fessler, A.T., Kadlec, K. & Schwarz, S. Novel apramycin resistance gene apmA in bovine and porcine methicillin-resistant *Staphylococcus aureus* ST398 isolates. *Antimicrob Agents Chemother* **55**, 373-5 (2011).

79. Feßler, A.T. et al. Complete sequence of a plasmid from a bovine methicillin-resistant *Staphylococcus aureus* harbouring a novel ica-like gene cluster in addition to antimicrobial and heavy metal resistance genes. *Veterinary Microbiology* **200**, 95-100 (2017).

80. Kadlec, K., Feßler, A.T., Couto, N., Pomba, C.F. & Schwarz, S. Unusual small plasmids carrying the novel resistance genes dfrK or apmA isolated from methicillin-resistant or -susceptible staphylococci. *Journal of Antimicrobial Chemotherapy* **67**, 2342-2345 (2012).

81. Thoden, J.B. & Holden, H.M. Molecular structure of WlbB, a bacterial *N*-Acetyltransferase Involved in the Biosynthesis of 2,3-Diacetamido-2,3-dideoxy-d-mannuronic Acid. *Biochemistry* **49**, 4644-4653 (2010).

82. Rangarajan, E.S. et al. Structure and active site residues of PglD, an N-acetyltransferase from the bacillosamine synthetic pathway required for *N*-glycan synthesis in *Campylobacter jejuni*. *Biochemistry* **47**, 1827-1836 (2008).

83. Morrison, M.J. & Imperiali, B. Biochemical analysis and structure determination of bacterial acetyltransferases responsible for the biosynthesis of UDP-*N*,*N*'-diacetylbacillosamine. *Journal of Biological Chemistry* **288**, 32248-32260 (2013).

84. Thoden, J.B., Cook, P.D., Schäffer, C., Messner, P. & Holden, H.M. Structural and functional studies of QdtC: An *N*-acetyltransferase required for the biosynthesis of dTDP-3-acetamido-3, 6-dideoxy-α-D-glucose. *Biochemistry* **48**, 2699-2709 (2009).

85. Pfoestl, A., Hofinger, A., Kosma, P. & Messner, P. Biosynthesis of dTDP-3-acetamido-3, 6-dideoxy-α-D-galactose in *Aneurinibacillus thermoaerophilus* L420-91T. *Journal of Biological Chemistry* **278**, 26410-26417 (2003).

86. Thoden, J.B. et al. Catalytic mechanism of perosamine *N*-acetyltransferase revealed by high-resolution X-ray crystallographic studies and kinetic analyses. *Biochemistry* **51**, 3433-3444 (2012).

87. Kumar, P., Selvaraj, B., Serpersu, E.H. & Cuneo, M.J. Encoding of promiscuity in an aminoglycoside acetyltransferase. *Journal of medicinal chemistry* **61**, 10218-10227 (2018).

88. Plattner, M., Gysin, M., Haldimann, K., Becker, K. & Hobbie, S.N. Epidemiologic, phenotypic, and structural characterization of aminoglycoside-resistance gene *aac(3)-IV*. *Int J Mol Sci* **21**, 6133 (2020).

89. Davies, J. & O'Connor, S. Enzymatic modification of aminoglycoside antibiotics 3 N acetyltransferase with broad specificity that determines resistance to the novel aminoglycoside apramycin. *Antimicrobial Agents and Chemotherapy* **14**, 69-72 (1978).